

# **Roles and Mechanisms of Effector-Triggered Immunity in Plant Disease Resistance**

Bruno Pok Man Ngou

The Sainsbury Laboratory, Norwich

November 2020

This thesis has been submitted for the degree of Doctor of Philosophy

This copy of the thesis has been supplied on condition that anyone who consults it is understood to recognise that its copyright rests with the author and that use of any information derived therefrom must be in accordance with current UK Copyright Law. In addition, any quotation or extract must include full attribution.

## **Abstract**

The plant immune system involves extracellular receptors that detect pathogen-derived molecules, and intracellular receptors that recognize pathogen-secreted effectors. Surface receptor-mediated immunity, or PTI, has been extensively studied but intracellular receptor-mediated immunity, or ETI, has rarely been investigated in the absence of PTI. Previous studies on ETI have mostly been concluded from comparison between PTI and 'PTI + ETI'. Intracellular nucleotide-binding leucine-rich repeat (NLR) proteins activate ETI following recognition of pathogen-secreted effectors. The mechanisms by which NLR activation leads to pathogen resistance are largely unknown. An *Arabidopsis* line with inducible expression of the effector AvrRps4 has been generated to investigate the downstream immune responses triggered by the TIR (Toll-like, Interleukin-1 receptor, Resistance protein)-NLRs RRS1 and RPS4. Activation of ETI<sup>AvrRps4</sup> leads to upregulation of defence genes and enhanced resistance against *Pseudomonas syringae*, but does not lead to physiological responses such as ROS burst, MAPKs activation or macroscopic cell death. This implies that robust physiological changes during 'PTI + ETI' might be due to the interaction between PTI and ETI. Using the inducible-effector system, I discovered a mutual-potential relationship between PTI and ETI. PTI activates multiple protein kinases and NADPH oxidases to induce physiological responses, whereas ETI potentiates the activation of these signalling components during 'PTI + ETI'. Multiple PTI signalling components are highly upregulated during ETI through multiple mechanisms. Reciprocally, hypersensitive response triggered by ETI is enhanced by PTI. Activation of either PTI or ETI alone is insufficient to provide resistance against *P. syringae*. Thus, PTI and ETI mutually potentiates each other to provide robust resistance. These findings on the relationship between the two immune systems reshape our understanding of plant immunity.

## **Access Condition and Agreement**

Each deposit in UEA Digital Repository is protected by copyright and other intellectual property rights, and duplication or sale of all or part of any of the Data Collections is not permitted, except that material may be duplicated by you for your research use or for educational purposes in electronic or print form. You must obtain permission from the copyright holder, usually the author, for any other use. Exceptions only apply where a deposit may be explicitly provided under a stated licence, such as a Creative Commons licence or Open Government licence.

Electronic or print copies may not be offered, whether for sale or otherwise to anyone, unless explicitly stated under a Creative Commons or Open Government license. Unauthorised reproduction, editing or reformatting for resale purposes is explicitly prohibited (except where approved by the copyright holder themselves) and UEA reserves the right to take immediate 'take down' action on behalf of the copyright and/or rights holder if this Access condition of the UEA Digital Repository is breached. Any material in this database has been supplied on the understanding that it is copyright material and that no quotation from the material may be published without proper acknowledgement.

## Table of Contents

Abstract .....	2
Acknowledgement.....	7
Publications .....	8
Abbreviations.....	9
<b>Chapter 1: General introduction .....</b>	<b>14</b>
Plants and Pathogens .....	14
Pattern-triggered immunity (PTI): an overview.....	14
PRR proteins involved in pathogen recognition .....	15
Activation of PRR proteins and complex formation with co-receptors.....	17
RLCKs link receptor complexes to downstream responses.....	17
PTI downstream responses .....	19
Activation of calcium channels and calcium influxes .....	19
Activation of NADPH oxidases and ROS production.....	20
MAPKs activation.....	21
Other PTI-induced physiological responses .....	22
Negative regulation of PTI signalling pathway .....	23
An overview of PTI.....	25
Effector-triggered susceptibility (ETS) .....	25
Effector-triggered immunity (ETI): an overview.....	26
NLR proteins involved in effector recognition .....	27
Structure and activation of NLR proteins.....	29
ETI signalling components: helper NLRs .....	30
ETI signalling components: EP proteins and NDR1 .....	31
Downstream responses of ETI: Calcium influx, ROS production and MAPK activation.....	32
Downstream responses of ETI: Transcriptional regulation .....	33
Downstream responses of ETI: Defence-related phytohormones.....	35
Physiological response of ETI: Hypersensitive Response (HR).....	37
Regulation of ETI.....	38
Overview of ETI .....	39
Aims of the thesis.....	39
<b>Chapter 2: Materials and methods .....</b>	<b>43</b>
Materials .....	43
<i>Arabidopsis thaliana</i> .....	43
<i>Escherichia coli</i> .....	43
<i>Agrobacterium tumefaciens</i> .....	43
<i>Pseudomonas spp.</i> .....	43
Lysogeny Broth (LB) .....	44
King's B (KB).....	44

Murashige and Skoog ½ (MS media ½).....	44
Antibiotics concentration.....	44
Methods.....	44
Polymerase chain reaction (PCR) .....	44
Golden Gate Cloning.....	45
Plasmid purification and validation.....	45
Plasmid transformation.....	45
FastRed selection for transgenic Arabidopsis.....	45
Growing Arabidopsis on MS plates or solution.....	46
Confocal laser scanning microscopy (CLSM) imaging.....	46
RNA extraction and reverse transcription–quantitative PCR (RT–qPCR) for measuring relative gene expression .....	46
Hypersensitive cell death response phenotyping in Arabidopsis .....	47
Trypan blue staining.....	47
Electrolyte leakage assay.....	48
Immunoblotting.....	48
ROS burst assay .....	49
DAB staining .....	50
Bacterial growth assay.....	50
Plasma membrane extraction for the detection of phosphorylated RbohD and BIK1.....	50
Callose quantification.....	51
RNA-seq and data analysis.....	51
Cycloheximide and MG132 treatment .....	51
Enrichment of ribosome .....	51
Serial dilution to estimate protein abundance.....	52
Statistical data analysis.....	52
<b>Chapter 3: Inducible effector expression reveals distinct properties of NLR-mediated effector-triggered immunity.....</b>	<b>55</b>
Abstract .....	55
Introduction .....	55
A T-DNA construct with RRS1, RPS4 and inducible-AvrRps4 modules.....	56
Generation of transgenic Arabidopsis lines: SETI <sup>WT</sup> , SETI <sup>KRVY</sup> and SETI <sub>eds1-2</sub> .....	57
ETI <sup>AvrRps4</sup> leads to the upregulation of defence-related genes .....	57
ETI <sup>AvrRps4</sup> does not lead to macroscopic hypersensitive response (HR).....	58
ETI <sup>AvrRps4</sup> does not lead to MAPKs activation .....	58
ETI <sup>AvrRps4</sup> does not lead to ROS production .....	58
ETI <sup>AvrRps4</sup> leads to resistance against <i>Pseudomonas syringae</i> .....	59
ETI triggered by multiple NLRs leads to upregulation of defence-related genes .....	59
ETI triggered by CC-NLRs leads to macroscopic HR.....	60
ETI triggered by CC-NLRs leads to MAPK activation and ROS burst.....	60

ETI triggered by multiple NLRs does not lead to S39 phosphorylation in RbohD.....	61
Discussion.....	61
<b>Chapter 4: Mutual Potentiation of Plant Immunity by Cell-surface and Intracellular Receptors .....</b>	<b>73</b>
Abstract .....	73
Introduction .....	73
Pre-activation of ETI leads to enhanced PTI-induced ROS production.....	74
Co-activation of PTI and ETI leads to enhanced ROS production and accumulation .....	74
Additional physiological hallmarks of PTI are enhanced by ETI.....	75
Pre-activation of PTI and ETI leads to enhanced activation of PTI-signaling components ...	75
Co-activation of ETI leads to enhanced activation of PTI-signaling components.....	76
ETI leads to protein accumulation of PTI signaling components .....	76
ETI restore suppression of PTI during ETS.....	77
ETI functions through PTI.....	77
PTI potentiates ETI <sup>AvrRps4</sup> -induced hypersensitive response.....	78
PTI potentiates ETI-induced hypersensitive response.....	79
PTI potentiates ETI-induced HR through MAPKs and NADPH oxidases.....	79
Discussion.....	80
<b>Chapter 5: Investigation into the mechanisms of elevated immune signalling protein accumulation triggered by NLR activation .....</b>	<b>94</b>
Abstract .....	94
Introduction .....	94
ETI leads to transcript upregulation of PTI signaling components.....	95
ETI leads to global transcriptional upregulation of multiple PTI signaling components .....	95
EDS1, but not SARD1 and CBP60G, is required for upregulation of PTI signaling components during ETI <sup>AvrRps4</sup> .....	96
Robust accumulation of BIK1, RbohD and MPK3 during ETI <sup>AvrRps4</sup> is not due to prolonged transcriptional activation .....	97
Translation and protein turnover are involved in protein accumulation during ETI <sup>AvrRps4</sup> .....	98
Translation control during ETI <sup>AvrRps4</sup> .....	98
Discussion.....	99
<b>Chapter 6: General discussion .....</b>	<b>112</b>
Study of ETI in the absence of PTI.....	112
Differential and common downstream responses triggered by CC- and TIR-NLRs.....	112
Differential and common downstream responses triggered by PRRs and NLRs.....	113
The relationship between PRR- and NLR-mediated immunity .....	114
Coordination of multiple PRRs and NLRs during infection.....	115
Is potentiation between PTI and ETI local or systemic? .....	115
Mechanisms involved in the potentiation of PTI by ETI.....	116
Mechanisms involved in the potentiation of ETI by PTI.....	117

How general is the new zig-zag-zig model? .....	<b>118</b>
Perspective for agriculture .....	<b>119</b>
References .....	<b>120</b>

## **Acknowledgement**

I would like to thank Jonathan Jones for the opportunity to join his lab in TSL. Jonathan has been extremely supportive and encouraging during my PhD. He has also provided many novel ideas, one of which initiates this project. I have learnt a lot from him over the last four years. It really is an honour to reinvent the famous ‘zig-zag-zig’ model with Jonathan. I would also like to thank my supervisory team members. Pingtao Ding has been a great friend and post-doc mentor who has taught me a lot. Many of our exciting discussion has led to scientific discoveries and I wish him the best for his new position in Leiden University. I would like to thank Cyril Zipfel for providing his expertise during my PhD. Cyril has provided many solid advices to improve the work and I could not have asked for a better supervisory team.

Thank you to all the Jones lab members for the support, providing feedback to my work and creating a lively and fun working environment. I am especially thankful to Hee-Kyung Ahn for working closely with me on many projects and providing advice, support, and expertise. Special thanks for all the RRS1/RPS4 group members Hailong Guo, Shanshan Wang and Jianhua Huang for both scientific and non-scientific discussions. I would also like to thank the pass and current students in the JJ lab: Oliver Furzer, Yan Man, Zan Duxbury, Agathe Jouet, Baptiste Castel, Hannah Brown, Lanxi Hu, Craig MacKenzie, Danylo Gorenkin, Moffatt Makechemu, Joanna Feehan, Lila Grandgeorge, Sophie Johnson and Robert Heal for all the support and creating the loudest, meme-filled and best student office to work in. I wish you all the best for your future career. Thank you to the student community in TSL (TSLytherin) for the supportive environment. I am also very grateful to the support staff at TSL and the horticultural services in NRP.

For my PhD project, I would also like to thank Jeff Dangl, Shuta Asai, Roger Innes, Kenichi Tsuda, Shuqun Zhang, Cyril Zipfel, Jian Min Zhou, Albrecht von Arnim, Brian Staskawicz, Cecilia Cheval, Yasuhiro Kadota, Ruby O'Grady, Maddy Morris, Jack Rhodes, Maria Derkacheva, Marta Bjornson and Yuli Ding for providing materials, discussion and technical support. Special thanks to Minhang Yuan, Xiufang Xin and Sheng-Yang He for scientific discussions and support in preparing our back-to-back manuscripts. I thank the Gatsby Foundation (United Kingdom) for funding to the JDGJ laboratory and support by the Norwich Research Park Biosciences Doctoral Training Partnership from BBSRC.

Thank you to Ken Shirasu for hosting and supporting me in RIKEN CSRS during my PIPS. Special thanks to Yoko Nagai and Yasuhiro Kadota for helping me to settle in Tokyo. I am grateful to all the Shirasu lab members for the fun, friendly and positive environment. I would also like to thank all the friends I have met during my time in Tokyo.

Thank you to my family and all of my friends (Yannik, Cara, Filip, Alice, Zara, Philip, Kit, Sam, Yuli, Bella, Rok, Jones, Travis, Nicholas, Dee, Hendrick, Matteo, Andy, Billy, Jack, George and Benzo) for their love and support during my PhD.

Bruno,

The Sainsbury Laboratory, Norwich (Nov 2020)

## **Publications**

Castel, B., Ngou, P.-M., Cevik, V., Redkar, A., Kim, D.-S., Yang, Y., Ding, P., and Jones, J.D.G. (2019). Diverse NLR immune receptors activate defence via the RPW8-NLR NRG1. *New Phytol.* 222, 966–980.

Ding, P., Ngou, B.P.M., Furzer, O.J., Sakai, T., Shrestha, R.K., MacLean, D., and Jones, J.D.G. (2020). High-resolution expression profiling of selected gene sets during plant immune activation. *Plant Biotechnol. J.*

Ding, P., Sakai, T., Shrestha, R.K., Perez, N.M., Guo, W., Ngou, B.P.M., He, S., Liu, C., Feng, X., Zhang, R., et al. (2020). Chromatin accessibility landscapes activated by cell surface and intracellular immune receptors. *BioRxiv*.

Duxbury, Z., Wang, S., MacKenzie, C.I., Tenthorey, J.L., Zhang, X., Huh, S.U., Hu, L., Hill, L., Ngou, P.M., Ding, P., et al. (2020). Induced proximity of a TIR signaling domain on a plant-mammalian NLR chimera activates defense in plants. *Proc. Natl. Acad. Sci. USA* 117, 18832–18839.

Ngou, B.P.M., Ahn, H.-K., Ding, P., Redkar, A., Brown, H., Ma, Y., Youles, M., Tomlinson, L., and Jones, J.D.G. (2020). Estradiol-inducible AvrRps4 expression reveals distinct properties of TIR-NLR-mediated effector-triggered immunity. *J. Exp. Bot.* 71, 2186–2197.

Ngou, B.P.M., Ahn, H.-K., Ding, P., and Jones, J.D. (2020). Mutual Potentiation of Plant Immunity by Cell-surface and Intracellular Receptors. *BioRxiv*.

## Abbreviations

3-OH-C10:0/ C10:0 (3-hydroxydecanoic acid)  
ACD (accelerated cell death)  
ACS (1-aminocyclopropane-1-261 carboxylic acid synthase)  
ADR1 (activated disease resistance 1)  
AGB1 (arabidopsis g-protein beta subunit 1)  
AGG1/2 (arabidopsis g-protein gamma-subunit1/2)  
BAK1 (brassinosteroid insensitive 1)  
BIK1 (botrytis-induced kinase 1)  
BIR (bak1-interacting receptor-like kinase)  
BKK1 (bak1-like1)  
bp (basepair)  
BRI1 (brassinosteroid insensitive 1)  
Ca<sup>2+</sup> (calcium)  
CaM (calmodulin)  
CAMTA (calmodulin-binding transcription factor 3)  
CARD1 (cannot respond to 2,6-dimethoxy-1,4-benzoquinone 1)  
CBP0G (calmodulin binding protein 60-like g)  
CC-NLRs (coiled-coil nucleotide-binding leucine-rich repeat)  
CDKC (cyclin-dependent kinase)  
CHS3 (chilling sensitive 3)  
CNGC (cyclic nucleotide-gated channel)  
COI1 (coronatine-insensitive 1)  
CPK (calcium-dependent protein kinase)  
CSA1 (constitutive shade-avoidance 1)  
DAMP (damage-associated molecular pattern)  
dex (dexamethasone)  
DLL (disease like lesion)  
DMBQ (2,6-dimethoxy-1,4-benzoquinone)  
DND (defence, no death)  
EDS1 (enhanced disease susceptibility 1)  
EDS5 (enhanced disease susceptibility 5)

EFR (elongation factor-tu receptor)  
EF-Tu (elongation factor-Tu)  
EP proteins (EP-domain containing proteins)  
ERF (ethylene response factor1)  
est/E2 (estradiol)  
ET (ethylene)  
ETI (effector-triggered immunity)  
ETS (effector-triggered susceptibility)  
ExTI (extracellularly-triggered immunity)  
FER (feronia)  
FLS2 (flagellin sensing 2)  
FMO1 (flavin-containing monooxygenase 1)  
g (gram)  
GA (gibberellic acid)  
GSL (glucan synthase-like)  
h (hour)  
H<sub>2</sub>O<sub>2</sub> (hydrogen peroxide)  
HDAC (histone deacetylase)  
HELL (helo/helo-like)  
Hpa (Hyaloperonospora arabidopsidis)  
HPCA1 (hydrogen-peroxide-induced ca<sup>2+</sup> increases)  
HR (hypersensitive response)  
HSP (heat shock protein)  
IAA (indole acetic acid)  
ICS1/SID2 (isochorismate synthase 1)  
INR (inceptin receptor)  
InTI (intracellular-triggered immunity)  
IRMI (intracellular receptor-mediated immunity)  
JA (jasmonic acid)  
JA-Ile (jasmonyl-l-isoleucine)  
JAZ (jasmonate zim-domain)  
l (liter)

LLG1 (lorelei-like-gpi anchored protein 1)  
LORE (lipooligosaccharide-specific reduced elicitation)  
LRR (leucine-rich repeat)  
LSD (lesion simulating disease)  
LYK (lysm-containing receptor-like kinases)  
LysM (lysin motif)  
MAMP (microbe associated molecular patterns)  
MAPK/MPK (mitogen-activated protein kinase)  
MAPKK/MKK (mitogen-activated protein kinase kinase)  
MAPKKK/MEKK (mitogen-activated protein kinase kinase kinase)  
min (minute)  
MIN7 (hopm interactor 7)  
MKP1 (mapk phosphatase 1)  
MLKLs (mixed-lineage kinases)  
mM (millimolar)  
NADPH (Nicotinamide adenine dinucleotide phosphate)  
NDR1 (non-race-specific disease resistance 1)  
NIK1 (nuclear shuttle protein-interacting kinase 1)  
NINJA (novel interactor of jaz)  
NLPs (necrosis and ethylene-inducing peptide 1-like proteins)  
NLR (nucleotide-binding leucine-rich repeat)  
NLR-ID (NLR integrated domains)  
nM (nanomolar)  
NMI (NLR-mediated immunity)  
NPR (non-expressor of pathogenesis-related genes)  
NRC (nlr required for cell death)  
NRG1 (N requirement gene 1)  
OsPT8 (phosphate transporter protein)  
PAD4 (phytoalexin deficient 4)  
PAMP (pathogen associated molecular patterns)  
PBL (avrpphb susceptible 1-like)  
PBS3 (avrpphb susceptible 3)

PCD (programmed cell death)  
PL (post-LRR domain)  
PM (plasma membrane)  
PMI (PRR-mediated immunity)  
PMR4 (powdery mildew resistant 4)  
PP2A (protein phosphatases type 2a)  
PP2C (protein phosphatases type 2c)  
PR1 (pathogenesis-related 1)  
PROPEP1 (precursor of pep1)  
PRORALF23 (pro-rapid alkalinization factor 23)  
PRR (pattern recognition receptors)  
PTI (pattern-triggered immunity)  
PUB (e3 ubiquitin ligases plant u-box)  
qPCR (quantitative PCR)  
RAR1 (required for mLa12 resistance 1)  
RbohD (respiratory burst nadph oxidase homolog d)  
RHA3A/B (ring-h2 finger a3a/b)  
RIN4 (rpm1-interacting protein 4)  
RIPK (rpm1-induced protein kinase)  
RK (receptor kinase)  
RLCK (receptor-like cytoplasmic kinase)  
RLP (receptor-like protein)  
ROS (reactive oxygen species)  
RPM1 (resistance to *p. syringae* pv *maculicola* 1)  
RPP1 (resistance to *peronospora parasitica* 1)  
RPP2A/B (resistance to *peronospora parasitica* 2A/B)  
RPP4 (resistance to *peronospora parasitica* 4)  
RPS2 (resistant to *p. syringae* 2)  
RPS4 (resistant to *p. syringae* 4)  
RPS5 (resistant to *p. syringae* 5)  
RPW8 (rpw8-like coiled-coil domain)  
RRS1 (resistance to *ralstonia solanacearum* 1)

SA (salicylic acid)  
SAG101 (senescence-associated gene 101)  
SAR (systemic acquired resistance)  
SARD1 (systemic acquired resistance deficient 1)  
SCFCO11 (Skp1/Cullin/F-box)  
SERK (somatic embryogenesis related receptor-like kinase)  
SFN (sulforaphane)  
SGT1 (suppressor of the g2 allele of skp1)  
SNC1 (suppressor of npr1-1, constitutive 1)  
SOBIR1 (suppressor of bir1-1)  
SRMI (cell-surface receptor-mediated immunity)  
STP13 (sugar transporter 13)  
T3SS (type 3 secretion system)  
TF (transcription factor)  
TGA (tgacg-binding factor)  
TIR-NLRs (toll/interleukin-1 receptor/resistance nucleotide-binding leucine-rich repeat)  
TPL (topless)  
TPR (topless-related)  
UPF (up-frameshift 1)  
V (volt)  
vc-APDR (variant-cyclic-ADP-ribose)  
WRR4 (white rust resistance 4)  
Xa21 (xanthomonas oryzae pv. oryzae resistance 21)  
XLG2 (extra-large guanine nucleotide-binding protein 2)  
ZAR1 (hopZ-activated resistance 1)  
 $\mu$ M (micromolar)

## Chapter 1: General introduction

### Plants and Pathogens

Plants are infected by diverse organisms such as fungi, oomycetes and bacteria, and also by viruses. When a plant is susceptible to a virulent pathogen race, disease ensues. Plants have evolved multiple layers of defence mechanisms to confer resistance against pathogens and pathogens have also evolved to suppress plant immune responses. This interaction between pathogens and plants can be represented in a ‘zig-zag-zig’ scheme (Jones and Dangl, 2006). Plant cell surface pattern recognition receptors (PRRs) recognise conserved Pathogen- or microbe-associated molecular patterns (PAMP/MAMPs). Perception of PAMP/MAMPs via PRRs triggers a defence response known as pattern-triggered immunity (PTI) which restricts pathogen proliferation. Pathogens have evolved to evade or suppress this response through the deployment of secreted effector molecules, which leads to effector-triggered susceptibility (ETS). Plants have in turn evolved intracellular receptors that detect effectors. These are often encoded by *Resistance (R)*-genes which upon effector perception trigger effector-triggered immunity (ETI). ETI is often triggered in the presence of PAMPs and is rarely examined in the absence PTI. Pathogens have evolved effectors to evade or suppress ETI. The ‘zig-zag-zig’ scheme provides a conceptual framework of the plant immune system (Jones and Dangl, 2006).

### Pattern-triggered immunity (PTI): an overview

Pattern-triggered immunity (or PTI) is an immune response triggered by the detection of PAMPs or damage-associated molecular patterns (DAMPs) through cell surface PRRs. PTI has also been referred to as extracellularly triggered immunity (ExTI), PRR-mediated immunity (PMI) or cell-surface receptor-mediated immunity (SRMI) as the recognition of PAMPs by cell-surface receptors occur extracellularly (Ding et al., 2020; Lacaze and Joly, 2020; van der Burgh and Joosten, 2019). PAMPs, such as the flagellin protein from bacterial flagellum, chitin from fungal cell walls and bacterial elongation factor-Tu (EF-Tu) from the prokaryotic ribosome (Kunze et al., 2004), are conserved molecules from pathogens. Multiple enzymes from plants, such as proteases and chitinases, are involved in the release of PAMPs and DAMPs during infection. Recently, the glycosidase BGAL1 has been shown to deglycosylate flagellin, which subsequently leads to the release of the flagellin-derived 22-amino acid flg22 peptides during infection (Buscaill et al., 2019). Both receptor-like kinase (RLKs) and receptor-like proteins (RLPs) are cell-surface PRRs (Jones et al., 1994; Kaku et al., 2006; Zipfel, 2014). Binding of ligands to PRR leads to complex formation between the PRR and its co-receptor, which are usually members from the SERK

(SOMATIC EMBRYOGENESIS RELATED RECEPTOR-LIKE KINASE) family (Hohmann et al., 2017; Ma et al., 2016). This leads to the phosphorylation of these PRRs which then trigger downstream signalling activation via RECEPTOR-LIKE CYTOPLASMIC KINASES (RLCKs) (Liang and Zhou, 2018; Lin et al., 2013). The heterodimeric receptor complex associates with and phosphorylates RLCKs, which then phosphorylates downstream signalling components (Liang and Zhou, 2018; Macho and Zipfel, 2014). The activation of downstream signalling components, such as calcium channels, NADPH oxidases and mitogen-activated protein kinase (MAPKs), leads to physiological and cellular changes that restricts pathogen infection (Asai et al., 2002; Kadota et al., 2015; Meng and Zhang, 2013; Torres et al., 2002). I will now provide an overview of current knowledge of the PTI signalling pathway that leads to resistance against pathogens.

### **PRR proteins involved in pathogen recognition**

The tomato Cf-9 gene (an RLP) was the first identified PRR, it recognises an apoplastic effector, Avr9, from *Cladosporium fulvum* (Jones et al., 1994). Multiple RLPs that recognise apoplastic effectors, such as Cf-4 and Cf-2, were later identified (Dixon et al., 1996, 1998; Krüger et al., 2002; Luderer et al., 2002; Thomas et al., 1997). RLPs consist of a leucine-rich repeat (LRR) ectodomain and a transmembrane  $\alpha$ -helix. Unlike RKs, they do not have a cytoplasmic kinase domain and therefore require co-receptor RKs for signal transduction, such as SOBIR1 (SUPPRESSOR OF BIR1-1) (Bi et al., 2016; Gust and Felix, 2014; Liebrand et al., 2013). Another example of RLP is the *Arabidopsis* RLP23, which forms a heteromeric receptor complex with both the co-receptors SOBIR1 and BRASSINOSTEROID INSENSITIVE 1 (BAK1) upon binding of the ligand Nlp20. Nlp20 is an epitope of NECROSIS AND ETHYLENE-INDUCING PEPTIDE 1-LIKE PROTEINS (NLPs), which are present in diverse range of pathogens such as bacteria, oomycetes and fungi (Albert et al., 2015; Böhm et al., 2014a).

RKs consist of an extracellular ectodomain, a transmembrane  $\alpha$ -helix and cytoplasmic kinase domain. Approximately 50% of RKs have an extracellular LRR domain for ligand recognition (LRR-RLKs) (Fischer et al., 2016; Gou et al., 2010; Wu et al., 2016). Some well characterised LRR-RLKs are FLAGELLIN SENSING 2 (FLS2), ELONGATION FACTOR-TU RECEPTOR (EFR) and XANTHOMONAS ORYZAE PV. ORYZAE RESISTANCE 21 (Xa21), which recognises flg22, EF-Tu and *Xanthomonas* RaxX peptide respectively (Chinchilla et al., 2006, 2007; Felix et al., 1999; Gómez-Gómez and Boller, 2000; Luu et al., 2019; Pruitt et al., 2017; Zipfel et al., 2006). Binding of corresponding

ligands to the LRR domains of the LRR-RLKs lead to formation of a heterodimeric complex between these LRR-RLKs and their corresponding coreceptors (BAK1 for FLS2 and EFR, OsSERK2 for Xa21), which sequentially leads to immune activation (Chen et al., 2014; Chinchilla et al., 2007; Heese et al., 2007; Sun et al., 2013).

PRRs are also involved in the recognition of non-proteinaceous PAMPs. The perception of chitin ( $\beta$ -1,4-linked N-acetylglucosamine (GlcNAc) polymers) is through the LYK-family receptors (LYSM (Lysin motif)-CONTAINING RECEPTOR-LIKE KINASES). In *Arabidopsis*, CERK1/LYK1, LYK4 and LYK5 are involved in chitin perception (Cao et al., 2014; Miya et al., 2007; Wan et al., 2008, 2012). In addition, CERK1, together with the RLPs LYM1 and LYM3, can also perceive peptidoglycans derived from the bacterial cell wall (Willmann et al., 2011). Thus, LYK receptors can perceive a range of carbohydrate oligomers from diverse pathogens. *Arabidopsis* can also detect the bacterial metabolite 3-hydroxydecanoic acid (3-OH-C10:0 or C10:0) through the lectin S-domain receptor kinase LIPOOLIGOSACCHARIDE-SPECIFIC REDUCED ELICITATION (LORE) (Kutschera et al., 2019; Ranf et al., 2015). LORE does not require the co-receptors BAK1 or SOBIR1 to function, and the mechanism by which it activates downstream defence responses is currently unclear.

Plants can also detect modified self, or damage-associated molecular patterns (DAMPs), that are released from wounding or tissue damage during pathogen infection. Calcium influx induced by damage activates metacaspases, which then cleave the DAMP precursor, PRECURSOR OF PEP1 (PROPEP1), into the mature DAMP PEP1. PEP1 is then perceived by the LRR-RKs PEPR1/2 and activates immune responses with BAK1 (Hander et al., 2019; Huffaker et al., 2006; Yamaguchi et al., 2006, 2010). Recently it has been reported that the *Arabidopsis* LRR-RLK, HYDROGEN-PEROXIDE-INDUCED  $Ca^{2+}$  INCREASES (HPCA1), perceives hydrogen peroxide and induces stomata closure (Wu et al., 2020a). Interestingly, HPCA1 (also known as CANNOT RESPOND TO DMBQ 1, or CARD1), can also perceive plant-derived quinone compounds (particularly 2,6-dimethoxy-1,4-benzoquinone, or DMBQ) and trigger an immune response against parasitic plants (Laohavisit et al., 2020). In addition, proteolytic fragments of chloroplastic ATP synthase from caterpillar oral secretions (termed as inceptins, a herbivore-associated molecular pattern or HAMP) can be perceived by a *Vigna unguiculata* RLP (INCEPTIN RECEPTOR, INR), which induces immune responses against herbivores (Steinbrenner et al., 2019). These indicate that multiple DAMPs or plant-derived compounds are perceived by PRRs

during infection, which leads to the amplification or potentiation of PTI activation (Dressano et al., 2020).

### **Activation of PRR proteins and complex formation with co-receptors**

As mentioned, LRR-RLKs form heterodimeric complexes with a shape-complementary co-receptor (frequently from the SERK family) upon ligand binding. The ligand acts as a “molecular glue” and interacts with the LRR domains of both the LRR-RK and the co-receptor (Hohmann et al., 2017; Santiago et al., 2016; She et al., 2011; Sun et al., 2013). The binding affinity of the ligand to the LRR-RLK increases in the presence of the co-receptor, indicating that a stable complex is formed between the PRRs (Santiago et al., 2016). Not much is currently known about the mechanism of ligand binding and complex formation in non-LRR-RLKs. Heterodimeric complex formation between the LRR domains of the LRR-RLK and the co-receptor forces the cytoplasmic kinase domains into proximity, which then leads to a series of phosphorylation events that activate downstream signalling components.

The SERK family member BAK1 associates with multiple LRR-RKs, such as FLS2, EFR and BRASSINOSTEROID INSENSITIVE 1 (BRI1), to control immunity and growth/development. Epitope-tagging of BAK1 in the C-terminus specifically impairs immunity, but not brassinosteroid signalling (Ntoukakis et al., 2011). Similarly, *bak1-5*, a point mutation in the kinase domain (C408Y) is also specifically impaired in immunity, and not in brassinosteroid signalling (Schwessinger et al., 2011). These indicate that specific phosphosites in BAK1 control its specificity in different signalling pathways. Recently, the phosphosite (S612) that specifically determines the dichotomy between immunity and growth pathways by BAK1 has been identified (Perraki et al., 2018). It is assumed that upon association, the cytoplasmic kinase domains of the LRR-RK and the co-receptor auto- and trans-phosphorylate each other to initiate downstream signalling, since both complex formation and kinase activity of either PRRs are required for signal transduction (Cao et al., 2013; Schwessinger et al., 2011; Sun et al., 2013). Further work is required to dissect the sequence of PRR phosphorylation events following ligand binding. Regardless, the activated heterodimeric complex directly phosphorylates cytoplasmic substrates, which leads to downstream signalling events (Macho and Zipfel, 2014).

### **RLCKs link receptor complexes to downstream responses**

RECEPTOR-LIKE CYTOPLASMIC KINASES (RLCKs) do not have transmembrane or extracellular domains. *Arabidopsis* RLCK subfamily VII (RLCK-VII) play particularly important roles during PTI (Rowland et al., 2005). These RLCKs associate with the PRR

complex and are directly phosphorylated, which leads to activation and subsequent phosphorylation of other downstream signalling components (Liang and Zhou, 2018). In *Arabidopsis*, BOTRYTIS-INDUCED KINASE1 (BIK1) and AVRPPHB SUSCEPTIBLE 1-LIKE (PBLs) from RLCK-VII are the most well-characterised RLCKs that are involved in immunity. FLS2-BAK1 complex directly associates with BIK1 and BAK1 phosphorylates BIK1 at Y243 and Y250, which are required to mediate downstream immune responses (Lin et al., 2014; Lu et al., 2010). BIK1 and PBL1 are required for flg22-induced responses such as calcium influx, ROS burst, callose deposition, stomatal closure, and seedling growth inhibition, through the phosphorylation of multiple downstream signalling components (Kadota et al., 2014; Li et al., 2014b; Liu et al., 2013b; Lu et al., 2010; Ranf et al., 2014; Zhang et al., 2010a). This will be discussed in the following sections. In addition to BIK1 and PBL1, multiple members of the RLCK-VII family have also been reported to be involved in PTI-signalling, such as PCRK1, PCRK2, PBL27 and RLCK VII-4 subfamily members (Bi et al., 2018; Kong et al., 2016; Sreekanta et al., 2015; Yamada et al., 2016a).

RLCKs are regarded as the central players in the PTI signalling pathway, since they are required for the activation of multiple downstream signalling components (Liang and Zhou, 2018). BIK1 protein level is therefore the rate-limiting step during immune signalling and is tightly regulated. In the pre-activation state, the heterotrimeric G protein EXTRA-LARGE GUANINE NUCLEOTIDE-BINDING PROTEIN 2 (XLG2) directly interacts with BIK1, and together with ARABIDOPSIS G-PROTEIN BETA SUBUNIT1 (AGB1) and ARABIDOPSIS G-PROTEIN GAMMA-SUBUNIT1/2 (AGG1/2), XLG2 attenuates proteasome-mediated degradation of BIK1 (Liang et al., 2016). While the accumulation of BIK1 is negatively regulated by the phosphatase PP2C38, E3 ubiquitin ligases PLANT U-BOX 25/26 (PUB25/26) and CALCIUM-DEPENDENT PROTEIN KINASE 28 (CPK28) through phosphorylation and protein turnover (Couto et al., 2016; Monaghan et al., 2014; Wang et al., 2018). Following activation, PP2C38 is phosphorylated by MAPKKKK4 and dissociates from BIK1 to prevent dephosphorylation (Jiang et al., 2019). In addition, the *Arabidopsis* E3 ubiquitin ligases RING-H2 FINGER A3A/B (RHA3A/B) mono-ubiquitinates BIK1, which releases it from the PRR complex and activates immune signalling (Ma et al., 2020a). These components function together to fine-tune the amplitude of BIK1 activation to prevent over-/ under-activation of downstream immune responses.

### **PTI downstream responses**

Activation of RLCKs results in a range of cellular changes such as calcium influx, ROS production, MAPK phosphorylation and transcriptional reprogramming, which are induced by multiple PAMPs/PRRs (Böhm et al., 2014b; Couto and Zipfel, 2016; Liang and Zhou, 2018; Zipfel, 2014). These together lead to physiological changes that restrict pathogen infection locally and systemically through the accumulation of phytohormone salicylic acid (SA) and ethylene (Ding and Ding, 2020; Guan et al., 2015; Ryals et al., 1996). In the next few sections, I will focus on the substrates targeted by RLCKs, particularly BIK1, which leads to these physiological changes.

### **Activation of calcium channels and calcium influxes**

Until recently, the detailed mechanism of how calcium influxes are induced during PTI has been largely unknown. Three calcium channels have recently been reported to be phosphorylated by BIK1 during PTI. These include two cyclic nucleotide-gated channels (CNGC), CNGC2, CNGC4, and OSCA1.3 (Thor et al., 2020; Tian et al., 2019). CNGC2 together with CNGC4, which were previously identified as DEFENCE, NO DEATH 1 and 2 (DND1/2), form a calcium channel and are phosphorylated by BIK1 upon PAMP perception (Ali et al., 2007; Clough et al., 2000; Jurkowski et al., 2004; Yu et al., 1998). Activation of CNGC2 and CNGC4 leads to increased  $\text{Ca}^{2+}$  concentration in the cytosol (Tian et al., 2019). Similarly, BIK1 directly associates with and phosphorylates the  $\text{Ca}^{2+}$ -permeable channel OSCA1.3 upon PAMP perception. The activation of OSCA1.3 is required for stomatal closure during immune signalling (Thor et al., 2020). Two additional CNGCs, CNGC19 and CNGC20, have also been reported to form  $\text{Ca}^{2+}$ -permeable complexes that might be implicated in plant immunity and cell death control (Yu et al., 2019). However, CNGC19 and CNGC20 are directly phosphorylated by BAK1 instead of BIK1. Additional calcium channels might be involved in calcium influxes during PTI and are remained to be identified.

The induction of  $\text{Ca}^{2+}$  influxes lead to activation of multiple downstream signalling components.  $\text{Ca}^{2+}$ -dependent protein kinases (CDPK/CPK) are activated by increased cytosolic  $\text{Ca}^{2+}$  concentration. Kinase activities of CPK4, CPK5, CPK6 and CPK11 increase in the presence  $\text{Ca}^{2+}$ , these then phosphorylate downstream signalling components such as the WRKY transcription factors WRKY8, WRKY28 and WRKY48 (Boudsocq et al., 2010; Gao et al., 2013). CPK4, CPK5, CPK6 and CPK11 have also been shown to be positive regulators of reactive oxygen species (ROS) during PTI (Dubiella et al., 2013; Gao et al., 2013; Kadota et al., 2014, 2015; Li et al., 2014b). In addition, the activation of the

calmodulin-binding transcription factor CBP60g, which regulates defence gene expression, is dependent on  $\text{Ca}^{2+}$  through calmodulin-binding activity (Cheval et al., 2013; Wang et al., 2009; Zhang et al., 2010b). As mentioned, proteolytic activity of metacaspases is also dependent on  $\text{Ca}^{2+}$ , activation of metacaspases leads to PROPEP cleavage and release of DAMPs to potentiate PTI activation (Dressano et al., 2020; Hander et al., 2019). Thus,  $\text{Ca}^{2+}$  influx activates multiple signalling components that mediate downstream immune responses during PTI.

### **Activation of NADPH oxidases and ROS production**

The NADPH oxidases RESPIRATORY BURST NADPH OXIDASE HOMOLOG D (RbohD) and RESPIRATORY BURST NADPH OXIDASE HOMOLOG F (RbohF) are both required for reactive oxygen species (ROS) production during pathogen infection (Torres et al., 2002). The activation of RbohD during immunity is tightly regulated, while the regulation of RbohF is not well-studied. As mentioned, multiple *Arabidopsis* CPKs are involved in the regulation of ROS production during PTI (Dubiella et al., 2013; Gao et al., 2013; Kadota et al., 2014, 2015; Li et al., 2014b). CPK4/5/6/11 can directly phosphorylate S163 and S347 in RbohD (Kadota et al., 2014). CPK2/4/11 can also phosphorylate RbohD in S148 (Gao et al., 2013). In addition, BIK1 directly associates and phosphorylates RbohD in S39, S339, S343 and S347 upon PTI (Kadota et al., 2014; Li et al., 2014b). Phosphorylation of RbohD by BIK1 is independent of CPK5/6/11 (Kadota et al., 2014). However, BIK1-dependent phosphorylation is required but not sufficient for RbohD activation, as RbohD phospho-mimic mutants (in the BIK1-mediated phosphorylation sites) do not produce ROS in the absence of PAMPs (Kadota et al., 2014). Thus, the activation of RbohD requires both  $\text{Ca}^{2+}$ -dependent and  $\text{Ca}^{2+}$ -independent regulations, likely through multiple post-translational modifications by different regulators (Kadota et al., 2015; Kimura et al., 2012; Ogasawara et al., 2008).

Production of ROS has multiple consequences during plant immunity. ROS such as superoxide and hydrogen peroxide ( $\text{H}_2\text{O}_2$ ) are antimicrobial (Lambeth, 2004). In addition, ROS production triggers stomatal closure, which restricts pathogen entry (Macho et al., 2012).  $\text{H}_2\text{O}_2$  also promotes peroxidase-mediated proteins and phenolics cross-linking in callose appositions, which restrict fungal and oomycete infections (Bradley et al., 1992; Luna et al., 2011; Voigt, 2014). ROS can also trigger  $\text{Ca}^{2+}$  influx and ROS production in neighbouring cells (Dubiella et al., 2013; Fichman et al., 2019, 2020; Gilroy et al., 2014; Miller et al., 2009; Toyota et al., 2018). As mentioned, the LRR-RLK HPCA1 has recently been identified to perceive  $\text{H}_2\text{O}_2$  which triggers  $\text{Ca}^{2+}$  influx (Wu et al., 2020a). Since  $\text{Ca}^{2+}$

is also required for the activation of RbohD, perhaps the positive feedback between ROS and Ca<sup>2+</sup> contributes to rapid propagation of systemic signals to prime distal tissues upon pathogen detection (Gilroy et al., 2014).

### **MAPKs activation**

The MAPK cascade is another hallmark signalling pathway triggered by PTI. The activation of MAPKKK/MEKK activates downstream MAPKK/MKK, which activates downstream MAPK/MPK (Asai et al., 2002; He et al., 2018; Komis et al., 2018; MAPK Group, 2002). During PTI, activated MAPKKK3 and MAPKKK5 phosphorylates MKK4 and MKK5, which then activates MPK3 and MPK6. In parallel, MKK1/MKK2 also phosphorylate MPK4 (Asai et al., 2002; Rasmussen et al., 2012). It is unclear how the PRR complex activates MAPKKK that leads to the activation of downstream MAPKs. Flg22- and elf18-induced MAPK activation is largely, but not completely, abolished in *bak1-5 bkk-1* (BKK1, BAK1-LIKE1/SERK4) double mutant (Roux et al., 2011). This indicates that other RK coreceptors are involved in the activation of MEKKs. In addition, BIK1 and PBL1 are not required for the activation of MAPKs during flg22-/elf18-/pep2-/chitin-induced PTI (Feng et al., 2012; Rao et al., 2018). Recently, multiple *Arabidopsis* RLCKs such as PBL27, BSK1 and family members of RLCK-VII-4 (PBL19, PBL20, PBL39 and PBL40) have been proposed to activate MAPKs (Bi et al., 2018; Rao et al., 2018; Yamada et al., 2016a; Yan et al., 2018). The detailed signalling pathway by which PRR complex activates downstream MAPKs remains to be determined.

Activation of MKK4/MKK5 and MPK3/MPK6 is involved in immunity (Asai et al., 2002; Beckers et al., 2009; Boudsocq et al., 2010; Su et al., 2017, 2018; Xu et al., 2014). Interestingly, these MAPKs are also activated during stomatal formation, flower abscission and both embryo and pollen development (He et al., 2018). It is unclear how specificity in these individual signalling pathways is determined. Multiple immunity-related substrates of MPK3/MPK6 have been identified. These include 1-AMINOCYCLOPROPANE-1-CARBOXYLIC ACID SYNTHASE (ACS) isoforms ACS2 and ACS6, which are involved in ethylene production (Han et al., 2010; Liu and Zhang, 2004); the ETHYLENE-RESPONSIVE FACTOR ERF6 and ERF104, which are required for resistance against *Botrytis cinerea* (Bethke et al., 2009; Meng et al., 2013); the defence-related transcription factor WRKY33 and CYCLIN-DEPENDENT KINASES (CDKC) CDKC1 and CDKC2, which phosphorylate RNA polymerase II to regulate transcription (Li et al., 2014a; Mao et al., 2011). It has been suggested that ROS and MAPKs might be linked, since external application of H<sub>2</sub>O<sub>2</sub> leads to MAPK activation (perhaps due to HPCA1 activation, (Kovtun

et al., 2000)). However, an *rbohD* mutant does not affect flg22-induced MAPKs phosphorylation. Conversely, mutations in MPK3 and/or MPK6 do not affect flg22-induced ROS burst (Xu et al., 2014). This indicates that MPK3/MPK6 activation and NADPH oxidase activation are two independent pathways, which might converge and potentiate each other in downstream signalling (Adachi et al., 2015).

### **Other PTI-induced physiological responses**

Calcium influx, ROS production and MAPK activation together activate multiple downstream signalling components. These lead to transcription reprogramming, phytohormone biosynthesis and production of antimicrobial compounds (Bigeard et al., 2015; Macho and Zipfel, 2014), which restrict pathogen proliferation locally and systemically. Here I will summarise the reported physiological responses triggered by PTI that restrict pathogen infection.

During infection, pathogens target plant sugar transporters to induce sugar efflux for nutrients (Chen et al., 2010; Cohn et al., 2014). Plants counteract this by inducing sterol synthesis and membrane permeability to prevent nutrient efflux (Wang et al., 2012), or by direct regulation of sugar transporters upon PAMP perception. The SUGAR TRANSPORTER 13 (STP13) directly associates with and is phosphorylated by BAK1 after flg22 perception, which leads to enhanced sugar influx to restrict nutrients to pathogens (Yamada et al., 2016b). In addition to sugar, plants also restrict availability of other nutrients to pathogens during infection. *Arabidopsis* immune responses also suppress *Pseudomonas* iron acquisition, which affects bacterial proliferation (Nobori et al., 2018). In addition, the rice PHOSPHATE TRANSPORTER PROTEIN OsPT8 expression is suppressed upon PAMP perception, and the overexpression of OsPT8 leads to enhanced susceptibility against *Magnaporthe oryzae* and *Xanthomonas oryzae pv. oryzae* (Dong et al., 2019). These indicate that PTI might also affect phosphate uptake to restrict pathogen infection (Campos-Soriano et al., 2020).

Pathogens induce virulence through the secretion of effectors (effector triggered susceptibility; ETS). PAMP-pretreatment in both *Nicotiana tabacum* and *Arabidopsis thaliana* inhibits effector secretion through the Type 3 Secretion System (T3SS) in *Pseudomonas syringae* (Crabill et al., 2010). Genes encoding the T3SS are induced during the early stages of *Pseudomonas* infection, likely due to the perception of signals from plant hosts. These water-soluble plant signals are reduced in the *Arabidopsis* MAPK PHOSPHATASE 1 (*mkp1*) mutant, which leads to impaired T3SS expression and effector secretion (Anderson et al., 2014). A recent report suggests that an *Arabidopsis* secondary

metabolite, sulforaphane (SFN), directly inhibits T3SS gene expression via cysteine modification (C209) of the *Pseudomonas syringae* transcription factor HrpS (Wang et al., 2020a). Thus, plants deploy multiple mechanisms to suppress T3SS expression and effector secretion in bacteria (Nobori et al., 2018).

Callose deposition is another PTI hallmark which restricts pathogen invasion. This high-molecular weight  $\beta$ -(1,3)-glucan polymer is deposited on the cell wall in response to stimuli such as PAMPs or damage (Luna et al., 2011; Voigt, 2014; Voigt and Somerville, 2009). Callose synthases are required in the accumulation of callose during pathogen infection, such as POWDERY MILDEW RESISTANT 4 (PMR4) (Nishimura et al., 2003). In *Arabidopsis*, there are 12 glucan synthase-like (GSL) genes, which are proposed to form complexes for callose synthesis (Verma and Hong, 2001). The mechanism by which these enzymes are activated is largely unknown. Activation through post-translational modifications of callose synthases triggered by  $\text{Ca}^{2+}$  influx have been proposed (Kauss, 1986). Transcriptional regulation of these enzymes contributes to callose deposition as well, since SA induces transcript accumulation of *Arabidopsis* GLS5 (Jacobs et al., 2003; Ostergaard et al., 2002). As mentioned, ROS can be used by peroxidases to promote protein and phenolic cross-linking, which also facilitates callose deposition (Brown et al., 1998; Luna et al., 2011; Thordal-Christensen et al., 1997). The detailed signalling pathway by which activated PRR complex leads to callose synthesis and deposition remains to be determined.

There are likely other PTI-induced physiological responses which suppress pathogen invasion. Future research will reveal additional mechanisms and physiological changes triggered by PTI.

### **Negative regulation of PTI signalling pathway**

Excessive activation of PTI signalling pathway leads to autoimmunity and growth inhibition. Seedlings that are grown on medium containing flg22, elf18 or pep1 exhibits root growth inhibition (Bethke et al., 2009; Denoux et al., 2008; Poncini et al., 2017), due to the inhibition of the auxin and brassinosteroid pathways (Albrecht et al., 2012; Huot et al., 2014; Jiménez-Góngora et al., 2015; Malinovsky et al., 2014; Navarro et al., 2006). Thus, PTI signalling pathway is tightly regulated to ensure transient activation. Here I will focus on multiple mechanisms that are utilised by plants to achieve this.

LRR-RK BAK1-INTERACTING RECEPTOR-LIKE KINASE (BIR) family contains four RKs: BIR1, BIR2, BIR3 and BIR4 (Gao et al., 2009). These RKs associate with and sequester BAK1 to prevent auto-activation (Gao et al., 2009; Hohmann et al., 2018; Ma et

al., 2017). *bir1* mutants show constitutive activation of BAK1, which leads to enhanced cell death and constitutive defence activation (Gao et al., 2009). Ligand-bound PRRs (such as flg22-bound FLS2) can displace BIRs and form a receptor complex for PTI-signalling (Ma et al., 2017). Whether BIRs play a role in the negative regulation of PTI post-activation remains to be determined. Other PRRs, such as the LRR-RKs APEX and NUCLEAR SHUTTLE PROTEIN (NSP)-INTERACTING KINASE 1 (NIK1), also negatively regulate the association between FLS2 and BAK1 (Li et al., 2019; Smakowska-Luzan et al., 2018).

Following PAMP perception, the subtilase S1P (or SUBTILISIN-LIKE PROTEASE SBT6.1) cleaves endogenous PRO-RAPID ALKALINIZATION FACTOR 23 (PRO-RALF23) into RALF23 (Stegmann et al., 2017). RALF23 is perceived by a PRR complex that is comprised of the *Catharanthus roseus* RLK1-like (CrRLK1L) protein kinase subfamily member FERONIA (FER) and the LORELEI-LIKE-GPI ANCHORED PROTEIN 1 (LLG1). The perception of RALF23 by FER negatively regulates the formation of the FLS2-BAK1 complex (Stegmann et al., 2017; Xiao et al., 2019). Recently, it has been shown that kinase activity of FER is not required for its regulation in immune signalling, and FER regulates plasma membrane nanodomain organization to modulate plant immune signalling (Gronnier et al., 2020). Localisation of RKs within nanodomains constrains their interactions and is important for RK function regulation (Burkart and Stahl, 2017; Gronnier et al., 2018).

Phosphorylation of PRR complexes and downstream kinases activates PTI-signalling. This is negatively regulated by protein phosphatases. In rice, the XA21-BINDING PROTEIN 15 (XB15, PROTEIN PHOSPHATASES TYPE 2C (PP2C)) dephosphorylates and negatively regulates XA21 (Park et al., 2008). Similarly, *Arabidopsis* POLTERGEIST-LIKE 4 (PLL4) and PLL5 (orthologues of XB15) associates with EFR and negatively regulate elf18-induced responses (Holton et al., 2015). In addition, the PROTEIN PHOSPHATASE 2A (PP2A) negatively regulates BAK1 phosphorylation status (Segonzac et al., 2014). As mentioned, the phosphatase PP2C38 also controls BIK1 phosphorylation and turnover (Couto et al., 2016). The PP2Cs AP2C1 and PP2C5 also negatively regulate the phosphorylation of MPK3 and MPK6 (Brock et al., 2010). Taken together, multiple protein phosphatases are involved in the negative regulation of kinase phosphorylation status during PTI.

Upon flg22 perception, activated BAK1 phosphorylates U-BOX DOMAIN-CONTAINING PROTEIN 12 and 13 (PUB12 and PUB13). Phosphorylated PUB12 and PUB13 mediate polyubiquitination of FLS2, which leads to endocytosis of FLS2 and its

degradation (Lu et al., 2011). PUB12 and PUB13 have also been shown to mediate the degradation of LYK5 and BIR1 (Liao et al., 2017; Martins et al., 2015). In addition, PUB22, PUB23 and PUB24 have also been implicated as negative regulators of PTI signalling, but the ubiquitination target of these genes are currently unknown (Trujillo et al., 2008). Other than PRRs, the turnover of the central immune regulator BIK1 is also tightly regulated, as discussed in the previous chapter. Recently, PUB4 has been reported to promote BIK1 degradation before PAMP perception (Derkacheva et al., 2020). Thus, multiple PTI signalling components are regulated by protein turnover to prevent constitutive activation.

To summarise, multiple mechanisms are involved in the negative regulation of PTI signalling activation. These include regulation of PRR complex formation, localisation, kinase phosphorylation status and turnover of signalling components. Additional mechanisms, such as transcriptional reprogramming and phytohormones, can also negatively regulate PTI signalling pathway (Couto and Zipfel, 2016). How these mechanisms integrate to control the duration and amplitude of PTI responses remains to be determined.

### **An overview of PTI**

PTI serves as the first line of immunity against pathogens. Plant PRRs perceive a range of PAMPs/DAMPs that can be peptides, polysaccharides, peptidoglycans, fatty acids, and compounds such as quinones and hydrogen peroxide. Perception of PAMPs/DAMPs leads to, although not always necessary, complex formation between ligand-binding PRRs and coreceptors. A series of phosphorylation events leads to activation of RLCKs, which then phosphorylate downstream signalling components to mediate physiological responses (Figure 1.1). A range of cellular and physiological changes lead to PTI that restricts pathogen proliferation. Trade-off between growth and immunity means that PTI activation must be negatively regulated. Multiple mechanisms are involved to prevent prolonged or hyper-activation of PTI. Pathogens also deploy effectors to suppress PTI, which will be discussed in the next section.

### **Effector-triggered susceptibility (ETS)**

Multiple effectors have been shown to target the PRR signalling pathway, which highlights the importance of PTI during immunity. Here, I will summarise the reported effectors that target PTI. Unless specified otherwise, the effectors mentioned from this section are from various *Pseudomonas syringae* strains.

AvrPto targets the FLS2-BAK1 complex and inhibit their kinase activities (Meng and Zhang, 2013; Shan et al., 2008; Xiang et al., 2008; Xing et al., 2007). Similarly, a conserved fungal effector NIS1 also targets receptor kinases complex to suppress PTI (Irieda et al., 2019). On the other hand, AvrPtoB has E3 ligase activity that leads to the degradation of multiple PRRs (Göhre et al., 2008; Lu et al., 2011). The effector HopB1 cleaves BAK1 to suppress PTI signalling activation (Li et al., 2016b). A tyrosine phosphatase, HopAO1, directly dephosphorylates EFR to prevent its activation (Macho et al., 2014). RLCKs, as central immune regulators, are also targeted by multiple effectors. AvrAC from *Xanthomonas campestris* uridylylates BIK1 and PBL2 (Feng et al., 2012; Wang et al., 2015). HopZ1a acetylates RLCKs and AvrPphB is a cysteine protease that degrades pseudo-RLCKs such as BIK1, PBS1 and PBL1 (Bastedo et al., 2019; Zhang et al., 2010a). Downstream PTI signalling components are also targeted by effectors. The ADP-ribosyltransferase HopF2 has been shown to target both BAK1 and MKK5 to suppress PTI signalling (Wang et al., 2010; Zhou et al., 2014). HopAI1 inactivates MPK3, MPK4 and MPK6 by its phosphothreonine lyase activity (Zhang et al., 2007). AvrRpt2 has also been shown to suppress MPK4/11 activation during PTI (Eschen-Lippold et al., 2016). Interestingly, there are many parallels between the suppression of PTI by host mechanisms and by pathogenic effectors (Figure 1.2).

Pathogen effectors also target other cellular processes to facilitate invasion. As mentioned, pathogens target host sugar transporters to sequester nutrients (Chen et al., 2010; Cohn et al., 2014). HopM1, a conserved effector found in most *P. syringae* strains, induces the establishment of an aqueous apoplast via targeting *Arabidopsis* HOPM INTERACTOR 7 (MIN7) (Xin et al., 2016). Effectors also target phytohormone signalling to suppress immunity (DebRoy et al., 2004). AvrPtoB has been shown to target NPR1 to disrupt SA signalling (Chen et al., 2017). HopZ1a targets JAZ transcriptional repressors and activates jasmonate signalling, which antagonises SA signalling (Jiang et al., 2013). Small RNAs are important mediators of both antiviral and antifungal immunity (Cai et al., 2018; Hamilton and Baulcombe, 1999; Ratcliff et al., 1997; Rybak and Robatzek, 2019). Multiple *Phytophthora* effectors have been shown to target gene silencing to promote infection (Hou et al., 2019; Qiao et al., 2013, 2015; Xiong et al., 2014). In conclusion, effectors promote virulence via targeting PTI and other cellular processes during infection.

### **Effector-triggered immunity (ETI): an overview**

Effector-triggered immunity (or ETI) is an immune response triggered by the detection of effectors through intracellular NUCLEOTIDE-BINDING, LEUCINE-RICH REPEAT

(NLR) immune receptor proteins. ETI has also been referred to as intracellular-triggered immunity (InTI), intracellular receptor-mediated immunity (IRMI) or NMI as it is triggered intracellularly (Ding et al., 2020; van der Burgh and Joosten, 2019). As mentioned, pathogens deliver multiple effectors to suppress PTI and other cellular processes to facilitate infection. NLRs detect effectors through either direct binding or guarding authentic targets or decoys. There are three main classes of NLRs: the helical COILED-COIL (CC) NLRs (CC-NLRs/CNLs), TOLL/INTERLEUKIN-1RECEPTOR/RESISTANCE (TIR) NLRs (TIR-NLRs/TNLs) and RPW8-LIKE COILED-COIL DOMAIN (RPW8) NLRs (RPW8-NLRs/RNLs) (Jones et al., 2016). CC-NLRs and TIR-NLRs act as receptor-NLRs and recognise effectors, while RPW8-NLRs act as helper-NLRs to transduce downstream signals (Feehan et al., 2020). Recognition of effectors by both CC- and TIR-NLRs leads to oligomerisation and formation of the ‘resistosome’ (Martin et al., 2020; Wang et al., 2019a, 2019b). CC-NLR resistosomes are proposed to form ion channels, while TIR-NLR resistosomes are proposed to act as NAD<sup>+</sup>-cleaving enzymes to promote cell death (Horsefield et al., 2019; Wan et al., 2019; Wang et al., 2019a). Multiple RPW8-NLRs then mediate downstream signalling activation in coordination with EP-domain containing proteins (EP-proteins) such as ENHANCED DISEASE SUSCEPTIBILITY 1 (EDS1), PHYTOALEXIN DEFICIENT 4 (PAD4) and SENESCENCE-ASSOCIATED GENE 101 (SAG101) (Castel et al., 2019; Gantner et al., 2019; Lapin et al., 2019, 2020; Wu et al., 2019). Activation of these signalling components leads to defence-gene induction, salicylic acid biosynthesis and hypersensitive cell death response (HR) (Jones and Dangl, 2006). Other physiological responses, such as calcium influx, ROS accumulation and MAPK activation are also strongly activated when ETI is triggered together with PTI (Grant and Loake, 2000; Grant et al., 2000; Jones and Dangl, 2006; Sohn et al., 2014; Su et al., 2018; Tao et al., 2003; Thilmony et al., 2006; Tsuda et al., 2013). These together further restrict pathogen infection. I will now provide an overview of current knowledge of the ETI signalling pathway that leads to resistance.

### **NLR proteins involved in effector recognition**

NLRs recognise effectors either by direct binding or guarding proteins (either guardee or decoy proteins) that are targeted by effectors (Van der Biezen and Jones, 1998; Dangl and Jones, 2001). For example, the TIR-NLR RESISTANCE TO PERONOSPORA PARASITICA 1 (RPP1, TIR-NLR) recognises the *Hyaloperonospora arabidopsidis* (*Hpa*) effector ATR1 through direct binding (Krasileva et al., 2010; Rehmany et al., 2005). RESISTANCE TO PERONOSPORA PARASITICA 4 (RPP4, TIR-NLR) also associates with the *Hpa* effector ATR4 (or AvrRpp4/ HaRxL103) in the nucleus to confer resistance

(Asai et al., 2018). Examples of indirect recognition include *Arabidopsis* RESISTANCE TO *P. SYRINGAE* PV *MACULICOLA* 1 (RPM1, CC-NLR) and RESISTANT TO *P. SYRINGAE* 2 (RPS2, CC-NLR). RPM1-INTERACTING PROTEIN 4 (RIN4) is guarded by both RPM1, RPS2 and TAO1. *Pseudomonas* effectors AvrRpm1 and AvrB lead to the phosphorylation of RIN4 by RPM1-INDUCED PROTEIN KINASE (RIPK), which leads to RPM1 activation. AvrRpt2 is a cysteine protease which cleaves RIN4, this leads to RPS2 activation (Axtell and Staskawicz, 2003; Axtell et al., 2003; Bent et al., 1994; Jones and Dangl, 2006; Liu et al., 2011; Mackey et al., 2002, 2003; McNellis et al., 1998). Another example is *Pseudomonas* AvrPphB, which is also a cysteine protease that degrades RLCKs such as BIK1, PBS1 and PBL1. PBS1 is guarded by *Arabidopsis* RESISTANT TO *P. SYRINGAE* 5 (RPS5, CC-NLR) (DeYoung et al., 2012; Qi et al., 2014; Shao et al., 2003; Zhang et al., 2010a). AvrAC and HopZ1a are pathogen effectors that target the RLCKs PBL2 and ZED1 respectively. Both effectors are recognized by the *Arabidopsis* HOPZ-ACTIVATED RESISTANCE 1 (ZAR1, CC-NLR) as it guards both PBL2 and ZED1. Recently, ZAR1 has been shown to confer recognition to multiple *Pseudomonas* effector families, such as HopX, HopO and HopBA (Laflamme et al., 2020). Thus, RLCKs are guarded by multiple NLRs.

NLR proteins can also work in pairs to confer effector recognition. These NLR pairs sometimes appear in a head-to-head orientation next to each other in the genome (Narusaka et al., 2009). The *Arabidopsis* (Ws-2 accession) paired NLR RESISTANCE TO *RALSTONIA SOLANACEARUM* 1 (RRS1-R, TIR-NLR) and RESISTANT TO *P. SYRINGAE* 4 (RPS4, TIR-NLR) confer recognition of AvrRps4 from *Pseudomonas*, PopP2 from *Ralstonia* and an unknown effector(s) from *Colletotrichum higginsianum* (Narusaka et al., 2009). The WRKY domain on RRS1-R acts as a decoy and interacts with both AvrRps4 and PopP2, which triggers the activation of RPS4 and thus ETI (Sarris et al., 2015). RRS1/RPS4 paralog RRS1B/RPS4B only recognises AvrRps4 (Saucet et al., 2015). On the other hand, RRS1 (RRS1-S)/RPS4 from the *Arabidopsis* Col-0 accession only recognises AvrRps4, but not PopP2. This is due to the requirement of PopP2 recognition by C-terminus phosphorylation in RRS1-R, but not in RRS1-S (Guo et al., 2020; Ma et al., 2018). Other examples of paired NLRs include the rice Pik-1/Pik-2 (CC-NLRs), which recognise AVR-Pik from *Magnaporthe oryzae* (Zhai et al., 2011). RGA4/RGA5 (CC-NLRs) in rice also recognise AVR1-CO39 and AVR-Pia from *Magnaporthe oryzae* (Cesari et al., 2013; Césari et al., 2014; Okuyama et al., 2011). *Arabidopsis* RESISTANCE TO *PERONOSPORA PARASITICA* 2A and 2B (RPP2A and RRP2, TIR-NLRs) appear in

head-to-tail orientation in the genome and are both required for resistance against the *Hpa Cala2* strain (Sinapidou et al., 2004).

### **Structure and activation of NLR proteins**

As mentioned, NLRs are classified into three classes according to their N-terminal domain: CC domain-containing NLRs (CC-NLRs), TIR domain-containing NLRs (TIR-NLRs) and RPW8-NLRs (RPW8-NLRs). Plant NLRs also have NB-ARC (NUCLEOTIDE BINDING AND ARC MOTIFS) domain in the middle and the LRR (LEUCINE RICH REPEAT) domain at the C-terminus. These domains are variable between NLRs and additional non-canonical domains can be integrated into NLRs (also known as NLR-integrated domains or NLR-ID). NLR-IDs allow plants to recognise a range of effectors from different pathogens (Baggs et al., 2017; El Kasmi and Nishimura, 2016; Maekawa et al., 2011, 2012). The function of different domains in each NLR varies. The LRR domain consists of a number of LxxLxL motif repeats and is involved in direct or indirect recognition of effectors (Dodds et al., 2006; Krasileva et al., 2010). The NB-ARC has weak ATPase activity and was proposed to act as a switch for NLR activation (Takken and Tameling, 2009; Takken et al., 2006). The CC-domain is involved in effector recognition and can interact directly with effectors as well as guarder proteins (Cai et al., 2011). Recently, the CC-domain has been suggested to oligomerise to form ion channels that lead to cell death (Adachi et al., 2019; Wang et al., 2019a). TIR-domains can also self-associate or associate with TIRs from other NLRs, which is crucial for the activation of multiple TNLs, such as RPS4, N and L6 (Caplan et al., 2008; Duxbury et al., 2020; Williams et al., 2014; Zhang et al., 2017). TIR-domains also exhibit NADase activity which leads to the production of variant-cyclic-ADP-ribose (vcADPR) (Horsefield et al., 2019; Wan et al., 2019). NLR-IDs can function as decoys of effector targets, such as the WRKY domain in RRS1 and the HMA domain in RGA5 (Cesari et al., 2013; Sarris et al., 2015).

Upon effector perception, NLRs are activated and this leads to ETI signalling. The molecular switch model suggests that effector perception allows NLRs to switch from an 'off' to an 'on' state (Takken and Tameling, 2009). It has also been suggested that effector recognition pushes the equilibrium of the NLR to the 'active' ATP-bound confirmation (Bernoux et al., 2016). In animals, activated NLRs such as NLRC4 oligomerise to form inflammasomes to activate defence (Halff et al., 2012). A cryo-EM structure of the CC-NLR ZAR1 has been published (Wang et al., 2019a, 2019b). In the resting state, ZAR1 forms a complex with the RLCK RKS1. *Xanthomonas* effector AvrAC uridylylates PBL2, which then binds to RKS1. Inactive ZAR1 together with RKS1 and the uridylylated PBL2

undergo conformational changes that expel ADP from the NB-ARC domain, which allows the binding of dATP (Wang et al., 2019b). The binding of dATP activates ZAR1 and allows it to oligomerise into a pentangular ‘resistosome’. Activated ZAR1 resistosomes associate with the plasma membrane (PM) (Wang et al., 2019a). PM-associated resistosomes are suggested to form pores that might act as ion channels, which subsequently activate downstream immune responses (Dangl and Jones, 2019; Wang et al., 2019a, 2019b). Recently, the structure of *Nicotiana benthamiana* TIR-NLR Roq1 has also been solved (Martin et al., 2020). *Xanthomonas euvesicatoria* effector XopQ directly binds to the LRR and Post-LRR (PL) domain of Roq1. Binding of XopQ leads to the release of the NB-ARC domain from the LRR domain. Roq1 then undergoes a conformational change into the ATP-bound state, which allows it to oligomerise into a tetrameric resistosome. The formation of this resistosome allows binding and induces proximity of the TIR domains, which exposes the NADase active site (Martin et al., 2020). This might lead to enhanced NADase activity which triggers downstream immune responses (Duxbury et al., 2020; Horsefield et al., 2019; Wan et al., 2019). Together, these structures suggest that both CC- and TIR-NLRs form oligomeric resistosomes. Oligomerisation enables different classes of NLRs to trigger immune responses through different signalling mechanisms, such as ion influxes and production of *vc*-ADPR.

### **ETI signalling components: helper NLRs**

The TNL N confers resistance to tobacco mosaic virus (TMV) (Whitham et al., 1996). *Nicotiana benthamiana* N REQUIREMENT GENE 1 (NRG1), a RPW8-NLR, was identified as a helper NLR required for N-mediated resistance (Peart et al., 2005). Three other *Arabidopsis* RPW8-NLRs, ACTIVATED DISEASE RESISTANCE 1 (ADR1), ADR1-LIKE 1 (ADR1-L1) and ADR1-L2 (collectively known as ADR1s), were later shown to be required for RPS2-mediated HR and resistance. *Arabidopsis* NRG1A and NRG1B are also required for immune responses mediated by multiple NLRs including RRS1/RPS4, RPP1, RPP2, RPP4, WHITE RUST RESISTANCE 4 (WRR4A), CHILLING SENSITIVE 3 (CHS3)/ CONSTITUTIVE SHADE-AVOIDANCE1 (CSA1), SUPPRESSOR OF NPR1-1, CONSTITUTIVE 1 (SNC1) and CHS1/SOC3 (Castel et al., 2019; Wu et al., 2019). NLR REQUIRED FOR CELL DEATH 2 (NRC2), NRC3 and NRC4 have also been previously identified as helper NLRs for multiple sensor NLRs in *Nicotiana benthamiana* (Wu et al., 2017). Helper NLRs are suggested to form ‘networks’ with upstream sensor NLRs to mediate downstream signalling upon effector perception (Wu et al., 2018).

Different sensor NLRs require different helper NLRs to mediate downstream signalling. For example, RPS2-mediated bacterial resistance and HR requires ADR1s, but not NRG1A/B. On the other hand, RRS1/RPS4-mediated HR requires NRG1A/B but not ADR1s, while RRS1/RPS4-mediated bacterial resistance requires ADR1s but not NRG1A/B. In addition, NLRs like RPM1 and ZAR1 do not require ADR1s or NRG1A/B to mediate bacterial resistance or HR. (Bonardi et al., 2011; Castel et al., 2019; Saile et al., 2020; Wu et al., 2019). Thus, there is unequal redundancy between the NRG1s and ADR1s when mediating immune responses from sensor NLRs. The current view is that NRG1 mainly contributes to HR triggered by TIR-NLRs, and ADR1 mainly contributes to defence-gene regulation that leads to SA accumulation (Feehan et al., 2020). It is unclear how sensor NLRs can activate helper NLRs. Perhaps sensor NLRs directly associate with and activate helper NLRs, or other signalling components such as vc-ADPRs or Ca<sup>2+</sup> influx can indirectly trigger helper NLRs. Emerging data have suggested that NRG1s function in association with the EP proteins such as SAG101, PAD4 and EDS1 to mediate downstream signalling activation (Gantner et al., 2019; Lapin et al., 2019; Qi et al., 2018). This will be further discussed in the next section. In addition, the RPW8-like domain in RPW8-NLRs is highly similar to the HeLo domain in the human mixed-lineage kinases (MLKLs) and the fungal HeLo/HeLo-Like (HELL) domain. It has therefore been proposed that RPW8-like domains might function similarly to the HeLo domains of MLKLs, which trigger cell death by forming pores on the membrane (Barragan et al., 2019; Daskalov et al., 2016; Feehan et al., 2020; Jubic et al., 2019; Li et al., 2020a). Recently, it has been reported that the *Arabidopsis* MLKLs (AtMLKLs) are involved in TIR-NLR-mediated resistance (Mahdi et al., 2020). Whether RPW8-NLRs function like CC-NLRs to form oligomers and membrane ion channels remains to be tested.

### **ETI signalling components: EP proteins and NDR1**

EDS1 is a lipase-like protein which is required for TIR-NLRs to mediate HR and resistance (Parker et al., 1996). While most CC-NLRs do not require EDS1, it was shown that RPS2-mediated resistance requires either EDS1 or salicylic acid biosynthesis (*eds1-2 sid2-1* double mutant loses RPS2 function) (Cui et al., 2017). EDS1 interacts with the two other lipase-like EP proteins PAD4 and SAG101 to induce HR and resistance (Feys et al., 2005; Wagner et al., 2013). How TIR-NLR activates EDS1 and other EP proteins is unclear. It has been proposed that vc-ADPR produced by TIR domains can trigger the activation of EDS1 (Horsefield et al., 2019; Wan et al., 2019). The mechanism by which EP proteins function is also unclear. It has been proposed that RPW8-NLRs function in cohort with the EP proteins to mediate downstream responses (Feehan et al., 2020; Lapin et al., 2019). In

*Arabidopsis*, NRG1s and SAG101 are required for TIR-NLR-induced HR but not bacterial resistance, while ADR1s and PAD4 are required for TIR-NLR-induced SA biosynthesis and resistance, but not HR (Lapin et al., 2019, 2020). In addition, the ‘*helperless*’ mutant that lacks both ADR1s and NRG1s phenocopies *eds1* and *pad4/sag101* (Saile et al., 2020; Wu et al., 2019). The detailed mechanisms of how these modules function with each other to mediate specific downstream responses remain to be determined.

NON-RACE-SPECIFIC DISEASE RESISTANCE1 (NDR1) is a plasma membrane-localised protein required for resistance mediated by RPM1, RPS2 and RPS5 (Century et al., 1997). NDR1 has been shown to interact with RIN4 (Day et al., 2006). Since NDR1 exhibits structural homology with mammalian integrins, it has been proposed to function as an integrin-like protein to mediate plasma membrane or cell wall adhesions, which allows CC-NLRs to function properly (Knepper et al., 2011). Interestingly, flg22-induced responses are also slightly impaired in the *ndr1* mutant, suggesting that NDR1 might play a role in both NLR- and PRR-mediated responses (Knepper et al., 2011).

To summarise, NLRs require different downstream signalling components to mediate downstream responses. While CC-NLRs, such as RPS2 requires NDR1, ADR1 and potentially EDS1 to mediate downstream responses, ZAR1 does not seem to require any downstream signalling components. TIR-NLRs in general require helper NLRs and EP proteins to mediate resistance and HR. The biological implications of different downstream signalling components required by NLRs are unknown. Perhaps a complex network would require a cohort of pathogen effectors to be manipulated. In the next section, I will focus on the downstream physiological and cellular changes triggered by ETI.

### **Downstream responses of ETI: Calcium influx, ROS production and MAPK activation**

Perception of PAMPs leads to calcium ( $\text{Ca}^{2+}$ ) influx and ROS production via activation of calcium channels and NADPH oxidases. PRR activation also leads to MAPK activation. *Pseudomonas syringae* delivering AvrRpm1 or AvrB (triggers ‘PTI + ETI<sup>AvRpm1</sup>’) triggers biphasic and prolonged  $\text{Ca}^{2+}$  influx compared to *P. syringae* carrying empty vector (PTI + ETS, which only triggers initial calcium burst) (Grant et al., 2000). Expression of AvrB, AvrRpm1 and AvrRpt2 in protoplasts also leads to CPK phosphorylation, indicating that  $\text{Ca}^{2+}$  influx is induced during RPM1 and RPS2 activation (Gao et al., 2013). In addition,  $\text{Ca}^{2+}$  channel blockers,  $\text{LaCl}_3$  inhibit RPM1- and RPS2-mediated HR and WKRY46 gene expression (Gao et al., 2013; Grant et al., 2000). Thus  $\text{Ca}^{2+}$  influx is important for ETI-induced resistance and HR. The mechanism by which NLRs lead to  $\text{Ca}^{2+}$  influx is unclear.

CNGC2 and CNGC4, also known as DEFENSE, NO DEATH 1 (DND1) and DND2, are required for RPS2- and RPM1-mediated cell death, but not resistance (Clough et al., 2000; Jurkowski et al., 2004; Yu et al., 1998). Perhaps plasma membrane localised NLRs can activate calcium channels to trigger  $\text{Ca}^{2+}$  influx and HR.

Similar to  $\text{Ca}^{2+}$  influx, activation of ‘PTI + ETI’ induces biphasic and prolonged ROS burst compared to PTI alone (Glazener et al., 1996; Lamb and Dixon, 1997; Orlandi et al., 1992). It is therefore assumed that NLR activation can trigger prolonged ROS accumulation, as the activation of ‘PTI + ETI’ often triggers stronger  $\text{H}_2\text{O}_2$  accumulation than PTI alone (Choi et al., 2007; Hatsugai et al., 2016; Torres et al., 2002). The NADPH oxidases AtRbohD and AtRbohF are both required for RPS2- and RPM1-induced  $\text{H}_2\text{O}_2$  accumulation and HR (Torres et al., 2002). Thus, ‘PTI + ETI’ leads to the activation of AtRbohD and AtRbohF, which leads to  $\text{H}_2\text{O}_2$  accumulation and HR. Recently, it has been reported that RPS2 activation alone ( $\text{ETI}^{\text{AvrRpt2}}$ ) leads to S343 and S347 phosphorylation in RbohD, which in turn triggers ROS accumulation (Kadota et al., 2019). It is unclear how the activated RPS2 triggers RbohD phosphorylation.

MAPK activation during PTI is transient (Bigeard et al., 2015). Activation of PTI together with ETI triggered by AvrRpm1, AvrRpt2, AvrB and AvrRps4 leads to prolonged activation of MAPKs compared to PTI alone (Su et al., 2018). In addition, the activation of  $\text{ETI}^{\text{AvrRpt2}}$  alone can also trigger activation of MAPKs (Tsuda et al., 2013). How activated RPS2 triggers MAPK activation is unclear. It has been reported that prolonged activation of MPK3 and MPK6 during ‘PTI + ETI’ leads to photosynthetic inhibition, which allows the accumulation of chloroplastic ROS and accelerated HR (Su et al., 2018). In conclusion, calcium influx, ROS production and MAPK activation are all enhanced and prolonged during ‘PTI + ETI’ compared to PTI alone. The prolonged activation of these physiological responses leads to stronger defence gene expression and HR, which will be discussed in the next sections.

### **Downstream responses of ETI: Transcriptional regulation**

Both PTI and ETI leads to rapid and robust transcriptional reprogramming, which allows plants to switch from growth and development into defence against pathogens. There is large overlap between PTI- and ETI- transcriptional reprogramming (Jacob et al., 2018; Zhang and Fan, 2020). Thus, PTI and ETI are likely to share transcription factors which lead to defence gene expression. Specific genes that are highly induced during ETI, but not during PTI, were identified by comparing expression profiles between plants activated with ‘PTI+ETI<sup>PopP2</sup>’ and PTI alone (Sohn et al., 2014). Many of these genes are involved in

phytohormone synthesis, such as the SA biosynthesis genes *ISOCHORISMATE SYNTHASE 1* (*ICS1* or *SID2*), *ENHANCED DISEASE SUSCEPTIBILITY 5* (*EDS5*) and *AVRPPHB SUSCEPTIBLE 3* (*PBS3*), genes involved in pipecolic acid biosynthesis (PIP) such as *FLAVIN-CONTAINING MONOOXYGENASE 1* (*FMO1*) and also transcription factors that are involved in SA and PIP biosynthesis such as *SYSTEMIC ACQUIRED RESISTANCE DEFICIENT 1* (*SARD1*) (Ding and Ding, 2020; Hartmann et al., 2018; Nawrath et al., 2002; Rekhter et al., 2019; Torrens-Spence et al., 2019; Wildermuth et al., 2001; Zhang et al., 2010b). Similarly, ‘‘PTI+ETI<sup>AvrRpm1</sup>’’, ‘‘PTI+ETI<sup>AvrRpt2</sup>’’, ‘‘PTI+ETI<sup>AvrRps4</sup>’’ also induce stronger expression of *ICS1* and *EDS5* compared to PTI alone (Saile et al., 2020). This results in a stronger SA biosynthesis and accumulation during ‘‘PTI+ETI’’ compared to PTI (Castel et al., 2019; Liu et al., 2020; Sun et al., 2018, 2020).

One mechanism by which defence genes are upregulated is via the action of transcription factors (TFs). Putative defence-related TF families include ERF, MYC, TGA and WRKY (Buscaill and Rivas, 2014; Eulgem, 2005). The defence-related transcription factor *SARD1* was originally identified from reverse genetic screening of systemic acquired resistance (SAR) defective mutants. *ICS1* expression and SA induction are partially compromised in the *sard1* mutant, and over-expression of *SARD1* enhances resistance (Zhang et al., 2010b). *SARD1* belongs to the *Arabidopsis* CALMODULIN-BINDING PROTEIN 60 (CBP60) family. A *sard1/cbp60g* double mutant shows defects in SAR, and *ICS1* expression is completely compromised during *Pseudomonas* infection (Zhang et al., 2010b). ChIP-seq analysis with *SARD1* shows that it binds to the promoters of many of defence-related genes, including *ICS1*, *EDS5*, *PBS3*, *FMO1*, *EDS1*, *ADR1*, *PAD4* and *WRKY70* (Sun et al., 2015). Interestingly, *SARD1* also binds to the promoters of defence-negative regulators such as *PUB13*, *WRKY40* and *WRKY60*. Similarly, CBP60g also binds to the promoters of the above genes (Sun et al., 2015). This implies that *SARD1* and CBP60g have a broad role in regulating expression of defence-related genes. The mechanism by which *SARD1*/CBP60g is activated during ETI is currently unknown. CBP60g, but not *SARD1*, has been shown to bind to calmodulin (CaM) (Zhang et al., 2010b). Perhaps Ca<sup>2+</sup> influx and other post-translational modifications can activate *SARD1* and CBP60G. Recently, the transcription factor TGACG-BINDING FACTOR 1 (TGA1) and TGA4 has been shown to positively regulate *SARD1* and *CBP60G* expression, while the transcription factors CALMODULIN-BINDING TRANSCRIPTION FACTOR 3 (CAMTA3) negatively regulate *SARD1* and *CBP60G* expression (Sun et al., 2018, 2020). Thus, transcriptional control is also involved in the regulation/activation of *SARD1* and CBP60G.

WRKY transcription factors are also involved in defence-related gene expression, such as WRKY18, WRKY33, WRKY40 (Birkenbihl et al., 2017; Pandey et al., 2010). The transcription corepressor TOPLESS-RELATED 1 (TPR1), TPR4 and TOPLESS (TPL) have also been implicated in transcriptional regulation during SNC1-triggered autoimmunity (Garner et al., 2020; Zhu et al., 2010). In addition, NLRs can directly associate with TFs to regulate gene expression. Recognition of Avr10 by *Hordeum vulgare* (barley) CC-NLR MLA10 allows it to directly associate with WRKY1/2 and de-repress defence gene expression (Chang et al., 2013). SA also leads to transcriptional reprogramming via the TGAs and SA receptors NON-EXPRESSION OF PATHOGENESIS-RELATED GENES 1 (NPR1), NPR3 and NPR4 (Cao et al., 1998; Ding et al., 2018; Fu et al., 2012; Pieterse et al., 1998; Zhang et al., 1999), which will be discussed in the next section.

### **Downstream responses of ETI: Defence-related phytohormones**

Salicylic acid (SA), jasmonic acid (JA) and ethylene (ET) are phytohormones that are involved in immunity (Bari and Jones, 2009). SA is induced rapidly upon ETI through the upregulation of ICS1, PBS3 and EDS5, which are involved in the biosynthesis of SA (Nawrath et al., 2002; Rekhter et al., 2019; Torrens-Spence et al., 2019; Wildermuth et al., 2001). Accumulation of SA leads to NPR1-dependent transcriptional reprogramming, *Pathogenesis Related (PR)* gene expression and enhanced resistance against hemi-/biotrophs (Cao et al., 1998; Ding et al., 2018; Fu et al., 2012; Pieterse et al., 1998; Zhang et al., 1999). With low SA concentration, NPR1 remains in an oligomeric form, while NPR3 and NPR4 suppress the expression of SA-responsive genes. With high SA concentration, redox changes in the cell convert oligomeric NPR1 into monomers, which then translocate into the nucleus and induce SA-responsive genes with TGA transcription factors. In addition, SA binds to both NPR3 and NPR4 to derepress SA-responsive gene expression. (Ding et al., 2018; Fu et al., 2012; Wang et al., 2020b; Yan and Dong, 2014; Zhang et al., 1999, 2003, 2006). ETI also leads to robust *AGD2-like defense response protein 1 (ALD1)*, *FMO1* and *SARD4* expression, which is required for the biosynthesis of pipercolic acid (PIP or N-hydroxypipercolic acid) (Chen et al., 2018; Ding et al., 2016; Hartmann et al., 2018; Návarová et al., 2012; Sohn et al., 2014). SA and PIP together prime distal tissues for secondary infection through SAR (Ding and Ding, 2020; Kim et al., 2020; Sun et al., 2020). NPR1, NPR3 and NPR4 contribute to both PTI- and ETI-mediated resistances and are also involved in regulating HR (Fu et al., 2012; Liu et al., 2020; Zavaliev et al., 2020). The mechanisms by which SA signaling intersects with PTI, ETI and HR remain to be determined.

JA enhances resistance against herbivores and necrotrophic pathogens (Buscaill and Rivas, 2014). In the resting state, JASMONATE ZIM-DOMAIN (JAZs), together with corepressors NOVEL INTERACTOR OF JAZ (NINJA) and TOPLESS (TPL), act as a complex to repress the expression of JA-responsive genes (Pauwels et al., 2010). This repressor complex interacts with Histone DeAcetylase (HDAC) proteins, such as HDA6 and HDA19, to establish a 'closed' chromatin state to repress the expression of JA-responsive genes (Jiang et al., 2020; Liu et al., 2014; Zhou et al., 2005; Zhu et al., 2011). During immune responses against pests and necrotrophic pathogens, Jasmonyl-L-Isoleucine (JA-Ile) is synthesised and is perceived by JAZ and F-box protein CORONATINE-INSENSITIVE 1 (COI1) (Katsir et al., 2008; Sheard et al., 2010). COI1 acts together with the Skp1/Cullin/F-box (SCFCOI1) complex as an E3 ubiquitin ligase, which leads to the degradation of JAZs via the 26S proteasome (Sheard et al., 2010; Thines et al., 2007). The degradation of JAZ allows MYC2 to form complexes with MYC3 and MYC4, which bind to the G-box in the promoter region of JA-responsive genes (Dombrecht et al., 2007; Fernández-Calvo et al., 2011). MYC2 then interacts with MED25 and recruits the transcriptional machinery to initiate the transcription of JA-responsive genes (Kazan and Manners, 2013). The ET and JA signalling pathways converge to activate ETHYLENE RESPONSE FACTOR1 (ERF1) which enhances resistance against necrotrophs (Huang et al., 2016). JA is also highly induced during ETI, and JA signalling pathway mutants exhibit reduced resistance towards *Pst* AvrRpt2 (Liu et al., 2016).

The reciprocal antagonism between SA and JA pathways has been well characterised across several plant species (Koornneef and Pieterse, 2008). Exogenous application of SA leads to the downregulation of JA-mediated PDF1.2 in *Arabidopsis* (Ndamukong et al., 2007). JA signalling suppression by SA has been shown to be NPR1-dependent and is regulated by WRKY70 and TGAs (Ndamukong et al., 2007). On the other hand, the JA analogue coronatine produced by *P. syringae* suppresses the SA-signalling pathway (Bender et al., 1999; Zhao et al., 2003). In addition, JAZ2 has been shown to repress EIN3/EIL1, which inhibits SA synthesis through *ICS1* promoter binding (Zhu et al., 2011). Despite much evidence showing the antagonism between SA and JA, a study suggests that SA perception by NPR3/4 leads to the degradation of JAZ, which activates the JA pathway to trigger HR and resistance against *P. syringae* (Liu et al., 2016). Thus, the spatiotemporal interaction between JA and SA orchestrates immune responses to both biotrophic and necrotrophic pathogens. Indole acetic acids (IAA or auxin) and gibberellic acid (GA) are phytohormones that regulate growth and development (Navarro et al., 2008; Weiss and Ori, 2007). PTI suppresses the auxin signalling pathway through miRNA (Navarro et al., 2006). Exogenous

application of SA also suppresses the expression of auxin-related genes (Wang et al., 2007). GAs degrade the plant growth repressor proteins DELLAs to promote growth. Perception of flg22 stabilises DELLAs, which upregulates JA-mediated resistance and downregulates growth (Navarro et al., 2008; Weiss and Ori, 2007). In conclusion, crosstalk between different phytohormones allows plants to switch from growth and/or development to defence in the presence of pathogens.

### **Physiological response of ETI: Hypersensitive Response (HR)**

HR is a type of programmed cell death (PCD) in plants that results in chromatin condensation, vacuole shrinkage, organelle degradation and collapse of the plasma membrane. It is triggered by multiple cellular processes such as  $\text{Ca}^{2+}$  influx, ROS accumulation, photosynthetic inhibition and phytohormone signalling (Dalio et al., 2020; Lam, 2004; Mur et al., 2008). The calcium channels CNGC2, CNGC4, CNGC19 and CNGC20 have been implicated to regulate HR (Ali et al., 2007; Clough et al., 2000; Jurkowski et al., 2004; Yu et al., 2019).  $\text{Ca}^{2+}$  channel blockers also inhibit HR during ‘‘PTI + ETI’’, indicating that  $\text{Ca}^{2+}$  influx is required for cell death (Gao et al., 2013; Grant et al., 2000).  $\text{Ca}^{2+}$  influx is linked to ROS production (Gilroy et al., 2014; Kimura et al., 2012; Ogasawara et al., 2008; Wu et al., 2020a). Activation of NADPH oxidases such as RbohD and RbohF leads to apoplastic ROS accumulation (Lamb and Dixon, 1997; Torres et al., 2002; Yun et al., 2011). In addition, MPK3/MPK6-mediated photosynthetic inhibition leads to chloroplastic ROS accumulation (Su et al., 2018). Both MPK3/MPK6 and RbohD/F are required for NLR-mediated HR (Su et al., 2018; Torres et al., 2002). Taken together, the activation of calcium channels, NADPH oxidases and MAPK contribute to cell death during ‘‘PTI + ETI’’.

SA has been shown to be a positive regulator of HR (Lorrain et al., 2003). Lesion mimic (*les*) mutants exhibit spontaneous cell death. Multiple *les* mutants were crossed with plants containing the *nahG* transgene, which prevents SA-accumulation by converting it to catechol (van Wees and Glazebrook, 2003). In *LESION SIMULATING DISEASE RESISTANCE 1 (lsd1)*, *ACCELERATED CELL DEATH 5 (acd5)*, *acd6*, *acd11* and *DISEASE LIKE LESIONI (dll1)*, *nahG* suppresses spontaneous HR, which suggests the role of SA as a positive regulator of HR (Bruggeman et al., 2015; Moeder and Yoshioka, 2008). On the other hand, SA-deficient mutants exhibit enhanced HR and exogenous application of SA leads to reduced HR-mediated by RPS2 (Radojićić et al., 2018; Zavaliev et al., 2020). Recently it has been proposed that NPR1 forms condensates in adjacent cells at infection sites to suppress the spread of HR to promote cell survival (Zavaliev et al.,

2020). The mechanisms by which SA regulates HR in both the infection site and adjacent tissues remain to be determined, but it has been proposed that moderate levels of SA can reduce HR, and low or high levels promote HR.

The role of HR was proposed to be to halt hemi/biotrophic pathogen infection by confining and restricting nutrient availability. NRG1 and SAG101 are both genetically required for HR induced by TIR-NLRs (Castel et al., 2019; Gantner et al., 2019; Lapin et al., 2019; Wu et al., 2019). However, only ETI-induced HR, but not resistance against *Pseudomonas*, is abolished in these mutants. Similarly, *cngc2/4* mutants only affect ETI-induced HR but not resistance (hence the name *defence, no death*) (Clough et al., 2000; Jurkowski et al., 2004; Yu et al., 1998). This implies that HR might not be required for resistance against bacterial pathogens. However, NRG1 is required for TIR-NLR-mediated resistance against viral, fungal and oomycete pathogens (Castel et al., 2019; Peart et al., 2005; Wu et al., 2019). The role and contribution of HR in resistance against different pathogens remains to be determined.

### **Regulation of ETI**

Since the activation of ETI leads to robust immune responses and HR, NLRs are tightly regulated to prevent autoimmunity. REQUIRED FOR MLA12 RESISTANCE 1 (RAR1), SUPPRESSOR OF THE G2 ALLELE OF SKP1 (SGT1), and HEAT SHOCK PROTEIN 90 (HSP90) function together to regulate the folding, localisation and turnover of NLRs (Azevedo et al., 2002; Peart et al., 2002; Shirasu, 2009; Takahashi et al., 2003). Phosphorylation of SGT1 by MAPKs is required for NLR activation, implying that ETI is regulated by SGT1 following PAMP perception (Hoser et al., 2013; Yu et al., 2020). Interestingly, PTI also leads to the degradation of nonsense-mediated mRNA decay (NMD) factors UP-FRAMESHIFT1 (UPF1), UPF2, and UPF3, which in turn leads to multiple TIR-NLR transcripts accumulation (Jung et al., 2020). In addition, “PTI + ETI” leads to alternative splicing of multiple NLRs such as RPS4, which is important for both NLR stability and activation (Zhang and Gassmann, 2007). Recently, the plant E3 ligases SNIPER1 and SNIPER2 were shown to ubiquitinate and regulate the homeostasis of multiple NLRs in *Arabidopsis* (Wu et al., 2020b). To summarise, transcriptional-, post-transcriptional- and post-translational-regulation prevents NLRs from over-accumulating and misfolding. Perception of PAMPs can ‘prime’ NLRs to ensure robust ETI can be activated upon effector perception. It is unclear whether transcriptional and/or post-translational modifications are important for the activation and/or stability of signalling components such as helper NLRs and EP proteins. Phosphorylation of the C-terminus of

RRS1-R is crucial for PopP2 recognition (Guo et al., 2020). PAMP perception also leads to *ADRI* and *NRG1* induction (Bonardi et al., 2011; Brendolise et al., 2018). Perhaps helper NLRs also require transcriptional and post-translational regulation to function efficiently.

NLR expression is also regulated by microRNAs (miRNAs). *Solanum lycopersicum* miR482 targets multiple CC-NLR mRNAs and suppresses their expression. MiR482-mediated silencing is suppressed by both viral and bacterial infections, which leads to enhanced CC-NLR expression. This system has therefore been proposed to act as surveillance for pathogenic suppression of host RNA silencing (Shivaprasad et al., 2012). Recently, the *Arabidopsis* miR825 has been shown to target and suppress TIR-NLR expression. In addition, PAMP treatment leads to down-regulation of miR825, suggesting that PTI can suppress RNA silencing and enhance NLR expression (López-Márquez et al., 2020). The regulation of ETI-signalling components pre- and post-activation remains to be investigated.

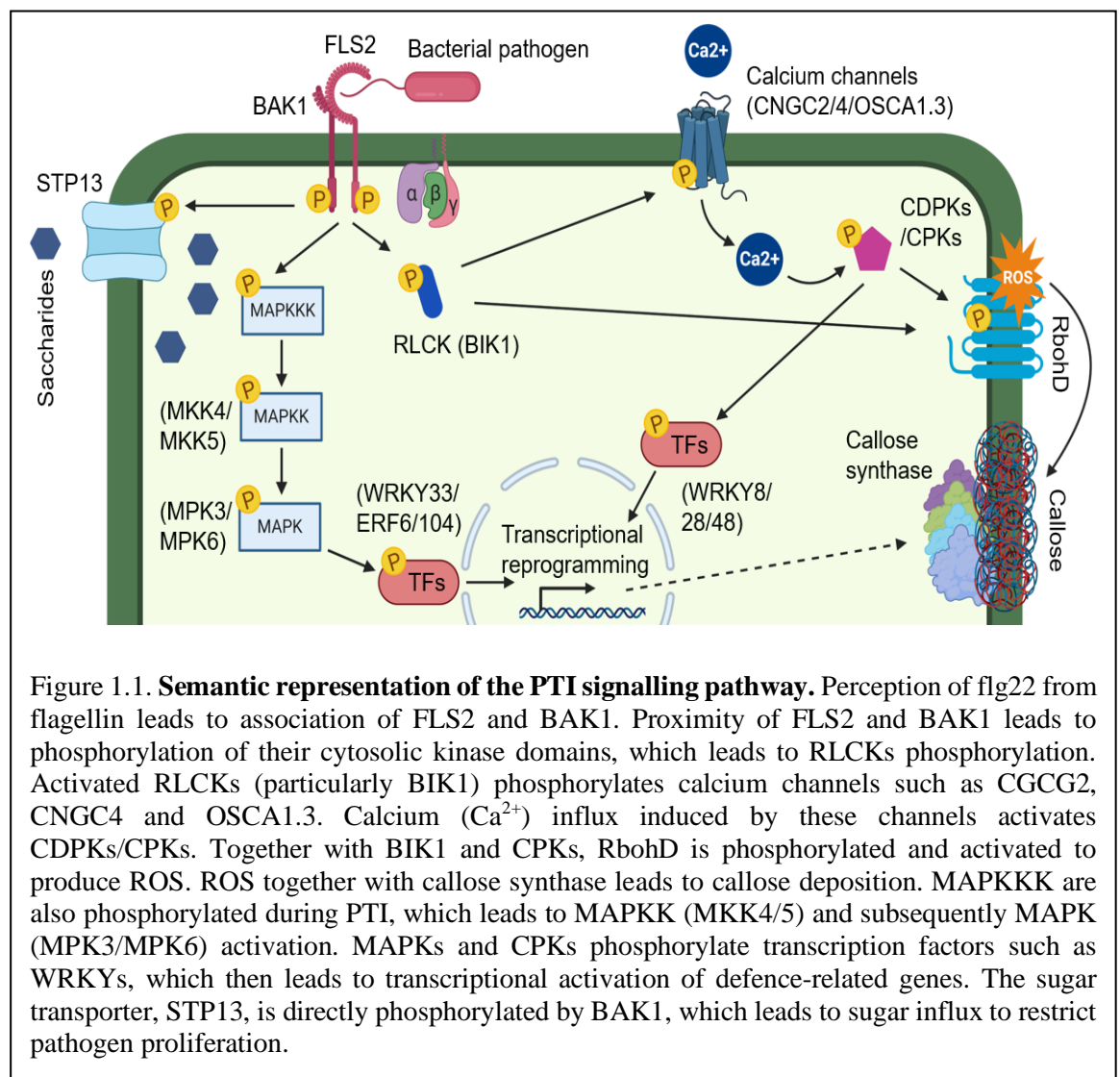
### **Overview of ETI**

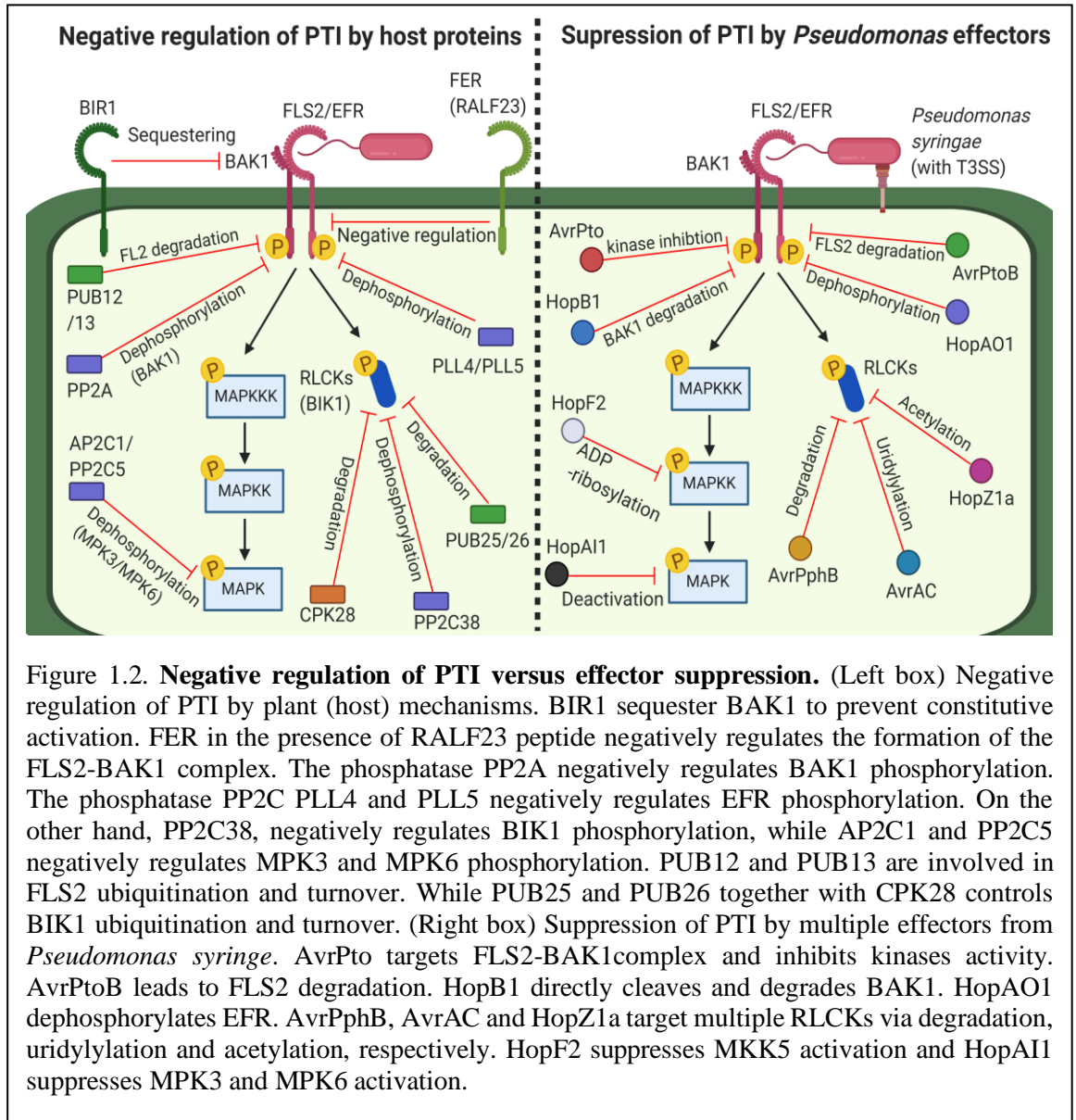
NLRs recognise effectors either by direct-binding or guarding proteins that are targeted by effectors. Recognition of effectors leads to oligomerisation and formation of resistosomes, which activates downstream signalling components by either pore-formation or production of *vc*-ADPR. Different helper NLRs and EP proteins are then activated to transduce signals from sensor NLRs. Activation of “PTI + ETI” results in enhanced  $Ca^{2+}$  influx, ROS production and MAPK activation, which leads to transcriptional regulation and HR to restrict pathogen infection. Genes involved in biosynthesis of defence-related phytohormones are also highly upregulated during ETI, which leads to SA and PIP accumulation and induction of SAR. NLRs are tightly regulated by multiple mechanisms to prevent autoactivation.

### **Aims of the thesis**

Despite recent advances in understanding PTI and ETI signalling pathway, whether PTI and ETI interacts is unclear. In addition, the mechanisms by which NLR activation thwart pathogens are largely unknown. Previous studies on ETI have mostly been concluded from comparison between PTI and ‘PTI + ETI’. ETI is rarely studied in the absence of PTI. An *Arabidopsis* line with inducible expression of AvrRps4 was generated to trigger RRS1/RPS4-dependent ETI. Since no pathogens were used to deliver AvrRps4, PTI would not be triggered. The aim of this thesis is to investigate downstream immune responses triggered by ETI alone. Surprisingly, the activation of ETI<sup>AvrRps4</sup> (in the absence of PTI) does not lead to physiological responses such as ROS burst or MAPK activation, which led

me to investigate the interaction between PTI and ETI. Using the inducible system, I discovered PTI and ETI mutually potentiated each other through various mechanisms. Importantly, activation of PTI or ETI alone is insufficient for resistance against *P. syringae* pv tomato strain DC3000, further implying that PTI and ETI function together to provide robust resistance. To summarize, the aim of the thesis is to 1) investigate immune responses triggered by ETI alone, 2) investigate the interaction between PTI and ETI, and 3) investigate the molecular mechanisms by which PTI and ETI mutually potentiates each other.





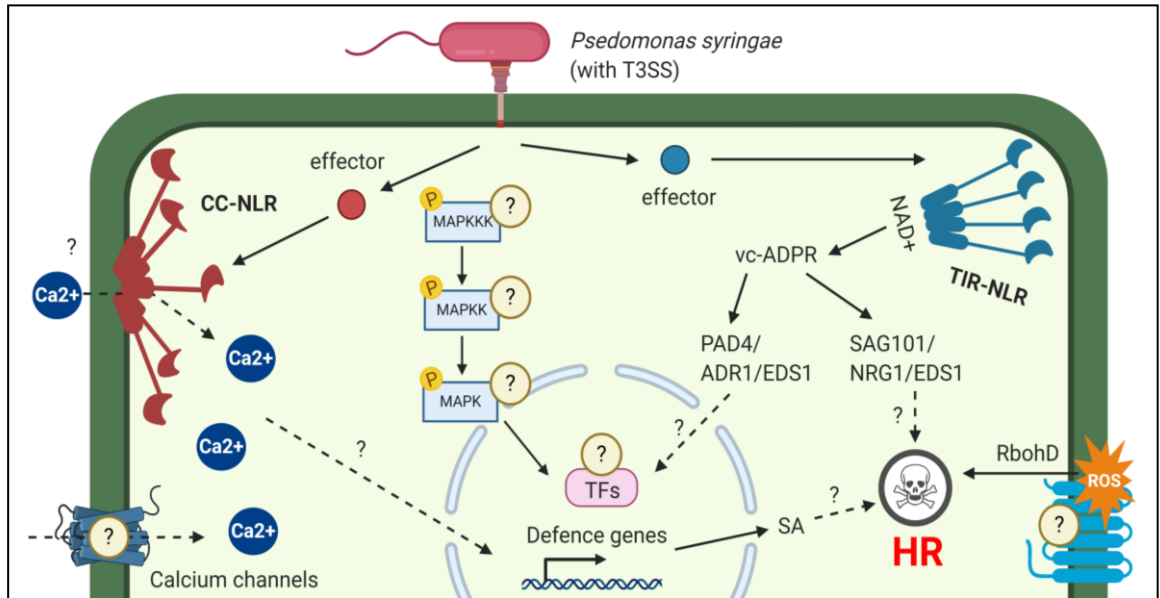


Figure 1.3. **Semantic representation of the activation of ETI signalling pathway.** CC-NLRs recognise effectors and oligomerise into resistosomes. CC-NLR resistosomes, such as ZAR1, has been proposed to form pore/ calcium channels on the plasma membrane, which activates downstream responses through unknown mechanisms. TIR-NLRs, such as Roq1, also oligomerise into resistosomes. TIR domains in close-proximity act as NAD<sup>+</sup>-cleaving enzymes (NADases), which produces vc-ADPR. vc-ADPR is proposed to activate downstream signalling components such as helper NLRs (NRG1 and ADR1) and EP proteins (EDS1, PAD4 and SAG101). PAD4/EDS1/ADR1 function together to induce transcriptional reprogramming and resistance, while SAG101/NRG1/EDS1 function together to induce HR. Multiple transcription factors are proposed to be activated during ETI, which leads to transcriptional reprogramming. SA-biosynthesis gene are highly upregulated, SA are then synthesised to regulate HR and induced SAR. Calcium influx, MAPK activation and ROS production are also strongly induced during “PTI + ETI”. However, the mechanisms by which these are triggered is unknown.

## Chapter 2: Materials and methods

### Materials

#### *Arabidopsis thaliana*

*Arabidopsis thaliana* (abbreviated as Arabidopsis) wild type line used in this study is Col-0. The mutant lines used in this study are Col-0\_ *rrs4-2-rps4b-2* (Saucet et al., 2015), Col-0\_ *eds1-2* (Falk et al., 1999), Col-0\_ *bak1-5-bkk1-1* (Roux et al., 2011; Schwessinger et al., 2011), and Col-0\_ *sard1-cbp60g* (Zhang et al., 2010b). Seeds were sown on compost and plants were grown at 21°C, with 10 hours of light and 14 hours of dark, and at 70 % humidity. For seed collection, 5-weeks old plants were grown at 21 °C, with 16 hours of light and 8 hours of dark, 70 % humidity. The light level is ~180–200 μmol with fluorescent tubes.

#### *Escherichia coli*

*Escherichia coli* (*E. coli*) strain DH10B genotype F–*mcrA* Δ(*mrr-hsdRMS-mcrBC*) Φ80*lacZ*Δ*M15* Δ*lacX74* *recA1* *endA1* *araD139* Δ(*ara leu*) 7697 *galU galK rpsL nupG* λ– was used for cloning purposes. *E. coli* were grown at 37 °C overnight in LB media with antibiotic dependent on the plasmid-carried selectable marker.

#### *Agrobacterium tumefaciens*

*Agrobacterium tumefaciens* (*A. tumefaciens*) strains GV3101 was used in this study for *Arabidopsis* transformation. *A. tumefaciens* were grown at 28°C overnight for 48 hours in LB media with gentamycin, rifampicin and additional antibiotics dependent on the plasmid-carried selectable marker.

#### *Pseudomonas spp.*

*Pseudomonas syringae* pv *tomato* strain DC3000 (DC3000) and *Pseudomonas fluorescens* strain Pf0-1 engineered with Type III Secretion System (T3SS) (Thomas et al., 2009) were used in this study.

DC3000 strains were grown at 28°C for 48 hours on KB media with rifampicin (rifampicin only for *DC3000 hrcC*<sup>-</sup> strain) and kanamycin (for other DC3000 strain carrying the pVSP61 vector). DC3000 with pVSP61 vector were expressing the following constructs: pVSP61 or pVSP61::AvrRps4 (Sohn et al., 2009; Williams et al., 2014).

Pf0-1 strains were grown at 28°C for 24 hours on KB media with chloramphenicol, tetracycline and kanamycin (for pEDV6::empty vector) or gentamycin (for pBBR1MCS-5::AvrRps4 and pBBR1MCS-5::AvrRps4-KRVYAAAA). (Sohn et al., 2009, 2014)

#### Lysogeny Broth (LB)

For 1 litre solution, 10 g tryptone, 5 g yeast extract, 5 g NaCl, 1 g glucose, pH was adjusted to 7.0. For solid medium, 10 g agar was added.

#### King's B (KB)

For 1 litre solution, 20 g peptone, 10 mL glycerol, 1.6 g potassium hydrogen phosphate, 10 mL glycerol. pH was adjusted to 5.8. For solid medium, 15 g agar was added.

#### Murashige and Skoog ½ (MS media ½)

For 1 litre solution, 2.2 g of Murashige and Skoog medium, 30 g sucrose. pH was adjusted to 5.8. For solid medium, 10 g agar was added.

#### Antibiotics concentration

Carbenicillin: 100 mg/mL in water (stock solution), 100 µg/mL (working concentration);  
Chloramphenicol: 10 mg/mL in water (stock solution), 10 µg/mL (working concentration);  
Gentamycin: 10 mg/mL in water (stock solution), 10 µg/mL (working concentration);  
Kanamycin: 150 mg/mL in water (stock solution), 150 µg/mL (working concentration);  
Rifampicin: 10 mg/mL in methanol (stock solution), 10 µg/mL (working concentration);  
Spectinomycin: 100 mg/mL in water (stock solution), 100 µg/mL (working concentration);  
Tetracycline: 5 mg/mL in ethanol (stock solution), 5 µg/mL (working concentration).

### **Methods**

#### Polymerase chain reaction (PCR)

PCR were performed with DreamTaq DNA Polymerase (Thermo Scientific). Reaction mix, annealing and extension temperature were defined according to primers and manufacturer's instructions. PCR were performed in thermocyclers. Gel electrophoresis was used to determine product size and quantity. Gels were run in 1 % agarose, 1X TAE buffer with 0.02 µl/mL ethidium bromide at ~100-120 V and then visualized under UV light. Gel extractions were performed with QIAquick Gel Extraction Kit (QIAGEN) following the manufacturer's instructions.

### Golden Gate Cloning

The Golden Gate assembly enables the assembly of multiple modules into a destination vector simultaneously, using type II restriction endonucleases and DNA ligase T4 (Engler et al., 2009, 2014). Compatible 4 bp overhangs at the junction in each module are designed to ensure the assembly in the right position (Engler et al., 2014). Multiple modules were assembled in a single reaction (diglig, digestion and ligation reaction): 0.02 pmol of each module and vector (backbone), 0.5 µl BsaI-HF® (20,000 units/mL, NEB) / BpiI® (10,000 units/mL, ThermoFisher), 0.15 µl 10 X BSA (2 mg/mL, NEB), 1 µl T4 DNA ligase (400,000 units/mL, NEB) and 1.5 µl CutSmart® buffer (NEB). Water was added to a final volume of 15 µl. The reactions were carried out in a thermocycler: initial digestion at 37°C for 1 min, 25 cycles of 37 °C for 3 mins (digestion) and 16°C for 4 mins (ligation), denaturing at 50 °C for 5 mins and then 80°C for 5 mins. 5µl product were used for transformation in *E. coli* for amplification.

### Plasmid purification and validation

White colonies were cultivated in liquid LB media with antibiotics and incubated O/N at 37°C (*E. coli*) or 28°C (*A. tumefaciens*). QIAprep Spin Miniprep Kit (QIAGEN) was used to extract plasmids from bacteria following the manufacturer's instruction. Plasmid DNA was eluted in water and checked by restriction enzyme digestion and gel electrophoresis. Plasmids sequences were further confirmed with Illumina sequencing service from GATC Biotech.

### Plasmid transformation

Plasmid were transformed with approximately  $5 \times 10^8$  cells in 0.1 cm cuvette and micropulser on settings recommended by manufacturer (Bio-Rad). Afterwards, cells were suspended in LB media and incubated at 37 °C for 30 mins. Liquid culture was then spread on L-plate with antibiotics and/or x-gal (40 mg/mL) for white/ blue selection (for golden gate cloning). *E. coli* were incubated at 37 °C O/N and *A. tumefaciens* were incubated at 28 °C for 2 days.

### FastRed selection for transgenic *Arabidopsis*

Transgenic *Arabidopsis* seeds were harvested and resuspended in 0.1 % agarose. The suspension was then exposed under fluorescence microscope on DsRed filter (for red fluorescent protein). Seeds with red fluorescence signal are selected with a glass pipette as positive transformants for sowing.

### Growing Arabidopsis on MS plates or solution

Arabidopsis seeds were sterilized with bleach (100 mL 10 % sodium hypochlorite solution 10 % + 2 mL 30 % hydrochloric acid) O/N. The seeds were then washed with 70 % ethanol twice, resuspended in water and sown on 1/2 MS plates (with or without 50  $\mu$ M estradiol for selection) or 1/2 MS solution in 12-well plates (3 mL/ well).

### Confocal laser scanning microscopy (CLSM) imaging

Seedlings were imaged with the Leica DM6000/TCS SP5 confocal microscope (Leica Microsystems) to confirm expression of AvrRps4-mNeonGreen (or mNeon) (Shaner et al., 2013). Roots of Arabidopsis seedlings were sprayed with 50  $\mu$ M estradiol and imaged 24 hours after. mNeon was excited at 500 nm and fluorescence signals were detected at between 520-540 nm. CLSM images of root cells were then recorded and images were analysed by Leica application Suite and Fiji software (Schindelin et al., 2012).

### RNA extraction and reverse transcription–quantitative PCR (RT–qPCR) for measuring relative gene expression

All RNA samples were isolated from Arabidopsis tissues after indicated treatment (Table 2.3) with RNeasy® Plant Mini Kit (Qiagen) and treated with RNase-free DNase (4716728001; Merck-Roche). Reverse transcription was carried out with SuperScript IV Reverse Transcriptase (18090050; ThermoFisher Scientific) under manufacturer's instructions. qPCR was performed using a CFX96 Touch™ Real-Time PCR Detection System with KAPA SYBR® FAST (Roche). Primers for qPCR analysis are listed in the table below (Table 2.1). Data were analysed using the double delta Ct method (Livak and Schmittgen, 2001).

Primer name	Gene	5' to 3' sequence
EF1 $\alpha$ _qPCR-F	<i>EF1<math>\alpha</math></i> (AT5G60390)	CAGGCTGATTGTGCTGTTCTTA
EF1 $\alpha$ _qPCR-R	<i>EF1<math>\alpha</math></i> (AT5G60390)	GTTGTATCCGACCTTCTTCAGG
ICS1_qPCR-F	<i>ICS1</i> (AT1G74710)	CAATTGGCAGGGAGACTTACG
ICS1_qPCR-R	<i>ICS1</i> (AT1G74710)	GAGCTGATCTGATCCCGACTG
PR1_qPCR-F	<i>PR1</i>	ATACACTCTGGTGGGCCTTACG
PR1_qPCR-R	<i>PR1</i>	TACACCTCACTTTGGCACATCC
AvrRpm1_qPCR-F	<i>AvrRpm1</i>	ATGGGCTGTGTATCGAGCACT
AvrRpm1_qPCR-R	<i>AvrRpm1</i>	TCTGAGTCAGACTGAACAGCT
AvrRpt2_qPCR-F	<i>AvrRpt2</i>	CACCATGAAAATTGCTCCAGTTGCCATAAATC
AvrRpt2_qPCR-R	<i>AvrRpt2</i>	GTAGCGGTAGAGCATTGCGTGTGGAAC
AvrPphB_qPCR-F	<i>AvrPphB</i>	GGTGGCAGTGCGCAATTGGG
AvrPphB_qPCR-R	<i>AvrPphB</i>	TCCCTCACAGGAGCACGCGAT
AvrRps4_qPCR-F	<i>AvrRps4</i>	ATGACTCGAATTTCAACC
AvrRps4_qPCR-R	<i>AvrRps4</i>	GGTCCACCCAATAGGGATTTGGGTG

AvrRpp4_qPCR-F	<i>AvrRpp4</i>	GATGCTGGCGGAGGACTTAG
AvrRpp4_qPCR-R	<i>AvrRpp4</i>	CTGCCACGTGACCAGATGAT
BAK1_qPCR-F	<i>BAK1 (AT4G33430)</i>	TGTCCTGACGCTACAAGTTCTGG
BAK1_qPCR-R	<i>BAK1 (AT4G33430)</i>	AGCAACTCCTCCCGCAATCG
BIK1_qPCR-F	<i>BIK1 (AT2G39660)</i>	ACTTATGGGTACGCCGCGCCTGAGT
BIK1_qPCR-R	<i>BIK1 (AT2G39660)</i>	GGCACGGACCACTTGGTCCA
RbohD_qPCR-F	<i>RbohD (AT5G47910)</i>	CGAATGGCATCCTTTCTCAATC
RbohD_qPCR-R	<i>RbohD (AT5G47910)</i>	GTCACCGAGAGTGCGGATATG
MPK3_qPCR-F	<i>MPK3 (AT3G45640)</i>	TGACGTTTGACCCCAACAGA
MPK3_qPCR-R	<i>MPK3 (AT3G45640)</i>	CTGTTCCCTCATCCAGAGGCTG
FLS2_qPCR-F	<i>FLS2 (AT5G46330)</i>	ACTCTCCTCCAGGGGCTAAGGAT
FLS2_qPCR-R	<i>FLS2 (AT5G46330)</i>	AGCTAACAGCTCTCCAGGGATGG
MPK4_qPCR-F	<i>MPK4 (AT4G01370)</i>	CGTTGTGCCACCCATATTT
MPK4_qPCR-R	<i>MPK4 (AT4G01370)</i>	AAAATTGAACGGCCTCACAC
RbohF_qPCR-F	<i>RbohF (AT1G64060)</i>	CTTGGCATTGGTGCAACTCC
RbohF_qPCR-R	<i>RbohF (AT1G64060)</i>	TCTTTCGTCTTGGCGTGTCA
MPK6_qPCR-F	<i>MPK6 (AT2G43790)</i>	CCGACAGTGCATCCTTTAGCT
MPK6_qPCR-R	<i>MPK6 (AT2G43790)</i>	TGGGCCAATGCGTCTAAAAC
CERK1_qPCR-F	<i>CERK1 (AT3G21630)</i>	CAAATCAAGAGATGGTGTGGTGC
CERK1_qPCR-R	<i>CERK1 (AT3G21630)</i>	CACCACCCAAACCTCCACT
SOBIR1_qPCR-F	<i>SOBIR1 (AT2G31880)</i>	TACCAGGAAGCAATGGGAAG
SOBIR1_qPCR-R	<i>SOBIR1 (AT2G31880)</i>	TACCAGGAAGCAATGGGAAG
FRK1_qPCR-F	<i>FRK1 (AT2G19190)</i>	CGGTCAGATTTCAACAGTTGTC
FRK1_qPCR-R	<i>FRK1 (AT2G19190)</i>	AATAGCAGGTTGGCCTGTAATC
NHL10_qPCR-F	<i>NHL10 (AT2G35980)</i>	TTCCTGTCCGTAACCCAAAC
NHL10_qPCR-R	<i>NHL10 (AT2G35980)</i>	CCCTCGTAGTAGGCATGAGC
FOX1_qPCR-F	<i>FOX1 (AT1G26380)</i>	GGCTGCACTTCAACCCTTAC
FOX1_qPCR-R	<i>FOX1 (AT1G26380)</i>	TTACTCTCTGTGGCGTTTGG
PER4_qPCR-F	<i>PER4 (AT1G14540)</i>	CGTTTAGGGCTATCGCAGAC
PER4_qPCR-R	<i>PER4 (AT1G14540)</i>	ACGTGAGGCATTGAGCTTG
WRKY31_qPCR-F	<i>WRKY31 (AT4G22070)</i>	ACGGTGGATGATGGACTATCAATGG
WRKY31_qPCR-R	<i>WRKY31 (AT4G22070)</i>	CGGCAACAAGTTGCATTTGTAAGG

**Table 2.1.** Primers used in this study.

#### Hypersensitive cell death response phenotyping in Arabidopsis

The abaxial surfaces of 5-week-old Arabidopsis leaves were hand-infiltrated with indicated elicitors or solution (Table 2.3) with 1-mL needleless syringes. Cell death was monitored as indicated time-point after infiltration.

#### Trypan blue staining

Either 50  $\mu$ M estradiol or 1% DMSO was hand-infiltrated into 5-week-old Arabidopsis leaves (abaxial surfaces) with 1-mL needleless syringes. Six leaves per sample were

collected 24 hours post infiltration. Leaves were boiled in trypan blue solution (with 1.25 mg mL<sup>-1</sup> trypan blue dissolved in 12.5 % glycerol, 12.5 % phenol, 12.5 % lactic acid and 50% ethanol) for 1 min and de-stained with chloral hydrate (2.5 g mL<sup>-1</sup>). De-stained leaves were mounted onto glass slides, and pictures were taken under a Leica M165FC fluorescent stereomicroscope. All images were taken with identical settings with 2.5 × magnification. Scale bars = 0.5 mm.

#### Electrolyte leakage assay

5-week-old Arabidopsis leaves were infiltrated with indicated solutions (Table 2.3) by a 1-mL needleless syringe. Leaf discs were collected with a 2.4-mm-diameter cork borer. Discs were dried and washed with deionized water and then kept in 10 mL deionized water (15 discs per technical replicate, three technical replicated per biological replicate). Electrolyte leakage was measured as conductivity with Pocket Water Quality Meters (LAQUAtwin-EC-33; Horiba) at indicated time points.

#### Immunoblotting

Arabidopsis tissues were treated with different treatment solution as indicated (Table 2.3). Samples were collected at indicated time point and snap-frozen in liquid-nitrogen. Samples were lysed and proteins were extracted with GTEN buffer (10 % glycerol, 25 mM Tris pH 7.5, 1 mM EDTA, 150 mM NaCl) with 10 mM DTT, 1% NP-40 and protease inhibitor cocktail (cOmplete™, EDTA-free; Merck), phosphatase inhibitor cocktail 2 (Sigma-Aldrich; P5726) and phosphatase inhibitor cocktail 3 (Sigma-Aldrich; P0044). After centrifugation at 13,000 rpm for 10 mins, protein concentration was measured and normalised with the Bradford assay (Protein Assay Dye Reagent Concentrate; Bio-Rad). After normalization, extracts were heated in 2× TruPAGE™ LDS Sample Buffer (Sigma-Aldrich) at 70 °C for at least 5 mins. Different percentage SDS-PAGE gels were used to run samples of difference sizes. After transferring proteins from gels to PVDF membranes (Merck-Millipore) with Trans-Blot Turbo System (Bio-Rad), membranes were blocked with 5% non-fat dried milk in TBST for 1 hour, immunoblotted with antibodies specified in the table below (Table 2.2). Anti-Rabbit IgG (whole molecule)–Peroxidase antibody produced in goat (A0545; Merck-Sigma-Aldrich) was used as secondary antibody following the use of primary antibodies. Ponceau S solution (P7170; Sigma-Aldrich) was used to stain PVDF membranes as loading controls.

Antibody	Target	Working concentration	Source
MPK3	MPK3 (AT3G45640)	1:4000	Sigma-Aldrich (M8318)

MPK4	MPK4 (AT4G01370)	1:1000	Published material (Menke et al., 2004)
MPK6	MPK6 (AT2G43790)	1:5000	Sigma-Aldrich (A7104)
BIK1	BIK1 (AT2G39660)	1:3000	Agrisera (AS16 4030)
BAK1	BAK1 (AT4G33430)	1:3000	Published material (Roux et al., 2011)
CERK1	CERK1 (AT3G21630)	1:1000	Agrisera (AS16 4037)
SOBIR1	SOBIR1 (AT2G31880)	1:1000	Agrisera (AS16 3204)
RbohD	RbohD (AT5G47910)	1:1000	Agrisera (AS15 2962)
FLS2	FLS2 (AT5G46330)	1:2000	Agrisera (AS12 1857)
RbohD (pS39)	Phosphorylated S39 in RbohD (AT5G47910)	1:500	Published material (Li et al., 2014b)
RbohD (pS343)	Phosphorylated S343 in RbohD (AT5G47910)	1:500	Published material (Li et al., 2014b)
p-p42/44	Phosphorylated forms of MAPKs	1:2000	Cell Signaling Technology (4370)
Rabbit	HRP antibody raised for rabbit	1:10000	Sigma-Aldrich (A0545)
HA	HA epitope tag with conjugated HRP	1:3000	Sigma-Aldrich (H6533)
Actin	Actin (AT2G37620)	1:3000	Agrisera (AS13 2640)
RPS6	Small ribosomal subunit (AT4G31700)	1:5000	Published material (Enganti et al., 2017)
RPL10a	Large ribosomal subunit L10a (AT4G31700)	1:5000	Abcam (ab226381)

**Table 2.2.** Antibodies used in this study.

#### ROS burst assay

Arabidopsis leaf discs were harvested with a 6-mm-diameter cork borer and placed on 96-well plates with 200  $\mu$ l of deionized water (with abaxial surface of the leaves face down) O/N in dark. 200  $\mu$ l of 20 mM luminol (Sigma-Aldrich, A8511), 0.02 mg/mL horseradish peroxidase (Sigma-Aldrich, P6782) and indicated PTI/ ETI elicitors (Table 2.3) were added into each well. ROS production was measured with a Photek camera (East Sussex, UK) over indicated time. Data from each treatment from each genotype is represented by 40 leaf discs in each biological replicate.

### DAB staining

3,3'-diaminobenzidine (DAB, Sigma-Aldrich D8001) was dissolved in water (1 mg/mL) and pH was adjusted to 6 with sodium hydroxide solution. Arabidopsis leaves following indicated treatments (Table 2.3) were vacuum-infiltrated with DAB solution for at least 30 mins and incubated in dark (room temperature) for at least 2 hours. DAB solution was then replaced with 100 % ethanol and boiled for at least 1 min. The leaves are then slowly de-stained with 70 % ethanol in room temperature. De-stained leaves were mounted and scanned with EPSON Perfection V600 Photo.

### Bacterial growth assay

*Pseudomonas syringae* strain DC3000 were cultured, resuspended in 10 mM MgCl<sub>2</sub> and the concentration was adjusted to OD<sub>600</sub> 0.001. 5-week-old Arabidopsis leaves were infiltrated on the abaxial surfaces with indicated bacterial suspension (Table 2.3) by 1-mL needleless syringes. To quantify bacteria, two leaf discs per leaf were harvested with a 6-mm diameter cork borer. For day 0, samples were grounded in infiltration buffer (10 mM MgCl<sub>2</sub>) and spotted (10 µl per spot) on selective KB media. For day 3, samples were grounded in infiltration buffer, serially diluted into 5, 50, 500, 5000, and 50 000 × and spotted (6µl per spot) on selective KB media. The number of colonies (CFU, colony forming unit) was counted and growth was represented as CFU cm<sup>-2</sup> in leaf tissues.

### Plasma membrane extraction for the detection of phosphorylated RbohD and BIK1

Minute™ Plant Plasma Membrane Protein Isolation Kit (Invent Biotechnologies, SM-005-P) was used to extract microsomal fraction from Arabidopsis tissues according to manufacturer's instructions. Protein concentration (cytosolic fraction) from each sample was measured and normalised with the Bradford assay (Protein Assay Dye Reagent Concentrate; Bio-Rad). Total membrane fractions were heated in 2 × TruPAGE™ LDS Sample Buffer (Sigma-Aldrich) at 70 °C for 5 mins (in a minimal volume of 80 µl). 6% SDS-PAGE gels were used to run the samples in 90 V. After transferring proteins from gels to PVDF membranes (Merck-Millipore) using Trans-Blot Turbo System (Bio-Rad), membranes were blocked with 5 % non-fat dried milk in TBST for 1 hour and immunoblotted with pS39-RbohD/ pS343-RbohD antibodies O/N (specified in table 2.2) (Li et al., 2014b). Anti-Rabbit IgG (whole molecule)–Peroxidase antibody (A0545; Merck-Sigma-Aldrich) was used as the secondary antibody. Ponceau S solution (P7170; Sigma-Aldrich) was used to stain PVDF membranes as loading control.

### Callose quantification

5-week-old *Arabidopsis* leaves were hand-infiltrated with indicated solutions (Table 2.3) and covered for 24 hours. Leaves were then hand-infiltrated with 0.01 % Aniline Blue in 1× PBS buffer solution. Leaf discs were then harvested by a 6-mm-diameter cork borer for imaging. Images were taken with an epifluorescence microscope on UV filter (excitation, 365/10 nm; emission, 460/50 nm). The number of callose dots was calculated by ImageJ. One disc was harvested per leaf and at least 7 leaves (from individual plants) were tested per treatment in one biological replicate.

### RNA-seq and data analysis

5-week-old *Arabidopsis* leaves from SETI<sup>WT</sup> or SETI<sup>KRVY</sup> (Ngou et al., 2020a) were hand-infiltrated with 50 µM estradiol for 0 or 4 hours. Samples were snap-frozen and total RNA were extracted by TRI Reagent<sup>®</sup> (T9424; Sigma-Aldrich) and RNA Clean & Concentrator-25 Kit (R1018; Zymo Research). RNA samples are prepared by BGI and libraries are sequenced with BGISEQ-500 sequencing platform. 10M single-end 50-bp reads (at least per library) were obtained from each RNA-seq library. Adaptor-trimmed clean reads have been uploaded to the European Nucleotide Archive (ENA, accession ID: PRJEB34955). After FastQC, Kallisto was used to map and quantify the RNA-seq reads (Bray et al., 2016), kallisto\_quant output files were then submitted to 3D RNA-seq tool for statistics and data visualization (Guo et al., 2019).

### Cycloheximide and MG132 treatment

*Arabidopsis* seedlings of 1-week-old (grown in liquid 1/2 MS media with 1% sucrose) were first pre-treated with 50 µM estradiol or mock (0.1% DMSO) for 3h. 50 µM cycloheximide, 10 µM MG132, or combination of both were then added to seedlings in addition to estradiol or mock solution. Seedlings were then harvested at indicated time points and protein were extracted as described above. Protein concentration from each sample was measured and normalised with the Bradford assay, and samples were analyzed by immunoblotting as described above.

### Enrichment of ribosome

Ribosome enrichment was performed with modified protocol based on previous publications (Cho et al., 2013; Ingole et al., 2020). 5-week old *Arabidopsis* SETI<sup>WT</sup> leaves were infiltrated with mock (1 % DMSO) or 50 µM estradiol for 6 hours. 0.6 g of leaves were collected, ground in liquid nitrogen and extracted in 5 mL extraction buffer (0.2 M Tris-HCl, pH 8.4 50 mM KCl, 25 mM MgCl<sub>2</sub>, 0.5 % Nonidet P-40, 50 µg/mL

cycloheximide and RNase inhibitor (RNasin®, Promega)). After centrifugation at 13,000 rpm for 10 min to removed cell debris, supernatant was loaded on top of a 1.6 M sucrose cushion. Samples were ultracentrifuged at 170,000 g for 16 hours to extract the ribosomal pellet. Pellets were then resuspended in 1 mL DEPC-treated water, 800 µL of which was used for RNA extraction and 200 µL of which for protein extraction (as described above).

#### Serial dilution to estimate protein abundance

BIK1, RbohD and MPK3 protein accumulation during ETI<sup>AvrRps4</sup> is estimated via serial dilution. Protein samples of ETI<sup>AvrRps4</sup> at 8 hours were diluted to 2× (1/2), 4× (1/4), 8× (1/8), 16× (1/16) and 32× (1/32) in 2 × TruPAGE™ LDS Sample Buffer (Sigma-Aldrich). Samples were loaded side-by-side with protein samples of ETI<sup>AvrRps4</sup> at 0 hour and ran on 10% SDS-PAGE gels. After transferring the proteins from SDS gel to PVDF membrane (Merck-Millipore) with Trans-Blot Turbo System (Bio-Rad), PVDF membranes were blocked with 5% non-fat dried milk in TBST for 1 hour and immunoblotted with primary antibodies O/N specified in table 2.2. Anti-Rabbit IgG (whole molecule)–Peroxidase antibody (A0545; Merck-Sigma-Aldrich) was used as secondary antibody. Ponceau S solution (P7170; Sigma-Aldrich) was used to stain PVDF membranes as loading control.

#### Statistical data analysis

Statistical data were analyzed with the R software (<https://www.r-project.org/>), and data were plotted with the Origin software (<https://www.originlab.com/>). For statistical analysis, data were tested for normal distribution with the Shapiro-Wilk test, homoscedasticity with the Levene’s test, and either parametric one-way ANOVA analysis followed by the Tukey’s post-hoc HSD test, or non-parametric Kruskal-Wallis test followed by the Dunn’s test were calculated to test for statistical significance. Data points with different letters indicate significant differences of P<0.01 for the Tukey’s HSD test results, and P<0.05 for the Dunn’s test. Data points are plotted with Origin. Number of samples analyzed for each experiment are indicated in the figure legends. Three biological replicates were tested, and individual biological replicates are indicated as different shapes. qPCR results were analyzed with t-test for statistical significance between samples.

Figure	Experiment	Conc of est/ dex	OD <sub>600</sub> of bacteria	Conc of PAMPs/ DAMP	Note
Figure 3.3a	Plate assay	50 µM	-	-	-
Figure 3.3b	Confocal imaging	50 µM	-	-	-
Figure 3.4	qPCR	50 µM	-	-	-

Figure 3.5	HR assay, trypan blue staining and conductivity assay	50 $\mu$ M	-	-	-
Figure 3.6a	Immunoblotting	50 $\mu$ M	-	100 nM flg22	-
Figure 3.6b-c	ROS assay	50 $\mu$ M	-	100 nM flg22	-
Figure 3.6d	DAB staining	50 $\mu$ M	-	-	-
Figure 3.7	Bacterial growth assay	50 $\mu$ M	0.001	-	-
Figure 3.8a	qPCR	50 $\mu$ M	-	-	-
Figure 3.8b	HR assay	50 $\mu$ M	-	-	-
Figure 3.9a	Immunoblotting	50 $\mu$ M	-	100 nM flg22	-
Figure 3.9b-c	ROS assay	50 $\mu$ M	-	100 nM flg22	-
Figure 3.9d	Immunoblotting	50 $\mu$ M	-	100 nM flg22	-
Figure 4.1b-e	ROS assay	50 $\mu$ M	-	100 nM flg22	-
Figure 4.2b-g	ROS assay	50 $\mu$ M	-	100 nM flg22	-
Figure 4.3	ROS assay	50 $\mu$ M	-	100nM elf18, pep1, C10:0, nlp20 or 1mg/mL chitin	-
Figure 4.4a	DAB staining	50 $\mu$ M	0.2	-	-
Figure 4.4b-c	Callose deposition	50 $\mu$ M	0.05	-	Concentration lowered to prevent callose saturation
Figure 4.4d	qPCR	50 $\mu$ M	0.2	-	-
Figure 4.5c-d	Immunoblotting	50 $\mu$ M	-	100 nM flg22	-
Figure 4.5f-g	Immunoblotting	50 $\mu$ M	0.2	-	-
Figure 4.6	Immunoblotting	50 $\mu$ M	-	-	-
Figure 4.7a	Immunoblotting	50 $\mu$ M	0.005	-	OD <sub>600</sub> lowered to prevent chlorosis caused by <i>Pst</i>
Figure 4.8a-b	Bacterial growth assay	-	0.001	-	-
Figure 4.8c-d	ROS assay	-	-	100 nM flg22	-
Figure 4.8e	Immunoblotting	-	-	100 nM flg22	-
Figure 4.9a-b	HR assay	50 $\mu$ M	0.2	-	-
Figure 4.10a	HR assay	50 $\mu$ M	0.2	1 $\mu$ M flg22, elf18, pep1	-
Figure 4.10b	HR assay	50 $\mu$ M	-	Stated in figure	-
Figure 4.10c	HR assay	Stated	Stated	-	-

Figure 4.11a	HR assay	-	0.1	-	1 $\mu$ M NA-PP1
Figure 4.11b	HR assay	-	Stated	-	-
Figure 5.1a-b	qPCR	50 $\mu$ M	-	-	-
Figure 5.2	RNAseq	50 $\mu$ M	-	-	-
Figure 5.3					
Figure 5.4a	qPCR	50 $\mu$ M	-	-	-
Figure 5.4b	Immunoblotting	50 $\mu$ M	-	-	-
Figure 5.5a	qPCR	50 $\mu$ M	-	-	-
Figure 5.6a					
Figure 5.5b	Immunoblotting	50 $\mu$ M	-	-	-
Figure 5.6b-c					
Figure 5.7a	qPCR and immunoblotting	50 $\mu$ M	0.01	-	-
Figure 5.8a	qPCR	50 $\mu$ M	-	-	-
Figure 5.8b-d	Immunoblotting	50 $\mu$ M	-	-	50 $\mu$ M CHX and/or 10 $\mu$ M MG132
Figure 5.9	Ribosome enrichment and qPCR	50 $\mu$ M	-	-	-

**Table 2.3.** Concentration of reagents and/or bacteria used in this study.

### **Chapter 3: Inducible effector expression reveals distinct properties of NLR-mediated effector-triggered immunity**

This chapter is largely identical to (Ngou et al., 2020a) and (Ngou et al., 2020b) and appears with permissions from Pingtao Ding and Hee-Kyung Ahn. Both publications are under the CC-BY license. Unless specified, experiments were performed by Bruno Pok Man Ngou.

#### **Abstract**

NLR proteins activate effector-triggered immunity following recognition of pathogen-secreted effectors. The mechanism of which NLR activation leads to pathogen resistance is largely unknown. Previous studies on ETI have mostly comprise comparisons between PTI and ‘PTI + ETI’. Activation of ETI in the absence of PTI has rarely been studied in detail. An Arabidopsis line with inducible expression of the effector AvrRps4 has been generated to investigate the downstream immune responses triggered by the TIR-NLRs RRS1 and RPS4. Activation of ETI<sup>AvrRps4</sup> leads to upregulation of defense genes and enhanced resistance against *P. syringae*, but does not lead to ROS burst, MAPK activation or macroscopic cell death. Interestingly, activation of CC-NLRs (such as RPM1, RPS2 and RPS5) can lead to ROS burst, MAPK activation and macroscopic cell death.

#### **Introduction**

Two approaches are commonly used to study ETI: (i) assays in which pathogens are used to deliver effectors into plant cells; or (ii) transient expression, in which Agrobacterium/biolytic bombardment are used to transiently express effectors in plant cells (Sainsbury and Lomonosoff, 2014). The presence of PAMPs and/or DAMPs from either approach triggers PTI. While PTI has been extensively studied, ETI is rarely investigated in the absence of PTI. It is also unclear whether PTI influences ETI, or vice versa.

An inducible system allows conditional expression of a gene by an inducer. Inducible systems contain two components: a transcription factor regulated by an inducer and a promoter/repressor that can be activated/derepressed by the transcription factor. A glucocorticoid-regulated transcription factor, GVG, in combination with the glucocorticoid-inducible promoter, 6×UAS<sub>gal4</sub>, induces the expression of the effector AvrRpt2 only in the presence of the inducer dexamethasone (dex) (McNellis et al., 1998). GVG is a chimeric transcription factor consisting of 3 different domains: a DNA-binding domain of the yeast GAL4 protein (G), a transactivating domain in the VP16 protein from the herpes simplex virus (V) and a glucocorticoid-binding domain from a rat receptor (G). After translation, GVG interacts with HSP70 and HSP90 and remains inactive (GVG<sub>i</sub>). In

the presence of dex, GVG<sub>i</sub> is activated (GVG<sub>a</sub>) and is transported into the nucleus (Aoyama and Chua, 1997). The DNA-binding domain of GVG<sub>a</sub> then binds to the promoter 6×UAS<sub>gal4</sub>, which then induces the expression of AvrRpt2 and triggers ETI<sup>AvrRpt2</sup> via RPS2 (McNellis et al., 1998). A similar inducible system has been generated (Tornerio et al., 2002; Zuo et al., 2000), in which estrogen receptor (E) was used instead of the glucocorticoid-binding domain (GVE). The effector AvrRpm1 is expressed in the presence of estradiol (est), which in turns triggers ETI<sup>AvrRpm1</sup> via RPM1 (Tornerio et al., 2002). These transgenic *Arabidopsis* lines have been established to study ETI in the absence of PTI. Three methods to investigate ETI has been summarised in figure 3.1.

Historically, ETI has been considered as a stronger version of PTI (Jones and Dangl, 2006). In previous reports, ‘PTI + ETI’, induced by patho-assay, was shown to induce stronger transcriptional reprogramming, cell death, calcium influx, MAPK activation and ROS production compared to PTI alone (Grant and Loake, 2000; Grant et al., 2000; Jones and Dangl, 2006; Sohn et al., 2014; Su et al., 2018; Tao et al., 2003; Thilmony et al., 2006; Tsuda et al., 2013). These reports have led to the assumption that i) ETI leads to stronger immune responses compared to PTI, ii) ETI alone can trigger transcriptional reprogramming, cell death, calcium influx, MAPK activation and ROS production and iii) the physiological output during ‘PTI + ETI’ is a mere additive effect of PTI and ETI. I used the inducible system to test if ETI alone can indeed trigger these physiological responses.

#### **A T-DNA construct with RRS1, RPS4 and inducible-AvrRps4 modules**

A stable transgenic inducible-AvrRps4 line was generated by Pingtao Ding to study RRS1/RPS4-induced ETI<sup>AvrRps4</sup>. A T-DNA construct with NLR modules (RRS1 and RPS4) and an inducible-AvrRps4 module was assembled using Golden Gate Modular Cloning (Engler et al., 2014). Since imbalanced expression of RRS1 and RPS4 can cause autoimmunity (Huh et al., 2017), the promoters pAt2 and pAt3 were used to express RRS1 and RPS4, respectively, due to their moderate and comparable expression. pAt2 is a ribosomal protein S16 promoter (AT4G34620 or RPS16-1) and pAt3 is a cysteine synthase isomer CysC1 promoter (AT3G61440 or CYSC1). The C-terminal of RRS1 and RPS4 were tagged with the epitope HF (His6-TEV-FLAG<sub>3</sub>) and HA<sub>6</sub> (hemagglutinin) respectively (Gauss et al., 2005; Soleimani et al., 2013) (Figure 3.2 a-b). Chimeric transcription factor XVE (DNA-binding domain of the bacterial repressor LexA (X)-VP16 (V)-Estrogen receptor (E)), in the presence of estradiol, de-represses the LexA operator, which leads to the expression of AvrRps4-mNeon (Figure 3.2 c-d). This multi-gene stacking binary construct was generated and named ‘Super ETI’ (SETI<sup>WT</sup> construct). The residues 135–138

of AvrRps4, lysine–arginine–valine–tyrosine (KRVY), are required for its recognition by RRS1 and RPS4 (Sohn et al., 2009). A construct with inducible AvrRps4<sup>KRVY-AAAA</sup>-mNeon (AvrRps4<sup>KRVY</sup>-mNeon) was also generated as negative control (SETI<sup>KRVY</sup> construct).

### **Generation of transgenic Arabidopsis lines: SETI<sup>WT</sup>, SETI<sup>KRVY</sup> and SETI<sub>eds1-2</sub>**

*Arabidopsis thaliana* accession Col-0 was transformed with SETI<sup>WT</sup> and SETI<sup>KRVY</sup> constructs. Approximately 20 positive T1 lines were selected by the FastRed selection marker (Shimada et al., 2010). Seedlings from the T2 generation of 3 independent T1 lines were further selected through their response to estradiol treatment. SETI<sup>WT</sup> transgenic lines display severe growth arrest on estradiol-containing growth medium (Figure 3.3a). Finally, one of the lines, T1-#8\_T2-#4 (abbreviated as SETI<sup>WT</sup>), was selected for subsequent experiments. SETI<sup>WT</sup> was also crossed with *eds1-2* mutant and homozygous SETI<sub>eds1-2</sub> was selected as an additional negative control. To further validate these transgenic lines, SETI<sup>WT</sup>, SETI<sup>KRVY</sup> and SETI<sub>eds1-2</sub> seedlings were sprayed with mock (0.1% DMSO) or 50 µM estradiol. Fluorescence signals of AvrRps4 were detected in root cells 24 hours after estradiol treatment (Figure 3.3b). The experiments described above were performed by Pingtao Ding.

### **ETI<sup>AvrRps4</sup> leads to the upregulation of defence-related genes**

One of the hallmarks of ETI is the upregulation of defence-related genes. Genes involved in the biosynthesis of salicylic acid and pipecolic acid are highly induced during ‘PTI + ETI’ compared to PTI alone. Some of these include *Isochorismate Synthase 1 (ICS1)*, *Enhanced Disease Susceptibility 5 (EDS5)*, *AvrPphB Susceptible 3 (PBS3)* and *Flavin Containing Dimethylaniline Monooxygenase (FMO1)* (Ding and Ding, 2020; Saile et al., 2020; Sohn et al., 2014). I tested if the induction of ETI<sup>AvrRps4</sup> alone is sufficient to trigger the expression of defence-related genes. *ICS1* is highly upregulated 4 hours after estradiol treatment (50 µM) in SETI<sup>WT</sup>, but not in SETI<sup>KRVY</sup> or SETI<sub>eds1-2</sub> (Figure 3.4a). Furthermore, the salicylic-acid responsive gene *Pathogenesis-Related protein 1 (PR1)* is upregulated 8 hours after estradiol treatment in SETI<sup>WT</sup>, but not in SETI<sup>KRVY</sup> or SETI<sub>eds1-2</sub> (Figure 3.4b). ETI<sup>AvrRps4</sup> in the absence of PTI is therefore sufficient to upregulate defence-related genes such as *ICS1*, which leads to the accumulation of salicylic acid and subsequently *PR1* expression.

To explore the dynamics of gene expression induced by ETI<sup>AvrRps4</sup>, SETI<sup>WT</sup> leaves were infiltrated with estradiol (50 µM) and RNA samples were collected over a time-course of 24 hours. The expression of *AvrRps4* peaks 2 hours post estradiol treatment, *ICS1* is

upregulated afterwards and peaks at 4 hours post treatment. *PRI* is highly upregulated from 6 hours and sustained for 24 hours (Figure 3.4c-f). In summary, ETI<sup>AvrRps4</sup> leads to both early (*ICSI*) and late (*PRI*) defence-related gene expression.

### **ETI<sup>AvrRps4</sup> does not lead to macroscopic hypersensitive response (HR)**

The hypersensitive response (HR) is a hallmark of ETI and restricts the spread of pathogens. I tested if the induction of ETI<sup>AvrRps4</sup> alone is sufficient to induce HR in *Arabidopsis*. SETI<sup>WT</sup>, SETI<sup>KRVY</sup> and SETI<sub>*eds1-2*</sub> leaves were infiltrated with 50 µM estradiol. No macroscopic HR was observed one day post infiltration (dpi) in all three genotypes compared to mock treatment (0.1 % DMSO) (Figure 3.5a). Since macroscopic HR cannot be observed, trypan blue staining was performed to test if ETI<sup>AvrRps4</sup> can trigger microscopic HR. Slightly stronger blue stains were observed in SETI leaves infiltrated with estradiol compared to mock treatment, and this difference was not observed in SETI<sup>KRVY</sup> or SETI<sub>*eds1-2*</sub> leaves (Figure 3.5b). This suggests that ETI<sup>AvrRps4</sup> can trigger microscopic HR, which leads to cell membrane disruption and electrolyte leakage. Conductivity assay was performed to confirm if ETI<sup>AvrRps4</sup> leads to electrolyte leakage. Estradiol treatment leads to significantly stronger ion leakage compared to mock treatment in SETI<sup>WT</sup>, but not in SETI<sup>KRVY</sup> or SETI<sub>*eds1-2*</sub> (Figure 3.5c). These results confirmed that ETI<sup>AvrRps4</sup> leads to electrolyte leakage and microscopic cell death, but not strong enough to cause macroscopic HR or tissue collapse.

### **ETI<sup>AvrRps4</sup> does not lead to MAPKs activation**

MAPKs, such as MPK3, MPK4, MPK6 and MPK11, have been shown to be phosphorylated in response to PTI triggered by multiple PAMPs or DAMPs. PTI-triggered MAPK phosphorylation is a transient response which occurs within minutes following elicitation (Macho and Zipfel, 2014). To test whether ETI<sup>AvrRps4</sup> can trigger MAPKs activation, seedlings of Col-0, SETI<sup>WT</sup>, SETI<sup>KRVY</sup> and SETI<sub>*eds1-2*</sub> were soaked in 50 µM estradiol and samples were collected over a time-course of 8 hours (soaking assay to prevent wounding response which also triggers MAPK activation). MAPK activation was only observed with 100 nM flg22 treatment, but not with estradiol treatment at any timepoint in all genotypes (Figure 3.6a). This implies that ETI<sup>AvrRps4</sup> cannot trigger MAPK phosphorylation.

### **ETI<sup>AvrRps4</sup> does not lead to ROS production**

PTI triggered by multiple PAMPs or DAMPs also leads to rapid production of ROS (ROS burst) through activation of NADPH oxidases (Respiratory Burst Oxidase Homologs or

RBOHs) (Kadota et al., 2015). To test whether ETI<sup>AvrRps4</sup> can trigger ROS burst, leaf discs of SETI<sup>WT</sup> were soaked in mock solution, 100 nM flg22 or 50 µM estradiol and ROS production was measured over a time-course of 24 hours (soaking assay to prevent wounding response which also triggers ROS production). A ROS burst was only observed with flg22 treatment, but not with estradiol treatment at any timepoint over 24 hours (Figure 3.6b-c). Hydrogen peroxide (a type of ROS) can be visualised through 3,3'-diaminobenzidine (DAB) staining (Daudi and O'Brien, 2012). SETI<sup>WT</sup> leaves were either infiltrated with mock or 50 µM estradiol and stained with DAB solution after 2dpi. No visible hydrogen peroxide can be observed after estradiol treatment (Figure 3.6d). This implies that ETI<sup>AvrRps4</sup> does not lead to significant ROS production or accumulation.

### **ETI<sup>AvrRps4</sup> leads to resistance against *Pseudomonas syringae***

Since many of the physiological responses are not triggered by ETI<sup>AvrRps4</sup>, it was unclear whether ETI<sup>AvrRps4</sup> is sufficient to provide resistance against pathogens. Col-0 and SETI<sup>WT</sup> leaves were infiltrated with mock or 50 µM estradiol (triggers ETI<sup>AvrRps4</sup>) for 24 hours and then infected with virulent bacteria *Pseudomonas syringae* pv. *tomato* (*Pst*) DC3000 (triggers PTI). Estradiol pre-treatment (ETI<sup>AvrRps4</sup>) leads to enhanced resistance against *Pst* DC3000 compared to mock pre-treatment only in SETI<sup>WT</sup> (Figure 3.7a). Thus, pre-activation of ETI<sup>AvrRps4</sup> leads to resistance against *Pseudomonas syringae* through transcriptional reprogramming and perhaps other unknown mechanisms.

In addition, it was unclear whether the timing of ETI activation is crucial to induced resistance. To test this, SETI<sup>WT</sup> and Col-0 leaves were treated with estradiol either one day before (-1d, pre-activation), on the same day during (0 d, co-activation), or one day after (+1d, delayed activation) *Pst* DC3000 infection. Pre-activation (-1d) or co-activation (0 d) of ETI<sup>AvrRps4</sup> both lead to enhanced resistance against *Pst* DC3000. However, delayed ETI<sup>AvrRps4</sup> activation (+1d) in SETI<sup>WT</sup> does not lead to enhanced resistance (Figure 3.7b). This suggests that early activation is crucial for ETI<sup>AvrRps4</sup>-induced resistance against *Pst* infection.

### **ETI triggered by multiple NLRs leads to upregulation of defence-related genes**

Although many physiological responses are not triggered by ETI<sup>AvrRps4</sup>, it was unclear whether ETI triggered by other NLRs is similar to RRS1/RPS4. Other effector-inducible effector lines, including est:AvrRpp4, est:AvrRpt2, dex:AvrRpm1 and est:AvrPphB, have been published (Asai et al., 2018; Qi et al., 2014; Tornero et al., 2002; Tsuda et al., 2013). Induced expression of these effectors leads to activation of ETI<sup>AvrRpp4</sup> (activated by the TIR-NLR RPP4), ETI<sup>AvrRpt2</sup>, ETI<sup>AvrRpm1</sup> and ETI<sup>AvrPphB</sup> (activated by CC-NLRs RPS2, RPM1

and RPS5) respectively. Dex:AvrRpm1, est:AvrRpt2, est:AvrPphB, SETI<sup>WT</sup> and est:AvrRpp4 leaves were infiltrated with 50 µM dexamethasone (dex, for dex:AvrRpm1) or 50 µM estradiol (for est:AvrRpt2, est:AvrPphB, SETI<sup>WT</sup> and est:AvrRpp4) respectively. Samples were collected at 0, 4 and 8 hpi for RNA extraction and qPCR. Expression of AvrRpm1, AvrRpt2, AvrPphB, AvrRps4 and AvrRpp4 all leads to the upregulation of *ICS1* at 4 or 8 hpi (Figure 3.8a). This implies that ETI<sup>AvrRpm1</sup>, ETI<sup>AvrRpt2</sup>, ETI<sup>AvrPphB</sup>, ETI<sup>AvrRps4</sup> and ETI<sup>AvrRpp4</sup> can induce defence-related genes.

### **ETI triggered by CC-NLRs leads to macroscopic HR**

Activation of ETI<sup>AvrRps4</sup> only leads to microscopic HR. I tested if ETI triggered by other NLRs would trigger macroscopic HR. Dex:AvrRpm1, est:AvrRpt2, est:AvrPphB, SETI<sup>WT</sup> and est:AvrRpp4 leaves were infiltrated with 50 µM dex (for dex:AvrRpm1) or 50 µM estradiol (for est:AvrRpt2, est:AvrPphB, SETI<sup>WT</sup> and est:AvrRpp4 respectively). High dosage of dex and estradiol were used to ensure maximal expression of these effectors. Activation of ETI<sup>AvrRpm1</sup>, ETI<sup>AvrRpt2</sup> and ETI<sup>AvrPphB</sup> (triggered by CC-NLRs) leads to macroscopic HR and tissue collapse at 3 dpi, while activation of ETI<sup>AvrRps4</sup> and ETI<sup>AvrRpp4</sup> (both triggered by TIR-NLRs) does not (Figure 3.8b). This implies that ETI triggered by CC-NLRs, but not TIR-NLRs, leads to macroscopic HR.

### **ETI triggered by CC-NLRs leads to MAPK activation and ROS burst**

Since CC-NLRs trigger macroscopic HR, I tested if ETI triggered by CC-NLRs also leads to phosphorylation of MAPKs. Dex:AvrRpm1, est:AvrRpt2, est:AvrPphB, SETI<sup>WT</sup> and est:AvrRpp4 seedlings were soaked in 50 µM dex (for dex:AvrRpm1) or 50 µM estradiol (for est:AvrRpt2, est:AvrPphB, SETI<sup>WT</sup> and est:AvrRpp4) over a time course of 8 hours. Activation of ETI<sup>AvrRpm1</sup>, ETI<sup>AvrRpt2</sup> and ETI<sup>AvrPphB</sup> leads to weak but prolonged MAPKs phosphorylation compared to flg22 treatment, while activation of ETI<sup>AvrRps4</sup> and ETI<sup>AvrRpp4</sup> does not (Figure 3.9a). This implies that ETI triggered by CC-NLRs, but not TIR-NLRs, can lead to MAPK activation.

Furthermore, I tested if ETI triggered by CC-NLR also leads to ROS burst. Leaf discs of Est:AvrRpt2 plants were soaked in mock solution, 100 nM flg22 or 50 µM estradiol and ROS production was measured over a time-course of 24 hours (soaking assay to prevent wounding response which also triggers ROS production). Activation of ETI<sup>AvrRpt2</sup> leads to a relatively weak ROS burst (compared to flg22-induced ROS burst) at around 3 hours (Figure 3.9b-c). Previous reports have also shown hydrogen peroxide accumulation 3 hours post ETI<sup>AvrRpt2</sup> activation (Kadota et al., 2019). These suggest that ETI triggered by CC-NLRs can lead to ROS accumulation.

## **ETI triggered by multiple NLRs does not lead to S39 phosphorylation in RbohD**

The NADPH oxidase Respiratory Burst Oxidase Homolog D (RbohD) has previously been reported to be phosphorylated during PTI at multiple sites such as 39<sup>th</sup>, 343<sup>rd</sup> and 347<sup>th</sup> serine residues, which subsequently leads to activation and ROS production (Kadota et al., 2014; Li et al., 2014b). It has also been reported that ETI<sup>AvrRpt2</sup> leads to phosphorylation of S343 and S347, but not S39 in RbohD (Kadota et al., 2019). It was unclear whether ETI triggered by other NLRs alone leads to S39 phosphorylation in RbohD. Col-0, Dex:AvrRpm1, est:AvrRpt2, est:AvrPphB, SETI<sup>WT</sup> and est:AvrRpp4 seedlings were soaked in either mock, 100 nM flg22 (15 mins; for Col-0), 50 µM dex (6 hours; for dex:AvrRpm1) or 50 µM estradiol (6 hours; for est:AvrRpt2, est:AvrPphB, SETI<sup>WT</sup> and est:AvrRpp4). S39 phosphorylation was detected by RbohD-pS39 antibody from (Li et al., 2014b). I could not detect S39 phosphorylation during ETI<sup>AvrRpm1</sup>, ETI<sup>AvrRpt2</sup>, ETI<sup>AvrPphB</sup>, ETI<sup>AvrRps4</sup> and ETI<sup>AvrRpp4</sup> activation, while flg22 treatment leads to S39 phosphorylation as reported (Figure 3.9d; Note: The RbohD-S39 antibody is not sensitive enough to detect RbohD phosphorylation very well. A 35S::FLAG-RbohD sample was added as a positive control. Other methods such as mass spectrometry should be considered for better detection of RbohD phospho-peptides.) (Li et al., 2014b). Phosphorylation of S343 and S347 on RbohD during PTI (flg22 treatment) could not be detected with immunoblotting by RbohD-pS343, pS347 and pS343/S347 antibodies (Li et al., 2014b). It is therefore unclear whether activation of ETI<sup>AvrRpm1</sup>, ETI<sup>AvrRpt2</sup>, ETI<sup>AvrPphB</sup>, ETI<sup>AvrRps4</sup> and ETI<sup>AvrRpp4</sup> leads to phosphorylation of S343 or S347 on RbohD. More sensitive methods, such as in-vitro phosphorylation and selected reaction monitoring (SRM) mass spectrometry, should be used in the future to detect phosphorylation of other residues in RbohD during ETI (Kadota et al., 2019; Picotti and Aebersold, 2012).

## **Discussion**

The conventional wisdom has long been that ETI leads to stronger immune responses compared to PTI, and that ETI alone can trigger transcriptional reprogramming, cell death, calcium influx, MAPK activation and ROS production (Grant and Loake, 2000; Grant et al., 2000; Jones and Dangl, 2006; Sohn et al., 2014; Su et al., 2018; Tao et al., 2003; Thilmony et al., 2006; Tsuda et al., 2013). An inducible-AvrRps4 line was generated to investigate whether ETI<sup>AvrRps4</sup> triggered by a pair of TIR-NLRs can activate these defence responses. Surprisingly, activation of ETI<sup>AvrRps4</sup> only triggers defence gene expression and microscopic cell death, but not tissue collapse, MAPK activation or ROS burst. Since PTI can activate MAPKs and ROS burst, it can be assumed that PTI and ETI<sup>AvrRps4</sup> activate different signalling pathways, while there could be convergent signalling pathways that

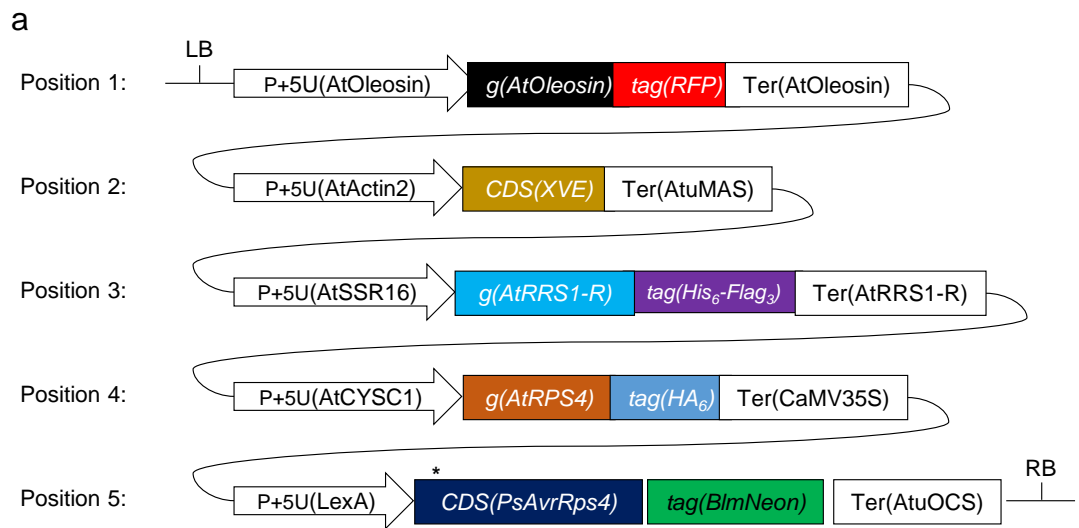
lead to transcriptional reprogramming. Although ETI<sup>AvrRps4</sup> only triggers defence gene expression and microscopic cell death, it does lead to enhanced resistance against *Pst* DC3000. This implies that ETI<sup>AvrRps4</sup> provides resistance against pathogens either through transcriptional reprogramming, microscopic cell death or other unknown mechanisms.

The CC-NLR ZAR1, on activation, forms a “resistosome” and induces cell death via its CC-domain (Wang et al., 2019a, 2019b). TIR-NLR immune activation requires the NADase activities of their TIR-domains (Horsefield et al., 2019; Martin et al., 2020; Wan et al., 2019). In addition, CC-NLRs and TIR-NLRs require different helper NLRs and signalling components for immune activation (Castel et al., 2019; Feehan et al., 2020; Qi et al., 2018; Saile et al., 2020; Wu et al., 2017, 2019). This implies that CC- and TIR-NLRs activate distinct signalling pathways and potentially different physiological responses. Using individual inducible lines that activate ETI<sup>AvrRpm1</sup>, ETI<sup>AvrRpt2</sup>, ETI<sup>AvrPphB</sup>, ETI<sup>AvrRps4</sup> and ETI<sup>AvrRpp4</sup>, immune responses triggered by different NLRs were compared (summarized in Figure 3.10). Activation of CC-NLRs, such as RPM1, RPS2 and RPS5, leads to MAPKs activation, ROS burst and macroscopic cell death; while TIR-NLRs, such as RRS1, RPS4 and RPP4, does not. Since RPM1, RPS2 and RPS5 are localised in the plasma membrane whereas RRS1, RPS4 and RPP4 are localised in the nucleus, differential responses triggered by NLRs could be due to i) requirement of different helper NLRs and signalling components, ii) their localisation, or iii) combination of the above two. Further work is required to dissect the biological implication of differential immune responses triggered by different NLRs, and the mechanisms that lead to these differences.

Since ETI<sup>AvrRps4</sup> does not trigger macroscopic cell death, ROS accumulation or MAPKs activation, it is puzzling how “PTI + ETI<sup>AvrRps4</sup>” triggers macroscopic cell death and prolonged MAPK activation (Saucet et al., 2015; Sohn et al., 2014; Su et al., 2018). As mentioned, it was assumed that the physiological outputs of “PTI + ETI” are merely additive. If this were true, these physiological responses during PTI + ETI<sup>AvrRps4</sup> would have been the same as PTI (since ETI<sup>AvrRps4</sup> does not trigger any of these physiological responses). Furthermore, the interaction between PTI and ETI is not well studied, as ETI cannot be dissected independently without the inducible system. The next chapter will focus on the interaction between these two immune systems.

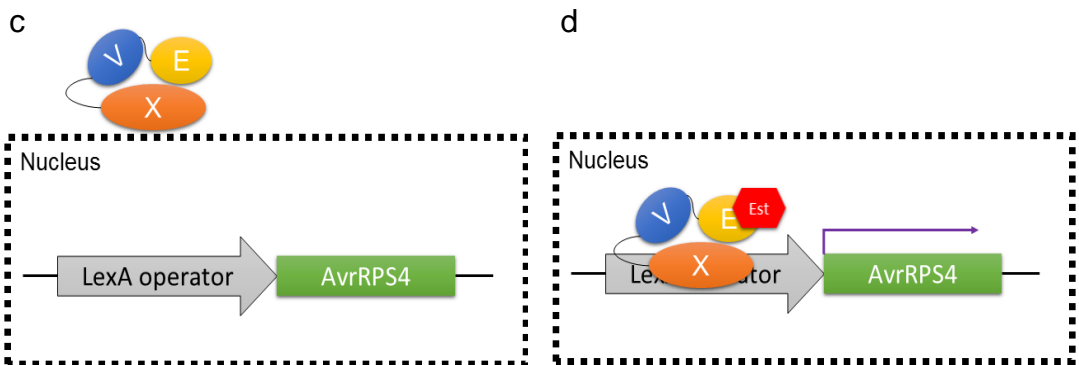
System	Patho-assay	Transient expression	Inducible system
Pre-activation	<p>PRRs NLR</p>		<p>TF</p>
Post-activation	<p>Pathogen Effector</p>	<p>Agrobacterium T-DNA</p>	<p>Estradiol (Inducer) TF</p>
Triggers PTI	✓	✓	✗
Advantage	Relatively authentic compared to the other two systems	Does not required stable transgenic lines (less time consuming)	Activates ETI in the absence of PTI

Figure 3.1. **Three methods to study ETI.** Patho-assay using pathogens, such as bacteria and fungi, to deliver effectors into plant cells. This triggers “PTI + ETI”. Transient expression with Agrobacterium. Agrobacteria deliver T-DNA into plant cells for effector expression. This also triggers “PTI + ETI”. Effector expression is induced by inducer (such as estradiol or dexamethasone) in transgenic inducible line. This allows the activation of ETI in the absence of PTI.



**b**

Module	Promoter	Gene	Function
1. Selection marker	P+5U' AtOleosin	Oleosin-RFP	Seed-specific selection (FastRED)
2. XVE module	P+5U' AtActin2	XVE	Inducible module
3. RRS1-R-HF	pAt2 (P+5U' AtSSR16)	RRS1-HF	RRS1-R with HF tag
4. RPS4-HA	pAt3 (P+5U' AtCYSC1)	RPS4-HA	RPS4 with HA tag
5. AvrRps4-mNeon/ AvrRps4 <sup>KRVY</sup> -mNeon	LexA operator (P+5U' LexA_)	AvrRps4-mNeon/ AvrRps4 <sup>KRVY</sup> -mNeon	AvrRps4 or AvrRps4 mutant with mNeon tag



**Figure 3.2. Inducible ETI<sup>AvrRps4</sup> line (SETI) design.** **a**) Illustrative layout of the SETI construct. Five individual expression units are listed as positions 1–5. Position 1, the FastRed selection marker (Shimada et al., 2010). Positions 2 and 5, chimeric trans-activator XVE (LexA-VP16-ER) and the corresponding LexA-inducible operator to express AvrRps4 (\*) or its mutant variant (AvrRps4<sup>KRVY</sup>) in the presence of estradiol treatment. Positions 3 and 4 are full-length RRS1-R and RPS4 proteins with epitope tags His<sub>6</sub>-Flag<sub>3</sub> and HA<sub>6</sub>, respectively. **b**) Tabular layout of the SETI construct. **c**) LexA operator suppresses the expression of AvrRps4 in the absence of estradiol. **d**) In the presence of estradiol, the chimeric trans-activator XVE moves into the nucleus to de-repress the expression of AvrRps4 and triggers ETI<sup>AvrRps4</sup>. This figure has also been published in Ngou et al, 2020a and appears here with permission.

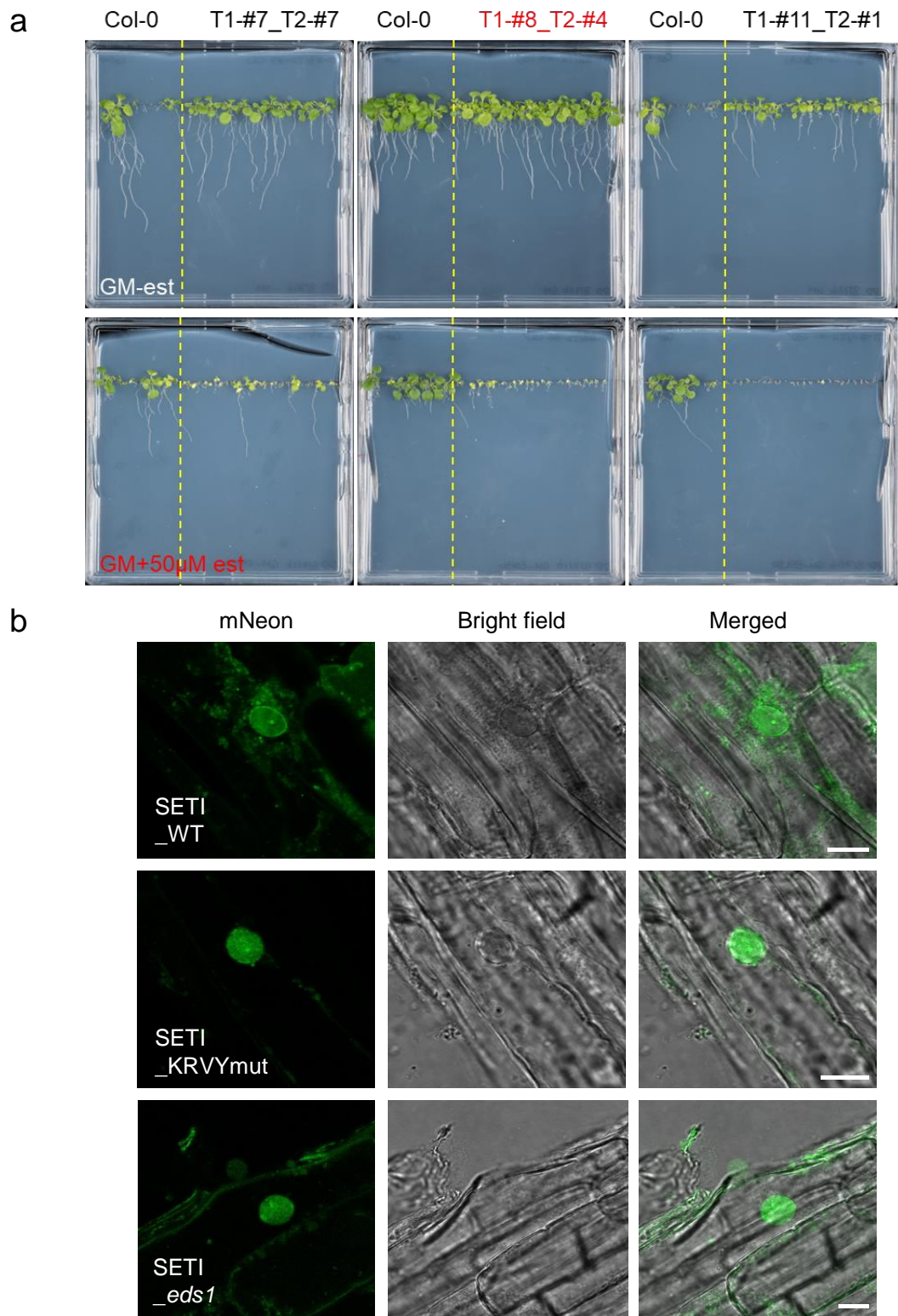


**Figure 3.3. Generation of transgenic *Arabidopsis* lines: SETI<sup>WT</sup>, SETI<sup>KRVY</sup> and SETI<sub>eds1-2</sub>.** **a)** SETI<sup>WT</sup>-transformed *Arabidopsis thaliana* transgenic seedlings were sown in GM with either 50µM estradiol (red, est) or its solvent 0.1% DMSO (-est). Images were taken 14 days post germination. Activation of ETI<sup>AvrRps4</sup> leads to growth inhibition and stunting. T1-#8 T2-#14 (red, SETI<sup>WT</sup>) was selected for further experiments. **b)** Confocal images of SETI<sup>WT</sup>, SETI<sup>KRVY</sup> and SETI<sub>eds1-2</sub> root cells expressing AvrRps4-mNeon (SETI<sup>WT</sup>, and SETI<sub>eds1-2</sub>), and AvrRps4<sup>KRVY-AAAA</sup>-mNeon (SETI<sup>KRVY</sup>) induced by 50 µM estradiol for 24 h. The mNeon channel indicates nucleocytoplasmic localization of AvrRps4. Bright field channel, a merged image of mNeon and bright field channel are also shown. Scale bars=10 µm. This figure has also been published in Ngou et al, 2020a and appears here with permission.

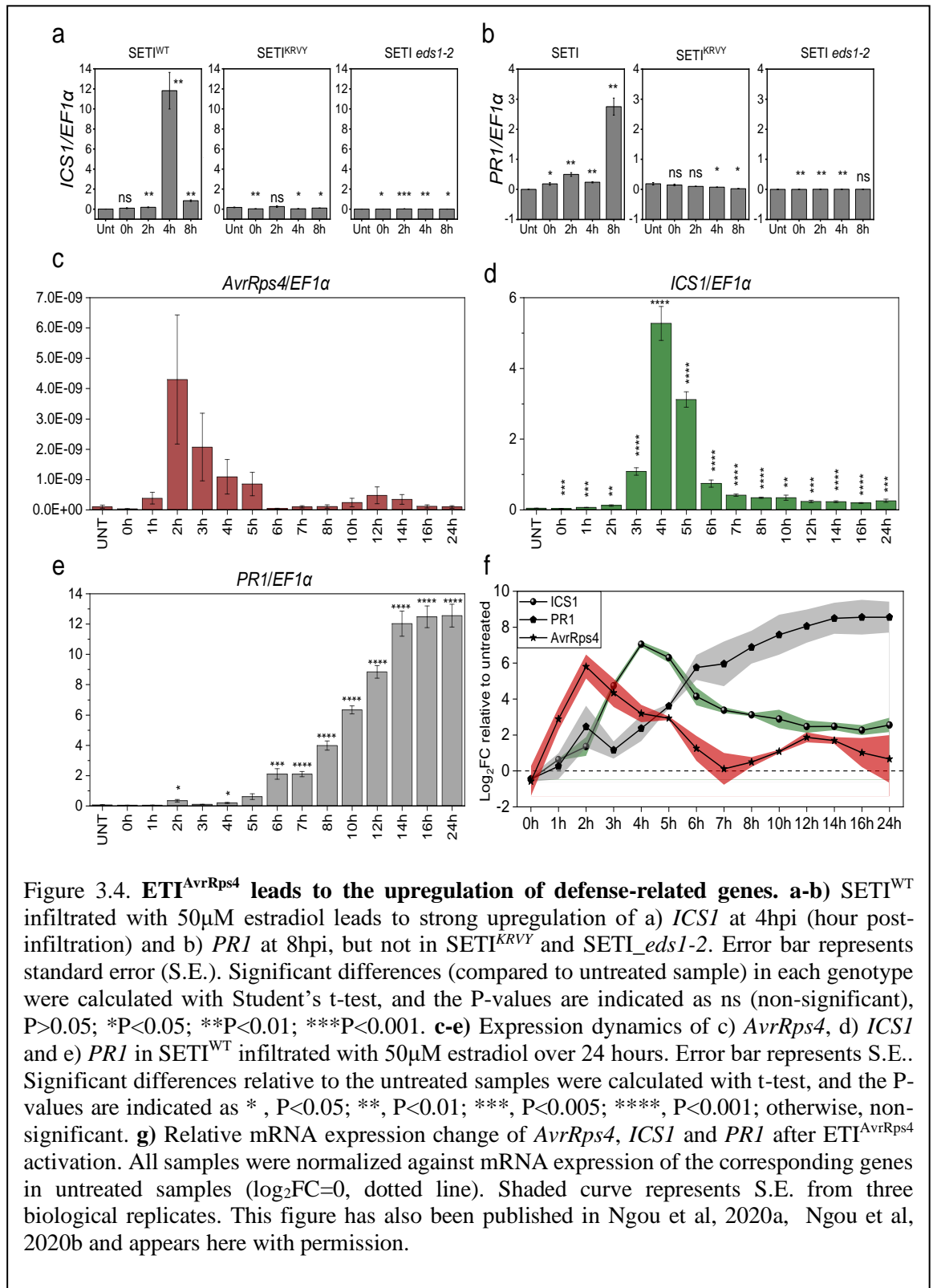


Figure 3.4. **ETI<sup>AvrRps4</sup> leads to the upregulation of defense-related genes.** **a-b)** SETI<sup>WT</sup> infiltrated with 50 $\mu$ M estradiol leads to strong upregulation of a) *ICS1* at 4hpi (hour post-infiltration) and b) *PR1* at 8hpi, but not in SETI<sup>KRVY</sup> and SETI *eds1-2*. Error bar represents standard error (S.E.). Significant differences (compared to untreated sample) in each genotype were calculated with Student's t-test, and the P-values are indicated as ns (non-significant),  $P > 0.05$ ; \* $P < 0.05$ ; \*\* $P < 0.01$ ; \*\*\* $P < 0.001$ . **c-e)** Expression dynamics of c) *AvrRps4*, d) *ICS1* and e) *PR1* in SETI<sup>WT</sup> infiltrated with 50 $\mu$ M estradiol over 24 hours. Error bar represents S.E.. Significant differences relative to the untreated samples were calculated with t-test, and the P-values are indicated as \*,  $P < 0.05$ ; \*\*,  $P < 0.01$ ; \*\*\*,  $P < 0.005$ ; \*\*\*\*,  $P < 0.001$ ; otherwise, non-significant. **g)** Relative mRNA expression change of *AvrRps4*, *ICS1* and *PR1* after ETI<sup>AvrRps4</sup> activation. All samples were normalized against mRNA expression of the corresponding genes in untreated samples ( $\log_2FC = 0$ , dotted line). Shaded curve represents S.E. from three biological replicates. This figure has also been published in Ngou et al, 2020a, Ngou et al, 2020b and appears here with permission.

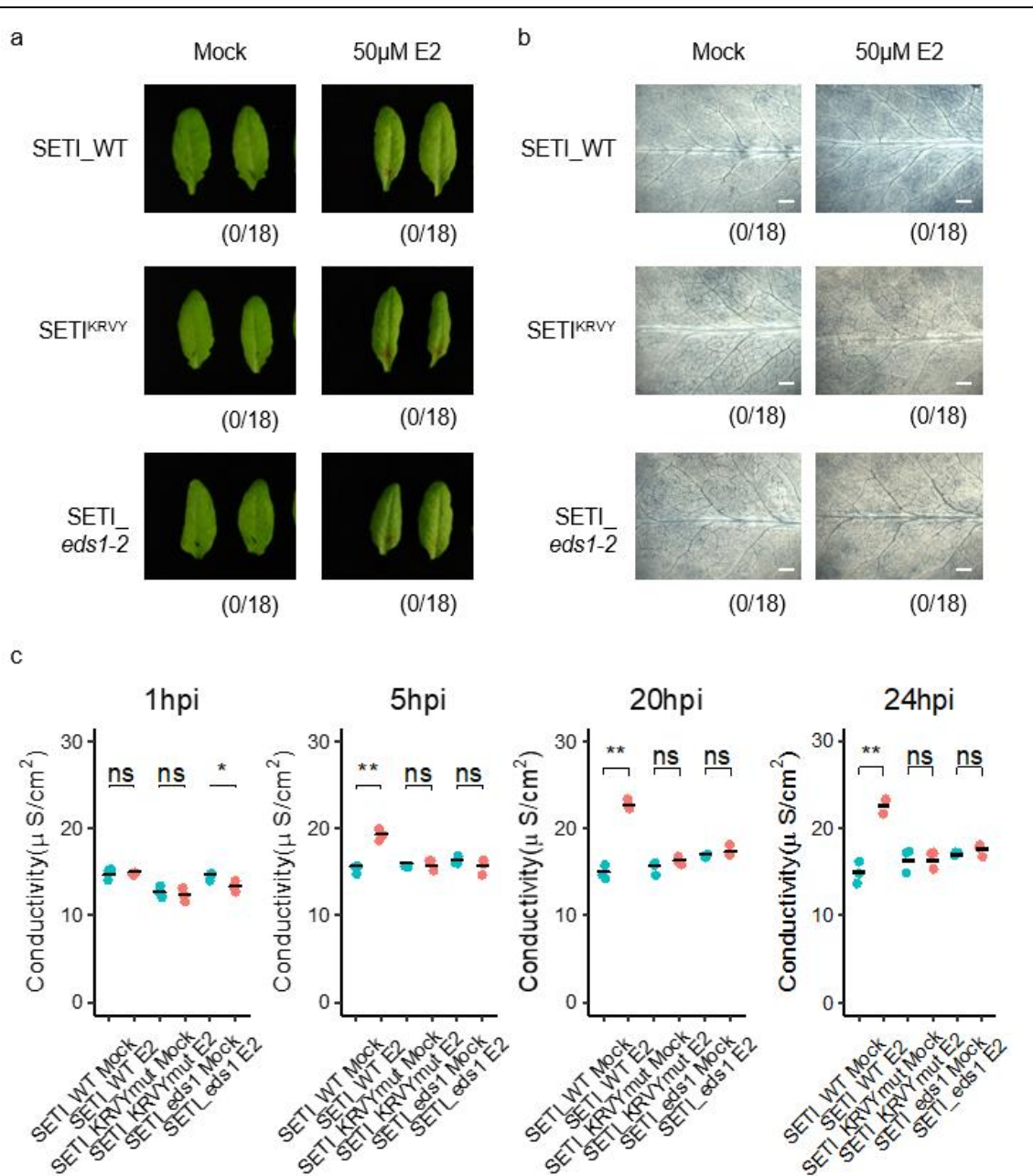
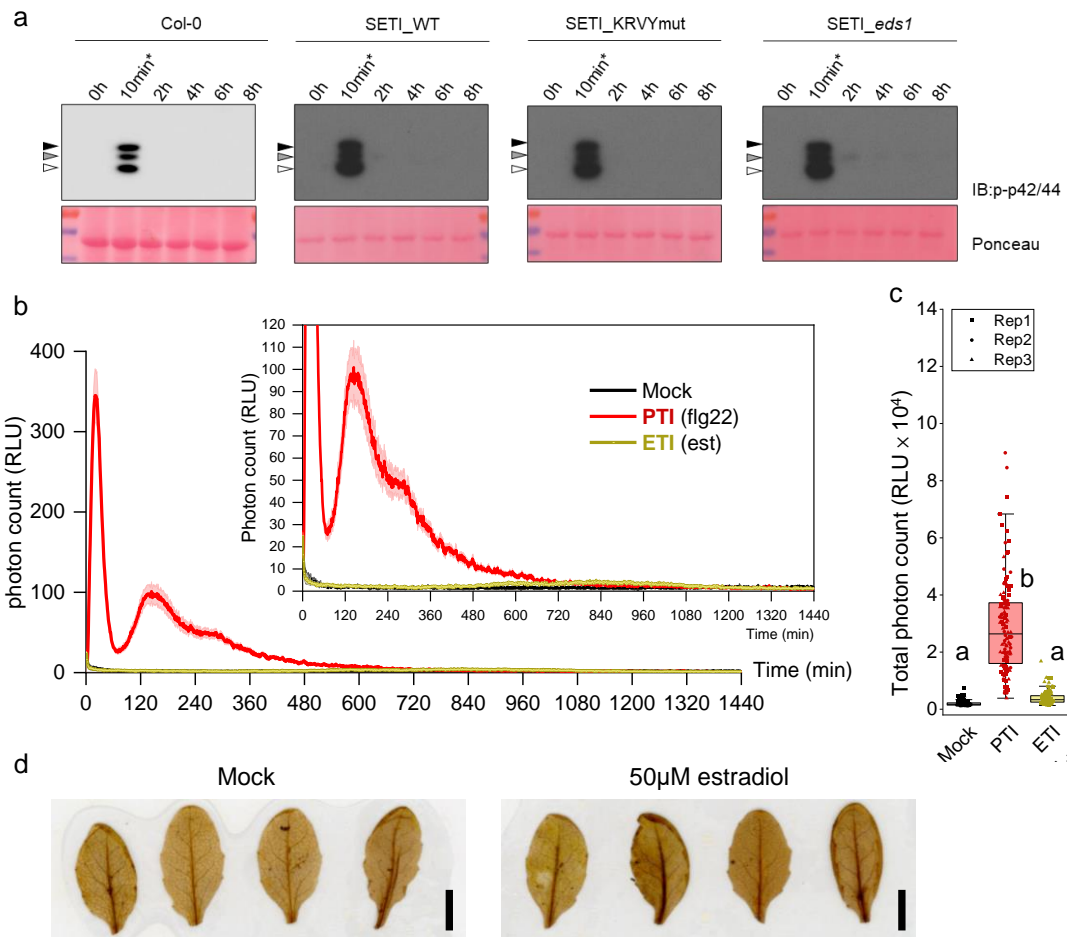
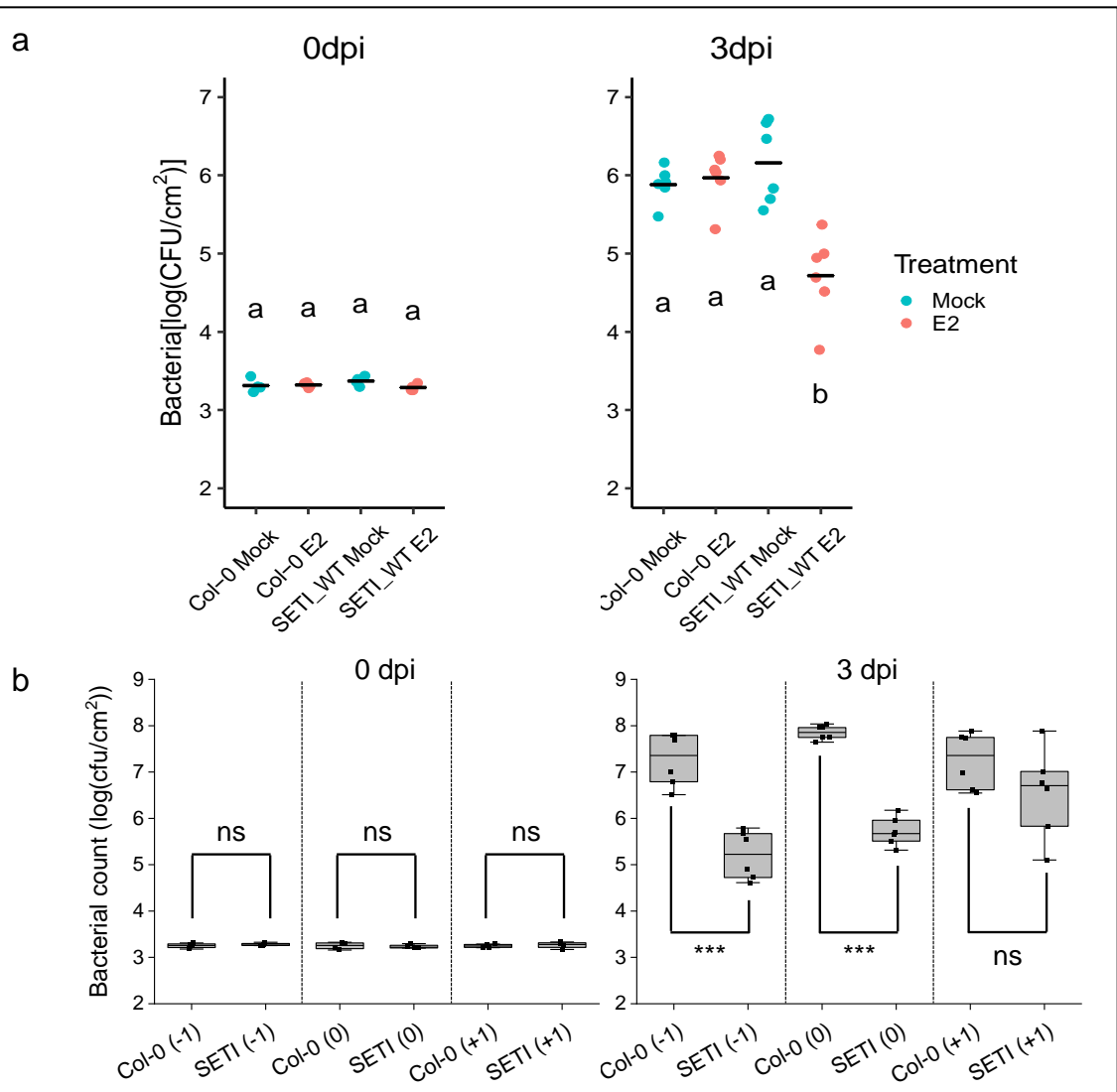


Figure 3.5. **ETI<sup>AvrRps4</sup> does not lead to macroscopic hypersensitive response (HR)** **a)** SETI<sup>WT</sup>, SETI<sup>KRVY</sup> and SETI<sub>eds1-2</sub> are infiltrated with 50 µM estradiol (E2) or mock (1% DMSO). Images were taken at 1 dpi (day post-infiltration). Numbers indicate the number of leaves displaying cell death out of the total number of infiltrated leaves. For positive control, refer to figure 3.8, 4.9 and 4.10. **b)** SETI<sup>WT</sup>, SETI<sup>KRVY</sup> and SETI<sub>eds1-2</sub> are infiltrated with 50 µM estradiol (E2) or mock (1% DMSO). After 1dpi, leaves were then stained with trypan blue solution, destained and imaged with a stereoscopic microscope. Scale bar = 0.5 mm. **c)** Five-week old SETI<sup>WT</sup>, SETI<sup>KRVY</sup> and SETI<sub>eds1-2</sub> leaves were infiltrated with mock solution (1% DMSO) or infiltrated with 50 µM estradiol (E2). Leaf discs were then collected for electrolyte leakage assay. Conductivity was measured at 1, 5, 20, and 24 hpi (hour post-infiltration). Each data point represents one technical replicate from 15 leaf discs, and three technical replicates are included per treatment and genotype in one biological replicate. Black line represents the mean. Significant differences (compared to the mock treatment) in each genotype were calculated with t-test, and the P-values are indicated as ns (non-significant), P>0.05; \*P<0.05; \*\*P<0.01; \*\*\*P<0.001. This figure has also been published in Ngou et al, 2020a and appears here with permission.



**Figure 3.6. *ETI<sup>AvrRps4</sup>* does not lead to MAPKs activation or ROS production** **a)** Col-0, *SETI<sup>WT</sup>*, *SETI<sup>KRVY</sup>* and *SETI<sup>eds1-2</sup>* seedlings were soaked in 50µM estradiol or 100 nM flg22 solution (\*, as positive control for 10 mins). Samples were taken at the indicated time-point for protein extraction. Phosphorylated MAPKs were detected using p-p42/44 antibodies. Arrowheads indicate phosphorylated MAPKs (black, pMPK6; grey, pMPK3; white, pMPK4/11). Ponceau staining was used as loading control. **b)** *SETI<sup>WT</sup>* leaf discs were soaked in mock (1% DMSO), 100 nM flg22 and 50 µM estradiol and ROS production was measured with a Photek camera over 24 hours. The y-axis was adjusted to show data from mock and ETI (in box). **c)** Total ROS production over 24 hours in mock, PTI and ETI. Data points from 3 biological replicates were analyzed with one-way ANOVA followed by Tukey's HSD test. Data points with different letters indicate significant differences of  $P < 0.01$ . **d)** *SETI<sup>WT</sup>* were infiltrated with mock (1% DMSO) or 50 µM estradiol. Leaves were stained with DAB solution 2 dpi (days post infiltration) and de-stained. Scale bars represent 1 cm. This figure has also been published in Ngou et al, 2020a, Ngou et al, 2020b and appears here with permission.



**Figure 3.7. *ETI<sup>AvrRps4</sup>* leads to resistance against *Pseudomonas syringae*** **a**) Five-week-old *SETI<sup>WT</sup>* and *Col-0* leaves were infiltrated with mock solution (1% DMSO) or with 50  $\mu$ M estradiol (E2). After 1 day, leaves were then inoculated with *Pst* DC3000 (0-day post infiltration, 0 dpi). Bacteria growth were then quantified as colony-forming units (CFU) at 0 and 3 dpi. Each data point represents two leaf discs collected from one plant. Samples from four plants were collected for 0 dpi and samples from six plants were collected for 3 dpi. The black line represents the mean. Biological significance was calculated by one-way ANOVA followed by post-hoc Tukey HSD analysis. Letters above the data points indicate significant differences between samples ( $P < 0.05$ ). **b**) Five-week-old *SETI<sup>WT</sup>* and *Col-0* leaves were infiltrated with 50  $\mu$ M estradiol one day before (-1), on the same day during (0), or one day after (+1) *Pst* DC3000 inoculation. Bacteria growth were then quantified as CFU at 0- and 3-days post *Pst* inoculation. Each data point represents two leaf discs collected from one plant. Samples from four plants were collected for 0 dpi and samples from six plants were collected for 3 dpi. Biological significance between *Col-0* and *SETI<sup>WT</sup>* with different treatments was calculated with Student's t-test, and the P-values are indicated as ns (non-significant),  $P > 0.05$ ; \* $P < 0.05$ ; \*\* $P < 0.01$ ; \*\*\* $P < 0.001$ . This figure has also been published in Ngou et al, 2020a and appears here with permission.

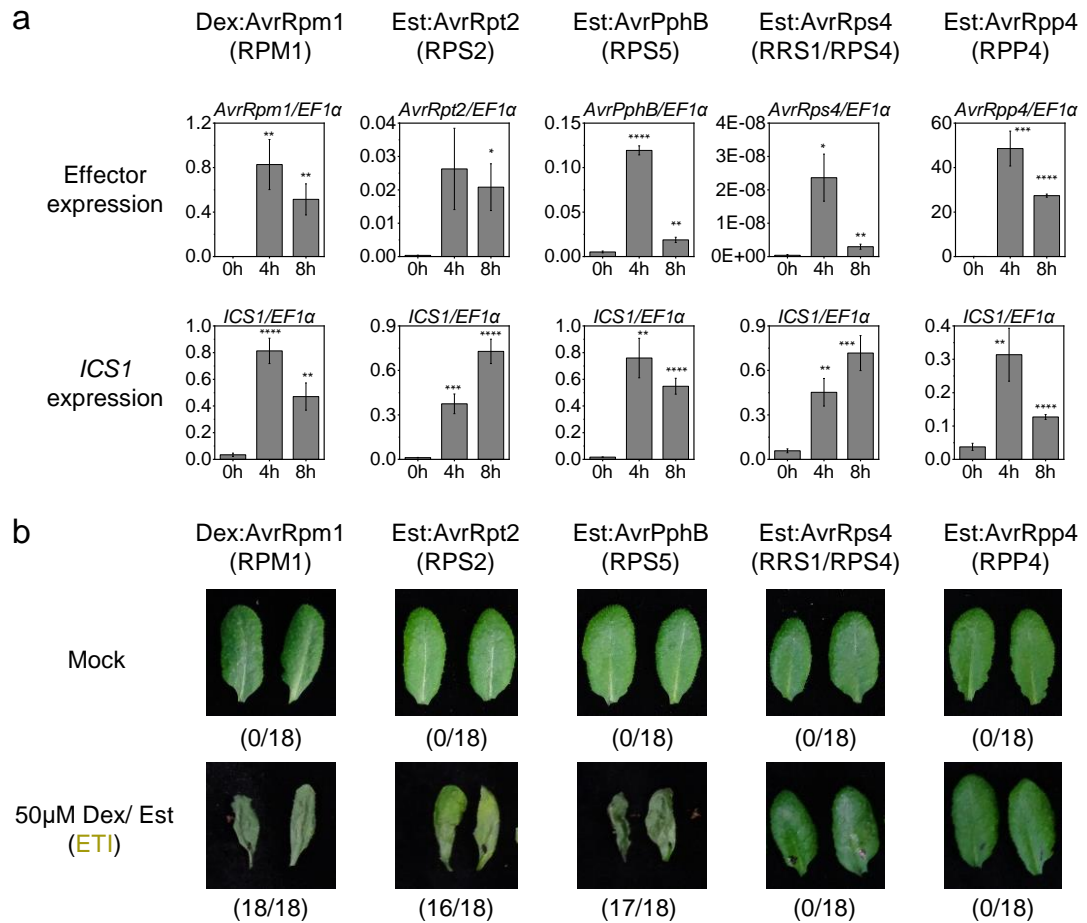


**Figure 3.8. Defense responses triggered by multiple NLRs** **a**) 5-week old dex:AvrRpm1, est:AvrRpt2, est:AvrPphB, SETI<sup>WT</sup> (est:AvrRps4) and est:AvrRpp4 leaves were infiltrated with 50 μM dexamethasone (for dex:AvrRpm1) or 50 μM estradiol (for est:AvrRpt2, est:AvrPphB, SETI<sup>WT</sup> and est:AvrRpp4) respectively. Samples were collected at indicated time point for qPCR analysis. Expression level is presented as relative to *EF1α*. The average of data points from 3 biological replicates were plotted onto the graphs, with standard error as error bars. Student's t-test was used to analyze significance in differences of 4 h, 8 h data points from 0 h. (\*,  $P \leq 0.05$ ; \*\*,  $P \leq 0.01$ ; \*\*\*,  $P \leq 0.005$ ; \*\*\*\*,  $P \leq 0.001$ ; otherwise, not significant). **b**) 5-week old dex:AvrRpm1, est:AvrRpt2, est:AvrPphB, SETI<sup>WT</sup> (est:AvrRps4) and est:AvrRpp4 leaves were infiltrated with 50 μM dexamethasone (for dex:AvrRpm1) or 50 μM estradiol (for est:AvrRpt2, est:AvrPphB, SETI<sup>WT</sup> and est:AvrRpp4) respectively. All pictures were taken 3 days post infiltration. The numbers indicate the number of leaves displaying HR out of the total number of leaves infiltrated. This figure has also been published in Ngou et al, 2020b and appears here with permission.

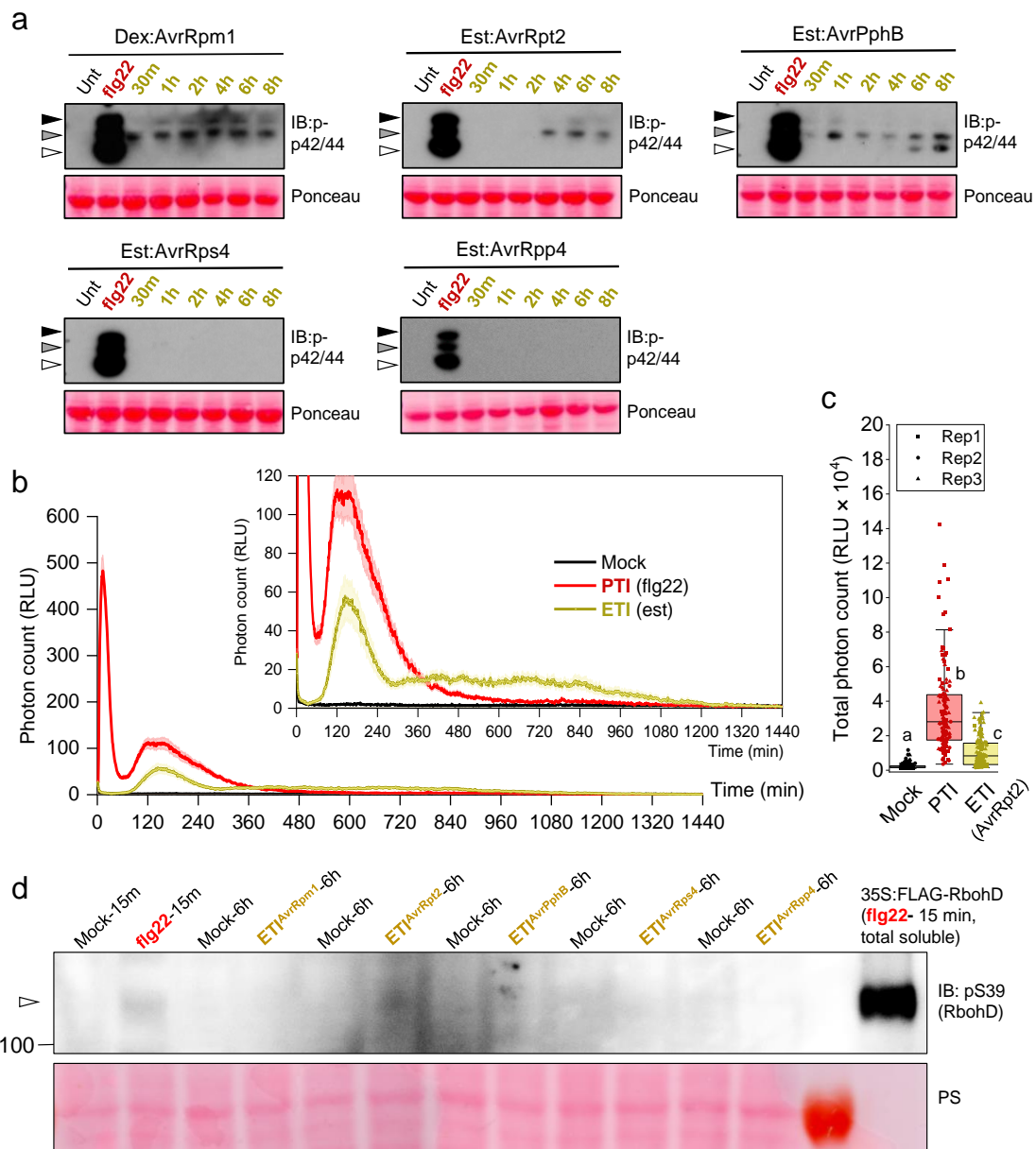


**Figure 3.9. Cellular responses triggered by multiple NLRs** **a)** Seedlings of dex:AvrRpm1, est:AvrRpt2, est:AvrPphB, SETI<sup>WT</sup> (est:AvrRps4) and est:AvrRpp4 leaves were soak in 100nM flg22 (for 15 mins as positive control), or 50  $\mu$ M dexamethasone (for dex:AvrRpm1) or 50  $\mu$ M estradiol (for est:AvrRpt2, est:AvrPphB, SETI<sup>WT</sup> and est:AvrRpp4) respectively. Samples were collected at indicated time point for immunoblotting with p-p42/44 antibodies. Arrowheads indicate phosphorylated MAPKs (black, pMPK6; grey, pMPK3; white, pMPK4/11). Ponceau staining (PS) was used as loading control. **b)** Est:AvrRpt2 leaf discs were soaked in mock (1% DMSO), 100 nM flg22 and 50  $\mu$ M estradiol and ROS production was measured with a Photek camera over 24 hours. The y-axis was adjusted to show data form mock and ETI (in box). **c)** Total ROS production over 24 hours in mock, PTI and ETI. Data points from 3 biological replicates were analyzed with one-way ANOVA followed by Tukey's HSD test. Data points with different letters indicate significant differences of  $P < 0.01$ . **d)** Seedlings of Col-0, dex:AvrRpm1, est:AvrRpt2, est:AvrPphB, SETI<sup>WT</sup> (est:AvrRps4) and est:AvrRpp4 leaves were soak in mock or 100 nM flg22 (Col-0, for 15 mins as positive control), 50  $\mu$ M dexamethasone or 50  $\mu$ M estradiol (for 6 h) respectively. Samples were collected at indicated time point for microsomal protein extraction. RbohD with S39 phosphorylation were detected using pS39 antibodies (white arrowhead). Total soluble protein extraction from RbohD over-expression line (35S::FLAG-RbohD) treated with 100 nM flg22 (for 15 mins) was used as additional positive control. Ponceau staining (PS) was used as loading control. This figure has also been published in Ngou et al, 2020b and appears here with permission.

Immune response	HR (Macroscopic)	MAPK phosphorylation	RbohD phosphorylation (S39, S343, S347)	ROS burst	Salicylic acid biosynthesis gene ( <i>ICS1</i> ) induction
PTI	✗	✓ (Transient)	✓ (S39, S343, S347)	✓ (Transient)	✓ (Relatively weak)
CC-ETI (Activated by CC-NLRs)	✓	✓ (Relatively weak but prolonged)	✓ (ETI <sup>AvrRpt2</sup> , only on S343 and S347)	✓ (ETI <sup>AvrRpt2</sup> , relatively weak)	✓ (Relatively stronger)
TIR-ETI (Activated by TIR-NLRs)	✗ (Microscopic)	✗	✗	✗	✓ (Relatively stronger)

Figure 3.10. **Comparison of physiological changes induced by different immune responses in Arabidopsis.** Macroscopic HR cannot be induced by PTI or ETI activated by TIR-NLRs (TIR-ETI) alone. PTI leads to robust but transient ROS burst and MAPKs phosphorylation (Macho and Zipfel, 2014). ETI activated by CC-NLRs (CC-ETI) leads to weak but prolonged ROS burst and MAPK phosphorylation. RbohD has been reported to be phosphorylated at S39, S343 and S347 during PTI (Kadota et al., 2014; Li et al., 2014b). ETI<sup>AvrRpt2</sup> can also lead to S343 and S347, but not S39 phosphorylation in RbohD (Kadota et al., 2019). S39 phosphorylation in RbohD also cannot be observed during ETI triggered by AvrRpm1, AvrRpt2, AvrPphB, AvrRps4 or AvrRpp4. PTI can induce relatively weak *ICS1* expression compared to ETI (Sohn et al., 2014), ETI triggered by AvrRpm1, AvrRpt2, AvrPphB, AvrRps4 and AvrRpp4 can all induce relatively strong *ICS1* expression.

## **Chapter 4: Mutual Potentiation of Plant Immunity by Cell-surface and Intracellular Receptors**

This chapter is largely identical to (Ngou et al., 2020b). The publication is under the CC-BY license.

### **Abstract**

The plant immune system involves extracellular PRRs that detect pathogen-derived molecules such as PAMPs, and intracellular receptors that recognize pathogen-secreted effectors. Surface receptor-mediated immunity, or PTI, has been extensively studied but intracellular receptor-mediated immunity, or ETI, is rarely studied alone. How these two immune systems interact is therefore poorly understood. Using the inducible-effector system, a mutual potentiation relationship between these two systems was discovered. PTI leads to the activation of multiple protein kinases and NADPH oxidases, whereas ETI elevates the abundance of these proteins. Reciprocally, the hypersensitive response triggered by ETI is enhanced by the activation of PTI. Activation of either PTI or ETI alone is insufficient to provide resistance against *P. syringae* strain DC3000. Thus, PTI and ETI mutually potentiate each other to activate robust defense against pathogens. These findings on the relationship between the two immune systems reshape our understanding of plant immunity.

### **Introduction**

Pattern recognition receptors (PRRs) associate with plasma-membrane-associated co-receptor kinases and receptor-like cytoplasmic kinases (RLCKs) following PAMP recognition (Macho and Zipfel, 2014). Ligand-dependent association between these receptors triggers multiple cellular responses including calcium influx, rapid production of ROS, activation of MAPKs. These cellular changes lead to physiological responses including stomata closure, callose deposition and induction of defence genes (Bigeard et al., 2015; Couto and Zipfel, 2016; Macho and Zipfel, 2014). Together these responses lead to resistance by restricting pathogen invasion and propagation.

Virulent pathogens evade resistance through secretion of effectors, which target multiple cellular processes including PTI, to ensure successful infection (Zhang et al., 2017). Intracellular NLR receptors activate ETI upon recognition of these effectors, but in contrast to PTI responses, ETI-mediated downstream responses are poorly defined. Despite recent progress in understanding immune receptor activation, our understanding of how PTI and ETI co-function to protect plants from pathogens is incomplete.

### **Pre-activation of ETI leads to enhanced PTI-induced ROS production**

As shown in the previous chapter, pre-activation of ETI<sup>AvrRps4</sup> in SETI<sup>WT</sup> leads to enhanced resistance against virulent bacteria *Pst* DC3000. The enhanced resistance could be due to an enhanced PTI response during ETI. To test the effect of ETI on PTI, SETI<sup>WT</sup> was pre-treated with mock (0.1% DMSO) or estradiol (50  $\mu$ M) to pre-activate ETI<sup>AvrRps4</sup> for 6 hours; 100 nM flg22 was then added to induce ROS production (Figure 4.1a). Compared to mock pre-treatment, estradiol pre-treatment leads to elevated ROS production triggered by flg22. Induction of ETI<sup>AvrRps4</sup> alone does not activate ROS production (Figure 4.1b-c). The same experiment was repeated with SETI *eds1-2*. Pre-activation of ETI with estradiol does not lead to enhanced ROS production triggered by flg22 in *eds1-2* background (Figure 4.1d-e). These data indicate that ETI<sup>AvrRps4</sup> elevates PTI-induced ROS production.

### **Co-activation of PTI and ETI leads to enhanced ROS production and accumulation**

During pathogen infection, PTI is activated before effectors are delivered into the plant cell. To mimic this, SETI<sup>WT</sup> was treated with either mock, 100nM flg22 (to trigger PTI), 50  $\mu$ M estradiol (to trigger ETI<sup>AvrRps4</sup>), or flg22 + estradiol (to activate “PTI + ETI<sup>AvrRps4</sup>”) respectively (Figure 4.2a) and ROS production was measured. “PTI + ETI<sup>AvrRps4</sup>” leads to significantly stronger ROS accumulation compared to PTI alone, particularly during the third phase (phase III; 5-16 hours) of the ROS burst, while ETI<sup>AvrRps4</sup> alone does not trigger ROS burst at any time-point (Figure 4.2b-d). As shown in the previous chapter, ETI<sup>AvrRpt2</sup> can also activate weak ROS burst. Est:AvrRpt2 was treated with either mock, 100nM flg22, 50  $\mu$ M estradiol (to trigger ETI<sup>AvrRpt2</sup>), or flg22 + estradiol (to activate “PTI + ETI<sup>AvrRpt2</sup>”) and ROS production was measured over 16 hours. ETI<sup>AvrRpt2</sup> also potentiates flg22-induced ROS burst, especially during phase II (1-5 hours) (Figure 4.2e-g). Thus, ETI triggered by either TIR- or CC-NLRs can enhance ROS production triggered by PTI.

Furthermore, I tested if PTI triggered by multiple PAMPs or DAMP can also be potentiated by ETI<sup>AvrRps4</sup>. 100 nM elf18 (activates EFR and BAK1), 100 nM pep1 (activates PEPR1, PEPR2 and BAK1), 100 nM C10:0 (activates LORE), 100 nM nlp20 (activates RLP23, SOBIR1 and BAK1) and 1 mg/mL chitin (activates LYK5 and CERK1) were used to trigger PTI. “PTI + ETI<sup>AvrRps4</sup>” triggered by all PAMPs or DAMP leads to significantly stronger ROS accumulation compared to PTI alone, particularly during phase III (Figure 4.3). Thus, ETI can enhance PTI-induced ROS production triggered by multiple PRRs.

As “PTI + ETI” leads to an enhanced ROS burst, ETI might enhance H<sub>2</sub>O<sub>2</sub> accumulation triggered by PTI. SETI<sup>WT</sup> leaves were infiltrated with either mock, *Pst* DC3000 *hrcC* mutant (*hrcC*<sup>-</sup>; to trigger PTI), 50  $\mu$ M estradiol (to trigger ETI<sup>AvrRps4</sup>), or estradiol + *hrcC*

(to activate “PTI + ETI<sup>AvrRps4</sup>”) respectively and H<sub>2</sub>O<sub>2</sub> accumulation was monitored through DAB staining. Significant H<sub>2</sub>O<sub>2</sub> accumulation could be observed after “PTI + ETI<sup>AvrRps4</sup>” treatment, but not from PTI or ETI<sup>AvrRps4</sup> treatment alone (Figure 4.4a). This implies that ETI<sup>AvrRps4</sup> can enhance ROS accumulation triggered by PTI.

### **Additional physiological hallmarks of PTI are enhanced by ETI**

H<sub>2</sub>O<sub>2</sub> accumulation during PTI promotes cross-linking of proteins and phenolics in cell wall, which leads to callose deposition (Luna et al., 2011; Voigt, 2014). SETI<sup>WT</sup> leaves was infiltrated with either mock, *hrcC*, 50 μM estradiol or estradiol + *hrcC* respectively. Callose deposition was stained and quantified by aniline blue solution. Interestingly both PTI and ETI<sup>AvrRps4</sup> alone induce callose deposition. This implies that ETI<sup>AvrRps4</sup> leads to callose deposition in a H<sub>2</sub>O<sub>2</sub>-independent manner. More importantly, callose deposition induced by “PTI + ETI<sup>AvrRps4</sup>” is significantly higher than the sum of those induced by PTI and ETI<sup>AvrRps4</sup> alone (Figure 4.4b-c). This indicates that PTI and ETI function synergistically and mutually potentiate callose deposition.

Another hallmark of PTI is transcriptional reprogramming. Activation of MAPKs and CDPKs lead to the upregulation of PTI-responsive genes such as *FLG22-INDUCED RECEPTOR-LIKE KINASE 1 (FRK1)*, *NDR1/HIN1-LIKE 10 (NHL10)*, *FAD-LINKED OXIDOREDUCTASE 1 (FOX1)*, *PEROXIDASE 4 (PER4)* and *WRKY DNA-BINDING PROTEIN 33 (WRKY33)* (Boudsocq et al., 2010; Li et al., 2016a). SETI<sup>WT</sup> leaves were infiltrated with either mock, *hrcC*, 50 μM estradiol or estradiol + *hrcC* for 24 hours, and expression of these genes were determined by qPCR analysis. Expression of *FRK1*, *NHL10*, *FOX1*, *PER4* and *WRKY33* was significantly higher after “PTI + ETI<sup>AvrRps4</sup>” treatment compared to PTI or ETI<sup>AvrRps4</sup> treatment alone (Figure 4.4d). In contrast, expression of *ICS1*, which is highly induced during ETI, is similar between “PTI + ETI<sup>AvrRps4</sup>” treatment and ETI<sup>AvrRps4</sup> treatment alone (Figure 4.4d). In summary, physiological responses induced by PTI are potentiated by ETI.

### **Pre-activation of PTI and ETI leads to enhanced activation of PTI-signaling components**

Potentiation of PTI-induced physiological responses during ETI could be due to enhanced activation of signaling components. Upon PAMP recognition by PRRs, RLCK-VII family members, such as BIK1, are phosphorylated. This leads to the phosphorylation of the RbohD at its 39<sup>th</sup> and 343<sup>rd</sup> serine residues (S39 and S343), resulting in ROS accumulation and callose deposition. PTI also leads to the activation of MAPKs which contribute to transcriptional reprogramming and other downstream responses (Figure 4.5a).

SETI<sup>WT</sup> leaves were pre-treated with either mock or 50  $\mu$ M estradiol to pre-activate ETI<sup>AvrRps4</sup> for 6 hours; 100 nM flg22 was then infiltrated to activate PTI and samples were collected at different time points for immunoblotting analysis. Compared to mock pre-treatment, estradiol pre-treatment led to enhanced and prolonged phosphorylation of MPK3, BIK1 and RbohD (at S39 and S343) triggered by flg22 (Figure 4.5b-d). As shown in the previous chapter, induction of ETI<sup>AvrRps4</sup> by estradiol alone did not lead to MPK3 and RbohD phosphorylation at S39. Estradiol pre-treatment also does not lead to BIK1, MPK3 or RbohD phosphorylation until PTI is induced. These data indicate that ETI<sup>AvrRps4</sup> enhances activation of PTI-signaling components.

### **Co-activation of ETI leads to enhanced activation of PTI-signaling components**

To mimic natural infection, SETI<sup>WT</sup> leaves were treated with either *hrcC*<sup>-</sup> or estradiol + *hrcC*<sup>-</sup> and samples were collected over a time-course of 24 hours for immunoblotting analysis. Compared to PTI treatment, “PTI + ETI<sup>AvrRps4</sup>” treatment led to prolonged phosphorylation of MPK3, BIK1 and RbohD at S39 (Figure 4.5e-g). Since ETI<sup>AvrRps4</sup> alone does not activate these signaling components, the prolonged activation is not due to the additive effect of PTI and ETI<sup>AvrRps4</sup>, but the potentiation of PTI by ETI<sup>AvrRps4</sup>. In summary, activation of PTI-signaling components is enhanced during ETI, which in turn leads to enhanced PTI-induced physiological responses.

### **ETI leads to protein accumulation of PTI signaling components**

It was unclear how ETI potentiates the activation of PTI-signaling components. Pre-activation of ETI<sup>AvrRps4</sup> leads to stronger MPK3, BIK1 and RbohD accumulation than mock pre-treatment, and “PTI + ETI<sup>AvrRps4</sup>” leads to prolonged and stronger accumulation of MPK3, BIK1 and RbohD than PTI alone. To test whether ETI leads to accumulation of PTI signaling components, protein levels were monitored during ETI triggered by multiple effectors. Dex:AvrRpm1, est:AvrRps2, est:AvrPphB, SETI<sup>WT</sup> and est:AvrRpp4 were infiltrated with either 50  $\mu$ M dex (for dex:AvrRpm1) or 50  $\mu$ M est (for est:AvrRps2, est:AvrPphB, SETI<sup>WT</sup> and est:AvrRpp4) and samples were collected at 0, 4 or 8 hpi for immunoblotting analysis. ETI<sup>AvrRpm1</sup>, ETI<sup>AvrRpt2</sup>, ETI<sup>AvrPphB</sup>, ETI<sup>AvrRps4</sup> and ETI<sup>AvrRpp4</sup> activation leads to robust protein accumulation of BAK1, SOBIR1, BIK1, RbohD and MPK3, but not MPK4, MPK6, CERK1 or FLS2 (Figure 4.6). This is consistent with the previous observation that PTI-induced phosphorylation of MPK3, but not MPK4 or MPK6, is enhanced by ETI<sup>AvrRps4</sup>. Thus, ETI alone leads to robust protein accumulation of some PTI signaling components, which, in turn, enhances their activation during PTI.

## **ETI reverses suppression of PTI during ETS**

The original "zig-zag-zig" model suggested that ETI alone triggers a strong immune response to overcome effector-triggered susceptibility (ETS) from pathogen effectors (Jones and Dangl, 2006). It was unclear whether PTI and ETI activated the same or distinct mechanisms to induced defense, as the immune responses activated by ETI (in the absence of PTI) were rarely investigated. The data above (including previous chapter) led to the hypotheses that (i) PTI triggers the main defense mechanisms against pathogens and (ii) ETI functions primarily to restore and enhance effector-attenuated PTI by replenishing signaling components.

To test these hypotheses, SETI<sup>WT</sup> plants were challenged with non-virulent *Pst* DC3000 *hrcC*<sup>-</sup>. PTI was activated and protein levels of BIK1 and RbohD were slightly elevated. MAPKs were also activated as indicated by their elevated phosphorylation level (Figure 4.7a). When SETI<sup>WT</sup> plant were challenged the virulent strain *Pst* DC3000, PTI-induced MAPK activation and protein accumulation of BIK1 and RbohD were reduced compared to *hrcC*<sup>-</sup> infection (Figure 4.7a). This is caused by ETS from *Pst* DC3000. When SETI<sup>WT</sup> plant were challenged by virulent *Pst* DC3000 together with 50  $\mu$ M estradiol to induce ETI<sup>AvrRps4</sup>, reduced accumulation of BIK1, RbohD and MPK3 were restored and elevated. ETI<sup>AvrRps4</sup> also led to prolonged phosphorylation of MAPKs (Figure 4.7a). These results indicate that ETI can overcome ETS and restores PTI capacity. A refinement of the zig-zag-zig model is proposed, in which ETI provides robust resistance by restoring and elevating PTI through upregulation of PTI signaling components, compensating for their turnover and attenuation by ETS (Figure 4.7b).

## **ETI functions through PTI**

The above proposed model implies that NLR-mediated resistance or ETI functions through PRR-mediated resistance or PTI. ETI is rarely activated without PTI during natural infections. The requirement of PTI in NLR-dependent resistance was then tested by infecting the PTI-compromised mutant *bak1-5 bkk1-1* (PRR co-receptor mutant) with *Pst* DC3000 delivering AvrRps4. *bak1-5 bkk1-1* is as susceptible as *rps4-2 rps4b-2* mutant that is unable detect AvrRps4 (Figure 4.8a). A similar experiment was performed with *fls2 efr* (PRR mutant) and similar results were observed (Figure 4.8b). *fls2 efr* is not as susceptible as *bak1-5 bkk1-1*, likely due to other PAMPs or DAMPs (such as pep1 and C10:0) being recognized in the *fls2 efr* mutant. In addition, *rps4-2 rps4b-2* mutant is not deficient in PTI-induced ROS burst and MAPK activation (Figure 4.8c-e). Together, these demonstrate that

PTI is required for *RPS4/RRS1*-dependent resistance against *P. syringae*, and that activation of ETI in the absence of PTI is insufficient to provide effective resistance in *Arabidopsis*. In addition, (Yuan et al., 2020) also independently showed that PTI is required for resistance mediated by RPS2, RPS5 and RRS1/RPS4.

### **PTI potentiates ETI<sup>AvrRps4</sup>-induced hypersensitive response**

*P. fluorescens* is a soil bacterium without type-III secretion system (Grant et al., 2006; Ma et al., 2003). A *P. fluorescens* strain, named effector-to-host analyzer; or EtHAN (abbreviated as Pf0-1 here), was developed to deliver effectors into plant cell by introducing the *hrp/hrc* region from *Pseudomonas syringae pv. syringae 61* (Thomas et al., 2009). With Pf0-1 EtHAN system, we can study ETI/ETS triggered by a single effector without interference by other type-III effectors from *Pseudomonas syringae*. As shown in the previous chapter, ETI<sup>AvrRps4</sup> alone does not lead to macroscopic HR, while macroscopic HR and tissue collapse can be observed in Col-0 after infiltration with Pf0-1 delivering AvrRps4 (Pf0-1:AvrRps4<sup>WT</sup>, triggers “PTI + ETI<sup>AvrRps4</sup>”) (Sohn et al., 2009, 2014). It was then hypothesized that both PTI and ETI<sup>AvrRps4</sup> activation is required to induce macroscopic HR.

SETI<sup>WT</sup> leaves were infiltrated with either Pf0-1:AvrRps4<sup>WT</sup> (triggers “PTI + ETI<sup>AvrRps4</sup>”), Pf0-1 strain delivering AvrRps4<sup>KRVY</sup> (Pf0-1:AvrRps4<sup>mut</sup>, triggers PTI), 50  $\mu$ M estradiol (triggers ETI<sup>AvrRps4</sup>) or estradiol + Pf0-1:AvrRps4<sup>mut</sup> (mimics “PTI + ETI<sup>AvrRps4</sup>”). Co-infiltration of estradiol and Pf0-1:AvrRps4<sup>mut</sup> leads to similar macroscopic HR induced by Pf0-1:AvrRps4<sup>WT</sup> infiltration, while estradiol or Pf0-1:AvrRps4<sup>mut</sup> infiltration alone did not lead to macroscopic HR (Figure 4.9a). To validate these results, the same experiment was performed, and electrolyte leakage was monitored over a time-course of 24 hours. Co-infiltration of estradiol and Pf0-1:AvrRps4<sup>mut</sup> resulted in similar ion leakage induced by Pf0-1:AvrRps4<sup>WT</sup> infiltration, which is significantly higher than both estradiol or Pf0-1:AvrRps4<sup>mut</sup> infiltration alone (Figure 4.9b).

To test if PTI induced by other PAMPs or DAMPs could also potentiate HR, the estradiol co-filtration experiment was performed in SETI<sup>WT</sup> with either *hrcC*, a wild-type *P. fluorescens* strain (without type-III secretion system), a mixture of PAMPs and DAMP (1  $\mu$ M flg22, elf18 and pep1), or single PAMP/DAMP (1  $\mu$ M flg22, 1  $\mu$ M elf18, 1  $\mu$ M pep1, 1  $\mu$ M C10:0, 1  $\mu$ M nlp20 or 1 mg/mL chitin) to activate PTI. In all cases, co-infiltration of estradiol combined with PTI elicitors leads to macroscopic HR (Figure 4.10a-b). This implies that PTI activated by different PRRs can potentiate ETI<sup>AvrRps4</sup>-activated HR.

### **PTI potentiates ETI-induced hypersensitive response**

ETI<sup>AvrRpp4</sup> alone also cannot induce macroscopic HR. Co-activation of PTI (by *hrcC*) and ETI<sup>AvrRpp4</sup> in *est:AvrRpp4* leads to enhanced HR (Figure 4.10c). Therefore, HR triggered by the TIR-NLRs, RRS1, RPS4 and RPP4 can all be potentiated by PTI. As previously shown, activation of ETI<sup>AvrRpm1</sup>, ETI<sup>AvrRpt2</sup> and ETI<sup>AvrPphB</sup> can trigger macroscopic HR and tissue collapse in the absence of PTI. To test whether HR triggered by these CC-NLRs could also be potentiated by PTI, reduced quantities of estradiol or dexamethasone were used to prevent macroscopic cell death induced by AvrRpt2, AvrRpm1 and AvrPphB. At these levels, ETI<sup>AvrRpt2</sup>, ETI<sup>AvrRpm1</sup> and ETI<sup>AvrPphB</sup>-mediated HR was also enhanced by PTI (by *hrcC*) (Figure 4.10c). Thus, PTI activation enhances ETI-induced HR triggered by both CC- and TIR-NLRs.

### **PTI potentiates ETI-induced HR through MAPKs and NADPH oxidases**

Previously, multiple PTI signaling components, such as BAK1, MAPKs, RbohD and RbohF, have been reported to be involved in HR (Domínguez-Ferreras et al., 2015; Su et al., 2018; Torres et al., 2002; Yun et al., 2011). As shown in the previous chapter, MAPKs phosphorylation and ROS burst were observed during CC-NLR (ETI<sup>AvrRpm1</sup>, ETI<sup>AvrRpt2</sup> and ETI<sup>AvrPphB</sup>), but not TIR-NLR activation (ETI<sup>AvrRps4</sup> or ETI<sup>AvrRpp4</sup>). Macroscopic HR was also only observed during ETI<sup>AvrRpm1</sup>, ETI<sup>AvrRpt2</sup> and ETI<sup>AvrPphB</sup>, but not during ETI<sup>AvrRps4</sup> or ETI<sup>AvrRpp4</sup>. Thus, there is a positive correlation between MAPKs phosphorylation, ROS production and macroscopic HR. Since the activation of BIK1, MPK3 and RbohD is potentiated during ‘‘PTI + ETI’’, the enhanced HR by PTI might involve ETI-potentiated activities of MAPKs and NADPH oxidases.

I further investigated the requirement of MAPKs and NADPH oxidases in ‘‘PTI + ETI’’ induced HR. Since *mpk3 mpk6* double mutant is lethal, a chemical genetic approach was used. *MPK6SR* is a *mpk3 mpk6* double mutant complemented by a mutant *MPK6* allele (*MPK6*<sup>YG</sup>, with a relative bigger ATP binding pocket), whose activity can be specifically inhibited by the protein kinase inhibitor, 1-NA-PP1. 1-NA-PP1 is a bulky ATP analogue which specifically targets *MPK6*<sup>YG</sup> (Su et al., 2017; Xu et al., 2014). Col-0 and *MPK6SR* were pre-treated with either mock or 10  $\mu$ M 1-NA-PP1 for 3 hours, leaves were then infiltrated with pf0-1:empty vector (to activate PTI) or pf0-1:AvrRps4<sup>WT</sup> (to activate ‘‘PTI + ETI<sup>AvrRps4</sup>’’). *MPK6SR* pretreated with 1-NA-PP1 has attenuated macroscopic HR after Pf0-1:AvrRps4<sup>WT</sup> infiltration compared to Col-0, consistent with previous reports (Figure 4.11a) (Su et al., 2018). Furthermore, HR induced by Pf0-1:AvrRps4<sup>WT</sup> is reduced in the NADPH oxidase mutant *rbohD rbohF* (Figure 4.11b). Together, these results show that MAPKs and NADPH oxidase activation make indispensable contributions to the HR.

## Discussion

While the mechanism of PTI has been studied in detail, the consequences of activating ETI without PTI, and the relationship between PTI and ETI was poorly understood. As discussed, most mechanistic studies of ETI have been done by comparing PTI with “PTI + ETI”, with very few studies on ETI alone in the absence of PTI. The data in these two chapters show that PTI and ETI result in distinct physiological outputs and initiate distinct chains of signalling events. Through studying ETI alone, it was also discovered that the stronger immune response during “PTI + ETI” is not merely additive, but due to mutual potentiation between these two systems.

One of the main questions in the plant immunity field is how does ETI lead to resistance against pathogens. These data shed new light on how ETI provides effective resistance, by showing that ETI functions through restoring and potentiating PTI. PTI has been shown to halt pathogens through multiple mechanisms including restriction of nutrient supply, cell wall fortification, suppression of effector secretion and induction of antimicrobial compounds (Anderson et al., 2014; Crabill et al., 2010; Luna et al., 2011; Nobori et al., 2018; Voigt, 2014; Yamada et al., 2016b). Since ETI halts pathogens through the potentiation of PTI, it would be interesting to test if the above PTI-induced defence mechanisms are also prolonged or potentiated by ETI. In summary, surface receptor-mediated immunity (PTI) and intracellular receptor-mediated immunity (ETI) function together to provide a more robust disease resistance than either alone. These data, together with those of (Yuan et al., 2020), support a model in which cellular processes and physiological responses triggered by PTI act as the primary source of immunity, and ETI acts to replenish and enhance PTI signalling components and downstream signalling, counteracting its attenuation by either pathogen effectors or turnover upon activation. In turn, enhanced activation of MAPKs and Rboh proteins can potentiate macroscopic HR triggered by ETI to further restrict pathogen proliferation and colonisation (Figure 4.12).

ETI potentiates PTI through the upregulation of PTI signalling components. There could be additional mechanisms by which ETI potentiates PTI, other than increasing protein abundance. The stability of FLS2, RbohD and BIK1 are dependent on post-translational modifications such as ubiquitination (Lee et al., 2020; Lu et al., 2011; Ma et al., 2020a; Monaghan et al., 2014; Robatzek et al., 2006). Recent reports suggested that multiple signalling components are also ubiquitinated during PTI (Grubb et al., 2020; Ma et al., 2020b). Additional mechanisms, such as alternative splicing and protein inhibition, can also attenuate PTI activation (Couto and Zipfel, 2016; Dressano et al., 2020; Liang et al., 2016). Whether ETI leads to de-repression of these inhibitions remains to be determined. In

addition, the mechanisms by which ETI leads to increased protein abundance of PTI signalling components is unclear. These will be investigated further in the next chapter.

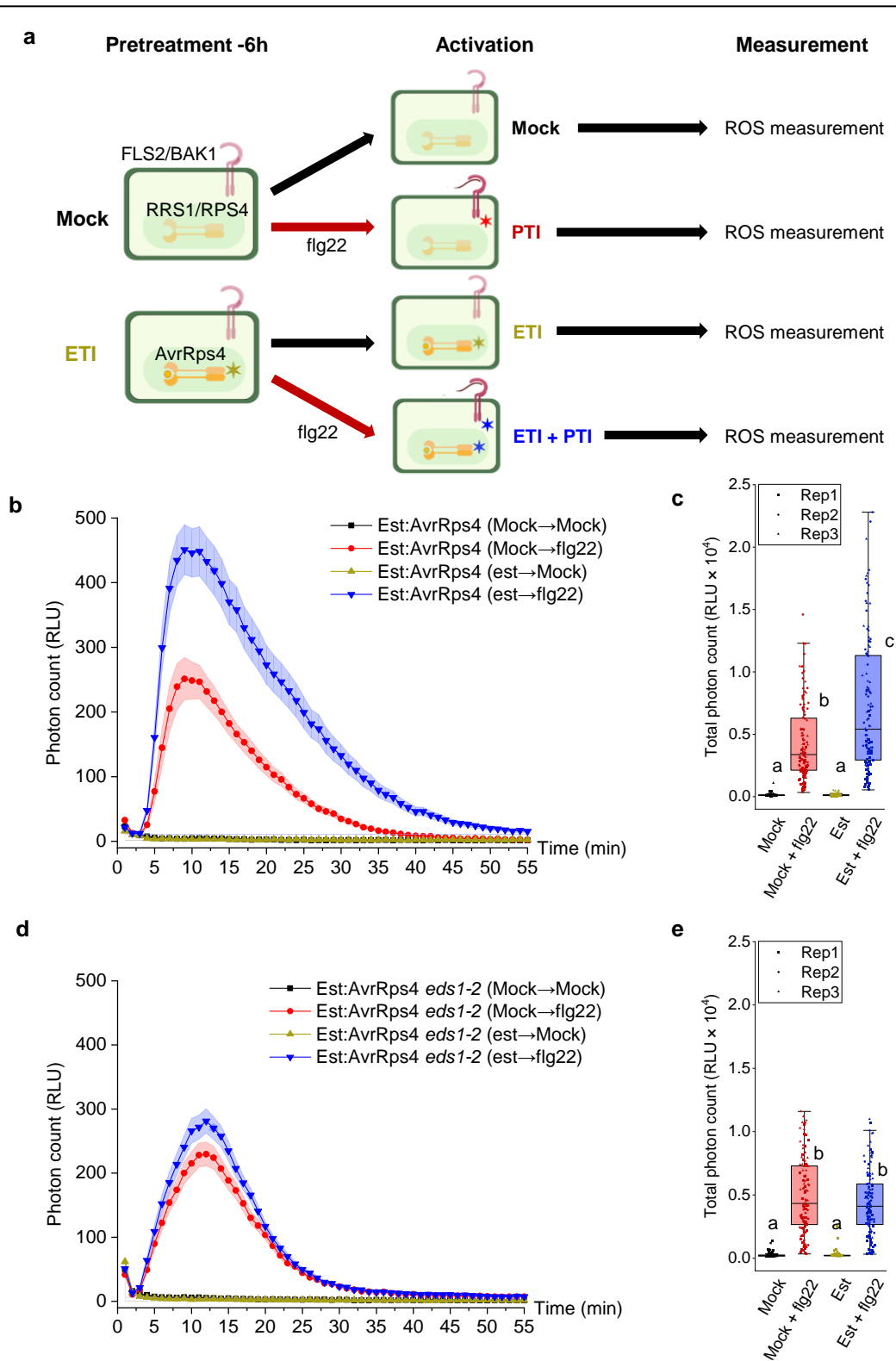
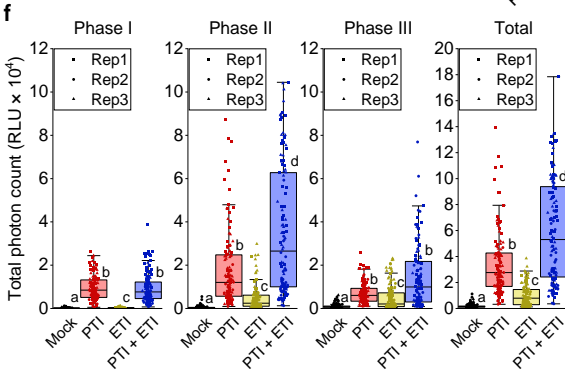
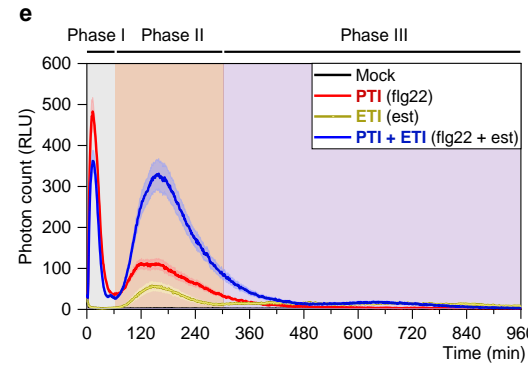
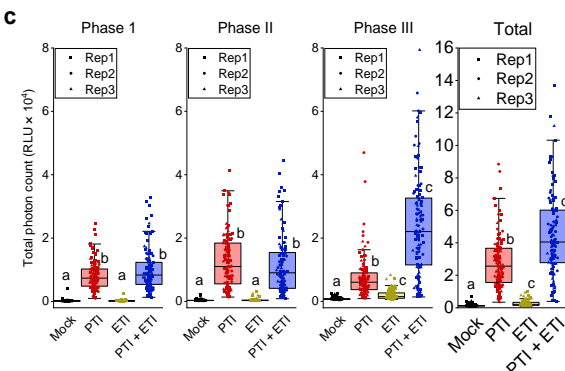
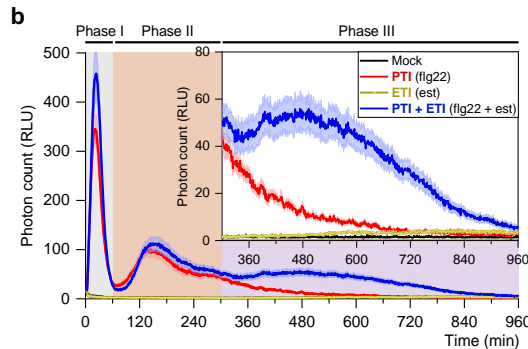
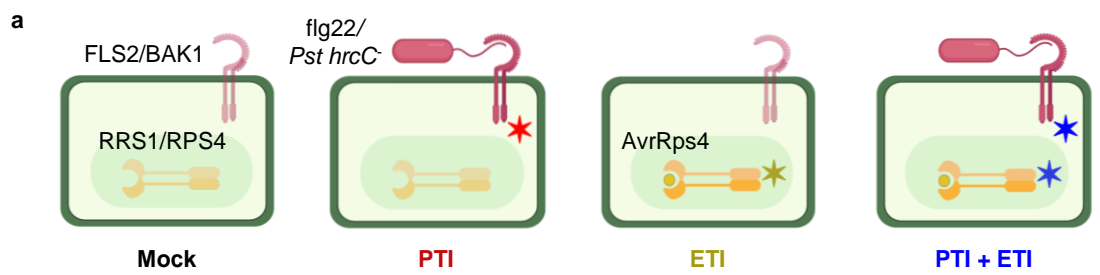


**Figure 4.1. Pre-activation of ETI leads to enhanced PTI-induced ROS production** **a)** Experiment design. Est:AvrRps4 (SETI<sup>WT</sup>) lines were treated with mock (1% DMSO) or 50  $\mu$ M estradiol for 6 h. Mock or 100 nM flg22 solution was then added and ROS production was measured for 55 mins. **b)** Est:AvrRps4 (SETI<sup>WT</sup>) leaves pre-treated with estradiol shows enhanced ROS burst induced by flg22. **c)** Total ROS production over 55 mins in different conditions. **d)** Est:AvrRps4 *eds1-2* leaves pre-treated with estradiol do not show enhanced ROS burst induced by flg22. **e)** Total ROS production over 55 mins in different conditions. **c, e)** Data points together from 3 biological replicates were analyzed with Kruskal-Wallis test followed by Dunn's test. Data points with different letters indicate significant differences of  $P < 0.05$ . This figure has also been published in Ngou et al, 2020b and appears here with permission.



Phase	Treatment			
	Mock	PTI (flg22)	ETI (AvrRps4)	PTI + ETI
Phase I (0-1h)	218 ±34	8097 ±409	212 ±20	9832 ±590
Phase II (1-5h)	376 ±21	12687 ±793	446 ±36	11526 ±837
Phase III (5-16h)	861 ±36	7533 ±592	2045 ±128	23963 ±1441
Total (0-16h)	1455 ±70	27369 ±1283	2702 ±154	44247 ±2381

Phase	Treatment			
	Mock	PTI (flg22)	ETI (AvrRpt2)	PTI + ETI
Phase I (0-1h)	216 ±14	9552 ±515	275 ±17	9546 ±620
Phase II (1-5h)	595 ±62	17738 ±1606	4675 ±526	35716 ±2715
Phase III (5-16h)	1121 ±89	6997 ±445	5064 ±548	14477 ±1332
Total (0-16h)	1932 ±143	34287 ±2297	10015 ±752	59739 ±3598

**Figure 4.2. Co-activation of PTI and ETI leads to enhanced ROS production and accumulation** **a**) Experiment design. SETI<sup>WT</sup> lines were treated with either mock (1% DMSO), 100 nM flg22 (PTI), 50 μM estradiol (ETI) or flg22 + estradiol (PTI + ETI). ROS production was measured over 16 hours. **b**) SETI<sup>WT</sup> leaves co-activated with PTI + ETI show enhanced ROS production during phase III (purple, 5-16 h). Standard error (S.E.) is shown as shade around curve. **c**) Total ROS production during phase I (0-1 h), phase II (1-5 h), phase III (5-16 h) and total (0-16 h) in SETI<sup>WT</sup> during different conditions. **e**) Est:AvrRpt2 leaves co-activated with PTI + ETI show enhanced ROS production during phase II and phase III (orange and purple, 1-16 h). S.E. is shown as shade around curve. **f**) Total ROS production during phase I, phase II, phase III and total in Est:AvrRpt2 during different conditions. **d, g**) Tabular summary of total ROS production during different phases and conditions. **c, f**) Data points together from 3 biological replicates were analyzed with Kruskal-Wallis test followed by Dunn's test. Data points with different letters indicate significant differences of P < 0.05. This figure has also been published in Ngou et al, 2020b and appears here with permission.

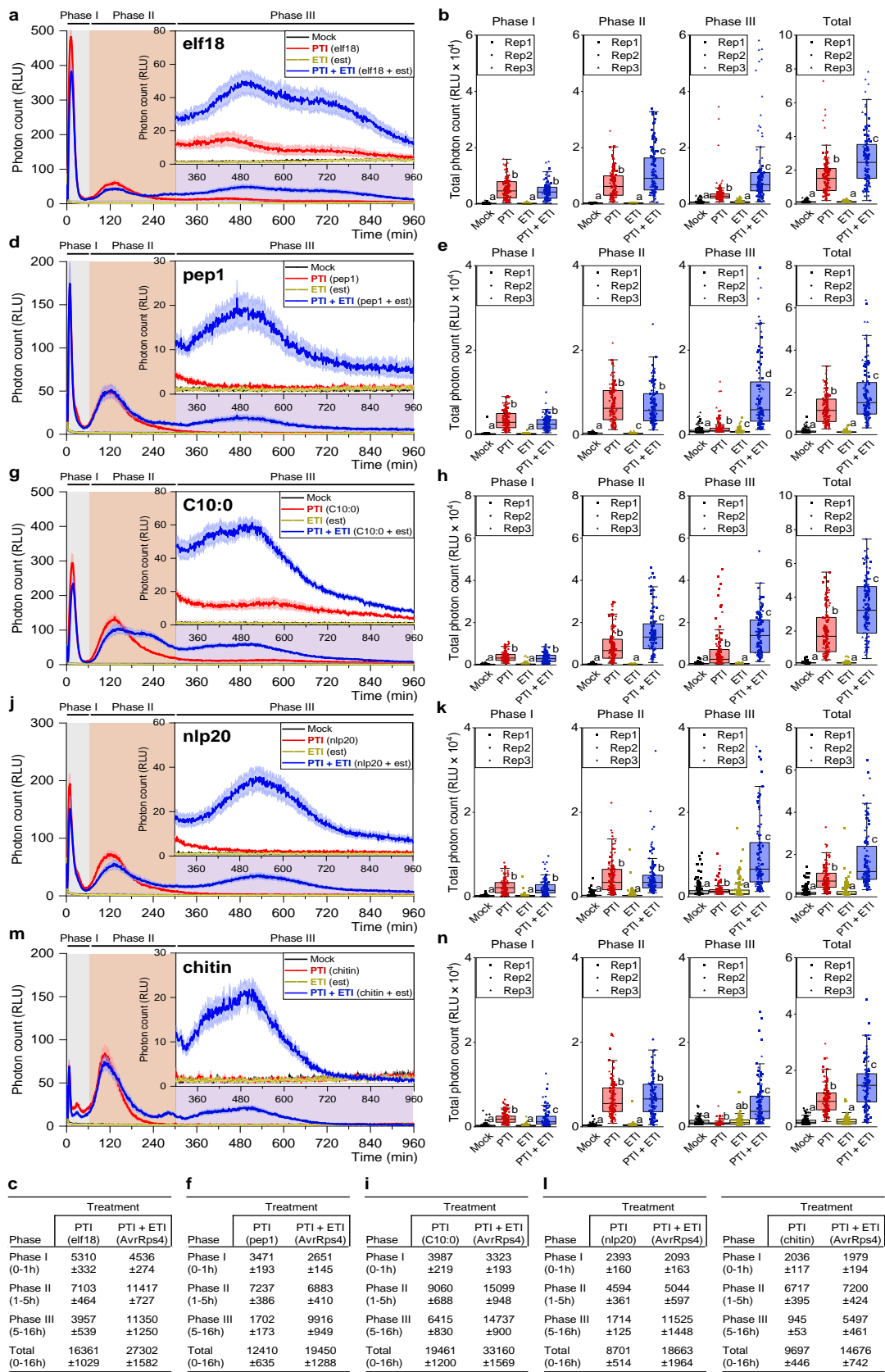


**Figure 4.3. Co-activation of PTI triggered by different PAMPs or DAMP and ETI leads to enhanced ROS accumulation** a) SET1<sup>WT</sup> lines were treated with either mock (1% DMSO), 100 nM elf18 (a-c)/ 100 nM pep1(d-f)/ 100 nM C10:0 (g-i)/ 100 nM nlp20 (j-l)/ 1 mg/mL chitin (m-o) (PTI), 50  $\mu$ M estradiol (ETI) or flg22 + estradiol (PTI+ETI). ROS production was measured over 16 hours. (a, d, g, j, m) Standard error is shown as shade around curve. (b, e, h, k, n) Data points together from 3 biological replicates were analyzed with Kruskal-Wallis test followed by Dunn's test. Data points with different letters indicate significant differences of  $P < 0.05$ . This figure has been published in Ngou et al, 2020b and appears here with permission.

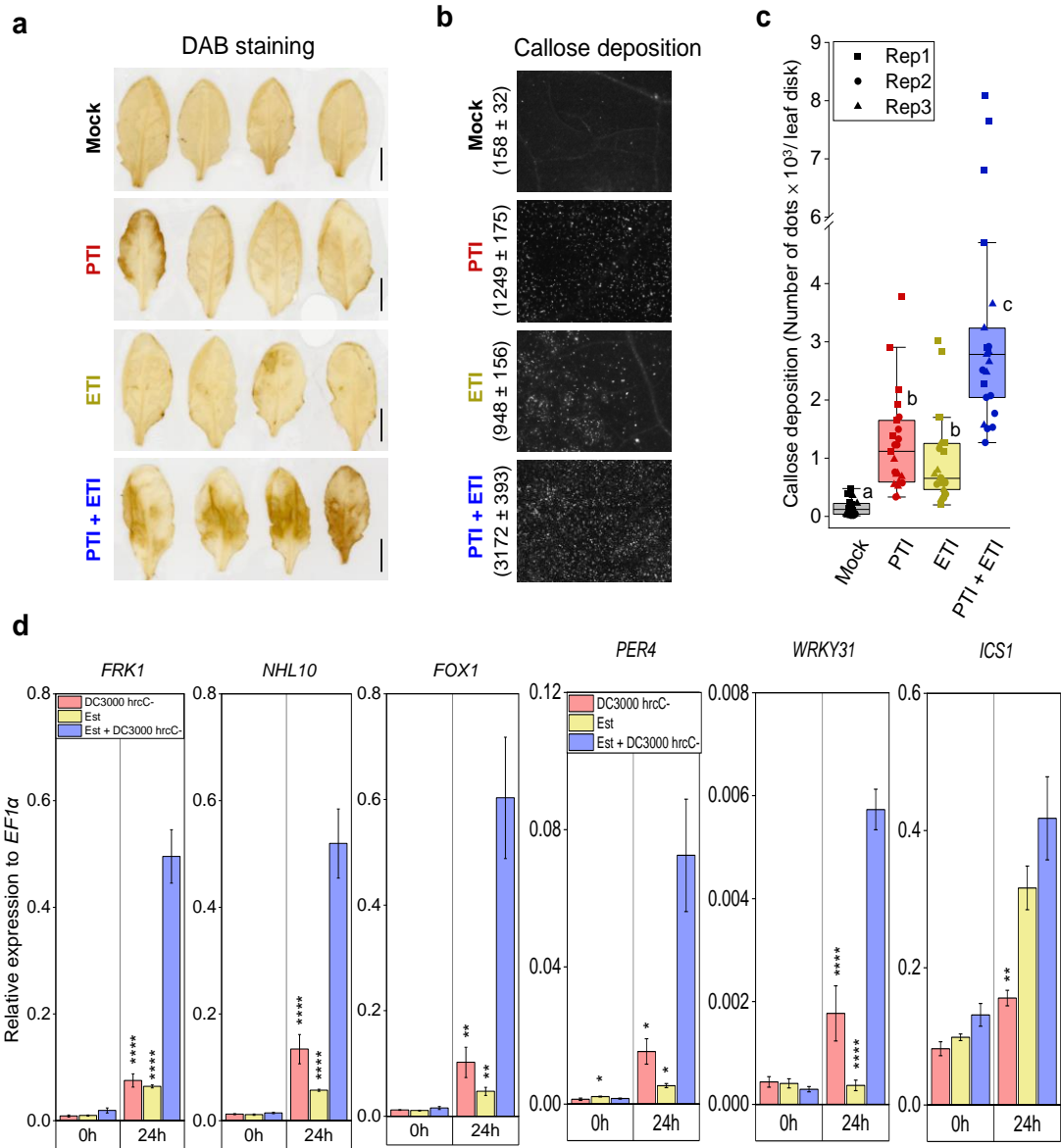


**Figure 4.4. Multiple physiological responses of PTI are enhanced by ETI** **a**) *SET1*<sup>WT</sup> lines were treated with either mock (1% DMSO), *hrcC* (PTI), estradiol (ETI) or *hrcC* + estradiol (PTI + ETI). Hydrogen peroxide was stained with DAB solution one day post infiltration (dpi). Scale bar represents 1 cm. **b**) *SET1*<sup>WT</sup> lines were treated with either mock (1% DMSO), *hrcC* (PTI), estradiol (ETI) or *hrcC* + estradiol (PTI + ETI). Callose deposition was visualized with analine blue solution 1 dpi. **c**) Total callose quantification in different conditions. Data points together from 3 biological replicates were analyzed with Kruskal-Wallis test followed by Dunn's test. Data points with different letters indicate significant differences of  $P < 0.05$ . **d**) *SET1*<sup>WT</sup> leaves were infiltrated with either, *hrcC* (PTI, red), estradiol (ETI, yellow) or *hrcC* + estradiol (PTI + ETI, blue). Samples were collected at indicated time point for qPCR analysis. PTI + ETI leads to a stronger *FRK1*, *NHL10*, *FOX1* (*AT1G26380*), *PER4* and *WRKY31* transcript accumulation compared to PTI or ETI alone. The average of data points from 3 biological replicates were plotted onto the graphs, with  $\pm$ S.E. for error bars. Student's t-test was used to analyze significance differences between PTI + ETI and PTI or ETI (\*,  $P \leq 0.05$ ; \*\*,  $P \leq 0.01$ ; \*\*\*,  $P \leq 0.005$ ; \*\*\*\*,  $P \leq 0.001$ ; otherwise, not significant). This figure has also been published in Ngou et al, 2020b and appears here with permission.

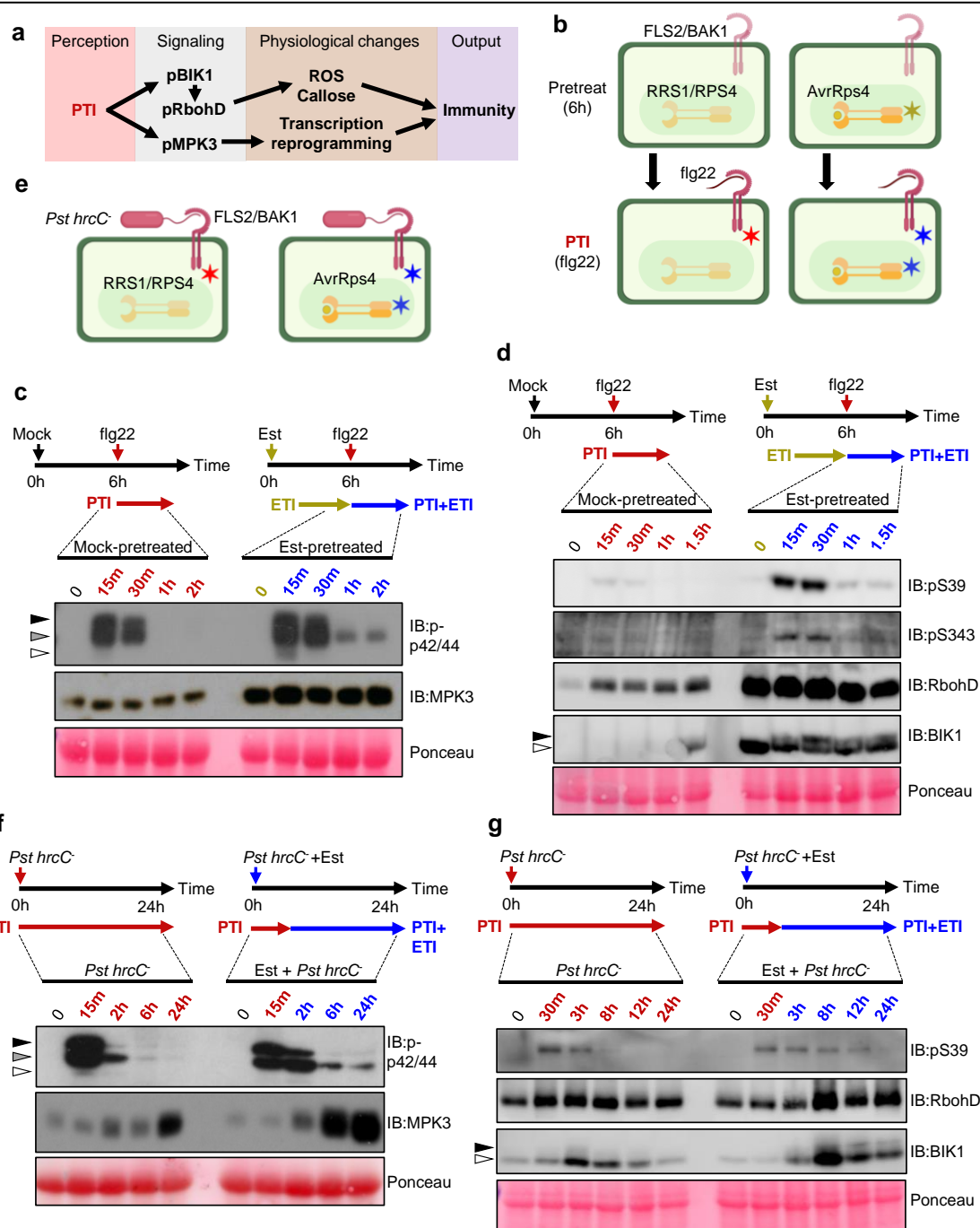


**Figure 4.5. Activation of PTI and together with ETI leads to enhanced activation of PTI-signalling components** a) PTI signaling pathway. b) Schematic representation of “ETI pre-activation” experimental design. ETI<sup>AvrRps4</sup> was pre-activated by spraying with 50  $\mu$ M estradiol for 6 h. \* indicates activated immune system. c) ETI<sup>AvrRps4</sup> pre-treatment leads to accumulation and prolonged phosphorylation of MPK3 compared to mock pre-treatment. Ponceau staining (PS) was used as loading control. d) ETI<sup>AvrRps4</sup> pre-treatment leads to accumulation and prolonged phosphorylation of BIK1 and RbohD (in S39 and S343) compared to mock pre-treatment. Microsomal fractions from each sample were isolated for immunoblotting. PS was used as loading control. e) Schematic representation of “natural infection mimicking” experimental design. ETI<sup>AvrRps4</sup> was co-activated with PTI. \* indicates activated immune system. f) PTI co-activated with ETI<sup>AvrRps4</sup> leads to stronger accumulation and prolonged phosphorylation of MPK3 compared to PTI. PS was used as loading control. g) PTI co-activated with ETI<sup>AvrRps4</sup> leads to stronger accumulation and prolonged phosphorylation of BIK1 and RbohD (in S39 and S343) compared to mock pre-treatment. Microsomal fractions from each sample were isolated for immunoblotting. PS was used as loading control. This figure has also been published in Ngou et al, 2020b and appears here with permission.

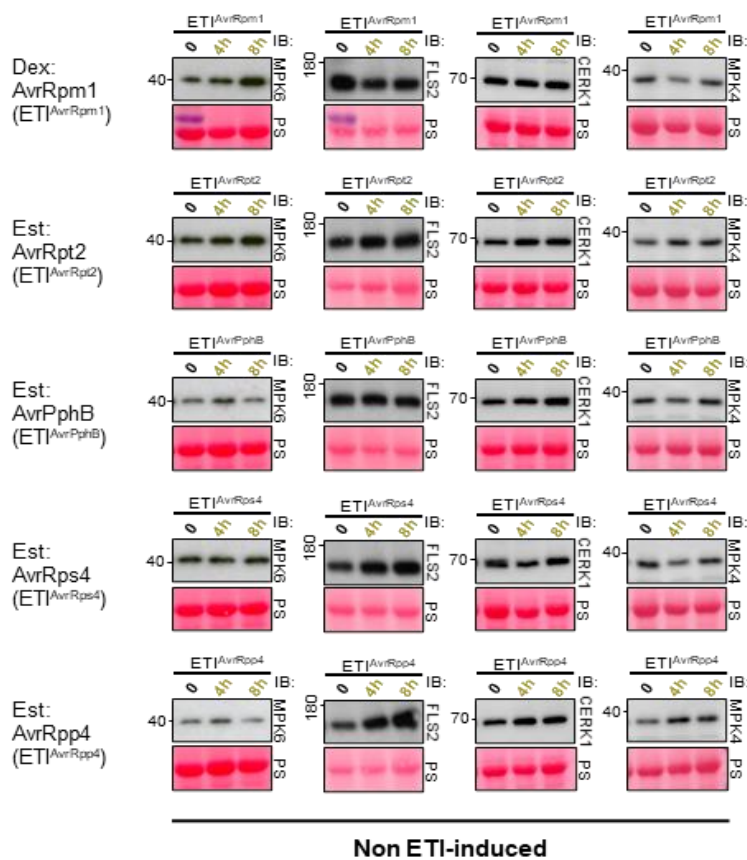
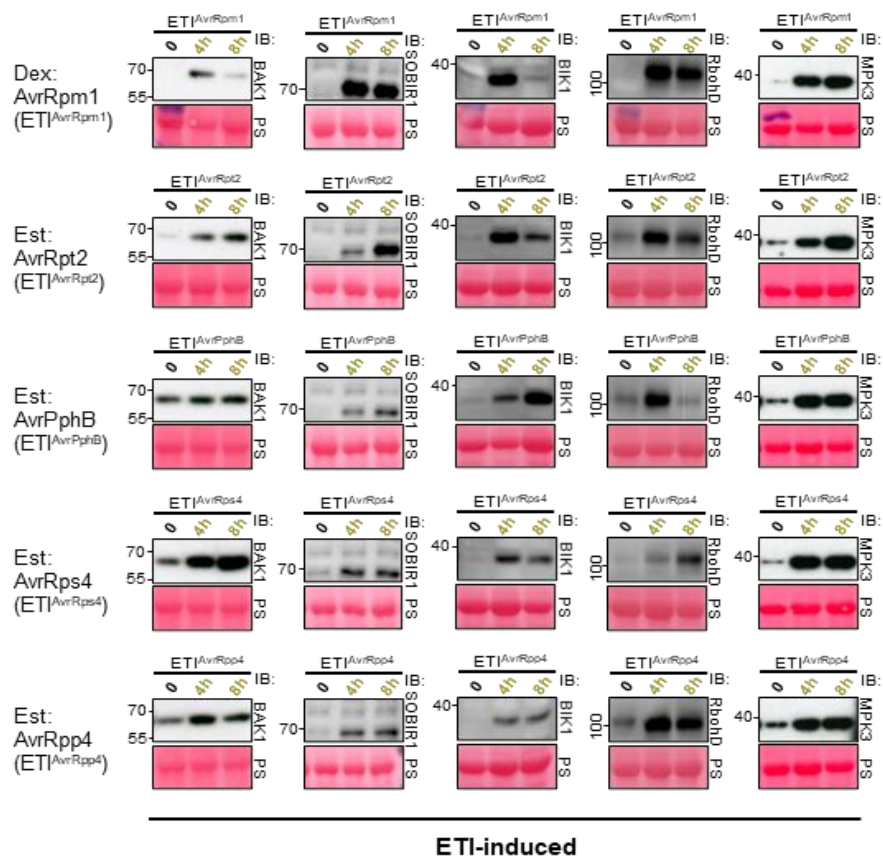


Figure 4.6. **Accumulation of PTI-signaling components during ETI.** Dex:AvrRpm1, est:AvrRpt2, est:AvrPphb, est:AvrRps4 (SET1<sup>WT</sup>) and est:AvrRpp4 were infiltrated with 50  $\mu$ M dexamethasone or estradiol. Samples were collected at indicated time-point for immunoblotting analysis. BAK1, SOBIR1, BIK1, RbohD MPK3, but not MPK6, FLS2, CERK1 or MPK4, are strongly accumulated during ETI. Ponceau staining (PS) was used as loading control. This figure has been published in Ngou et al, 2020b and appears here with permission.

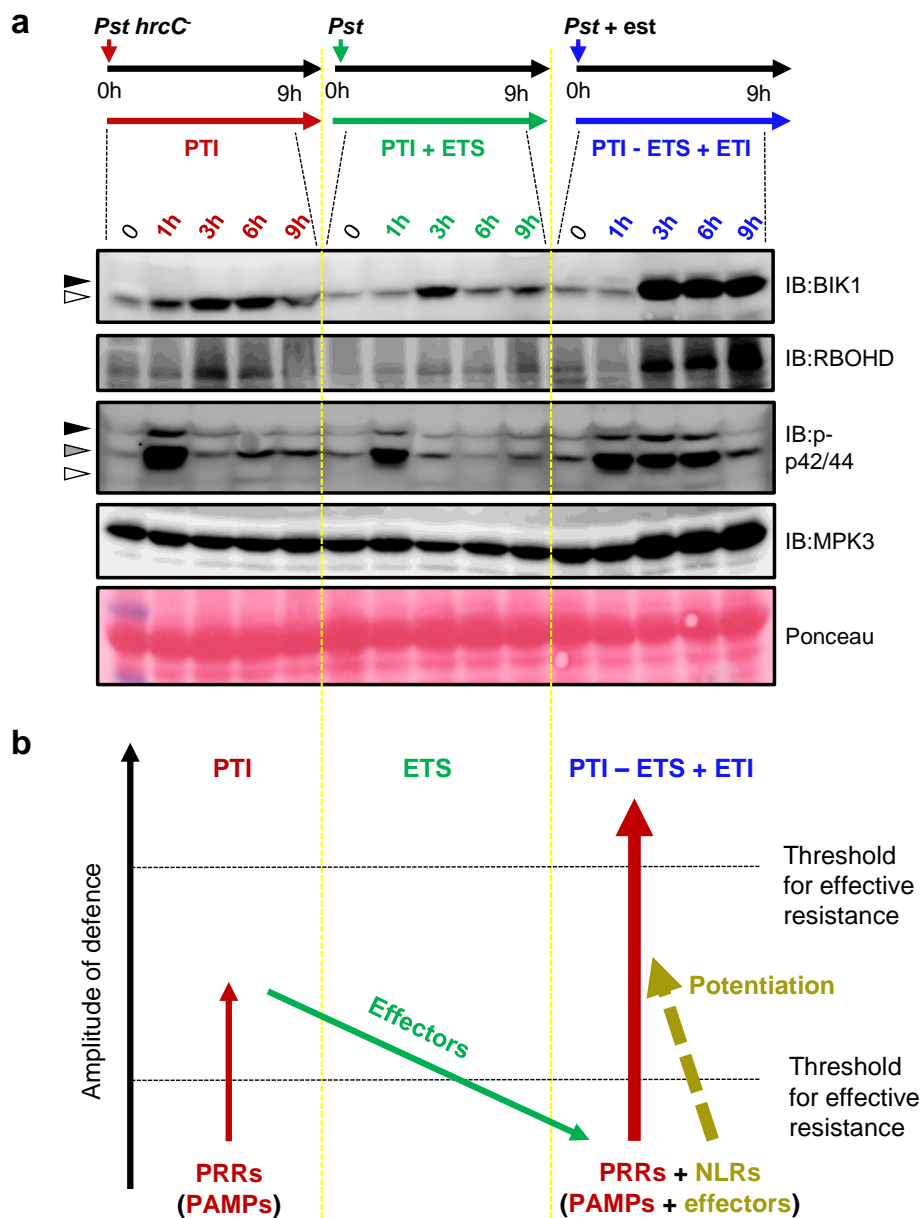
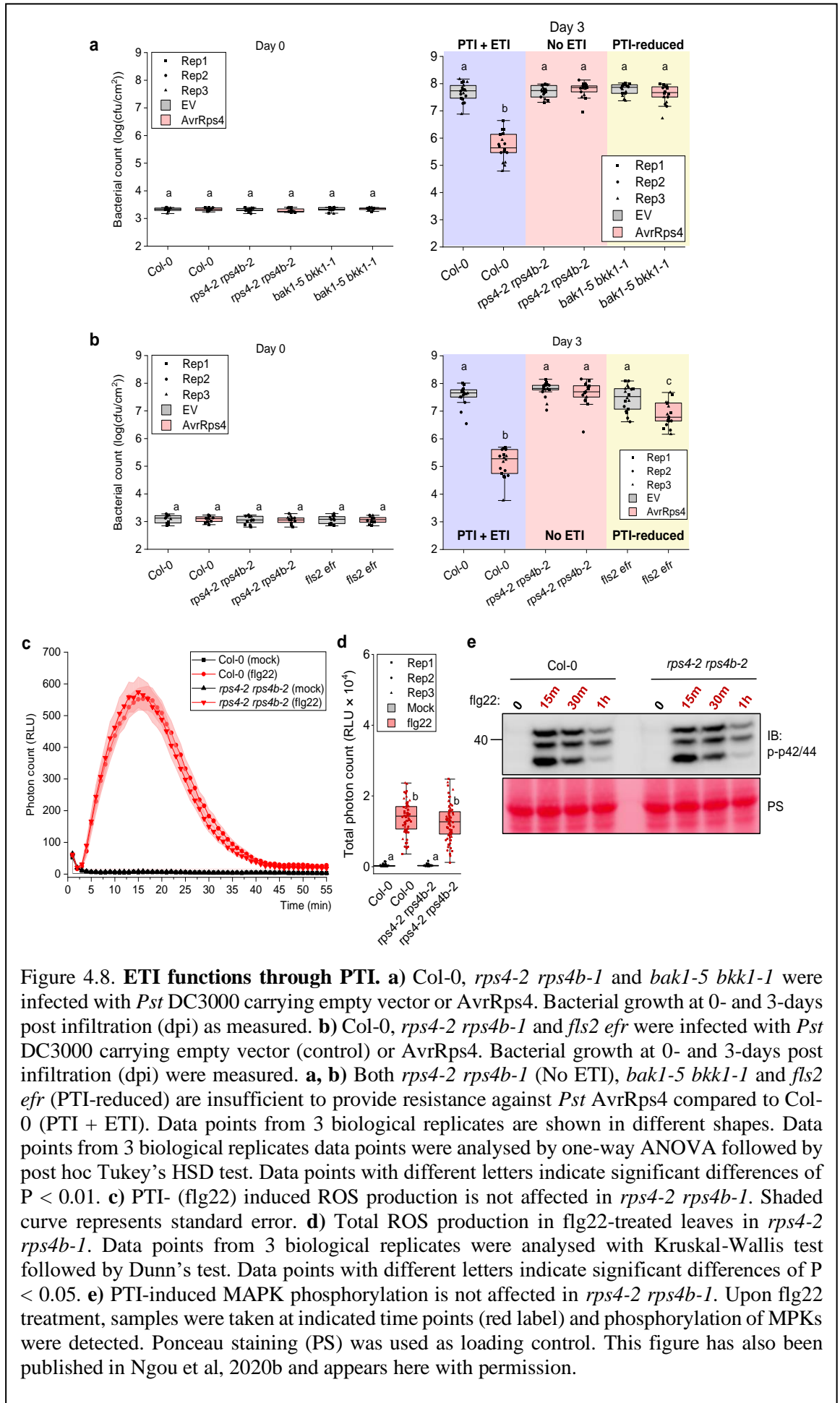
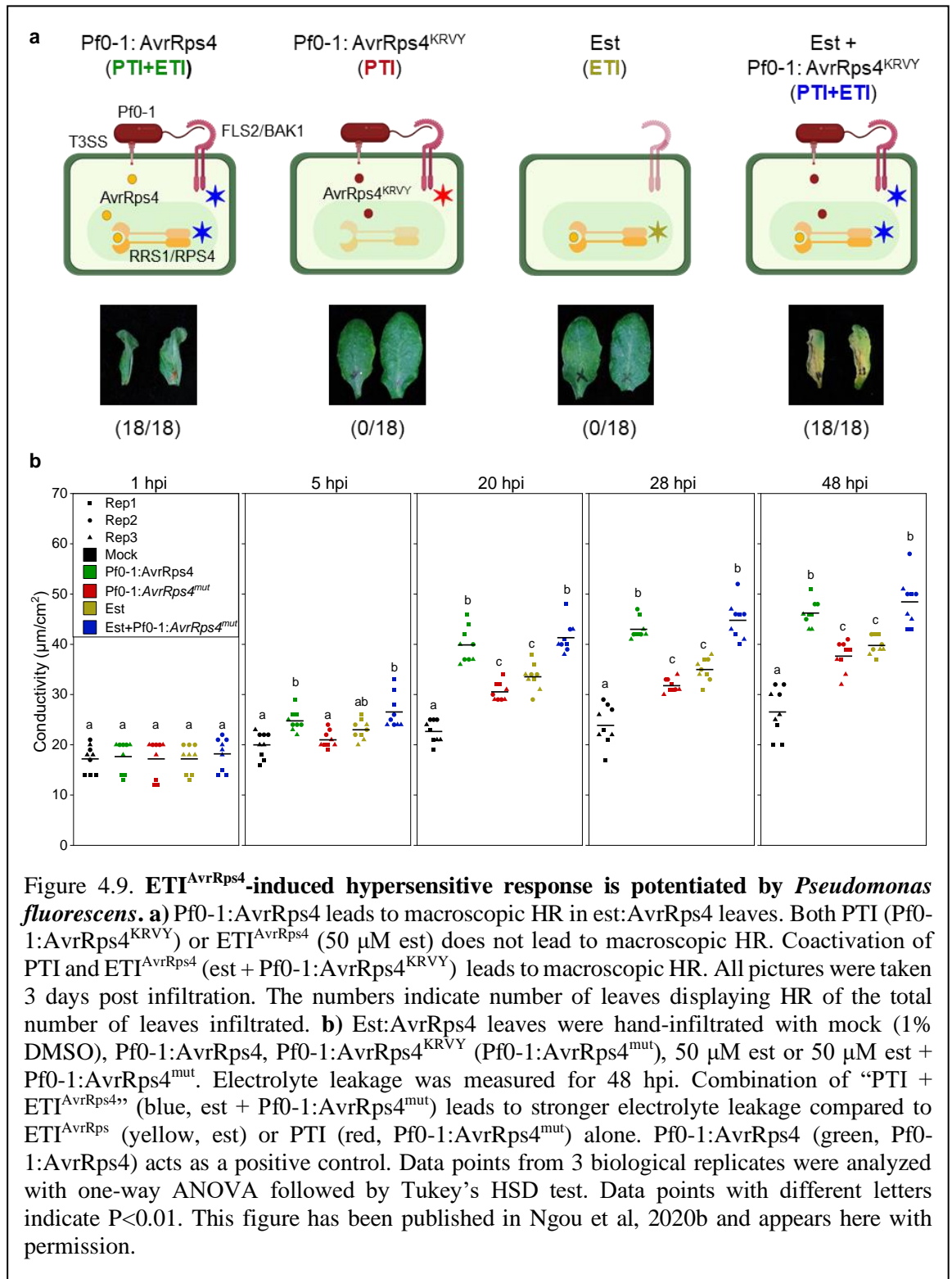
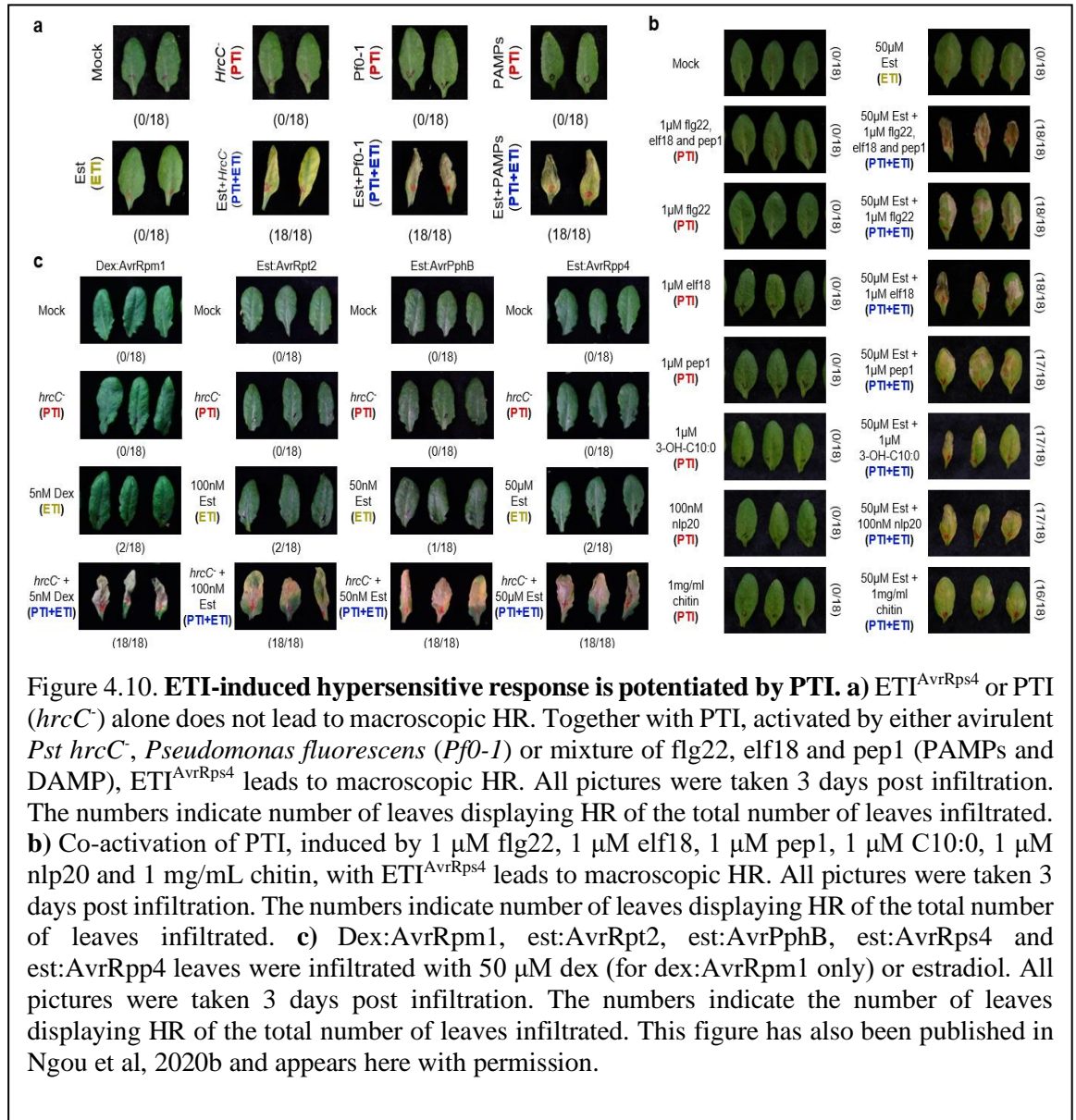
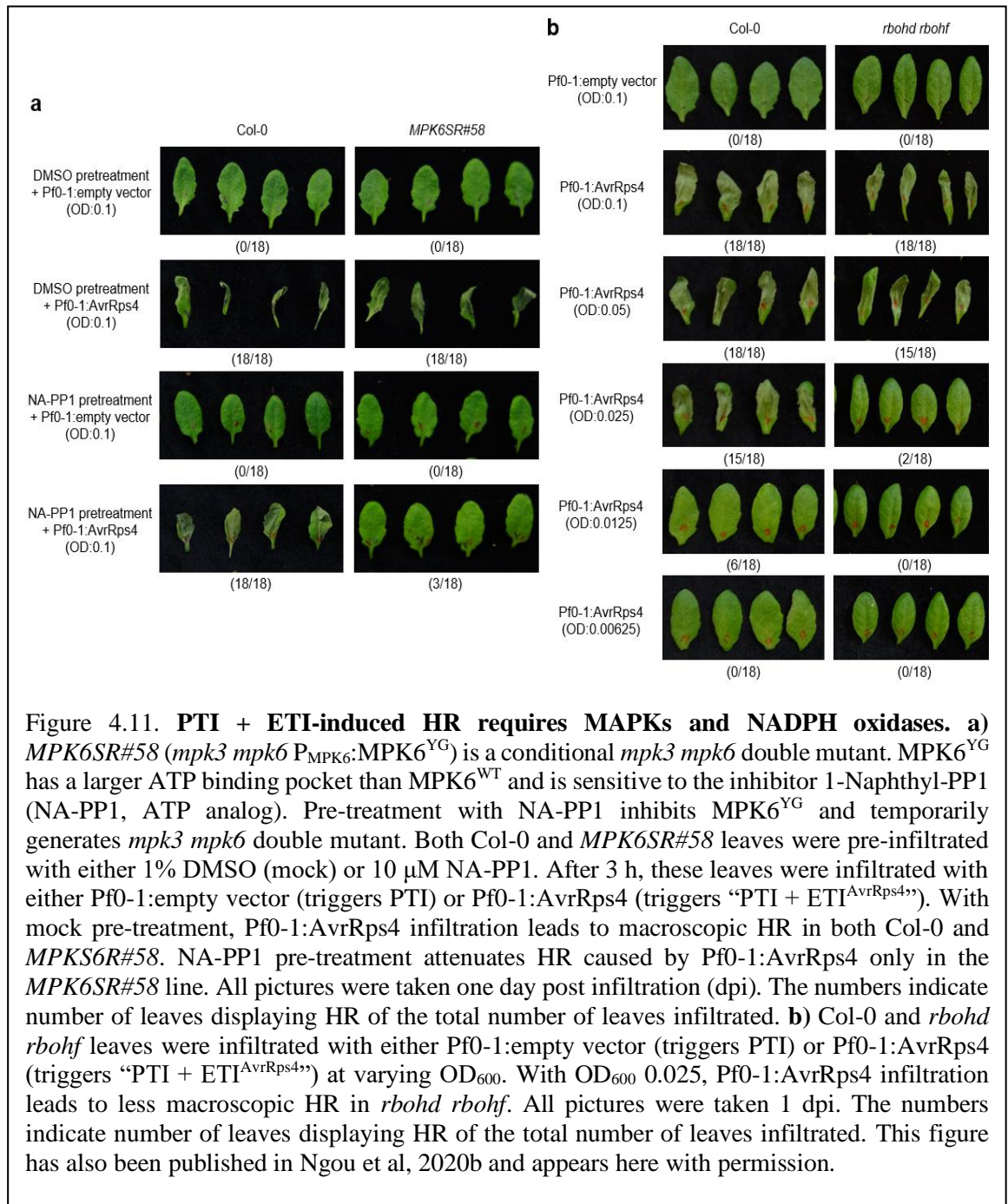


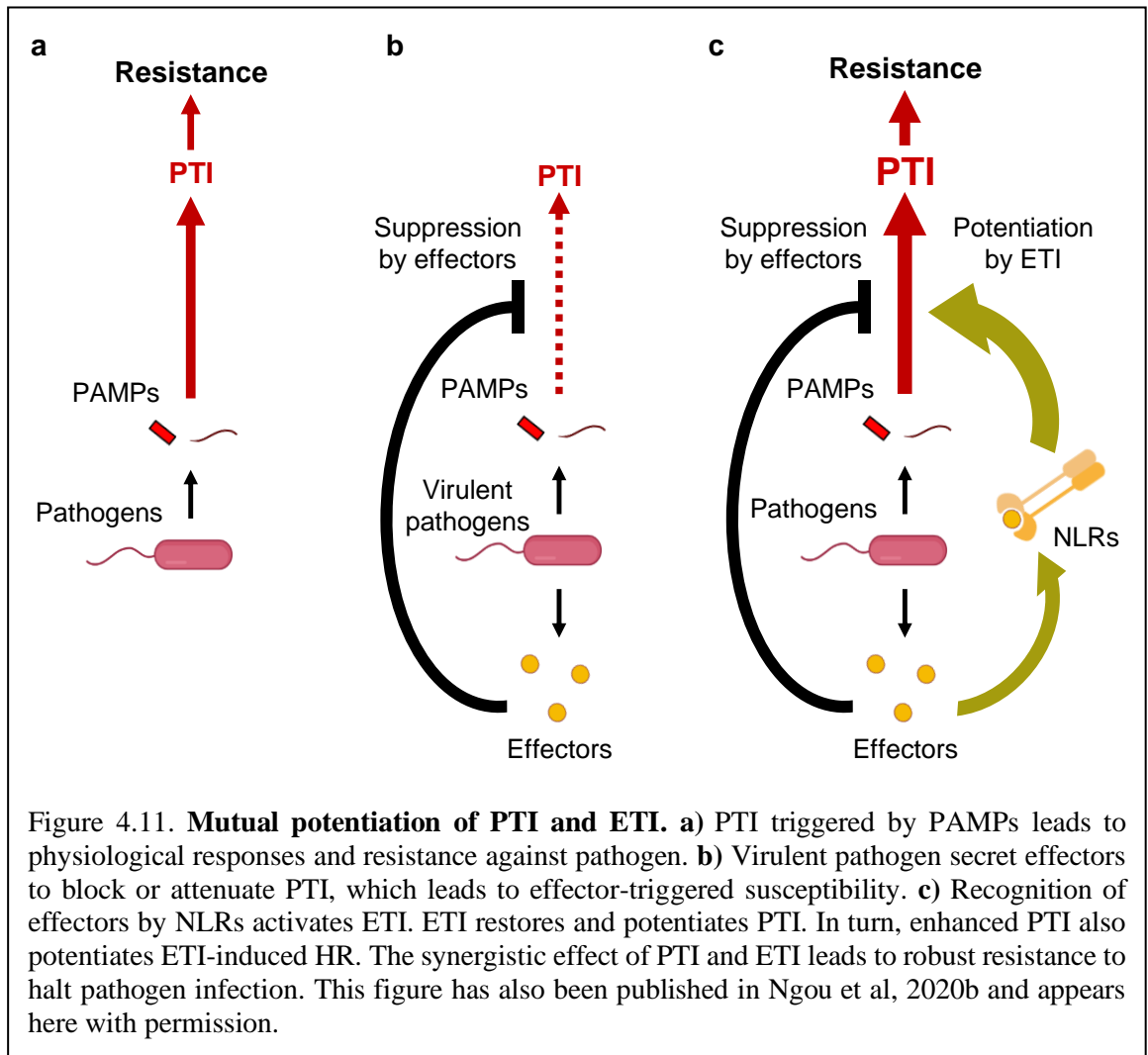
Figure 4.7. **ETI restores suppression of PTI during ETS.** **a)** Est:AvrRps (SETI<sup>WT</sup>) was infiltrated with *Pst hrcC* (PTI), *Pst DC3000* (PTI + ETS) and *Pst DC3000* together with estradiol to trigger ETI<sup>AvrRpr4</sup> (PTI - ETS + ETI). Samples were collected at indicated time-point for immunoblotting analysis. PTI leads to activation of MAPKs and accumulation of BIK1 and RbohD (red). *Pst* secretes effectors to block PTI (green). When PTI is coactivated with ETI, there is a stronger accumulation of MPK3, BIK1 and RbohD compared to that of PTI (blue). Ponceau staining (PS) was used as loading control. Arrows in IB: BIK1 indicate the phosphorylation of BIK1 (black: pBIK1, white: BIK1). Arrows in IB: p-p42/44 indicate the corresponding MAP kinases (black: pMPK6, grey: pMPK3, white: pMPK4/11). **b)** Updated version of the “zig-zag-zig” model. PAMPs from pathogen is detected by PRRs to trigger PTI. Successful pathogens secrete effectors to interfere with PTI, which leads to ETS. ETI is activated when effectors are recognized by NLRs. ETI restores and enhances PTI, which leads to effective resistance against virulent pathogens. This figure has also been published in Ngou et al, 2020b and appears here with permission.











## **Chapter 5: Investigation into the mechanisms of elevated immune signalling protein accumulation triggered by NLR activation**

This chapter is largely identical to (Ngou et al., 2020b) and appears with permissions from Pingtao Ding and Hee-Kyung Ahn. This publication is under the CC-BY license. Unless specified, experiments were performed by Bruno Pok Man Ngou.

### **Abstract**

Activation of NLRs leads to robust protein accumulation of PTI signaling components, which in turns potentiates PTI. How NLRs elevate the accumulation of these proteins is not well understood. Following activation of NLRs, transcript levels of multiple PTI signaling components are also induced. While EDS1 is required for both transcript and protein accumulation of these genes during ETI<sup>AvrRps4</sup>, the transcription factors SARD1 and CBP60G are not required. Furthermore, non-concordance between transcript and protein levels is observed for many components during ETI<sup>AvrRps4</sup>, indicating that post-transcriptional regulatory mechanisms are involved in the protein accumulation. Translation and proteasome inhibitors indicated that both de-novo protein synthesis and protein turnover regulate the accumulation of PTI-signaling components during ETI. Thus, multiple mechanisms are involved in the accumulation of different PTI signaling components during ETI. Further investigation would be required to fully dissect these mechanisms.

### **Introduction**

Following effector recognition, activated NLRs undergo a series of conformational changes. For example, ZAR1 oligomerises into a pentamer upon effector recognition, which leads to downstream signalling events (Wang et al., 2019a, 2019b). TIR domains on TIR-NLRs has also been shown to oligomerize (Martin et al., 2020), and produce variant cyclic-ADP-Ribose (vc-ADPR) through NADase activity upon activation (Horsefield et al., 2019; Wan et al., 2019). vc-ADPR was proposed to activate downstream signalling components, such as the lipase-like proteins EDS1, SAG101 and PAD4 (collectively known as EP proteins) (Lapin et al., 2019, 2020). In addition to EP proteins, the RPW8-NLR clade is also required for ETI triggered by diverse NLRs, likely through their contribution to HR and transcriptional reprogramming (Castel et al., 2019; Feehan et al., 2020; Saile et al., 2020; Wu et al., 2019). Downstream transcription factors SARD1 and CBP60G have been shown to be involved in the upregulation of *ICS1*, *FMO1* and *ALDI*, involved in the biosynthesis of defence-related phytohormones, during ETI. The upregulation of these genes leads to salicylic acid and pipelicolic acid biosynthesis, which activate system acquired resistance

and phytohormone-induced defence responses (Ding and Ding, 2020; Sun et al., 2015; Zhang et al., 2010b).

As shown in the previous chapter, ETI halts pathogen infection through the potentiation of PTI. PTI potentiation is achieved by elevated protein accumulation of its signalling components, such as BIK1, RbohD and MPK3. It is unclear whether elevated protein accumulation is controlled by transcriptional regulation or other unknown mechanisms. The genetic components required for the regulation of PTI signalling genes are also unknown. Moreover, recent reports have suggested that multiple processes, such as translation and protein turnover, are crucial in the regulation of protein dynamics during PTI (Dressano et al., 2020; Grubb et al., 2020; Lee et al., 2020; Ma et al., 2020a, 2020b; Xu et al., 2017).

### **ETI leads to transcript upregulation of PTI signaling components**

Transcription and translation are strongly correlated during ETI compared to PTI (Meteignier et al., 2017; Xu et al., 2017; Yoo et al., 2020). The elevated protein levels of PTI signaling components during ETI could be due to transcriptional induction. To test this, 5-week old leaves of dex:AvrRpm1, est:AvrRps2, est:AvrPphB, SETI<sup>WT</sup> and est:AvrRpp4 were infiltrated with either 50  $\mu$ M dex (for dex:AvrRpm1) or 50  $\mu$ M est (for est:AvrRps2, est:AvrPphB, SETI<sup>WT</sup> and est:AvrRpp4) to activate ETI in the absence of PTI. Samples were collected at 0, 4 or 8 hpi for qPCR analysis. ETI triggered by all NLRs leads to relatively strong upregulation of *BAK1*, *SOBIR1*, *BIK1*, *RbohD* and *MPK3*. *MPK6*, *CERK1*, *FLS2*, *MPK4* and *RbohF* are also weakly induced (Figure 5.1a-b). Interestingly, highly upregulated genes lead to protein accumulation and weakly induced genes do not (Figure 4.6). This indicates that elevated protein levels during ETI might be determined by transcriptional upregulation.

### **ETI leads to global transcriptional upregulation of multiple PTI signaling components**

To further explore the effect of ETI on transcription, SETI<sup>WT</sup> and SETI<sup>KRVY</sup> leaves were infiltrated with either mock or 50  $\mu$ M estradiol for 0 and 4 h and genome-wide expression profiling was performed (Figure 5.2a). Initial data analysis was performed by Pingtao Ding. Around 10% of the transcriptome shows significant differential gene expression upon ETI<sup>AvrRps4</sup> activation (2573 genes, adjusted p-value < 0.01). These genes were clustered according to their expression level (z-score) during different treatments, with cluster 7 and 8 being most highly upregulated during ETI<sup>AvrRps4</sup> (Figure 5.2b). I performed GO analysis with cluster 7 and 8. These upregulated genes are enriched in biological processes implicated in immune responses, especially PRR signaling pathways (Figure 5.2c),

molecular functions implicated in kinase activity and cellular components implicated in the plasma membrane (Figure 5.2d-e). This implies that ETI<sup>AvrRps4</sup> indeed leads to transcriptional upregulation of genes involved in the PTI signaling pathway.

I further investigated the PTI signaling components that are upregulated during ETI<sup>AvrRps4</sup>. In addition to *BAK1*, *BIK1*, *RbohD*, *MPK3*, *MPK4*, *MPK6*, *FLS2*, *CERK1*, *MPK4* and *RbohF*, multiple reported PTI signaling components are also upregulated during ETI<sup>AvrRps4</sup>. These include: LRR-RLKs, such as *PEPR1* and *PEPR2* (PRRs involved in pep1 perception (Yamaguchi et al., 2006, 2010)), EFR (PRR involved in elf18 perception (Zipfel et al., 2006)), *BKK1* (functionally redundant with *BAK1* (He et al., 2007)); LRR-RLPs, such as *RLP30* (PRR involved in proteinaceous elicitor SCFE1 perception (Zhang et al., 2013)); members of other PRR classes, such as *LORE* (PRR involved in C10:0 perception (Kutschera et al., 2019)) and *LYK5* (PRR involved in chitin perception (Cao et al., 2014)); members of the RLCK-VII family, such as *PBL39* and *PBL40* (involved in chitin-induced immune signaling (Liang et al., 2018)); G-proteins involved in PTI signaling regulation, such as *XLG2* and *AGB1* (Liu et al., 2013a; Zhu et al., 2009); CPKs involved in the phosphorylation of multiple immune signaling components, such as *CPK1*, *CPK2* and *CPK4* (Cheval et al., 2013; Gao et al., 2013; Seybold et al., 2014); GNGCs that are involved in PTI-induced calcium signaling, such as *CNGC19* (Meena et al., 2019; Yu et al., 2019); MAP kinases that are involved in the phosphorylation of MPK3 and MPK6, such as *MEKK1*, *MKK4* and *MKK5* (Asai et al., 2002; Rasmussen et al., 2012) (Figure 3a-b). Genes encoding enzymes that are required for the biosynthesis of defense-related phytohormone and metabolites, such as *ICS1*, *EDS5*, *PBS3*, *SARD4*, *FMO1* and *ALD1* are also upregulated during ETI<sup>AvrRps4</sup> (Ding and Ding, 2020; Huang et al., 2020) (Figure 5.3a-b). In addition, genes encoding PRRs involved in growth and development, such as *ERECTA*, *RDK1*, *BAM2* and *CLV2*, and genes required for photosynthesis, such as *Lhcb2*, *GUN4* and *ATAF1*, are down-regulated during ETI<sup>AvrRps4</sup> (Huot et al., 2014; Serrano et al., 2016; Su et al., 2018) (Figure 5.3a-b). In conclusion, ETI elevates transcript abundance of genes involved in PTI-signaling and biosynthesis of defense-related phytohormones, while genes that are involved in development and photosynthesis are downregulated.

### **EDS1, but not SARD1 and CBP60G, is required for upregulation of PTI signaling components during ETI<sup>AvrRps4</sup>**

To explore the genetic requirement of the upregulation of PTI signaling components during ETI<sup>AvrRps4</sup>, SETI<sup>WT</sup> was crossed with *sard1 cbp60g* (transcription factor double mutant highly diminished in the salicylic acid and pipecolic acid signaling pathway (Ding and Ding, 2020; Zhang et al., 2010b)). SETI<sup>WT</sup>, SETI<sup>KRVY</sup>, SETI *eds1-2* and SETI *sard1 cbp60g*

leaves were infiltrated with 50  $\mu$ M estradiol followed by qPCR and IB analysis. As expected, upregulation of *ICS1* and *PR1* in ETI<sup>AvrRps4</sup> is abolished in SETI<sup>KRVY</sup>, SETI *eds1-2* and highly reduced in SETI *sard1 cbp60g* (Figure 5.4a-b). I tested if ETI<sup>AvrRps4</sup>-induced BIK1, RbohD and MPK3 expression is affected in these mutant lines. While the upregulation of these genes is abolished in SETI<sup>KRVY</sup> and SETI *eds1-2*, it remains intact in SETI *sard1 cbp60g* (Figure 5.4a-b). This indicates that the transcription factor SARD1, CBP60G and salicylic acid signaling pathway are not required for the accumulation of BIK1, RbohD and MPK3 during the early stage of ETI<sup>AvrRps4</sup>, consistent with the report from (Yuan et al., 2020). As mentioned, other signaling components such as SAG101, PAD4 and helper NLRs are required for ETI<sup>AvrRps4</sup>-induced resistance. SETI lines will be generated carrying additional mutations to define the genetic components required for the accumulation of PTI-signaling components during ETI.

### **Robust accumulation of BIK1, RbohD and MPK3 during ETI<sup>AvrRps4</sup> is not due to prolonged transcriptional activation**

Previous studies suggest substantial overlap between PTI- and “PTI + ETI”-induced transcriptional reprogramming (Navarro et al., 2004; Zhang and Fan, 2020). I tested if the accumulation of PTI signaling components during ETI is solely due to prolonged transcriptional activation. Both the transcript and protein level of multiple PTI signaling components were tracked over 24 hours after ETI<sup>AvrRps4</sup>-induction. Consistent with previous results, *CERK1*, *MPK4* and *MPK6* expression was weakly induced during ETI and robust protein accumulation was not observed (Figure 5.5a-b, 5.6). Consistent with the protein levels, *BAK1* and *SOBIR1* transcript levels are induced and sustained following ETI<sup>AvrRps4</sup> activation (Figure 5.5a-b, 5.6). However, *BIK1*, *RbohD* and *MPK3* mRNAs rise briefly and then fall after 3 hours, while the induced protein levels are sustained over 24 hours (Figure 5.5a-b, 5.6). Interestingly, increases in both *XLG2* and *FLS2* transcript levels does not result in elevated protein accumulation at any time point (Figure 5.5a-b, 5.6). These data indicate a discrepancy between mRNA and protein level during ETI<sup>AvrRps4</sup>.

As reported in the last chapter, “PTI + ETI<sup>AvrRps4</sup>” leads to stronger accumulation of BIK1, RbohD and MPK3 compared to PTI alone. It was unclear whether ETI<sup>AvrRps4</sup> leads to stronger accumulation of these genes than PTI, or PTI and ETI<sup>AvrRps4</sup> together potentiates their induction. I tracked both the transcript and protein level of BIK1, RbohD and MPK3 during PTI, ETI<sup>AvrRps4</sup> and “PTI + ETI<sup>AvrRps4</sup>”. ETI<sup>AvrRps4</sup> and “PTI + ETI<sup>AvrRps4</sup>” both leads to stronger protein accumulation of BIK1, RbohD and MPK3 compared to PTI alone, which means ETI<sup>AvrRps4</sup> alone is sufficient for the induction of these genes. Surprisingly, the transcript levels of *BIK1*, *RbohD* and *MPK3* changes only slightly between different

conditions (Figure 5.7a). I investigated previously published transcriptomic data comparing PTI and “PTI + ETI”. “PTI + ETI” (activated by AvrRpm1, AvrRpt2, AvrRps4 and PopP2) leads to stronger expression of the salicylic acid biosynthesis genes *ICS1* and *EDS5* compared to PTI alone. However, the expression of *BAK1*, *BIK1*, *RbohD* and *MPK3* is only slightly higher during “PTI + ETI” compared to PTI alone (Figure 5.7b-c). Taken together, these results imply that the robust accumulation of PTI-signaling components during ETI<sup>AvrRps4</sup> might not solely involve transcriptional regulation.

### **Translation and protein turnover are involved in protein accumulation during ETI<sup>AvrRps4</sup>**

To investigate whether post-transcriptional controls are involved in the accumulation of PTI signaling components during ETI, Hee-Kyung Ahn tested the effect of the translation inhibitor cycloheximide (CHX) and the proteasome inhibitor MG132 on the accumulation of these genes during ETI<sup>AvrRps4</sup>. Mock, CHX, MG132 or CHX + MG132 were added into SETI<sup>WT</sup> seedlings pre-treated with mock or estradiol (to activate ETI<sup>AvrRps4</sup>) for 3 hours (Figure 5.8a). The translation inhibitor CHX blocks the accumulation of BIK1, RbohD, MPK3 and BAK1 during ETI, but MPK6 and Actin levels are unaffected (Figure 5.8a-b). This indicates that *de-novo* synthesis or translation is required for the accumulation of PTI-signaling components during ETI. Proteasome inhibitor MG132 treatment results in stronger accumulation of BIK1 and RbohD during ETI, but has no effect on MPK3, MPK6, BAK1, FLS2 or Actin (Figure 5.8b-d). In addition, MPK3 levels are similar between CHX + MG132 and CHX treatment, indicating that the induction of protein accumulation for MPK3 is due to increased protein translation. FLS2, BAK1, BIK1 and RbohD protein levels increase upon CHX+MG132 compared to CHX, implying that control of protein turnover also contributes to the accumulation of BAK1, BIK1 and RbohD, consistent with previous reports (Figure 5.8b-d) (Couto et al., 2016; Lee et al., 2020; Lu et al., 2011; Ma et al., 2020a; Segonzac et al., 2014). In summary, ETI elevates the protein levels of different PTI signaling components by multiple mechanisms.

### **Translation control during ETI<sup>AvrRps4</sup>**

Translational reprogramming has been shown to contribute to plant immunity (Meteignier et al., 2017; Xu et al., 2017; Yoo et al., 2020). Since translation is required for the accumulation of multiple PTI signaling components, ETI<sup>AvrRps4</sup> could lead to increased translation efficiency of these genes. Multiple factors, such as ribosomal association, translation elongation speed and tRNA concentration, can affect translation efficiency. Hee-Kyung Ahn and I tested if ETI<sup>AvrRps4</sup> enhances the association of transcripts with

ribosomes (Figure 5.9a). Total mRNA and ribosomal mRNA are extracted from SETI<sup>WT</sup> treated with either mock or estradiol (Figure 5.9b-c). The relative translation efficiency (T.E., relative to *EF1α*) is calculated from the ratio between ribosomal and total mRNA (Figure 5.9d). There is no significantly increased association of *ICS1*, *SOBIR1*, *BAK1*, *BIK1*, *RbohD*, *MPK3* with ribosomes during ETI<sup>AvrRps4</sup> compared to mock treatment (Figure 5.9e). Further investigation is required to dissect the role of translational control of PTI-signaling components during ETI<sup>AvrRps4</sup>.

## Discussion

The robust accumulation of PTI signalling components during ETI restores PTI from ETS. Transcript levels of multiple PTI signalling components are strongly upregulated during ETI. While most LRR-RLPs are upregulated, only half of the LRR-RLK family members are upregulated (such as *EFR*, *PEPR* and *BAK1*). LRR-RLKs involved in development, such as *ERECTA*, *RDK1* and *BAM2* are downregulated during ETI. This implies that ETI specifically upregulates PRRs involved in pathogen recognition. Since many RLKs and their corresponding ligands are unidentified, ETI transcriptomic data might be helpful to identify novel cell surface receptors in the future.

Other than PRRs, downstream signalling components of the PTI signalling components are also strongly upregulated. RLCK subfamily VII members, which mediate PTI signalling of multiple PRRs, are mostly upregulated during ETI. Interestingly, multiple components in the MAPK-signalling pathway are upregulated during ETI. The MAPK kinase (MAPKK) MKK4 and MKK5, which act upstream of MPK3 and MPK6, are also upregulated. Thus, enhanced activation of MPK3 during “PTI + ETI” could also be due to enhanced activation via MKK4 and MKK5 (Asai et al., 2002). In addition to Rboh proteins, CNGC family calcium (Ca<sup>2+</sup>) channel members and calcium dependent kinase CDPKs are also upregulated. Enhanced ROS production during “PTI + ETI” could also be due to enhanced Ca<sup>2+</sup> influx and activation of CDPKs (Kadota et al., 2014; Li et al., 2014b). It would be interesting to test if Ca<sup>2+</sup> influx triggered by PTI can also be enhanced by ETI.

Multiple signalling components, such as EDS1, PAD4, SAG101 (collectively known as EP proteins), NRG1s and ADR1s (NRG1a, NRG1b, ADR1, ADR1-L1 and ADR1-L2, collectively known as helper NLRs), are required for ETI induced by TIR-NLRs. EDS1 is indispensable for ETI<sup>AvrRps4</sup>-induced HR and resistance, PAD4 and ADR1s are involved in ETI<sup>AvrRps4</sup>-induced resistance (but are not involved in ETI<sup>AvrRps4</sup>-HR) while SAG101 and NRG1s are involved in ETI<sup>AvrRps4</sup>-induced HR (but dispensable for ETI<sup>AvrRps4</sup>-resistance) (Castel et al., 2019; Feehan et al., 2020; Gantner et al., 2019; Lapin et al., 2019; Wu et al., 2019). The helper NLRs together with EP proteins modulate TIR-NLR-induced immune

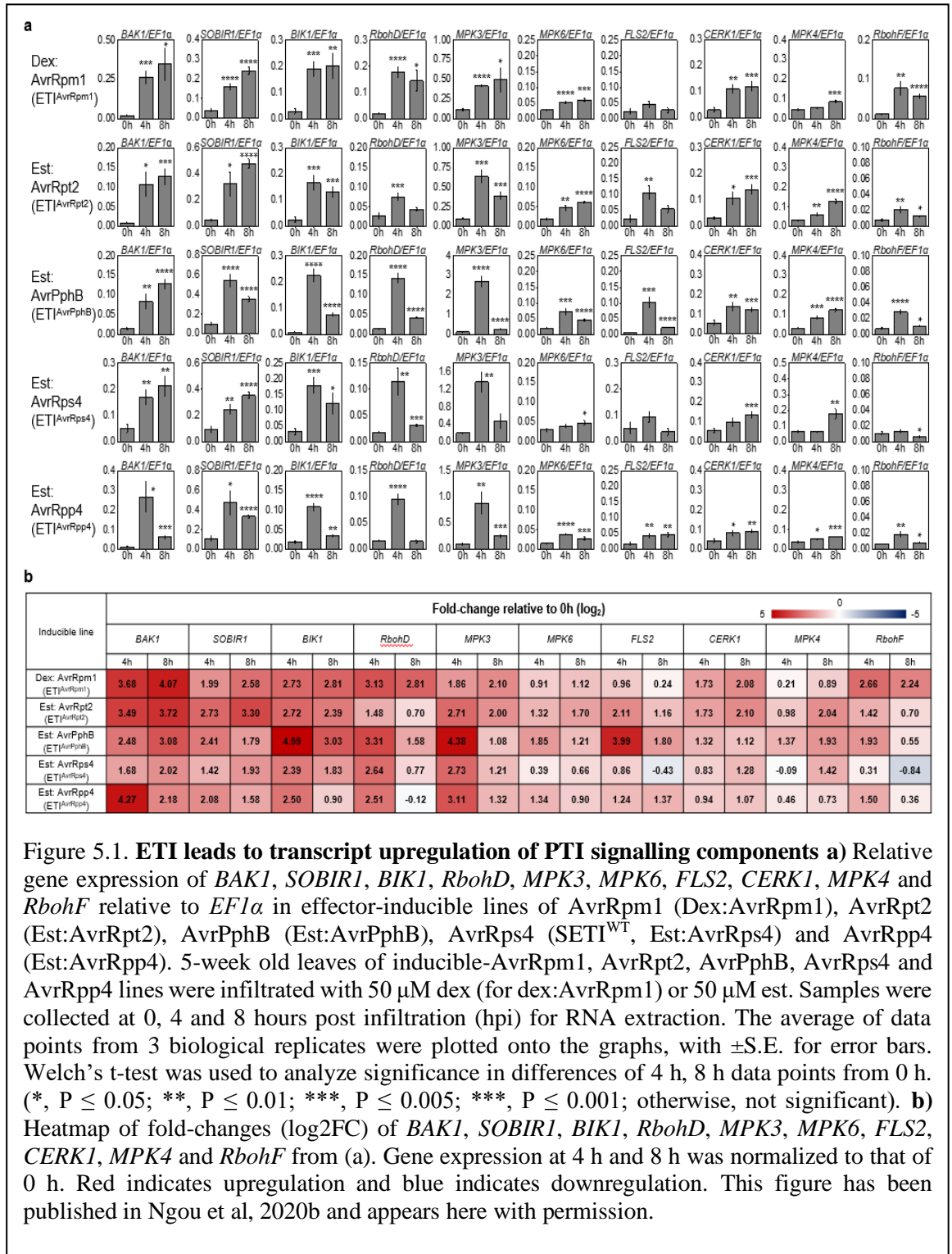
responses. ETI<sup>AvrRps4</sup>-induced upregulation of PTI-signalling components is EDS1 dependent. It is unclear whether PAD4, SAG101 and helper NLRs are also required. Recently it has been reported that ADR1s, but not NRG1s, are involved in RPS4-induced transcriptional reprogramming (Castel et al., 2019; Saile et al., 2020; Wu et al., 2019). Perhaps ADR1s and PAD4 are involved in the transcriptional upregulation of PTI-signalling components during ETI<sup>AvrRps4</sup>. ETI<sup>AvrRps4</sup>-induced upregulation of BIK1, RbohD and MPK3 are not affected in *sard1 cbp60g*. Since both salicylic acid and pipecolic acid pathways are highly diminished in *sard1 cbp60g*, defence-related phytohormones might not be required for the upregulation of PTI-signalling components (Sun et al., 2015; Yuan et al., 2020; Zhang and Fan, 2020; Zhang et al., 2010b). Further genetic analysis would be required to define the signalling pathway required for the upregulation of these genes.

SOBIR1, BIK1, RbohD and MPK3 protein levels are upregulated within 2 hours of AvrRps4 induction and sustained up to 24 hours. Rapid and prolonged accumulation ensures these signalling components can still be activated by PTI during early stage of infection. Similarly, transcript levels of these genes are also upregulated within an hour of AvrRps4 induction. Although the transcriptional upregulation of *SOBIR1* is sustained for 24 hours, *RbohD* and *MPK3* transcript levels are only upregulated for up to 6 hours. This indicates differential transcriptional regulation of these genes. More importantly, prolonged accumulation of BIK1, RbohD and MPK3 protein levels is not due to prolonged transcriptional upregulation of these genes. “PTI + ETI” leads to prolonged transcriptional upregulation of ICS1, SARD1 and EDS5 compared to PTI alone (Saile et al., 2020; Sohn et al., 2014). Surprisingly, “PTI + ETI<sup>AvrRps4</sup>” leads to stronger protein, but not transcript accumulation, of BIK1, RbohD and MPK3 compared to PTI. This is consistent with previously published data (Saile et al., 2020; Sohn et al., 2014). Thus, robust protein accumulation of these genes could not be predicted from transcriptomic data, indicating that post-transcriptional regulation might also be involved.

As expected, translation (de-novo synthesis) is required for elevated protein accumulation of BAK1, BIK1, RbohD and MPK3. Amino acid metabolic pathway and growth/developmental pathway are translationally regulated during ETI (Meteignier et al., 2017; Yoo et al., 2020). The PTI-signalling pathway could also be translationally upregulated during ETI, which leads to prolonged protein accumulation of BIK1, RbohD and MPK3. Although ETI does not lead to enhanced association of these transcripts to ribosomes, other factors, such as translation elongation speed, might affect translation efficiency during ETI. In addition, protein turnover of BAK1, BIK1 and RbohD also contributes to the accumulation of these genes. Ubiquitin ligase (ATL44/RHA3A),

phosphatase (PP2C38) and kinase (CPK28) has been shown to affect BIK1 stability (Couto et al., 2016; Ma et al., 2020a; Monaghan et al., 2014), while RbohD stability is also affected by its phosphorylation and ubiquitination status (Lee et al., 2020). Two recently published studies reveal large number of proteins that are ubiquitinated upon PTI (Grubb et al., 2020; Ma et al., 2020b), indicating that protein turnover could contribute to the accumulation of other PTI signalling components during ETI.

In conclusion, multiple PTI signalling components are transcriptionally upregulated during ETI. While transcript levels correlate with protein level in some genes (such as SOBIR1), protein accumulation cannot be predicted purely based on transcript level (such as XLG2), likely due to post-transcriptional regulations. Since protein levels of PTI signalling components are tightly regulated by multiple mechanisms, it would be difficult to determine the contribution of these regulations to the accumulation of each of these proteins. In the future, a systematic approach to profile mRNA and protein levels over a detailed time course would allow us to determine the role of transcription, translation, and protein turnover during plant immune responses, as has been done in mammalian cells (Figure 5.10) (Jovanovic et al., 2015).



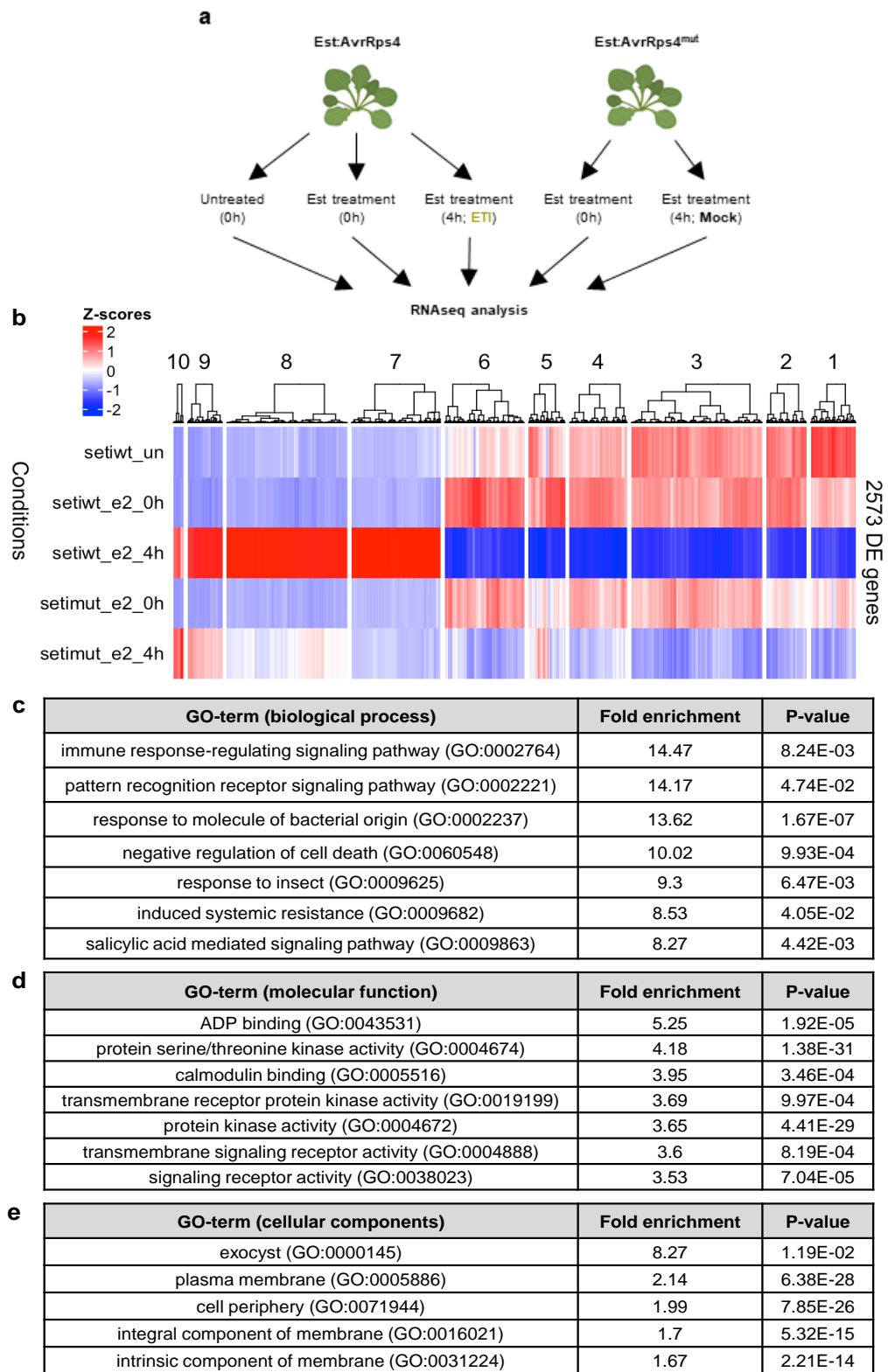
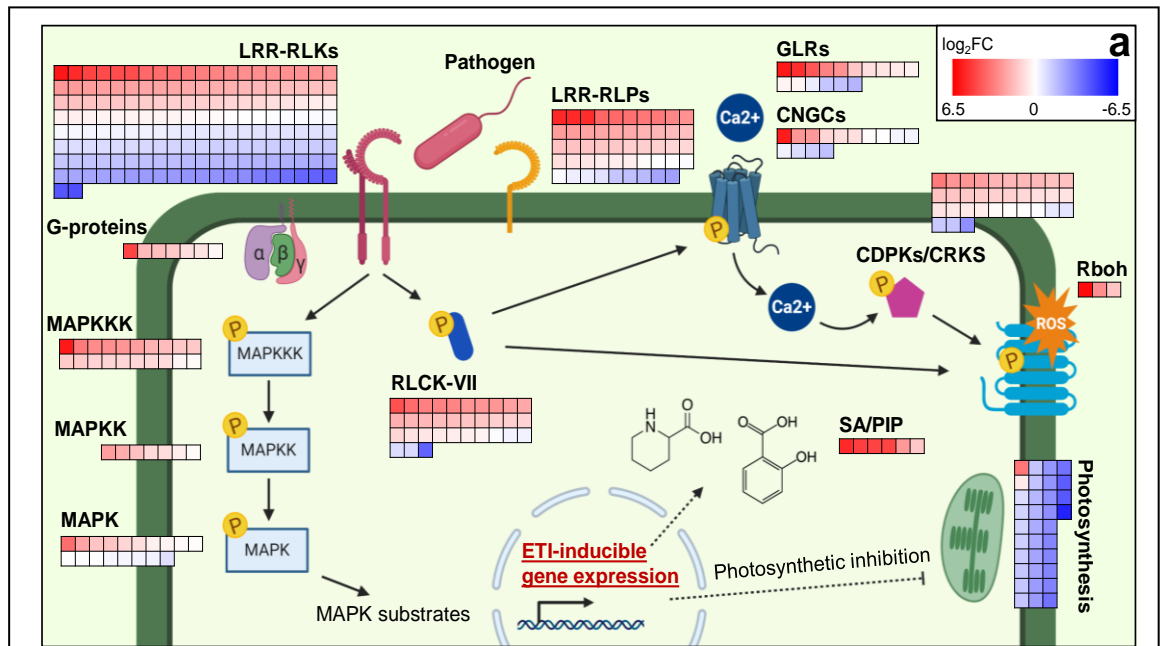


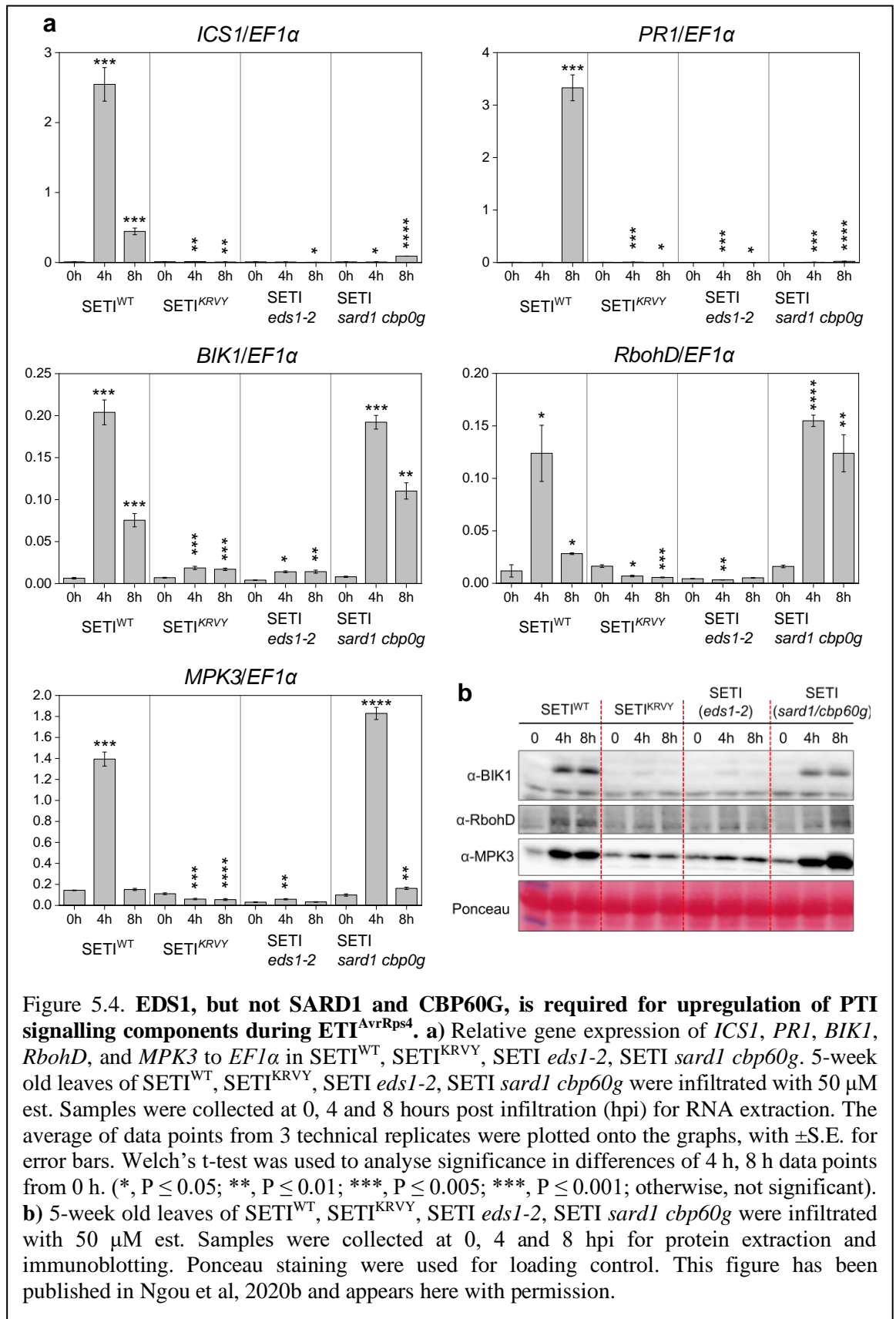
Figure 5.2. **PTI signalling pathway is upregulated during ETI<sup>AvrRps4</sup>**. **a**) Schematic design of RNAseq analysis. 5-week old inducible lines of wild-type AvrRps4 (SETI<sup>WT</sup>, Est:AvrRps4) and mutant AvrRps4 (AvrRps4<sup>KRYY135-138AAAA</sup> mutant; Est:AvrRps4<sup>mut</sup>) were hand-infiltrated with mock or 50µM est and samples were collected at 0 h, and 4 h. **b**) 2573 differential expressed (DE) genes were identified as significant in comparison between SETI<sup>WT</sup> treated with estradiol for 0 h (setiwt\_e2\_0h) and 4 h (setiwt\_e2\_4h). DE genes with adjusted p-value (adj.pval) < 0.01 is categorized as significant. Heatmap representing DE genes during 5 treatments shown in (a). Genes that are specifically upregulated during ETI<sup>AvrRps4</sup> are in cluster 7 and 8. **c-e**) GO enrichment analysis in (c) biological processes, (d) molecular functions, (e) cellular components of genes from cluster 7 and 8. This figure has been published in Ngou et al, 2020b and appears here with permission.

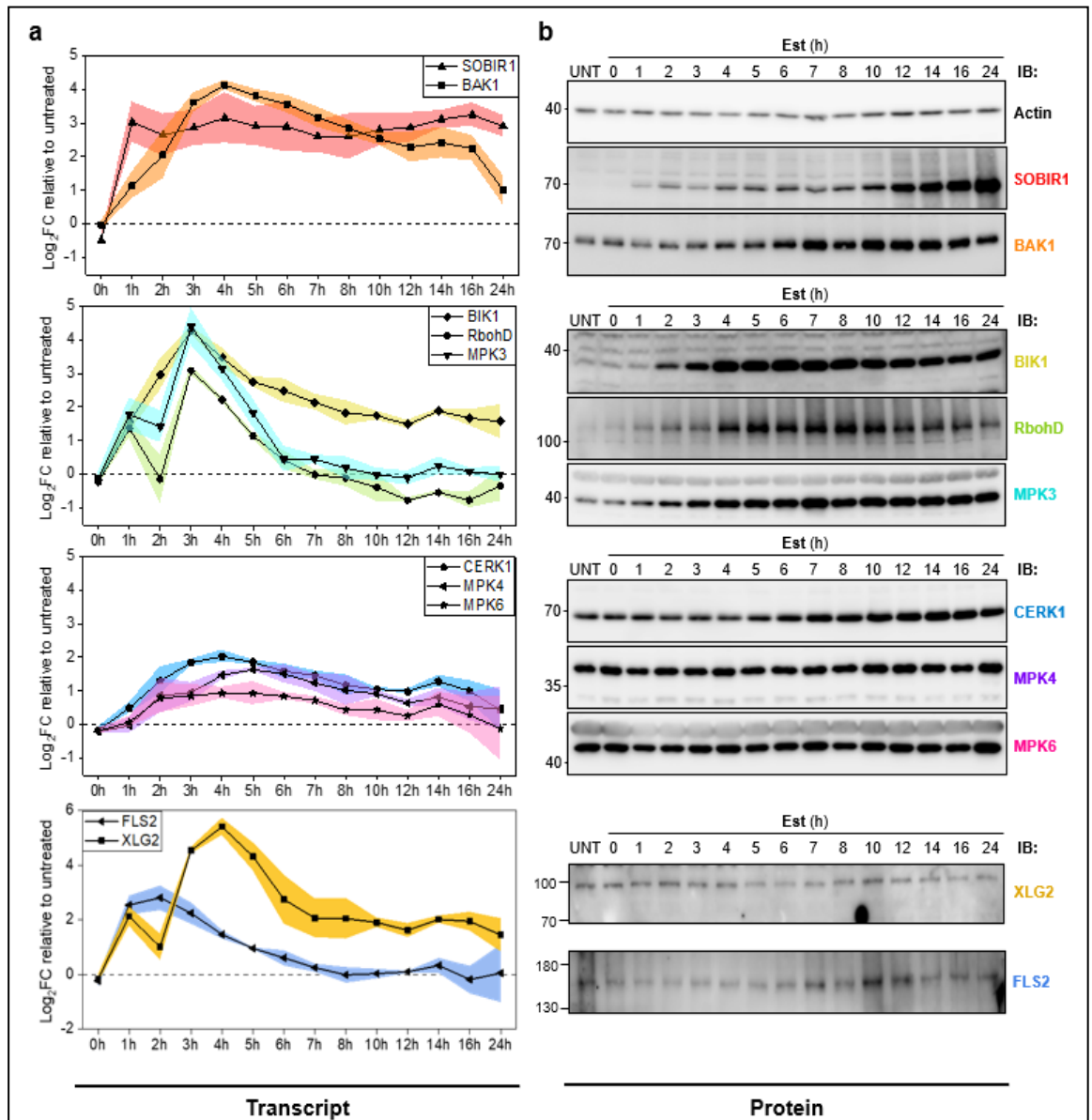


**b**

Target	log <sub>2</sub> FC	adj.pval
<b>LRR-RLKs</b>		
<i>PEPR2</i>	4.812	0.003
<i>NILR1</i>	4.519	0.005
<i>PEPR1</i>	3.813	0.007
<i>RLK7</i>	3.052	0.005
<i>BAK1</i>	2.797	0.001
<i>BKK1</i>	2.562	0.005
<i>FLS2</i>	2.317	0.018
<i>PSKR1</i>	2.289	0.002
<i>EFR</i>	2.083	0.005
<i>SOBIR1</i>	1.509	0.025
<i>BAM1</i>	-1.892	0.035
<i>IRK</i>	-2.536	0.016
<i>ERECTA</i>	-2.768	0.003
<i>RDK1</i>	-3.930	0.007
<i>BAM2</i>	-4.006	0.003
<i>ERECTA-LIKE2</i>	-4.967	0.040
<b>LRR-RLPs</b>		
<i>RLP30</i>	3.873	0.008
<i>CLV2</i>	-1.499	0.047
<b>Other PRRs</b>		
<i>LYK2</i>	4.304	0.043
<i>LORE</i>	3.250	0.001
<i>LYK5</i>	2.516	0.030
<i>CERK1</i>	1.646	0.005
<b>RLCK-VII</b>		
<i>BIK1</i>	3.101	0.002
<i>PBL40</i>	1.841	0.002
<i>PBL39</i>	1.645	0.002
<b>G-protein</b>		
<i>XLG2</i>	4.751	0.001
<i>GPA1</i>	1.624	0.006
<i>AGB1</i>	1.366	0.005
<b>CPKs</b>		
<i>AtCPK28</i>	2.676	0.001
<i>AtCPK4</i>	1.811	0.032
<i>AtCPK6</i>	1.772	0.006
<i>AtCPK1</i>	1.589	0.007
<i>AtCPK2</i>	1.564	0.018
<b>GNGC</b>		
<i>CNGC19</i>	5.768	0.002
<b>Rboh</b>		
<i>RbohC</i>	6.197	0.022
<i>RbohD</i>	2.869	0.003
<i>RbohF</i>	1.475	0.042
<b>MAPKKK</b>		
<i>MEK1</i>	1.957	0.002
<b>MAPKK</b>		
<i>MKK4</i>	2.083	0.003
<i>MKK5</i>	1.554	0.004
<b>MAPK</b>		
<i>MPK11</i>	3.680	0.002
<i>MPK3</i>	1.496	0.022
<i>MPK6</i>	1.061	0.012
<b>PROPEP</b>		
<i>PROPEP2</i>	6.183	0.002
<i>PROPEP3</i>	5.593	0.003
<b>SA/PIP (Phytohormone biosynthesis pathway)</b>		
<i>EDS5</i>	5.443	0.001
<i>FMO1</i>	4.781	0.005
<i>ICS1</i>	4.746	0.001
<b>Photosynthetic pathway genes</b>		
<i>Lhcb2</i>	-5.645	0.001
<i>ATAF1</i>	-4.266	0.003
<i>GUN4</i>	-4.176	0.002
<i>Lhcb4</i>	-3.616	0.001

Figure 5.3. **Multiple PTI signaling components are upregulated during ETI<sup>AvrRps4</sup>.** **a)** RNA-seq results of the upregulation of PTI signaling pathway during ETI<sup>AvrRps4</sup>. Heatmap representing the expression level of PTI signaling pathway genes, defense-related hormone salicylic acid (SA) and secondary metabolite pipecolic acid (PIP) biosynthesis pathway genes and photosynthetic pathway genes at 4 h after ETI<sup>AvrRps4</sup> induction. Red represents upregulation and blue represents downregulation. **b)** Expression level of known PTI-signalling components during ETI<sup>AvrRps4</sup>. Red (positive log<sub>2</sub>FC (fold change)) represents genes that are significantly induced and blue (negative log<sub>2</sub>FC) represents genes that are significantly repressed. Adjusted p-value (adj.pval) < 0.05 is considered as significant. Gradient of green colour indicates significance of the adjusted p-value. This figure has been published in Ngou et al, 2020b and appears here with permission.

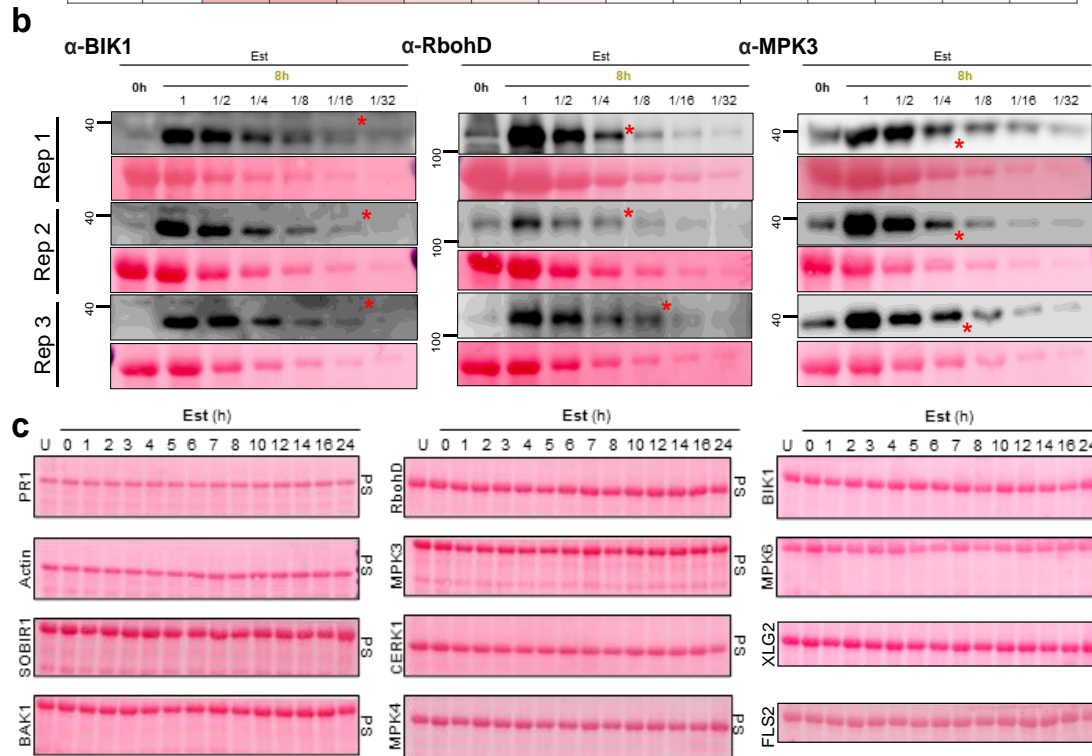




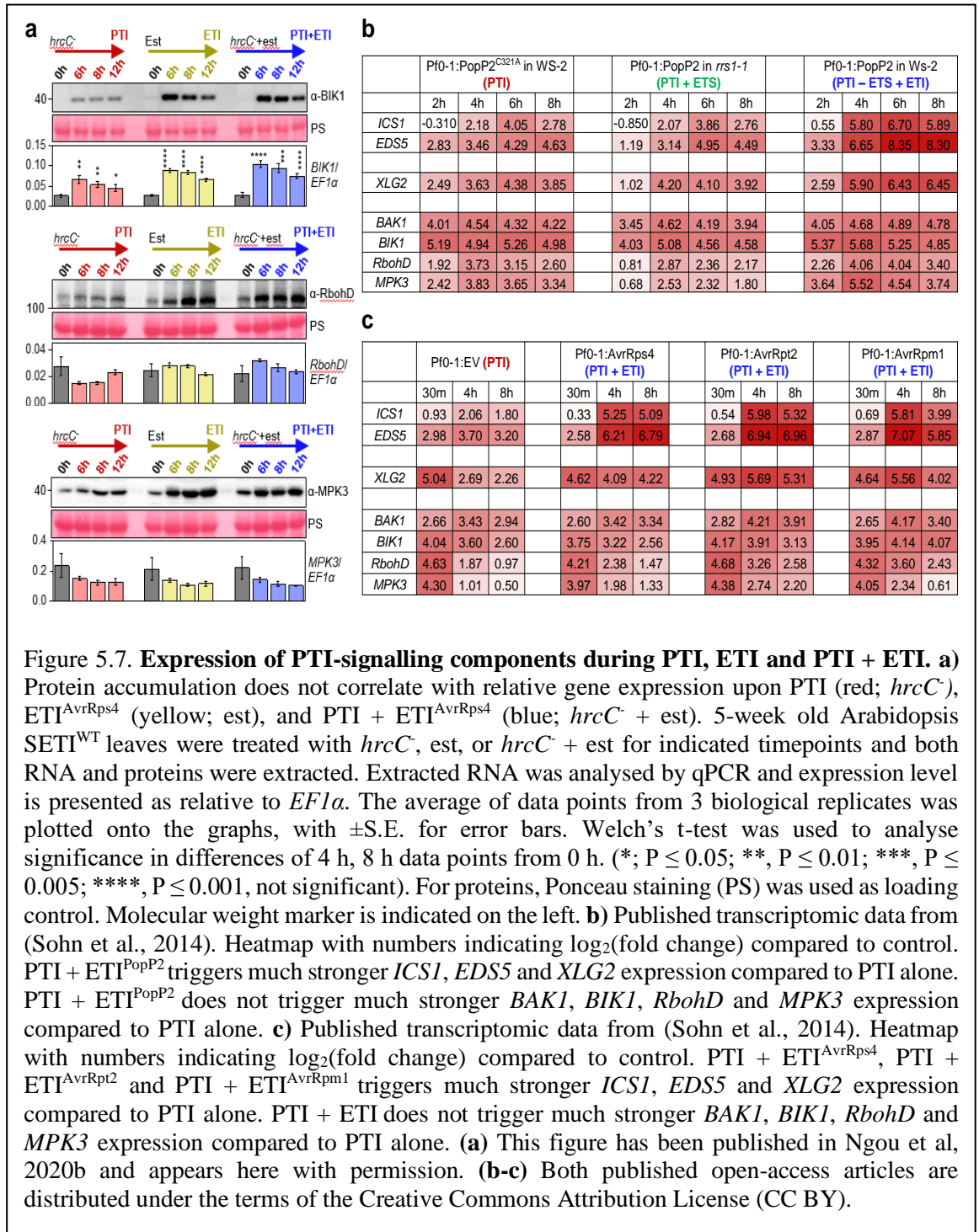
**Figure 5.5. Dynamic mRNA and protein expression of PTI-signalling components during  $ETI^{AvrRps4}$ .** **a**) Relative mRNA expression change of *SOBIR1*, *BAK1*, *BIK1*, *RbohD*, *MPK3*, *CERK1*, *MPK4*, *MPK6*, *XLG2* and *FLS2*. Samples were taken at indicated time points after  $ETI^{AvrRps4}$  activation. All samples were normalized against mRNA expression of the corresponding genes in untreated samples ( $\log_2FC=0$ , dotted line). Shaded curve represents standard error (S.E.). **b**) Protein accumulation of *SOBIR1*, *BAK1*, *BIK1*, *RbohD*, *MPK3*, *CERK1*, *MPK4*, *MPK6*, *XLG2* and *FLS2* at different time points. Actin was used as a loading control. Molecular weight is indicated. Ponceau staining (PS) was used as loading control and shown in Figure 5.6. This figure has been published in Ngou et al, 2020b and appears here with permission.

**a**

Gene	Log <sub>2</sub> (FC) relative to untreated													
	0h	1h	2h	3h	4h	5h	6h	7h	8h	10h	12h	14h	16h	24h
<i>ICS1</i>	-0.46	0.63	1.36	4.74	7.05	6.30	4.15	3.38	3.12	2.89	2.46	2.48	2.27	2.56
<i>PR1</i>	-0.45	0.26	2.46	1.16	2.37	3.60	5.76	5.96	6.88	7.58	8.06	8.49	8.55	8.56
<i>SOBIR1</i>	-0.47	3.03	2.64	2.86	3.15	2.91	2.89	2.61	2.59	2.80	2.87	3.11	3.24	2.91
<i>BAK1</i>	-0.03	1.14	2.05	3.61	4.13	3.81	3.56	3.17	2.84	2.53	2.28	2.42	2.24	1.01
<i>BIK1</i>	-0.15	1.55	2.96	4.27	3.47	2.75	2.48	2.14	1.82	1.74	1.49	1.88	1.68	1.57
<i>RbohD</i>	-0.23	1.37	-0.14	3.08	2.22	1.14	0.43	-0.01	-0.11	-0.38	-0.77	-0.54	-0.76	-0.34
<i>MPK3</i>	-0.10	1.78	1.42	4.39	3.14	1.83	0.45	0.45	0.19	-0.01	-0.11	0.25	0.08	0.00
<i>CERK1</i>	-0.17	0.50	1.30	1.85	2.03	1.86	1.59	1.47	1.18	1.06	0.99	1.29	1.00	0.44
<i>MPK4</i>	-0.21	-0.02	0.87	0.96	1.47	1.63	1.51	1.24	1.02	0.92	0.64	0.82	0.54	0.48
<i>MPK6</i>	-0.18	0.08	0.79	0.86	0.94	0.94	0.85	0.73	0.43	0.44	0.26	0.60	0.29	-0.12
<i>XLG2</i>	-0.16	2.13	1.00	4.54	5.41	4.32	2.74	2.06	2.05	1.90	1.62	2.01	1.94	1.45
<i>FLS2</i>	-0.24	2.54	2.81	2.25	1.47	0.96	0.61	0.25	-0.02	0.03	0.10	0.33	-0.19	0.05



**Figure 5.6. Dynamic mRNA and protein expression of PTI-signalling components during ETI<sup>AvrRps4</sup> (continued).** **a**) Relative mRNA expression change of *SOBIR1*, *BAK1*, *BIK1*, *RbohD*, *MPK3*, *CERK1*, *MPK4*, *MPK6*, *XLG2* and *FLS2*. Samples were taken at indicated time points after ETI<sup>AvrRps4</sup> activation. All samples were normalized against mRNA expression of the corresponding genes in untreated samples ( $\log_2FC=0$ , dotted line). Shaded curve represents standard error (S.E.). **b**) Fold changes of BIK1, RbohD and MPK3 protein accumulation upon ETI<sup>AvrRps4</sup>-activation is shown by serial dilution of ETI<sup>AvrRps4</sup> samples 8 h after est infiltration. Red asterisk indicates approximate fold differences between 0 h and 8 h est treatment. Ponceau staining was used as control. Molecular weight marker is indicated on the left. **c**) Ponceau staining (PS) was used as loading control for Figure 5.5b. This figure has been published in Ngou et al, 2020b and appears here with permission.



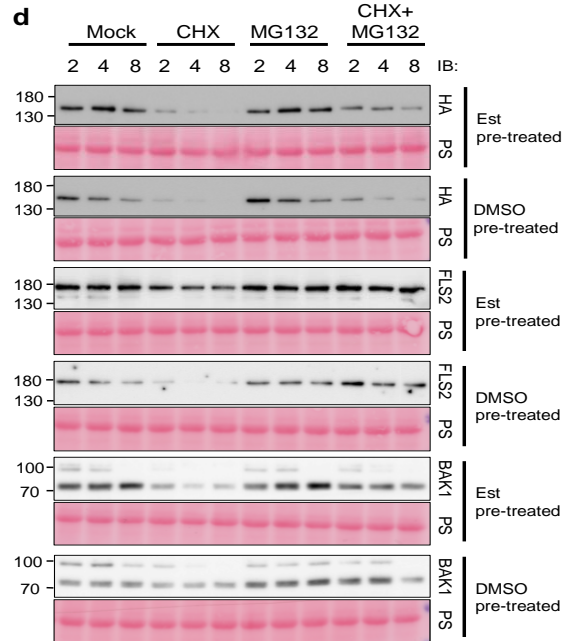
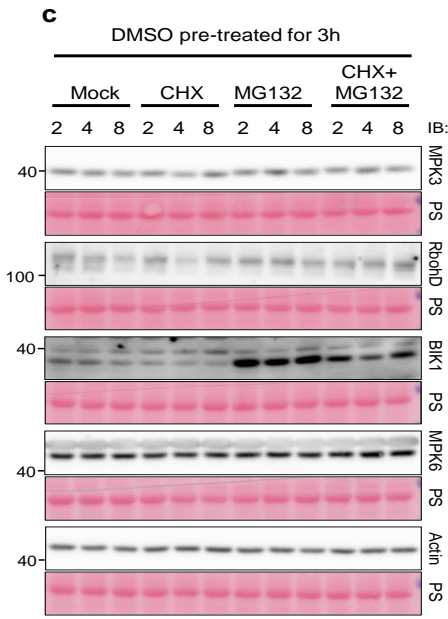
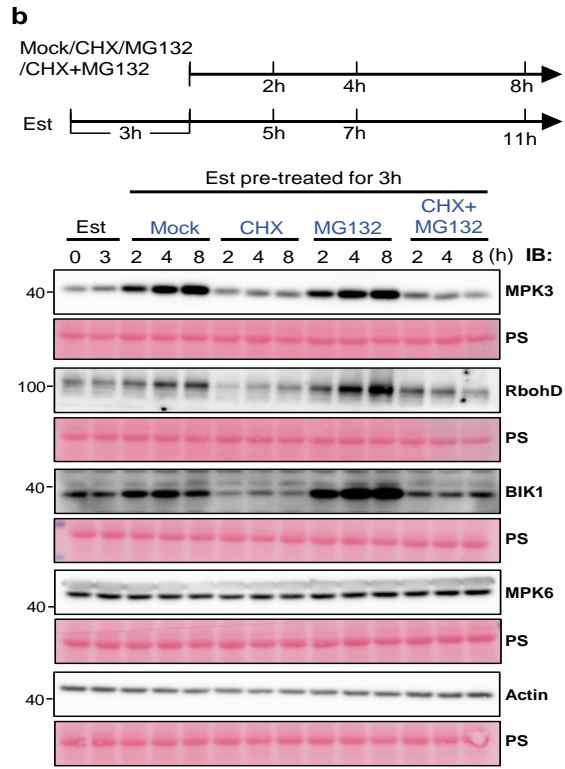
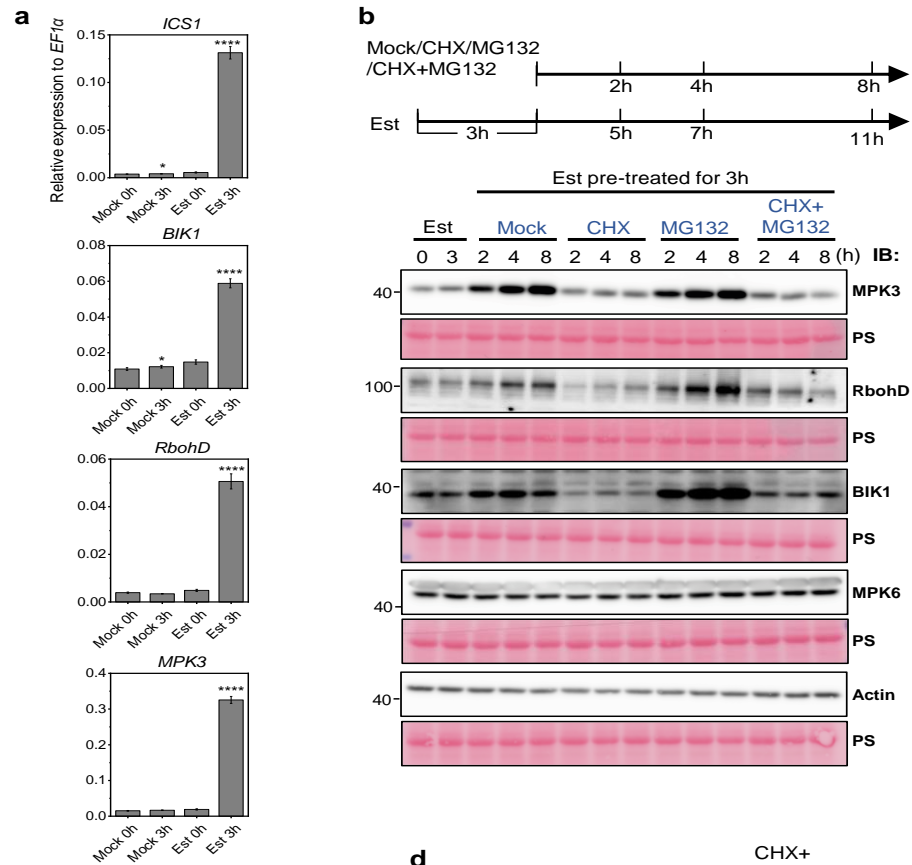


**Figure 5.8. Translation and protein turnover are involved in protein accumulation during  $ETI^{AvrRps4}$ .** **a)** Relative gene expression of *ICS1*, *BIK1*, *RbohD* and *MPK3* in seedlings pre-activated with  $ETI^{AvrRps4}$  3h prior to treatment with cycloheximide (CHX) and MG132. The average of data points from 3 biological replicates were plotted onto the graphs, with  $\pm$ S.E. for error bars. Welch's t-test was used to analyse significance in differences between 0 h and 3 h. (\*;  $P \leq 0.05$ ; \*\*,  $P \leq 0.01$ ; \*\*\*,  $P \leq 0.005$ ; \*\*\*\*,  $P \leq 0.001$ ; otherwise, not significant). **b-c)** Accumulation of MPK3, RbohD, BIK1 in  $SETI^{WT}$  seedlings pre-treated with estradiol (b) or mock (c) for 3 h and subsequently treated with cycloheximide (50mM; CHX), MG132 (10mM), or both for indicated times (2h, 4h, 8h). Actin and MPK6 was used as control. Ponceau staining (PS) of corresponding blots are shown below. **d)** Protein level of RPS4-HA, FLS2 and BAK1 in  $SETI^{WT}$  seedlings during different treatments as described above. Ponceau staining (PS) of corresponding blots are shown below. This figure has been published in Ngou et al, 2020b and appears here with permission.

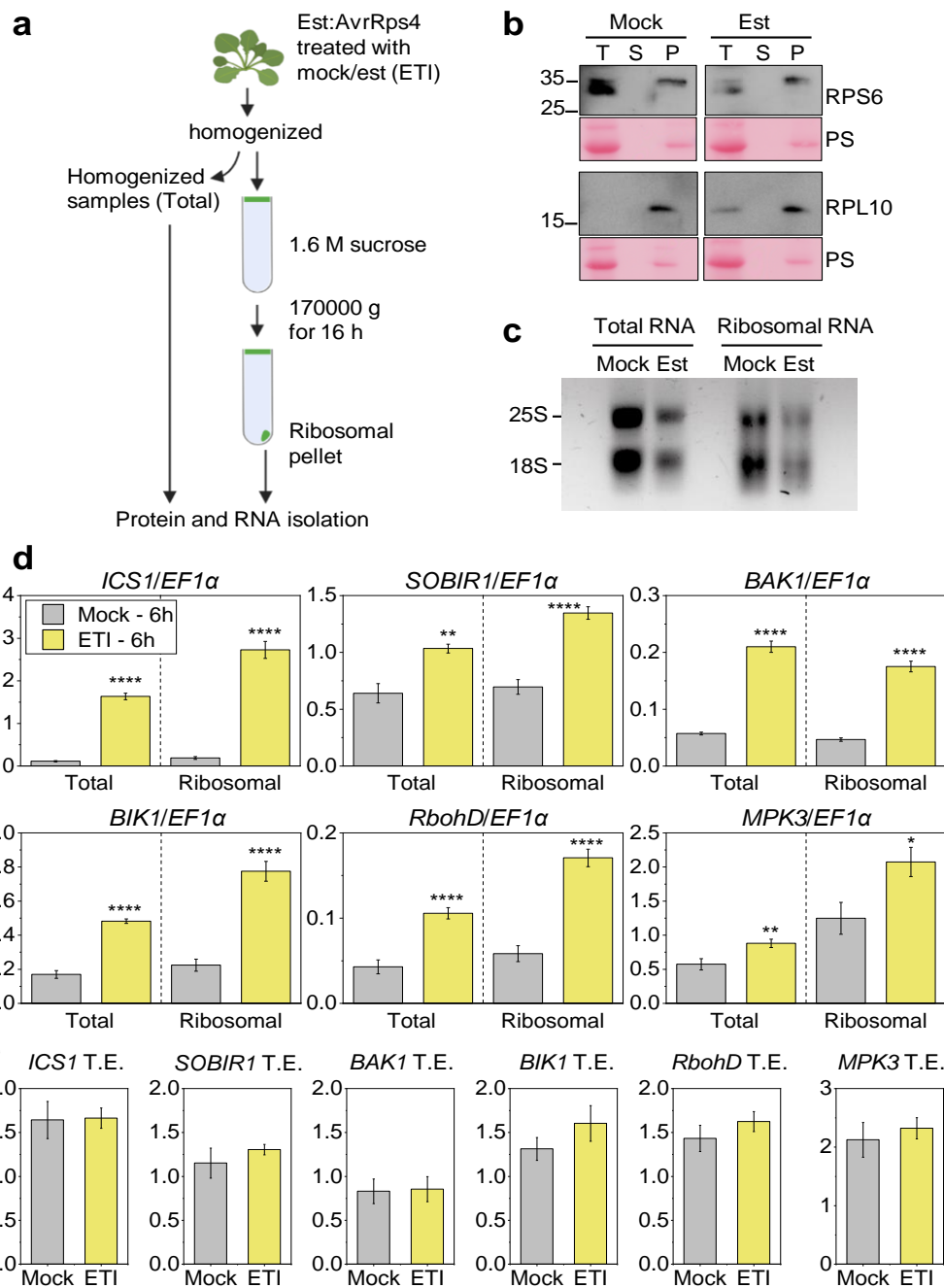


**Figure 5.9. Translation control during ETI<sup>AvrRps4</sup>.** **a)** Experiment design of ribosome enrichment with ultracentrifugation. SET1<sup>WT</sup> leaves treated with mock or estradiol solution were homogenized in extraction buffer. Part of it was used for total extraction (T) and the rest were ultra-centrifugated at 170000 g for 16 hours. Ribosomal pellet was then collected for ribosomal extraction (P). **b)** Total extract (T), supernatant (S), and ribosomal pellet (P) samples were blotted with RPS6 and RPL10 antibody. Ponceau staining was used as loading control. **c)** RNA extracted from total extract (total RNA) and ribosomal pellet (ribosome RNA) were loaded on a gel. 28S and 18S are indicated. **d)** Relative expression of *ICS1*, *SOBIR1*, *BAK1*, *BIK1*, *RbohD* and *MPK3* to *EF1α* from total RNA (Total) and ribosomal pellet RNA (Ribosomal). The average of data points from 3 biological replicates were plotted onto the graphs, with  $\pm$ S.E. for error bars. Welch's t-test was used to analyze significance in differences between mock and estradiol-treated samples. (\*;  $P \leq 0.05$ ; \*\*,  $P \leq 0.01$ ; \*\*\*,  $P \leq 0.005$ ; \*\*\*\*,  $P \leq 0.001$ ; otherwise, not significant, not significant;). **e)** Translational efficiency (T.E., relative to *EF1α*) was calculated from the ratio of transcripts retained from the ribosomal to total samples. T.E. of *ICS1*, *SOBIR1*, *BAK1*, *BIK1*, *RbohD* and *MPK3* is not significantly different between mock and ETI. This figure has also been published in Ngou et al, 2020b and appears here with permission.

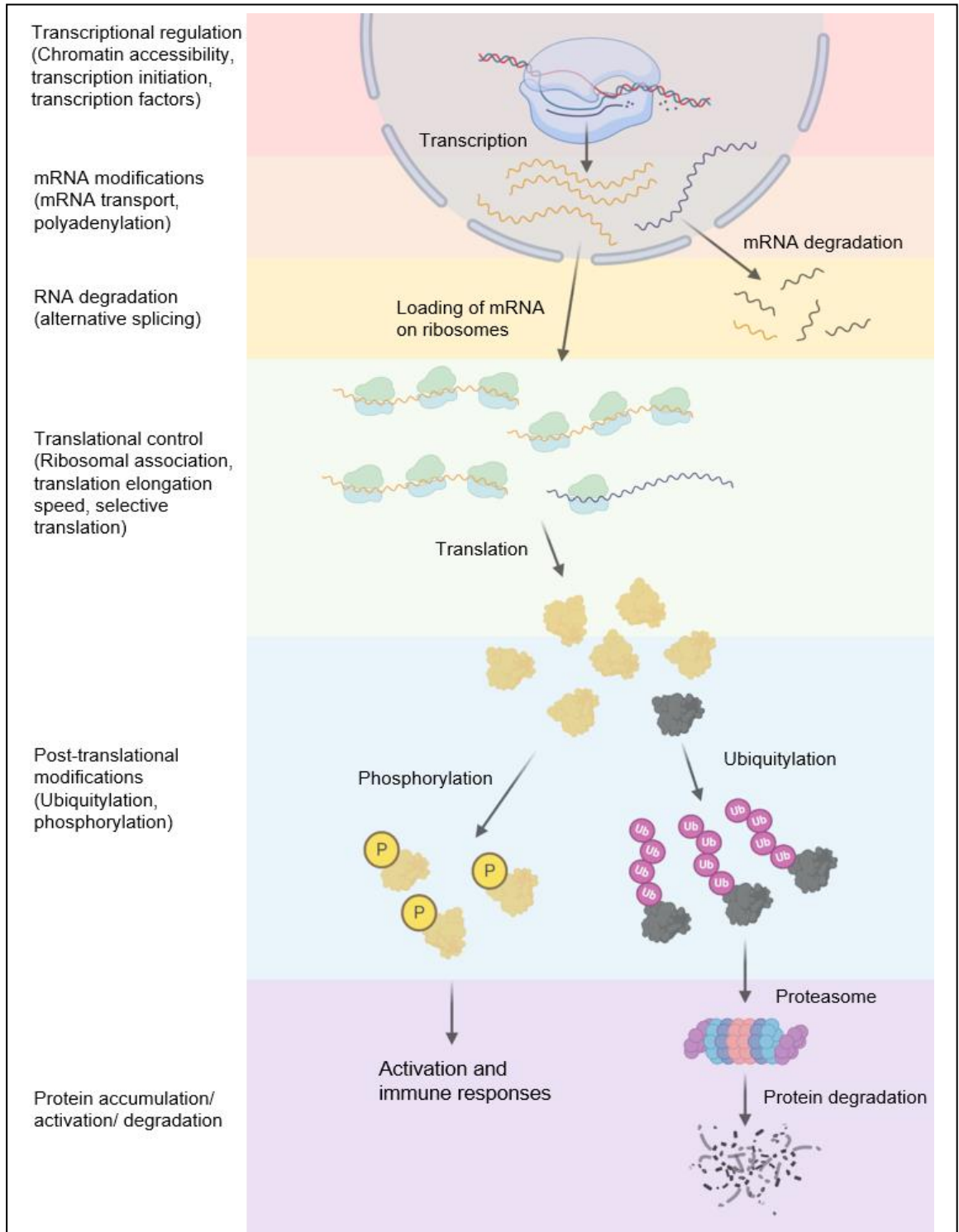


Figure 5.10. **Mechanisms that control protein accumulation during ETI.** Illustrated diagram of potential mechanisms that contributes to gene upregulation (yellow protein) or downregulation (black protein). ETI leads to transcriptional activation of PTI-signalling components. Modifications of transcripts (or mRNA) contribute to their stability. Transcripts are then loaded onto ribosomes for translation. Translation efficiency is determined by multiple factors such as ribosomal association, translation elongation speed, codon optimization and tRNA availability. Synthesized proteins are subjected to post-translational modifications, which leads to protein activation or turnover (degradation). These processes together determine the accumulation of PTI-signalling components during ETI.

## **Chapter 6: General discussion**

### **Study of ETI in the absence of PTI**

In most previous literature, investigations into ETI in which effectors are delivered either from pathogen strains or by Agro-infiltration, have unwittingly involved studying “PTI + ETI” rather than ETI alone, thus masking the mutual potentiation of the two immune systems. In contrast, in this thesis, I used inducible effector expression, revealing the roles and mechanisms of ETI in the absence of PTI, and also interactions between ETI and PTI. While the inducible system has its advantages, there are some limitations. Firstly, it is unclear whether the amounts of effectors that accumulate upon inducible expression resemble the amounts delivered into plant cells during authentic infections. Conceivably, over-expression of effectors might cause pleiotropic effects or artifacts. In addition, comparison between ETI triggered by different effectors/NLRs with individual inducible lines might not be accurate, due to variable number and/or position of genomic insertions. Furthermore, it is difficult to trigger ETI in specific locations in a plant since chemicals like estradiol or dexamethasone diffuse into neighboring tissues. Recent technological advances in optogenetics allow inducible gene expression in plants under specific wavelengths of light (Ochoa-Fernandez et al., 2020). This could enable local expression of effectors in a specific tissue, while avoiding the diffusion effects and wounding (release of DAMPs) triggered by infiltration of chemical inducers. Thus, optogenetic control of effector expression may allow the dissection of ETI locally and systemically in the future.

### **Differential and common downstream responses triggered by CC- and TIR-NLRs**

ETI triggered by CC-NLRs (RPM1, RPS2 and RPS5), if effector levels are sufficiently induced, activates MAPK, ROS burst and macroscopic cell death, while ETI triggered by TIR-NLRs (RRS1, RPS4 and RPP4) does not. Additional lines, such as inducible HopZ1a- (activates the CC-NLR ZAR1), inducible AvrAC- (activates ZAR1) and inducible AvrRpp2 (ATR2)- (activates the TIR-NLR RPP2) lines, should be tested in the future. RPM1, RPS2 and RPS5 are localized on the plasma membrane while RRS1, RPS4 and RPP4 are localized in the nucleus. Since RLCKs and NADPH oxidases are localized on the plasma membrane and MAPKs are localized in the cytosol and/or nucleus, the localization of NLRs might influence their downstream signaling. A recent report suggests that RPS2-induced ROS burst and RbohD phosphorylation (at S343 and S347) is dependent on BAK1, BKK1 and BIK1 (Yuan et al., 2020). RPM1, RPS2 and RPS5 also physically associate with FLS2 (Qi et al., 2011), implying that CC-NLRs might function through PTI-signaling components. On the other hand, the ZAR1-resistosome has been suggested to function as

pore-forming device on plasma membranes to directly trigger HR (Wang et al., 2019a). However, the N-terminal pore-forming motif (MADA motif) is only conserved in around 20% of plant CC-NLRs (Adachi et al., 2019). In addition, plasma membrane localized NLRs have recently been shown to target a P-type ATPase to induce plasma membrane depolarization and calcium influx (Choi et al., 2020). The signaling pathway activated by CC-NLRs that leads to MAPK activation, ROS burst and macroscopic cell death remains to be determined, but could result directly from ion fluxes that result from membrane perturbation.

Activation of RPM1, RPS2, RPS5, RRS1/RPS4 and RPP4 all lead to transcriptional upregulation of *ICS1* and PTI-signaling components. Similarly, robust protein accumulation of BAK1, SOBIR1, BIK1, RbohD and MPK3 are detected upon ETI triggered by these NLRs. This implies that salicylic acid biosynthesis and potentiation of PTI are shared defense mechanisms triggered by both CC- and TIR-NLRs. It is unclear whether CC- and TIR-NLRs share the same signaling pathways that lead to these defense responses. The transcription factors SARD1 and CBP60G are required for salicylic acid accumulation during both CC- and TIR-NLR activation (Sun et al., 2018; Zhang et al., 2010b). It is therefore possible that different NLRs activate common transcription factors, resulting in transcriptional upregulation during ETI.

### **Differential and common downstream responses triggered by PRRs and NLRs**

PTI has been shown to trigger physiological responses such as MAPK activation, ROS burst and calcium influx. Notably, PTI triggered by different PAMPs/ PRRs have yet to be compared. Whether different PRRs trigger similar physiological responses is unclear. As previously discussed, CC-NLRs can also activate these responses, possibly due to their action on membranes, shared signaling components and/ or other unknown mechanisms. The ability to activate PTI-signaling components by membrane localized-NLRs could allow them to restore PTI in the presence of ETS induced by effectors. On the other hand, nuclear-localized-NLRs recognize effectors which are unlikely to target membrane-associated PTI-signaling components. Other common physiological responses induced by PTI and ETI are callose deposition and transcriptional reprogramming. We noticed that callose spots induced by ETI<sup>AvrRps4</sup> are bigger than those triggered by PTI. In addition, ETI<sup>AvrRps4</sup>-induced callose deposition is likely to be ROS-independent. This indicates that ETI can trigger callose deposition through an unknown mechanism, perhaps by the induction of callose synthase. As mentioned, there is substantial overlap between genes induced by PRRs and NLRs (Navarro et al., 2004), possibly due to shared transcription

factors such as SARD1, CBP0G and CAMTA3 (Jacob et al., 2018; Sun et al., 2015; Zhang et al., 2010b). However, ETI leads to prolonged upregulation of salicylic acid biosynthesis genes such as *ICS1* and *EDS5*, and prolonged protein accumulation of multiple PTI-signaling components. Thus, signaling components, such as transcription factors, that are specifically utilized during ETI remain to be discovered. To summarize, there are some shared signaling components between PTI and ETI induced by CC-NLRs, while PTI and ETI induced by TIR-NLRs initiate distinct chains of signaling events and result in distinct physiological outputs. ETI also specifically leads to prolonged upregulation of salicylic acid biosynthesis and PTI-signaling pathway components, thus restoring and potentiating PTI.

### **The relationship between PRR- and NLR-mediated immunity**

Immune responses triggered by PRRs and NLRs have been extensively studied in the past couple of decades. While the signaling pathway of PTI is relatively well-defined, little is known about ETI-induced signaling and physiological responses. Previous reports and reviews have suggested ETI acts to “re-boot” PTI (Jacob et al., 2018; Nomura et al., 2011; Tao et al., 2003). However, because of the lack of unambiguous data, it was assumed that ETI acts independently of PTI upon activation. Yuan et al (Yuan et al., 2020) and our data (Ngou, et al., 2020) support a model that ETI restores and potentiates activation of signaling components by PTI during *Pst* infection, making PTI an indispensable component for ETI-induced resistance (Yuan et al., 2020). One of the major challenges in the plant immunity field is to understand the underlying mechanism of how activated NLRs exert resistance against pathogens. While there are likely other mechanisms involved (for example salicylic acid and pipecolic acid biosynthesis), we have shown that one of the major mechanisms of ETI is to enhance physiological responses induced by PTI. How PTI-induced physiological responses lead to resistance through nutrient restriction, cell wall fortification, inhibition of effector secretion and other unknown mechanisms remains to be determined (Anderson et al., 2014; Crabill et al., 2010; Luna et al., 2011; Nobori et al., 2018; Voigt, 2014; Wang et al., 2020a; Yamada et al., 2016b). Although we have only investigated a limited number of NLRs (RPM1, RPS2, RPS5, RRS1/RPS4 and RPP4) and PRRs (FLS2, EFR, PEPR1/2, LORE, RLP23 and LYK5) due to constraints in materials and available pathogens, this mechanism is likely to be conserved across a wide range of plant-pathogen interactions. In addition, while many effectors have been shown to target the PTI signaling pathway, recent reports suggest that the ETI signaling pathway could also be targeted by effectors (Li et al., 2020b; Lopez et al., 2019; Yu et al., 2020). Given that the mutual potentiation between PTI

and ETI is highly relevant to resistance, pathogens might have evolved effectors to target both processes.

### **Coordination of multiple PRRs and NLRs during infection**

During natural infection, multiple PRRs, and potentially NLRs, are activated simultaneously. For example, FLS2 (which recognizes flg22), EFR (recognizes elf18), LORE (recognizes C10:0), PEPR1/2 (recognizes PEPs) are all activated during *Pseudomonas* infection, while multiple NLRs (RPM1, RPS2, RPS5 and RRS1/RPS4) can also be activated. ETI<sup>AvrRps4</sup> can potentiate PTI activated by multiple PRRs, and PTI signaling components are upregulated during ETI triggered by multiple NLRs, indicating that any PRRs and NLRs can coordinate with each other during immunity. Since PTI is usually activated before ETI, ETI must be activated within a few hours following PTI to potentiate it. This might explain why delayed ETI activation does not lead to effective resistance against *Pseudomonas* (Figure 3.7b) (Bhandari et al., 2019). In addition, potentiation of PTI by RPS2 is faster (phase II, 1-3 hours) compared to RRS1/RPS4 (phase III, 3-16 hours), indicating that upregulation of PTI signaling components is more rapid during RPS2 activation. This is consistent with previous reports that RPM1 and RPS2 activate faster transcriptional reprogramming compared to RRS1/RPS4 (Saile et al., 2020). ETI<sup>AvrRps4</sup> alone leads to accumulation of PTI signaling components for up to 24 hours. It would be interesting to test if simultaneous activation of multiple NLRs can lead to stronger and prolonged upregulation of these genes. Recently it has been reported that cross-talk between the PRR co-receptors, BAK1 and CERK1, potentiates chitin-induced PTI responses upon bacterial perception (Gong et al., 2019). The cross-talk between PRRs and NLRs (PTI-PTI, ETI-ETI and PTI-ETI interaction) during natural infection is complex and will reward further investigation.

### **Is potentiation between PTI and ETI local or systemic?**

As mentioned, it is difficult to activate ETI in single-cell level with the chemical-inducible system since chemicals diffuse into neighboring tissues. Whole leaves or seedlings were treated with estradiol or dexamethasone in this study. Therefore, it is unclear whether the potentiation between PTI and ETI happens within the same cell (cell-autonomously) or systemically (or both). Potentiation of RbohD phosphorylation (in S343 and S347) during ‘‘PTI + ETI’’ occurs in both leaf tissues and protoplasts (Ngou et al., 2020b; Yuan et al., 2020). Thus, ETI potentiates PTI within the same cell. Whether ETI can prime PTI in neighboring cells is unknown. External application of salicylic acid can induce the upregulation of both MPK3 and RbohD (Beckers et al., 2009; Lukan et al., 2020; Pogány

et al., 2009), so perhaps salicylic acid induction during ETI allows the accumulation of PTI-signaling components in neighboring cells. In addition, it is unclear whether PTI activation can prime ETI in neighboring cells. The spatial regulation and potentiation of PTI and ETI during natural infection remains to be further explored.

### **Mechanisms involved in the potentiation of PTI by ETI**

One of the mechanisms of which ETI potentiates PTI is through elevating the abundance of PTI-signaling components. With pre- or co-activation with ETI, the abundance of the activated BIK1, RbohD and MPK3 increases, likely due to the increased amount of total protein. However, the proportion of these proteins that gets activated might also increase during ‘‘PTI +ETI’’, as upstream signaling components such as BAK1, CPKs, MKK4 and MKK5 are also upregulated during ETI. It is challenging to distinguish these possibilities since they might equally contribute to the enhanced activity of these proteins. PTI signaling components are heavily regulated to prevent hyper-activation or prolonged immune responses. Some of these mechanisms include regulation of PRR complex phosphorylation status, de-activation of signaling components and control of protein turnover (Couto and Zipfel, 2016). It is therefore possible that ETI enhances activation of PTI through the inhibition of these mechanisms. Interestingly, the U-box E3 ubiquitin ligases *PUB12* required for FLS2 degradation is down-regulated during ETI<sup>AvrRps4</sup> (Lu et al., 2011). The Arabidopsis E3 ubiquitin ligases *RHA3A* required for BIK1 mono-ubiquitination is also down-regulated during ETI<sup>AvrRps4</sup> (Ma et al., 2020a). Thus, ETI might reduce turnover of PTI signaling components as proposed in chapter 5. A recent report suggests that pep1 perception leads to alternative splicing and an inactive form of *CPK28*, which leads to reduction of BIK1 degradation and enhance PTI activation (Dressano et al., 2020). It would be interesting to test if ETI also leads to alternative splicing and inactive forms of negative PTI regulators.

In addition to protein turnover, transcriptional and translation regulation are also involved in the upregulation of PTI signaling components. Although the transcription factors *SARD1* and *CBP60G* have been shown to bind to BIK1 and MPK3 promoters, both transcript and protein induction of these genes are not affected during ETI<sup>AvrRps4</sup> in SETI *sard1 cbp60g*, indicating that additional transcription factors contribute to their upregulation. As mentioned, salicylic acid application leads to induction of both MPK3 and RbohD in both Arabidopsis and tobacco (Beckers et al., 2009; Lukan et al., 2020; Pogány et al., 2009; Zhang and Klessig, 1998). Since the upregulation of PTI signaling components is not abolished in both *sard1 cbp60g* or *ics1* (Ngou et al., 2020b; Yuan et al., 2020), salicylic acid might be involved in the prolonged accumulation of these genes at a later stage of

infection, and in preparing systemic leaves for a stronger response. In the future, reverse genetics and other discovery approaches, such as DAP-seq (O'Malley et al., 2016), will allow the identification of transcription factors required for the upregulation of these genes. During PTI, translation efficiency is low (Xu et al., 2017). This might serve as a mechanism to prevent prolonged activation of PTI. On the other hand, two independent reports show that translation is highly correlated to transcription during ETI<sup>AvrRpm1</sup> and ETI<sup>AvrRpt2</sup> (Meteignier et al., 2017; Yoo et al., 2020). This implies that translation inhibition is lifted during ETI. Consistent with these data, ETI<sup>AvrRps4</sup>-induced elevated mRNA levels for *BIK1*, *RbohD* and *MPK3* are matched by elevation in ribosome-loaded mRNAs for these genes (Figure 5.9). Whether ETI leads to elevated translation efficiency of these genes through other mechanisms remains to be investigated. It is challenging to determine the relative contribution of transcription, translation, and protein turnover in protein accumulation during ETI using inhibitors, since each of these steps affects one another. Interestingly, simultaneous mRNA and protein labeling in mouse dendritic cells suggests that protein accumulation during LPS-induced immunity is mainly determined by transcription, whereas translation and protein turnover contribute to the regulation of pre-existing proteome (Jovanovic et al., 2015). Whether a similar phenomenon occurs during plant immunity remains to be determined.

### **Mechanisms involved in the potentiation of ETI by PTI**

PTI potentiates HR triggered by ETI. We initially hypothesized that PTI might be required for ETI to be activated. However, ETI activation alone leads to *ICS1* expression and growth stunting in seedlings. “PTI + ETI” also does not lead to stronger *ICS1* induction than ETI alone. Thus, activation of ETI does not require pre-activation of PTI, and potentiated HR during “PTI + ETI” is therefore likely due to enhanced activation of downstream signaling components. Activation of MPK3 and MPK6 leads to photosynthetic inhibition and chloroplastic ROS accumulation, which can also promote HR (Su et al., 2018). Activation of RbohD/F also leads to ROS accumulation and HR (Torres et al., 2002; Yun et al., 2011). Since ETI alone triggers weak (CC-NLRs) or no MAPK and RbohD activation (TIR-NLRs), enhanced activation of these signaling components during “PTI + ETI” might contribute to the enhanced ROS accumulation and macroscopic HR.

There might be additional mechanisms that lead to enhanced HR during “PTI + ETI”. Recently, it has been reported that MPK3 and MPK6 activation during PTI leads to degradation of nonsense-mediated mRNA decay (NMD) factors and NLR transcript accumulation (Jung et al., 2020). Similarly, flg22 treatment can lead to induction of both

ADR1 and NRG1 (Bonardi et al., 2011; Brendolise et al., 2018). This indicates that PTI can prime ETI signaling components, thus potentiating ETI. In addition, MPK3 and MPK6 can also phosphorylate SGT1, and the phosphorylation of SGT1 is required for RPS2-mediated cell death (Yu et al., 2020). Thus, prolonged phosphorylation of multiple MAPKs substrates during ‘‘PTI + ETI’’ might contribute to the enhanced HR.

### **How general is the new zig-zag-zig model?**

We have shown the mutual potentiation relationship between PTI and ETI during *Pseudomonas syringae* infection. It is unclear whether this mechanism applies to resistance against other pathogens. It has been reported that the resistance against *Hyaloperonospora arabidopsidis* (*Hpa*) strains *Emoy2* and *Cala2* is BAK1- and BKK1- dependent (Roux et al., 2011). Since resistance against *Emoy2* and *Cala* are RPP4- and RPP2-dependent respectively (Asai et al., 2018; Sinapidou et al., 2004; van der Biezen et al., 2002), ETI-induced resistance against *Hpa* might also require PTI. In addition, RRS1/RPS4, which recognises an unknown effector(s) from the fungal pathogen *Colletotrichum higginsianum* (Narusaka et al., 2009), can potentiate ROS production and cell death triggered by chitin. This indicates that potentiation between PTI and ETI can occur during fungal and oomycete infection. During fungal and oomycete infection, penetration hyphae spread through plant tissues, and effectors are only secreted through the haustoria. As a result, ETI might not be triggered in all the plant cells that are in contact with the pathogen. Perhaps the activation of ETI can potentiate PTI in the neighbouring cells and restrict the spreading of hyphae. The detailed molecular interaction between PTI and ETI during infection by filamentous pathogens remains to be determined.

Similar to *Hpa*, a *bak1-5 bkk1-1* mutant shows enhanced susceptibility against multiple RNA viruses including oilseed rape mosaic virus (ORMV), tobacco mosaic virus (TMV) and turnip crinkle virus (TCV) (Kørner et al., 2013). So far, there have been no reports of PRRs that recognise PAMPs from viruses. Double-stranded RNAs (dsRNAs) has been shown to induce SERK1-dependent PTI responses and antiviral resistance against OMRV (Niehl et al., 2016), implying that PTI might be activated during viral infection. In addition, DAMPs such as pep1 and pep2 might to be released from HR induced by ETI. *N* activation during TMV infection in tobacco also leads to prolonged transcript and protein accumulation of WIPK (the tobacco ortholog of Arabidopsis MPK3) (Zhang and Klessig, 1998). Since viral infection spreads through plants via cell-to-cell movement, perhaps activation of ETI by viral effectors leads to the release of DAMPs and viral PAMPs, which then triggers enhanced PTI responses in surrounding tissues to restrict the spread of viruses.

Whether mutual potentiation occurs during viral infection would be determined when any PAMPs/PRRs involved in virus perception are better defined.

### **Perspective for agriculture**

The new zig-zag-zig model corrects the previous implication that ETI alone can lead to resistance. While the activation of ETI does not require PTI, resistance induced by ETI is dependent on PTI. Thus, physiological responses triggered by PTI might be the key physiological process that halts pathogen infection. The new model proposed is highly relevant to engineer crop disease resistance in the field. Firstly, multiple NLR-encoding genes have been shown to be semi-dominant, which suggest the strength of ETI is rate-limiting for resistance (Cevik et al., 2019; Jones et al., 2003). Thus, stacks of multiple NLR genes should provide physiologically stronger resistance through potentiation, as well as enhancing genetic durability. Secondly, interfamily transfer of the PRR, EFR, has been shown to confer broad-spectrum bacterial resistance (Lacombe et al., 2010). This implies that transferring multiple PRRs together with the appropriate effector-recognizing NLRs could provide both broad-spectrum and durable resistance against virulent pathogens. It will be interesting to determine whether mutual potentiation between PTI and ETI applies to other host-pathogen systems in the future.

## References

- Adachi, H., Nakano, T., Miyagawa, N., Ishihama, N., Yoshioka, M., Katou, Y., Yaeno, T., Shirasu, K., and Yoshioka, H. (2015). WRKY Transcription Factors Phosphorylated by MAPK Regulate a Plant Immune NADPH Oxidase in *Nicotiana benthamiana*. *Plant Cell* 27, 2645–2663.
- Adachi, H., Contreras, M.P., Harant, A., Wu, C.-H., Derevnina, L., Sakai, T., Duggan, C., Moratto, E., Bozkurt, T.O., Maqbool, A., et al. (2019). An N-terminal motif in NLR immune receptors is functionally conserved across distantly related plant species. *Elife* 8.
- Albert, I., Böhm, H., Albert, M., Feiler, C.E., Imkampe, J., Wallmeroth, N., Brancato, C., Raaymakers, T.M., Oome, S., Zhang, H., et al. (2015). An RLP23-SOBIR1-BAK1 complex mediates NLP-triggered immunity. *Nat. Plants* 1, 15140.
- Albrecht, C., Boutrot, F., Segonzac, C., Schwessinger, B., Gimenez-Ibanez, S., Chinchilla, D., Rathjen, J.P., de Vries, S.C., and Zipfel, C. (2012). Brassinosteroids inhibit pathogen-associated molecular pattern-triggered immune signaling independent of the receptor kinase BAK1. *Proc. Natl. Acad. Sci. USA* 109, 303–308.
- Ali, R., Ma, W., Lemtiri-Chlieh, F., Tsaltas, D., Leng, Q., von Bodman, S., and Berkowitz, G.A. (2007). Death don't have no mercy and neither does calcium: *Arabidopsis* CYCLIC NUCLEOTIDE GATED CHANNEL2 and innate immunity. *Plant Cell* 19, 1081–1095.
- Anderson, J.C., Wan, Y., Kim, Y.-M., Pasa-Tolic, L., Metz, T.O., and Peck, S.C. (2014). Decreased abundance of type III secretion system-inducing signals in *Arabidopsis* mkp1 enhances resistance against *Pseudomonas syringae*. *Proc. Natl. Acad. Sci. USA* 111, 6846–6851.
- Aoyama, T., and Chua, N.H. (1997). A glucocorticoid-mediated transcriptional induction system in transgenic plants. *Plant J.* 11, 605–612.
- Asai, S., Furzer, O.J., Cevik, V., Kim, D.S., Ishaque, N., Goritschnig, S., Staskawicz, B.J., Shirasu, K., and Jones, J.D.G. (2018). A downy mildew effector evades recognition by polymorphism of expression and subcellular localization. *Nat. Commun.* 9, 5192.
- Asai, T., Tena, G., Plotnikova, J., Willmann, M.R., Chiu, W.-L., Gomez-Gomez, L., Boller, T., Ausubel, F.M., and Sheen, J. (2002). MAP kinase signalling cascade in *Arabidopsis* innate immunity. *Nature* 415, 977–983.
- Axtell, M.J., and Staskawicz, B.J. (2003). Initiation of RPS2-specified disease resistance in *Arabidopsis* is coupled to the AvrRpt2-directed elimination of RIN4. *Cell* 112, 369–377.
- Axtell, M.J., Chisholm, S.T., Dahlbeck, D., and Staskawicz, B.J. (2003). Genetic and molecular evidence that the *Pseudomonas syringae* type III effector protein AvrRpt2 is a cysteine protease. *Mol. Microbiol.* 49, 1537–1546.
- Azevedo, C., Sadanandom, A., Kitagawa, K., Freialdenhoven, A., Shirasu, K., and Schulze-Lefert, P. (2002). The RAR1 interactor SGT1, an essential component of R gene-triggered disease resistance. *Science* 295, 2073–2076.
- Baggs, E., Dagdas, G., and Krasileva, K.V. (2017). NLR diversity, helpers and integrated domains: making sense of the NLR IDentity. *Curr. Opin. Plant Biol.* 38, 59–67.

- Bari, R., and Jones, J.D.G. (2009). Role of plant hormones in plant defence responses. *Plant Mol. Biol.* *69*, 473–488.
- Barragan, C.A., Wu, R., Kim, S.-T., Xi, W., Habring, A., Hagmann, J., Van deaana 1Weyer, A.-L., Zaidem, M., Ho, W.W.H., Wang, G., et al. (2019). RPW8/HR repeats control NLR activation in *Arabidopsis thaliana*. *PLoS Genet.* *15*, e1008313.
- Bastedo, D.P., Khan, M., Martel, A., Seto, D., Kireeva, I., Zhang, J., Masud, W., Millar, D., Lee, J.Y., Lee, A.H.-Y., et al. (2019). Perturbations of the ZED1 pseudokinase activate plant immunity. *PLoS Pathog.* *15*, e1007900.
- Beckers, G.J.M., Jaskiewicz, M., Liu, Y., Underwood, W.R., He, S.Y., Zhang, S., and Conrath, U. (2009). Mitogen-activated protein kinases 3 and 6 are required for full priming of stress responses in *Arabidopsis thaliana*. *Plant Cell* *21*, 944–953.
- Bender, C.L., Alarcón-Chaidez, F., and Gross, D.C. (1999). *Pseudomonas syringae* phytotoxins: mode of action, regulation, and biosynthesis by peptide and polyketide synthetases. *Microbiol. Mol. Biol. Rev.* *63*, 266–292.
- Bent, A.F., Kunkel, B.N., Dahlbeck, D., Brown, K.L., Schmidt, R., Giraudat, J., Leung, J., and Staskawicz, B.J. (1994). *RPS2* of *Arabidopsis thaliana*: a leucine-rich repeat class of plant disease resistance genes. *Science* *265*, 1856–1860.
- Bernoux, M., Burdett, H., Williams, S.J., Zhang, X., Chen, C., Newell, K., Lawrence, G.J., Kobe, B., Ellis, J.G., Anderson, P.A., et al. (2016). Comparative Analysis of the Flax Immune Receptors L6 and L7 Suggests an Equilibrium-Based Switch Activation Model. *Plant Cell* *28*, 146–159.
- Bethke, G., Unthan, T., Uhrig, J.F., Pöschl, Y., Gust, A.A., Scheel, D., and Lee, J. (2009). Flg22 regulates the release of an ethylene response factor substrate from MAP kinase 6 in *Arabidopsis thaliana* via ethylene signaling. *Proc. Natl. Acad. Sci. USA* *106*, 8067–8072.
- Bhandari, D.D., Lapin, D., Kracher, B., von Born, P., Bautor, J., Niefind, K., and Parker, J.E. (2019). An EDS1 heterodimer signalling surface enforces timely reprogramming of immunity genes in *Arabidopsis*. *Nat. Commun.* *10*, 772.
- Bi, G., Liebrand, T.W.H., Bye, R.R., Postma, J., van der Burgh, A.M., Robatzek, S., Xu, X., and Joosten, M.H.A.J. (2016). SOBIR1 requires the GxxxG dimerization motif in its transmembrane domain to form constitutive complexes with receptor-like proteins. *Mol. Plant Pathol.* *17*, 96–107.
- Bi, G., Zhou, Z., Wang, W., Li, L., Rao, S., Wu, Y., Zhang, X., Menke, F.L.H., Chen, S., and Zhou, J.-M. (2018). Receptor-Like Cytoplasmic Kinases Directly Link Diverse Pattern Recognition Receptors to the Activation of Mitogen-Activated Protein Kinase Cascades in *Arabidopsis*. *Plant Cell* *30*, 1543–1561.
- Van der Biezen, E.A., and Jones, J.D. (1998). Plant disease-resistance proteins and the gene-for-gene concept. *Trends Biochem. Sci.* *23*, 454–456.
- Bigeard, J., Colcombet, J., and Hirt, H. (2015). Signaling mechanisms in pattern-triggered immunity (PTI). *Mol. Plant* *8*, 521–539.
- Birkenbihl, R.P., Kracher, B., Roccaro, M., and Somssich, I.E. (2017). Induced Genome-Wide Binding of Three *Arabidopsis* WRKY Transcription Factors during Early MAMP-Triggered Immunity. *Plant Cell* *29*, 20–38.

- Böhm, H., Albert, I., Oome, S., Raaymakers, T.M., Van den Ackerveken, G., and Nürnberger, T. (2014a). A conserved peptide pattern from a widespread microbial virulence factor triggers pattern-induced immunity in *Arabidopsis*. *PLoS Pathog.* *10*, e1004491.
- Böhm, H., Albert, I., Fan, L., Reinhard, A., and Nürnberger, T. (2014b). Immune receptor complexes at the plant cell surface. *Curr. Opin. Plant Biol.* *20*, 47–54.
- Bonardi, V., Tang, S., Stallmann, A., Roberts, M., Cherkis, K., and Dangl, J.L. (2011). Expanded functions for a family of plant intracellular immune receptors beyond specific recognition of pathogen effectors. *Proc. Natl. Acad. Sci. USA* *108*, 16463–16468.
- Boudsocq, M., Willmann, M.R., McCormack, M., Lee, H., Shan, L., He, P., Bush, J., Cheng, S.-H., and Sheen, J. (2010). Differential innate immune signalling via Ca(2+) sensor protein kinases. *Nature* *464*, 418–422.
- Bradley, D.J., Kjellbom, P., and Lamb, C.J. (1992). Elicitor- and wound-induced oxidative cross-linking of a proline-rich plant cell wall protein: a novel, rapid defense response. *Cell* *70*, 21–30.
- Bray, N.L., Pimentel, H., Melsted, P., and Pachter, L. (2016). Near-optimal probabilistic RNA-seq quantification. *Nat. Biotechnol.* *34*, 525–527.
- Brendolise, C., Martinez-Sanchez, M., Morel, A., Chen, R., Dinis, R., Deroles, S., Peeters, N., Rikkerink, E.H.A., and Montefiori, M. (2018). NRG1-mediated recognition of HopQ1 reveals a link between PAMP and Effector-triggered Immunity. *BioRxiv*.
- Brock, A.K., Willmann, R., Kolb, D., Grefen, L., Lajunen, H.M., Bethke, G., Lee, J., Nürnberger, T., and Gust, A.A. (2010). The *Arabidopsis* mitogen-activated protein kinase phosphatase PP2C5 affects seed germination, stomatal aperture, and abscisic acid-inducible gene expression. *Plant Physiol.* *153*, 1098–1111.
- Brown, I., Trethowan, J., Kerry, M., Mansfield, J., and Bolwell, G.P. (1998). Localization of components of the oxidative cross-linking of glycoproteins and of callose synthesis in papillae formed during the interaction between non-pathogenic strains of *Xanthomonas campestris* and French bean mesophyll cells. *Plant J.* *15*, 333–343.
- Bruggeman, Q., Raynaud, C., Benhamed, M., and Delarue, M. (2015). To die or not to die? Lessons from lesion mimic mutants. *Front. Plant Sci.* *6*, 24.
- Burkart, R.C., and Stahl, Y. (2017). Dynamic complexity: plant receptor complexes at the plasma membrane. *Curr. Opin. Plant Biol.* *40*, 15–21.
- Buscaill, P., and Rivas, S. (2014). Transcriptional control of plant defence responses. *Curr. Opin. Plant Biol.* *20*, 35–46.
- Buscaill, P., Chandrasekar, B., Sanguankiatichai, N., Kourelis, J., Kaschani, F., Thomas, E.L., Morimoto, K., Kaiser, M., Preston, G.M., Ichinose, Y., et al. (2019). Glycosidase and glycan polymorphism control hydrolytic release of immunogenic flagellin peptides. *Science* *364*.
- Cai, Q., Qiao, L., Wang, M., He, B., Lin, F.-M., Palmquist, J., Huang, S.-D., and Jin, H. (2018). Plants send small RNAs in extracellular vesicles to fungal pathogen to silence virulence genes. *Science* *360*, 1126–1129.

- Cai, R., Lewis, J., Yan, S., Liu, H., Clarke, C.R., Campanile, F., Almeida, N.F., Studholme, D.J., Lindeberg, M., Schneider, D., et al. (2011). The plant pathogen *Pseudomonas syringae* pv. tomato is genetically monomorphic and under strong selection to evade tomato immunity. *PLoS Pathog.* 7, e1002130.
- Campos-Soriano, L., Bundó, M., Bach-Pages, M., Chiang, S.-F., Chiou, T.-J., and San Segundo, B. (2020). Phosphate excess increases susceptibility to pathogen infection in rice. *Mol. Plant Pathol.* 21, 555–570.
- Cao, H., Li, X., and Dong, X. (1998). Generation of broad-spectrum disease resistance by overexpression of an essential regulatory gene in systemic acquired resistance. *Proc. Natl. Acad. Sci. USA* 95, 6531–6536.
- Cao, Y., Aceti, D.J., Sabat, G., Song, J., Makino, S.-I., Fox, B.G., and Bent, A.F. (2013). Mutations in FLS2 Ser-938 dissect signaling activation in FLS2-mediated Arabidopsis immunity. *PLoS Pathog.* 9, e1003313.
- Cao, Y., Liang, Y., Tanaka, K., Nguyen, C.T., Jedrzejczak, R.P., Joachimiak, A., and Stacey, G. (2014). The kinase LYK5 is a major chitin receptor in *Arabidopsis* and forms a chitin-induced complex with related kinase CERK1. *Elife* 3.
- Caplan, J.L., Mamillapalli, P., Burch-Smith, T.M., Czymbek, K., and Dinesh-Kumar, S.P. (2008). Chloroplastic protein NRIP1 mediates innate immune receptor recognition of a viral effector. *Cell* 132, 449–462.
- Castel, B., Ngou, P.-M., Cevik, V., Redkar, A., Kim, D.-S., Yang, Y., Ding, P., and Jones, J.D.G. (2019). Diverse NLR immune receptors activate defence via the RPW8-NLR NRG1. *New Phytol.* 222, 966–980.
- Century, K.S., Shapiro, A.D., Repetti, P.P., Dahlbeck, D., Holub, E., and Staskawicz, B.J. (1997). NDR1, a pathogen-induced component required for Arabidopsis disease resistance. *Science* 278, 1963–1965.
- Cesari, S., Thilliez, G., Ribot, C., Chalvon, V., Michel, C., Jauneau, A., Rivas, S., Alaux, L., Kanzaki, H., Okuyama, Y., et al. (2013). The rice resistance protein pair RGA4/RGA5 recognizes the Magnaporthe oryzae effectors AVR-Pia and AVR1-CO39 by direct binding. *Plant Cell* 25, 1463–1481.
- Césari, S., Kanzaki, H., Fujiwara, T., Bernoux, M., Chalvon, V., Kawano, Y., Shimamoto, K., Dodds, P., Terauchi, R., and Kroj, T. (2014). The NB-LRR proteins RGA4 and RGA5 interact functionally and physically to confer disease resistance. *EMBO J.* 33, 1941–1959.
- Cevik, V., Boutrot, F., Apel, W., Robert-Seilaniantz, A., Furzer, O.J., Redkar, A., Castel, B., Kover, P.X., Prince, D.C., Holub, E.B., et al. (2019). Transgressive segregation reveals mechanisms of Arabidopsis immunity to Brassica-infecting races of white rust (*Albugo candida*). *Proc. Natl. Acad. Sci. USA* 116, 2767–2773.
- Chang, C., Yu, D., Jiao, J., Jing, S., Schulze-Lefert, P., and Shen, Q.-H. (2013). Barley MLA immune receptors directly interfere with antagonistically acting transcription factors to initiate disease resistance signaling. *Plant Cell* 25, 1158–1173.
- Chen, H., Chen, J., Li, M., Chang, M., Xu, K., Shang, Z., Zhao, Y., Palmer, I., Zhang, Y., McGill, J., et al. (2017). A bacterial type III effector targets the master regulator of

- salicylic acid signaling, NPR1, to subvert plant immunity. *Cell Host Microbe* 22, 777–788.e7.
- Chen, L.-Q., Hou, B.-H., Lalonde, S., Takanaga, H., Hartung, M.L., Qu, X.-Q., Guo, W.-J., Kim, J.-G., Underwood, W., Chaudhuri, B., et al. (2010). Sugar transporters for intercellular exchange and nutrition of pathogens. *Nature* 468, 527–532.
- Chen, X., Zuo, S., Schwessinger, B., Chern, M., Canlas, P.E., Ruan, D., Zhou, X., Wang, J., Daudi, A., Petzold, C.J., et al. (2014). An XA21-associated kinase (OsSERK2) regulates immunity mediated by the XA21 and XA3 immune receptors. *Mol. Plant* 7, 874–892.
- Chen, Y.-C., Holmes, E.C., Rajniak, J., Kim, J.-G., Tang, S., Fischer, C.R., Mudgett, M.B., and Sattely, E.S. (2018). N-hydroxy-pipecolic acid is a mobile metabolite that induces systemic disease resistance in *Arabidopsis*. *Proc. Natl. Acad. Sci. USA* 115, E4920–E4929.
- Cheval, C., Aldon, D., Galaud, J.-P., and Ranty, B. (2013). Calcium/calmodulin-mediated regulation of plant immunity. *Biochim. Biophys. Acta* 1833, 1766–1771.
- Chinchilla, D., Bauer, Z., Regenass, M., Boller, T., and Felix, G. (2006). The *Arabidopsis* receptor kinase FLS2 binds flg22 and determines the specificity of flagellin perception. *Plant Cell* 18, 465–476.
- Chinchilla, D., Zipfel, C., Robatzek, S., Kemmerling, B., Nürnberger, T., Jones, J.D.G., Felix, G., and Boller, T. (2007). A flagellin-induced complex of the receptor FLS2 and BAK1 initiates plant defence. *Nature* 448, 497–500.
- Cho, H.K., Ahn, C.S., Lee, H.-S., Kim, J.-K., and Pai, H.-S. (2013). Pescadillo plays an essential role in plant cell growth and survival by modulating ribosome biogenesis. *Plant J.* 76, 393–405.
- Choi, D., Lee, H.-Y., Seo, Y.-E., Lee, J.H., Lee, S.E., Oh, S., Kim, J., Jung, S., Kim, H., Park, H., et al. (2020). Plant NLR targets P-type ATPase for executing plasma membrane depolarization leading to calcium influx and cell death. *BioRxiv*.
- Choi, H.W., Kim, Y.J., Lee, S.C., Hong, J.K., and Hwang, B.K. (2007). Hydrogen peroxide generation by the pepper extracellular peroxidase CaPO2 activates local and systemic cell death and defense response to bacterial pathogens. *Plant Physiol.* 145, 890–904.
- Clough, S.J., Fengler, K.A., Yu, I.C., Lippok, B., Smith, R.K., and Bent, A.F. (2000). The *Arabidopsis* *dnd1* “defense, no death” gene encodes a mutated cyclic nucleotide-gated ion channel. *Proc. Natl. Acad. Sci. USA* 97, 9323–9328.
- Cohn, M., Bart, R.S., Shybut, M., Dahlbeck, D., Gomez, M., Morbitzer, R., Hou, B.-H., Frommer, W.B., Lahaye, T., and Staskawicz, B.J. (2014). *Xanthomonas axonopodis* virulence is promoted by a transcription activator-like effector-mediated induction of a SWEET sugar transporter in cassava. *Mol. Plant Microbe Interact.* 27, 1186–1198.
- Couto, D., and Zipfel, C. (2016). Regulation of pattern recognition receptor signalling in plants. *Nat. Rev. Immunol.* 16, 537–552.
- Couto, D., Niebergall, R., Liang, X., Bücherl, C.A., Sklenar, J., Macho, A.P., Ntoukakis, V., Derbyshire, P., Altenbach, D., Maclean, D., et al. (2016). The *Arabidopsis* protein

- phosphatase PP2C38 negatively regulates the central immune kinase BIK1. *PLoS Pathog.* *12*, e1005811.
- Crabill, E., Joe, A., Block, A., van Rooyen, J.M., and Alfano, J.R. (2010). Plant immunity directly or indirectly restricts the injection of type III effectors by the *Pseudomonas syringae* type III secretion system. *Plant Physiol.* *154*, 233–244.
- Cui, H., Gobbato, E., Kracher, B., Qiu, J., Bautor, J., and Parker, J.E. (2017). A core function of EDS1 with PAD4 is to protect the salicylic acid defense sector in *Arabidopsis* immunity. *New Phytol.* *213*, 1802–1817.
- Dalio, R.J.D., Paschoal, D., Arena, G.D., Magalhães, D.M., Oliveira, T.S., Merfa, M.V., Maximo, H.J., and Machado, M.A. (2020). Hypersensitive response (HR): from NLR pathogen recognition to cell death response. *Ann Appl Biol.*
- Dangl, J.L., and Jones, J.D. (2001). Plant pathogens and integrated defence responses to infection. *Nature* *411*, 826–833.
- Dangl, J.L., and Jones, J.D.G. (2019). A pentangular plant inflammasome. *Science* *364*, 31–32.
- Daskalov, A., Habenstein, B., Sabaté, R., Berbon, M., Martinez, D., Chaignepain, S., Couлары-Salin, B., Hofmann, K., Loquet, A., and Saupe, S.J. (2016). Identification of a novel cell death-inducing domain reveals that fungal amyloid-controlled programmed cell death is related to necroptosis. *Proc. Natl. Acad. Sci. USA* *113*, 2720–2725.
- Daudi, A., and O'Brien, J.A. (2012). Detection of hydrogen peroxide by DAB staining in *Arabidopsis* leaves. *Bio Protoc* *2*.
- Day, B., Dahlbeck, D., and Staskawicz, B.J. (2006). NDR1 interaction with RIN4 mediates the differential activation of multiple disease resistance pathways in *Arabidopsis*. *Plant Cell* *18*, 2782–2791.
- DebRoy, S., Thilmony, R., Kwack, Y.-B., Nomura, K., and He, S.Y. (2004). A family of conserved bacterial effectors inhibits salicylic acid-mediated basal immunity and promotes disease necrosis in plants. *Proc. Natl. Acad. Sci. USA* *101*, 9927–9932.
- Denoux, C., Galletti, R., Mammarella, N., Gopalan, S., Werck, D., De Lorenzo, G., Ferrari, S., Ausubel, F.M., and Dewdney, J. (2008). Activation of defense response pathways by OGs and Flg22 elicitors in *Arabidopsis* seedlings. *Mol. Plant* *1*, 423–445.
- Derkacheva, M., Yu, G., Rufian, J.S., Jiang, S., Derbyshire, P., Morcillo, R.J.L., Stransfeld, L., Wei, Y., Menke, F.L.H., Zipfel, C., et al. (2020). The *Arabidopsis* E3 ubiquitin ligase PUB4 regulates BIK1 homeostasis and is targeted by a bacterial type-III effector. *BioRxiv*.
- DeYoung, B.J., Qi, D., Kim, S.-H., Burke, T.P., and Innes, R.W. (2012). Activation of a plant nucleotide binding-leucine rich repeat disease resistance protein by a modified self protein. *Cell Microbiol.* *14*, 1071–1084.
- Ding, P., and Ding, Y. (2020). Stories of salicylic acid: A plant defense hormone. *Trends Plant Sci.*

- Ding, P., Rekhter, D., Ding, Y., Feussner, K., Busta, L., Haroth, S., Xu, S., Li, X., Jetter, R., Feussner, I., et al. (2016). Characterization of a pipecolic acid biosynthesis pathway required for systemic acquired resistance. *Plant Cell* 28, 2603–2615.
- Ding, P., Sakai, T., Shrestha, R.K., Perez, N.M., Guo, W., Ngou, B.P.M., He, S., Liu, C., Feng, X., Zhang, R., et al. (2020). Chromatin accessibility landscapes activated by cell surface and intracellular immune receptors. *BioRxiv*.
- Ding, Y., Sun, T., Ao, K., Peng, Y., Zhang, Y., Li, X., and Zhang, Y. (2018). Opposite roles of salicylic acid receptors NPR1 and NPR3/NPR4 in transcriptional regulation of plant immunity. *Cell* 173, 1454–1467.e15.
- Dixon, M.S., Jones, D.A., Keddie, J.S., Thomas, C.M., Harrison, K., and Jones, J.D. (1996). The tomato Cf-2 disease resistance locus comprises two functional genes encoding leucine-rich repeat proteins. *Cell* 84, 451–459.
- Dixon, M.S., Hatzixanthis, K., Jones, D.A., Harrison, K., and Jones, J.D. (1998). The tomato Cf-5 disease resistance gene and six homologs show pronounced allelic variation in leucine-rich repeat copy number. *Plant Cell* 10, 1915–1925.
- Dodds, P.N., Lawrence, G.J., Catanzariti, A.-M., Teh, T., Wang, C.-I.A., Ayliffe, M.A., Kobe, B., and Ellis, J.G. (2006). Direct protein interaction underlies gene-for-gene specificity and coevolution of the flax resistance genes and flax rust avirulence genes. *Proc. Natl. Acad. Sci. USA* 103, 8888–8893.
- Dombrecht, B., Xue, G.P., Sprague, S.J., Kirkegaard, J.A., Ross, J.J., Reid, J.B., Fitt, G.P., Sewelam, N., Schenk, P.M., Manners, J.M., et al. (2007). MYC2 differentially modulates diverse jasmonate-dependent functions in Arabidopsis. *Plant Cell* 19, 2225–2245.
- Domínguez-Ferreras, A., Kiss-Papp, M., Jehle, A.K., Felix, G., and Chinchilla, D. (2015). An Overdose of the Arabidopsis Coreceptor BRASSINOSTEROID INSENSITIVE1-ASSOCIATED RECEPTOR KINASE1 or Its Ectodomain Causes Autoimmunity in a SUPPRESSOR OF BIR1-1-Dependent Manner. *Plant Physiol.* 168, 1106–1121.
- Dong, Z., Li, W., Liu, J., Li, L., Pan, S., Liu, S., Gao, J., Liu, L., Liu, X., Wang, G.-L., et al. (2019). The rice phosphate transporter protein ospt8 regulates disease resistance and plant growth. *Sci. Rep.* 9, 5408.
- Dressano, K., Weckwerth, P.R., Poretsky, E., Takahashi, Y., Villarreal, C., Shen, Z., Schroeder, J.I., Briggs, S.P., and Huffaker, A. (2020). Dynamic regulation of Pep-induced immunity through post-translational control of defence transcript splicing. *Nat. Plants* 6, 1008–1019.
- Dubiella, U., Seybold, H., Durian, G., Komander, E., Lassig, R., Witte, C.-P., Schulze, W.X., and Romeis, T. (2013). Calcium-dependent protein kinase/NADPH oxidase activation circuit is required for rapid defense signal propagation. *Proc. Natl. Acad. Sci. USA* 110, 8744–8749.
- Duxbury, Z., Wang, S., MacKenzie, C.I., Tenthorey, J.L., Zhang, X., Huh, S.U., Hu, L., Hill, L., Ngou, P.M., Ding, P., et al. (2020). Induced proximity of a TIR signaling domain on a plant-mammalian NLR chimera activates defense in plants. *Proc. Natl. Acad. Sci. USA* 117, 18832–18839.

- El Kasmi, F., and Nishimura, M.T. (2016). Structural insights into plant NLR immune receptor function. *Proc. Natl. Acad. Sci. USA* *113*, 12619–12621.
- Enganti, R., Cho, S.K., Toperzer, J.D., Urquidi-Camacho, R.A., Cakir, O.S., Ray, A.P., Abraham, P.E., Hettich, R.L., and von Arnim, A.G. (2017). Phosphorylation of ribosomal protein RPS6 integrates light signals and circadian clock signals. *Front. Plant Sci.* *8*, 2210.
- Engler, C., Gruetzner, R., Kandzia, R., and Marillonnet, S. (2009). Golden gate shuffling: a one-pot DNA shuffling method based on type II restriction enzymes. *PLoS One* *4*, e5553.
- Engler, C., Youles, M., Gruetzner, R., Ehnert, T.-M., Werner, S., Jones, J.D.G., Patron, N.J., and Marillonnet, S. (2014). A golden gate modular cloning toolbox for plants. *ACS Synth. Biol.* *3*, 839–843.
- Eschen-Lippold, L., Jiang, X., Elmore, J.M., Mackey, D., Shan, L., Coaker, G., Scheel, D., and Lee, J. (2016). Bacterial AvrRpt2-Like Cysteine Proteases Block Activation of the Arabidopsis Mitogen-Activated Protein Kinases, MPK4 and MPK11. *Plant Physiol.* *171*, 2223–2238.
- Eulgem, T. (2005). Regulation of the Arabidopsis defense transcriptome. *Trends Plant Sci.* *10*, 71–78.
- Falk, A., Feys, B.J., Frost, L.N., Jones, J.D., Daniels, M.J., and Parker, J.E. (1999). EDS1, an essential component of R gene-mediated disease resistance in Arabidopsis has homology to eukaryotic lipases. *Proc. Natl. Acad. Sci. USA* *96*, 3292–3297.
- Feehan, J.M., Castel, B., Bentham, A.R., and Jones, J.D. (2020). Plant NLRs get by with a little help from their friends. *Curr. Opin. Plant Biol.* *56*, 99–108.
- Felix, G., Duran, J.D., Volko, S., and Boller, T. (1999). Plants have a sensitive perception system for the most conserved domain of bacterial flagellin. *Plant J.* *18*, 265–276.
- Feng, F., Yang, F., Rong, W., Wu, X., Zhang, J., Chen, S., He, C., and Zhou, J.-M. (2012). A *Xanthomonas* uridine 5'-monophosphate transferase inhibits plant immune kinases. *Nature* *485*, 114–118.
- Fernández-Calvo, P., Chini, A., Fernández-Barbero, G., Chico, J.M., Gimenez-Ibanez, S., Geerinck, J., Eeckhout, D., Schweizer, F., Godoy, M., Franco-Zorrilla, J.M., et al. (2011). The *Arabidopsis* bHLH transcription factors MYC3 and MYC4 are targets of JAZ repressors and act additively with MYC2 in the activation of jasmonate responses. *Plant Cell* *23*, 701–715.
- Feys, B.J., Wiermer, M., Bhat, R.A., Moisan, L.J., Medina-Escobar, N., Neu, C., Cabral, A., and Parker, J.E. (2005). Arabidopsis SENESCENCE-ASSOCIATED GENE101 stabilizes and signals within an ENHANCED DISEASE SUSCEPTIBILITY1 complex in plant innate immunity. *Plant Cell* *17*, 2601–2613.
- Fichman, Y., Miller, G., and Mittler, R. (2019). Whole-Plant Live Imaging of Reactive Oxygen Species. *Mol. Plant* *12*, 1203–1210.
- Fichman, Y., Myers, R.J., Grant, D.G., and Mittler, R. (2020). Plasmodesmata-localized proteins and reactive oxygen species orchestrate light-induced rapid systemic signaling in Arabidopsis. *BioRxiv*.

- Fischer, I., Diévert, A., Droc, G., Dufayard, J.-F., and Chantret, N. (2016). Evolutionary Dynamics of the Leucine-Rich Repeat Receptor-Like Kinase (LRR-RLK) Subfamily in Angiosperms. *Plant Physiol.* *170*, 1595–1610.
- Fu, Z.Q., Yan, S., Saleh, A., Wang, W., Ruble, J., Oka, N., Mohan, R., Spoel, S.H., Tada, Y., Zheng, N., et al. (2012). NPR3 and NPR4 are receptors for the immune signal salicylic acid in plants. *Nature* *486*, 228–232.
- Gantner, J., Ordon, J., Kretschmer, C., Guerois, R., and Stuttmann, J. (2019). An EDS1-SAG101 Complex Is Essential for TNL-Mediated Immunity in *Nicotiana benthamiana*. *Plant Cell* *31*, 2456–2474.
- Gao, M., Wang, X., Wang, D., Xu, F., Ding, X., Zhang, Z., Bi, D., Cheng, Y.T., Chen, S., Li, X., et al. (2009). Regulation of cell death and innate immunity by two receptor-like kinases in *Arabidopsis*. *Cell Host Microbe* *6*, 34–44.
- Gao, X., Chen, X., Lin, W., Chen, S., Lu, D., Niu, Y., Li, L., Cheng, C., McCormack, M., Sheen, J., et al. (2013). Bifurcation of *Arabidopsis* NLR immune signaling via Ca<sup>2+</sup>-dependent protein kinases. *PLoS Pathog.* *9*, e1003127.
- Garner, C.M., Spears, B.J., Su, J., Cseke, L., Smith, S.N., Rogan, C.J., and Gassmann, W. (2020). Opposing functions of the plant *TOPELESS* gene family during SNC1-mediated autoimmunity. *BioRxiv*.
- Gauss, R., Trautwein, M., Sommer, T., and Spang, A. (2005). New modules for the repeated internal and N-terminal epitope tagging of genes in *Saccharomyces cerevisiae*. *Yeast* *22*, 1–12.
- Gilroy, S., Suzuki, N., Miller, G., Choi, W.-G., Toyota, M., Devireddy, A.R., and Mittler, R. (2014). A tidal wave of signals: calcium and ROS at the forefront of rapid systemic signaling. *Trends Plant Sci.* *19*, 623–630.
- Glazener, J.A., Orlandi, E.W., and Baker, C.J. (1996). The active oxygen response of cell suspensions to incompatible bacteria is not sufficient to cause hypersensitive cell death. *Plant Physiol.* *110*, 759–763.
- Göhre, V., Spallek, T., Häweker, H., Mersmann, S., Mentzel, T., Boller, T., de Torres, M., Mansfield, J.W., and Robatzek, S. (2008). Plant pattern-recognition receptor FLS2 is directed for degradation by the bacterial ubiquitin ligase AvrPtoB. *Curr. Biol.* *18*, 1824–1832.
- Gómez-Gómez, L., and Boller, T. (2000). FLS2: an LRR receptor-like kinase involved in the perception of the bacterial elicitor flagellin in *Arabidopsis*. *Mol. Cell* *5*, 1003–1011.
- Gong, B.-Q., Guo, J., Zhang, N., Yao, X., Wang, H.-B., and Li, J.-F. (2019). Cross-Microbial Protection via Priming a Conserved Immune Co-Receptor through Juxtamembrane Phosphorylation in Plants. *Cell Host Microbe* *26*, 810–822.e7.
- Gou, X., He, K., Yang, H., Yuan, T., Lin, H., Clouse, S.D., and Li, J. (2010). Genome-wide cloning and sequence analysis of leucine-rich repeat receptor-like protein kinase genes in *Arabidopsis thaliana*. *BMC Genomics* *11*, 19.
- Grant, J.J., and Loake, G.J. (2000). Role of reactive oxygen intermediates and cognate redox signaling in disease resistance. *Plant Physiol.* *124*, 21–29.

- Grant, M., Brown, I., Adams, S., Knight, M., Ainslie, A., and Mansfield, J. (2000). The RPM1 plant disease resistance gene facilitates a rapid and sustained increase in cytosolic calcium that is necessary for the oxidative burst and hypersensitive cell death. *Plant J.* 23, 441–450.
- Grant, S.R., Fisher, E.J., Chang, J.H., Mole, B.M., and Dangl, J.L. (2006). Subterfuge and manipulation: type III effector proteins of phytopathogenic bacteria. *Annu. Rev. Microbiol.* 60, 425–449.
- Gronnier, J., Gerbeau-Pissot, P., Germain, V., Mongrand, S., and Simon-Plas, F. (2018). Divide and rule: plant plasma membrane organization. *Trends Plant Sci.* 23, 899–917.
- Gronnier, J., Franck, C.M., Stegmann, M., DeFalco, T.A., Cifuentes, A.A., Dünser, K., Lin, W., Yang, Z., Kleine-Vehn, J., Ringli, C., et al. (2020). FERONIA regulates FLS2 plasma membrane nanoscale dynamics to modulate plant immune signaling. *BioRxiv*.
- Grubb, L.E., Derbyshire, P., Dunning, K., Zipfel, C., Menke, F.L.H., and Monaghan, J. (2020). Large-scale identification of ubiquitination sites on membrane-associated proteins in *Arabidopsis thaliana* seedlings. *BioRxiv*.
- Guan, R., Su, J., Meng, X., Li, S., Liu, Y., Xu, J., and Zhang, S. (2015). Multilayered Regulation of Ethylene Induction Plays a Positive Role in Arabidopsis Resistance against *Pseudomonas syringae*. *Plant Physiol.* 169, 299–312.
- Guo, H., Ahn, H.-K., Sklenar, J., Huang, J., Ma, Y., Ding, P., Menke, F.L.H., and Jones, J.D.G. (2020). Phosphorylation-Regulated Activation of the Arabidopsis RRS1-R/RPS4 Immune Receptor Complex Reveals Two Distinct Effector Recognition Mechanisms. *Cell Host Microbe* 27, 769–781.e6.
- Guo, W., Tzioutziou, N., Stephen, G., Milne, I., Calixto, C., Waugh, R., Brown, J.W.S., and Zhang, R. (2019). 3D RNA-seq - a powerful and flexible tool for rapid and accurate differential expression and alternative splicing analysis of RNA-seq data for biologists. *BioRxiv*.
- Gust, A.A., and Felix, G. (2014). Receptor like proteins associate with SOBIR1-type of adaptors to form bimolecular receptor kinases. *Curr. Opin. Plant Biol.* 21, 104–111.
- Halff, E.F., Diebolder, C.A., Versteeg, M., Schouten, A., Brondijk, T.H.C., and Huizinga, E.G. (2012). Formation and structure of a NAIP5-NLRC4 inflammasome induced by direct interactions with conserved N- and C-terminal regions of flagellin. *J. Biol. Chem.* 287, 38460–38472.
- Hamilton, A.J., and Baulcombe, D.C. (1999). A species of small antisense RNA in posttranscriptional gene silencing in plants. *Science* 286, 950–952.
- Han, L., Li, G.-J., Yang, K.-Y., Mao, G., Wang, R., Liu, Y., and Zhang, S. (2010). Mitogen-activated protein kinase 3 and 6 regulate Botrytis cinerea-induced ethylene production in Arabidopsis. *Plant J.* 64, 114–127.
- Hander, T., Fernández-Fernández, Á.D., Kumpf, R.P., Willems, P., Schatowitz, H., Rombaut, D., Staes, A., Nolf, J., Pottier, R., Yao, P., et al. (2019). Damage on plants activates Ca<sup>2+</sup>-dependent metacaspases for release of immunomodulatory peptides. *Science* 363.

- Hartmann, M., Zeier, T., Bernsdorff, F., Reichel-Deland, V., Kim, D., Hohmann, M., Scholten, N., Schuck, S., Bräutigam, A., Hölzel, T., et al. (2018). Flavin Monooxygenase-Generated N-Hydroxypipicolinic Acid Is a Critical Element of Plant Systemic Immunity. *Cell* *173*, 456–469.e16.
- Hatsugai, N., Hillmer, R., Yamaoka, S., Hara-Nishimura, I., and Katagiri, F. (2016). The  $\mu$  Subunit of Arabidopsis Adaptor Protein-2 Is Involved in Effector-Triggered Immunity Mediated by Membrane-Localized Resistance Proteins. *Mol. Plant Microbe Interact.* *29*, 345–351.
- He, K., Gou, X., Yuan, T., Lin, H., Asami, T., Yoshida, S., Russell, S.D., and Li, J. (2007). BAK1 and BKK1 regulate brassinosteroid-dependent growth and brassinosteroid-independent cell-death pathways. *Curr. Biol.* *17*, 1109–1115.
- He, Y., Zhou, J., Shan, L., and Meng, X. (2018). Plant cell surface receptor-mediated signaling - a common theme amid diversity. *J. Cell Sci.* *131*.
- Heese, A., Hann, D.R., Gimenez-Ibanez, S., Jones, A.M.E., He, K., Li, J., Schroeder, J.I., Peck, S.C., and Rathjen, J.P. (2007). The receptor-like kinase SERK3/BAK1 is a central regulator of innate immunity in plants. *Proc. Natl. Acad. Sci. USA* *104*, 12217–12222.
- Hohmann, U., Lau, K., and Hothorn, M. (2017). The structural basis of ligand perception and signal activation by receptor kinases. *Annu. Rev. Plant Biol.* *68*, 109–137.
- Hohmann, U., Nicolet, J., Moretti, A., Hothorn, L.A., and Hothorn, M. (2018). Mechanistic analysis of the SERK3 elongated allele defines a role for BIR ectodomains in brassinosteroid signaling. *BioRxiv*.
- Holton, N., Nekrasov, V., Ronald, P.C., and Zipfel, C. (2015). The phylogenetically-related pattern recognition receptors EFR and XA21 recruit similar immune signaling components in monocots and dicots. *PLoS Pathog.* *11*, e1004602.
- Horsefield, S., Burdett, H., Zhang, X., Manik, M.K., Shi, Y., Chen, J., Qi, T., Gilley, J., Lai, J.-S., Rank, M.X., et al. (2019). NAD<sup>+</sup> cleavage activity by animal and plant TIR domains in cell death pathways. *Science* *365*, 793–799.
- Hoser, R., Zurczak, M., Lichocka, M., Zuzga, S., Dadlez, M., Samuel, M.A., Ellis, B.E., Stuttmann, J., Parker, J.E., Hennig, J., et al. (2013). Nucleocytoplasmic partitioning of tobacco N receptor is modulated by SGT1. *New Phytol.* *200*, 158–171.
- Hou, Y., Zhai, Y., Feng, L., Karimi, H.Z., Rutter, B.D., Zeng, L., Choi, D.S., Zhang, B., Gu, W., Chen, X., et al. (2019). A Phytophthora Effector Suppresses Trans-Kingdom RNAi to Promote Disease Susceptibility. *Cell Host Microbe* *25*, 153–165.e5.
- Huang, P.-Y., Catinot, J., and Zimmerli, L. (2016). Ethylene response factors in Arabidopsis immunity. *J. Exp. Bot.* *67*, 1231–1241.
- Huang, W., Wang, Y., Li, X., and Zhang, Y. (2020). Biosynthesis and Regulation of Salicylic Acid and N-Hydroxypipicolinic Acid in Plant Immunity. *Mol. Plant* *13*, 31–41.
- Huffaker, A., Pearce, G., and Ryan, C.A. (2006). An endogenous peptide signal in Arabidopsis activates components of the innate immune response. *Proc. Natl. Acad. Sci. USA* *103*, 10098–10103.

- Huh, S.U., Cevik, V., Ding, P., Duxbury, Z., Ma, Y., Tomlinson, L., Sarris, P.F., and Jones, J.D.G. (2017). Protein-protein interactions in the RPS4/RRS1 immune receptor complex. *PLoS Pathog.* *13*, e1006376.
- Huot, B., Yao, J., Montgomery, B.L., and He, S.Y. (2014). Growth-defense tradeoffs in plants: a balancing act to optimize fitness. *Mol. Plant* *7*, 1267–1287.
- Ingole, K.D., Dahale, S.K., and Bhattacharjee, S. (2020). Proteomic analysis of SUMO1-SUMOylome changes during defense elicitation in *Arabidopsis*. *BioRxiv*.
- Irieda, H., Inoue, Y., Mori, M., Yamada, K., Oshikawa, Y., Saitoh, H., Uemura, A., Terauchi, R., Kitakura, S., Kosaka, A., et al. (2019). Conserved fungal effector suppresses PAMP-triggered immunity by targeting plant immune kinases. *Proc. Natl. Acad. Sci. USA* *116*, 496–505.
- Jacob, F., Kracher, B., Mine, A., Seyfferth, C., Blanvillain-Baufumé, S., Parker, J.E., Tsuda, K., Schulze-Lefert, P., and Maekawa, T. (2018). A dominant-interfering camta3 mutation compromises primary transcriptional outputs mediated by both cell surface and intracellular immune receptors in *Arabidopsis thaliana*. *New Phytol.* *217*, 1667–1680.
- Jacobs, A.K., Lipka, V., Burton, R.A., Panstruga, R., Strizhov, N., Schulze-Lefert, P., and Fincher, G.B. (2003). An arabidopsis callose synthase, *GSL5*, is required for wound and papillary callose formation. *Plant Cell* *15*, 2503–2513.
- Jiang, J., Ding, A.B., Liu, F., and Zhong, X. (2020). Linking signaling pathways to histone acetylation dynamics in plants. *J. Exp. Bot.* *71*, 5179–5190.
- Jiang, S., Yao, J., Ma, K.-W., Zhou, H., Song, J., He, S.Y., and Ma, W. (2013). Bacterial effector activates jasmonate signaling by directly targeting JAZ transcriptional repressors. *PLoS Pathog.* *9*, e1003715.
- Jiang, Y., Han, B., Zhang, H., Mariappan, K.G., Bigeard, J., Colcombet, J., and Hirt, H. (2019). MAP4K4 associates with BIK1 to regulate plant innate immunity. *EMBO Rep.* *20*, e47965.
- Jiménez-Góngora, T., Kim, S.-K., Lozano-Durán, R., and Zipfel, C. (2015). Flg22-Triggered Immunity Negatively Regulates Key BR Biosynthetic Genes. *Front. Plant Sci.* *6*, 981.
- Jones, J.D.G., and Dangl, J.L. (2006). The plant immune system. *Nature* *444*, 323–329.
- Jones, D.A., Thomas, C.M., Hammond-Kosack, K.E., Balint-Kurti, P.J., and Jones, J.D.G. (1994). Isolation of the tomato *Cf-9* gene for resistance to *Cladosporium fulvum* by transposon tagging. *Science* *266*, 789–793.
- Jones, J.D.G., Brigneti, G., and Smilde, D. (2003). Putting plant disease resistance genes to work. In *Plant Biotechnology 2002 and Beyond*, I.K. Vasil, ed. (Dordrecht: Springer Netherlands), pp. 10–17.
- Jones, J.D.G., Vance, R.E., and Dangl, J.L. (2016). Intracellular innate immune surveillance devices in plants and animals. *Science* *354*.
- Jovanovic, M., Rooney, M.S., Mertins, P., Przybylski, D., Chevrier, N., Satija, R., Rodriguez, E.H., Fields, A.P., Schwartz, S., Raychowdhury, R., et al. (2015).

- Immunogenetics. Dynamic profiling of the protein life cycle in response to pathogens. *Science* 347, 1259038.
- Jubic, L.M., Saile, S., Furzer, O.J., El Kasmi, F., and Dangl, J.L. (2019). Help wanted: helper NLRs and plant immune responses. *Curr. Opin. Plant Biol.* 50, 82–94.
- Jung, H.W., Panigrahi, G.K., Jung, G.Y., Lee, Y.J., Shin, K.H., Sahoo, A., Choi, E.S., Lee, E., Man Kim, K., Yang, S.H., et al. (2020). Pathogen-Associated Molecular Pattern-Triggered Immunity Involves Proteolytic Degradation of Core Nonsense-Mediated mRNA Decay Factors During the Early Defense Response. *Plant Cell* 32, 1081–1101.
- Jurkowski, G.I., Smith, R.K., Yu, I., Ham, J.H., Sharma, S.B., Klessig, D.F., Fengler, K.A., and Bent, A.F. (2004). Arabidopsis DND2, a second cyclic nucleotide-gated ion channel gene for which mutation causes the “defense, no death” phenotype. *Mol. Plant Microbe Interact.* 17, 511–520.
- Kadota, Y., Sklenar, J., Derbyshire, P., Stransfeld, L., Asai, S., Ntoukakis, V., Jones, J.D.G., Shirasu, K., Menke, F., Jones, A., et al. (2014). Direct regulation of the NADPH oxidase RBOHD by the PRR-associated kinase BIK1 during plant immunity. *Mol. Cell* 54, 43–55.
- Kadota, Y., Shirasu, K., and Zipfel, C. (2015). Regulation of the NADPH oxidase RBOHD during plant immunity. *Plant Cell Physiol.* 56, 1472–1480.
- Kadota, Y., Liebrand, T.W.H., Goto, Y., Sklenar, J., Derbyshire, P., Menke, F.L.H., Torres, M.-A., Molina, A., Zipfel, C., Coaker, G., et al. (2019). Quantitative phosphoproteomic analysis reveals common regulatory mechanisms between effector- and PAMP-triggered immunity in plants. *New Phytol.* 221, 2160–2175.
- Kaku, H., Nishizawa, Y., Ishii-Minami, N., Akimoto-Tomiyama, C., Dohmae, N., Takio, K., Minami, E., and Shibuya, N. (2006). Plant cells recognize chitin fragments for defense signaling through a plasma membrane receptor. *Proc. Natl. Acad. Sci. USA* 103, 11086–11091.
- Katsir, L., Schillmiller, A.L., Staswick, P.E., He, S.Y., and Howe, G.A. (2008). COI1 is a critical component of a receptor for jasmonate and the bacterial virulence factor coronatine. *Proc. Natl. Acad. Sci. USA* 105, 7100–7105.
- Kauss, H. (1986). Ca<sup>2+</sup>-Dependence of Callose Synthesis and the Role of Polyamines in the Activation of 1,3-β-Glucan Synthase by Ca<sup>2+</sup>. In *Molecular and Cellular Aspects of Calcium in Plant Development*, A.J. Trewavas, ed. (Boston, MA: Springer US), pp. 131–137.
- Kim, Y., Gilmour, S.J., Chao, L., Park, S., and Thomashow, M.F. (2020). Arabidopsis CAMTA transcription factors regulate pipecolic acid biosynthesis and priming of immunity genes. *Mol. Plant* 13, 157–168.
- Kimura, S., Kaya, H., Kawarazaki, T., Hiraoka, G., Senzaki, E., Michikawa, M., and Kuchitsu, K. (2012). Protein phosphorylation is a prerequisite for the Ca<sup>2+</sup>-dependent activation of Arabidopsis NADPH oxidases and may function as a trigger for the positive feedback regulation of Ca<sup>2+</sup> and reactive oxygen species. *Biochim. Biophys. Acta* 1823, 398–405.

- Knepper, C., Savory, E.A., and Day, B. (2011). Arabidopsis NDR1 is an integrin-like protein with a role in fluid loss and plasma membrane-cell wall adhesion. *Plant Physiol.* *156*, 286–300.
- Komis, G., Šamajová, O., Ovečka, M., and Šamaj, J. (2018). Cell and Developmental Biology of Plant Mitogen-Activated Protein Kinases. *Annu. Rev. Plant Biol.* *69*, 237–265.
- Kong, Q., Sun, T., Qu, N., Ma, J., Li, M., Cheng, Y.-T., Zhang, Q., Wu, D., Zhang, Z., and Zhang, Y. (2016). Two Redundant Receptor-Like Cytoplasmic Kinases Function Downstream of Pattern Recognition Receptors to Regulate Activation of SA Biosynthesis. *Plant Physiol.* *171*, 1344–1354.
- Koornneef, A., and Pieterse, C.M.J. (2008). Cross talk in defense signaling. *Plant Physiol.* *146*, 839–844.
- Kørner, C.J., Klauser, D., Niehl, A., Domínguez-Ferreras, A., Chinchilla, D., Boller, T., Heinlein, M., and Hann, D.R. (2013). The immunity regulator BAK1 contributes to resistance against diverse RNA viruses. *Mol. Plant Microbe Interact.* *26*, 1271–1280.
- Kovtun, Y., Chiu, W.L., Tena, G., and Sheen, J. (2000). Functional analysis of oxidative stress-activated mitogen-activated protein kinase cascade in plants. *Proc. Natl. Acad. Sci. USA* *97*, 2940–2945.
- Krasileva, K.V., Dahlbeck, D., and Staskawicz, B.J. (2010). Activation of an Arabidopsis resistance protein is specified by the in planta association of its leucine-rich repeat domain with the cognate oomycete effector. *Plant Cell* *22*, 2444–2458.
- Krüger, J., Thomas, C.M., Golstein, C., Dixon, M.S., Smoker, M., Tang, S., Mulder, L., and Jones, J.D.G. (2002). A tomato cysteine protease required for Cf-2-dependent disease resistance and suppression of autonecrosis. *Science* *296*, 744–747.
- Kunze, G., Zipfel, C., Robatzek, S., Niehaus, K., Boller, T., and Felix, G. (2004). The N terminus of bacterial elongation factor Tu elicits innate immunity in *Arabidopsis* plants. *Plant Cell* *16*, 3496–3507.
- Kutschera, A., Dawid, C., Gisch, N., Schmid, C., Raasch, L., Gerster, T., Schäffer, M., Smakowska-Luzan, E., Belkhadir, Y., Vlot, A.C., et al. (2019). Bacterial medium-chain 3-hydroxy fatty acid metabolites trigger immunity in Arabidopsis plants. *Science* *364*, 178–181.
- Lacaze, A., and Joly, D.L. (2020). Structural specificity in plant-filamentous pathogen interactions. *Mol. Plant Pathol.* *21*, 1513–1525.
- Lacombe, S., Rougon-Cardoso, A., Sherwood, E., Peeters, N., Dahlbeck, D., van Esse, H.P., Smoker, M., Rallapalli, G., Thomma, B.P.H.J., Staskawicz, B., et al. (2010). Interfamily transfer of a plant pattern-recognition receptor confers broad-spectrum bacterial resistance. *Nat. Biotechnol.* *28*, 365–369.
- Laflamme, B., Dillon, M.M., Martel, A., Almeida, R.N.D., Desveaux, D., and Guttman, D.S. (2020). The pan-genome effector-triggered immunity landscape of a host-pathogen interaction. *Science* *367*, 763–768.
- Lam, E. (2004). Controlled cell death, plant survival and development. *Nat. Rev. Mol. Cell Biol.* *5*, 305–315.

- Lamb, C., and Dixon, R.A. (1997). The oxidative burst in plant disease resistance. *Annu. Rev. Plant Physiol. Plant Mol. Biol.* *48*, 251–275.
- Lambeth, J.D. (2004). NOX enzymes and the biology of reactive oxygen. *Nat. Rev. Immunol.* *4*, 181–189.
- Laohavisit, A., Wakatake, T., Ishihama, N., Mulvey, H., Takizawa, K., Suzuki, T., and Shirasu, K. (2020). Quinone perception in plants via leucine-rich-repeat receptor-like kinases. *Nature*.
- Lapin, D., Kovacova, V., Sun, X., Dongus, J.A., Bhandari, D.D., von Born, P., Bautor, J., Guarneri, N., Stuttmann, J., Beyer, A., et al. (2019). A coevolved EDS1-SAG101-NRG1 module mediates cell death signaling by TIR-domain immune receptors. *BioRxiv*.
- Lapin, D., Bhandari, D.D., and Parker, J.E. (2020). Origins and immunity networking functions of EDS1 family proteins. *Annu. Rev. Phytopathol.* *58*, 253–276.
- Lee, D., Lal, N.K., Lin, Z.-J.D., Ma, S., Liu, J., Castro, B., Toruño, T., Dinesh-Kumar, S.P., and Coaker, G. (2020). Regulation of reactive oxygen species during plant immunity through phosphorylation and ubiquitination of RBOHD. *Nat. Commun.* *11*, 1838.
- Li, B., Meng, X., Shan, L., and He, P. (2016a). Transcriptional Regulation of Pattern-Triggered Immunity in Plants. *Cell Host Microbe* *19*, 641–650.
- Li, B., Ferreira, M.A., Huang, M., Camargos, L.F., Yu, X., Teixeira, R.M., Carpinetti, P.A., Mendes, G.C., Gouveia-Mageste, B.C., Liu, C., et al. (2019). The receptor-like kinase NIK1 targets FLS2/BAK1 immune complex and inversely modulates antiviral and antibacterial immunity. *Nat. Commun.* *10*, 4996.
- Li, F., Cheng, C., Cui, F., de Oliveira, M.V.V., Yu, X., Meng, X., Intorne, A.C., Babilonia, K., Li, M., Li, B., et al. (2014a). Modulation of RNA polymerase II phosphorylation downstream of pathogen perception orchestrates plant immunity. *Cell Host Microbe* *16*, 748–758.
- Li, L., Li, M., Yu, L., Zhou, Z., Liang, X., Liu, Z., Cai, G., Gao, L., Zhang, X., Wang, Y., et al. (2014b). The FLS2-associated kinase BIK1 directly phosphorylates the NADPH oxidase RbohD to control plant immunity. *Cell Host Microbe* *15*, 329–338.
- Li, L., Kim, P., Yu, L., Cai, G., Chen, S., Alfano, J.R., and Zhou, J.-M. (2016b). Activation-Dependent Destruction of a Co-receptor by a *Pseudomonas syringae* Effector Dampens Plant Immunity. *Cell Host Microbe* *20*, 504–514.
- Li, L., Habring, A., Wang, K., and Weigel, D. (2020a). Atypical resistance protein RPW8/HR triggers oligomerization of the NLR immune receptor RPP7 and autoimmunity. *Cell Host Microbe* *27*, 405–417.e6.
- Li, Q., Wang, J., Bai, T., Zhang, M., Jia, Y., Shen, D., Zhang, M., and Dou, D. (2020b). A *Phytophthora capsici* effector suppresses plant immunity via interaction with EDS1. *Mol. Plant Pathol.* *21*, 502–511.
- Liang, X., and Zhou, J.-M. (2018). Receptor-Like Cytoplasmic Kinases: Central Players in Plant Receptor Kinase-Mediated Signaling. *Annu. Rev. Plant Biol.* *69*, 267–299.

- Liang, X., Ding, P., Lian, K., Wang, J., Ma, M., Li, L., Li, L., Li, M., Zhang, X., Chen, S., et al. (2016). Arabidopsis heterotrimeric G proteins regulate immunity by directly coupling to the FLS2 receptor. *Elife* 5, e13568.
- Liang, X., Ma, M., Zhou, Z., Wang, J., Yang, X., Rao, S., Bi, G., Li, L., Zhang, X., Chai, J., et al. (2018). Ligand-triggered de-repression of Arabidopsis heterotrimeric G proteins coupled to immune receptor kinases. *Cell Res.* 28, 529–543.
- Liao, D., Cao, Y., Sun, X., Espinoza, C., Nguyen, C.T., Liang, Y., and Stacey, G. (2017). Arabidopsis E3 ubiquitin ligase PLANT U-BOX13 (PUB13) regulates chitin receptor LYSIN MOTIF RECEPTOR KINASE5 (LYK5) protein abundance. *New Phytol.* 214, 1646–1656.
- Liebrand, T.W.H., van den Berg, G.C.M., Zhang, Z., Smit, P., Cordewener, J.H.G., America, A.H.P., Sklenar, J., Jones, A.M.E., Tameling, W.I.L., Robatzek, S., et al. (2013). Receptor-like kinase SOBIR1/EVR interacts with receptor-like proteins in plant immunity against fungal infection. *Proc. Natl. Acad. Sci. USA* 110, 10010–10015.
- Lin, W., Lu, D., Gao, X., Jiang, S., Ma, X., Wang, Z., Mengiste, T., He, P., and Shan, L. (2013). Inverse modulation of plant immune and brassinosteroid signaling pathways by the receptor-like cytoplasmic kinase BIK1. *Proc. Natl. Acad. Sci. USA* 110, 12114–12119.
- Lin, W., Li, B., Lu, D., Chen, S., Zhu, N., He, P., and Shan, L. (2014). Tyrosine phosphorylation of protein kinase complex BAK1/BIK1 mediates Arabidopsis innate immunity. *Proc. Natl. Acad. Sci. USA* 111, 3632–3637.
- Liu, Y., and Zhang, S. (2004). Phosphorylation of 1-aminocyclopropane-1-carboxylic acid synthase by MPK6, a stress-responsive mitogen-activated protein kinase, induces ethylene biosynthesis in Arabidopsis. *Plant Cell* 16, 3386–3399.
- Liu, J., Elmore, J.M., Lin, Z.-J.D., and Coaker, G. (2011). A receptor-like cytoplasmic kinase phosphorylates the host target RIN4, leading to the activation of a plant innate immune receptor. *Cell Host Microbe* 9, 137–146.
- Liu, J., Ding, P., Sun, T., Nitta, Y., Dong, O., Huang, X., Yang, W., Li, X., Botella, J.R., and Zhang, Y. (2013a). Heterotrimeric G proteins serve as a converging point in plant defense signaling activated by multiple receptor-like kinases. *Plant Physiol.* 161, 2146–2158.
- Liu, L., Sonbol, F.-M., Huot, B., Gu, Y., Withers, J., Mwimba, M., Yao, J., He, S.Y., and Dong, X. (2016). Salicylic acid receptors activate jasmonic acid signalling through a non-canonical pathway to promote effector-triggered immunity. *Nat. Commun.* 7, 13099.
- Liu, X., Yang, S., Zhao, M., Luo, M., Yu, C.-W., Chen, C.-Y., Tai, R., and Wu, K. (2014). Transcriptional repression by histone deacetylases in plants. *Mol. Plant* 7, 764–772.
- Liu, Y., Sun, T., Sun, Y., Zhang, Y., Radojičić, A., Ding, Y., Tian, H., Huang, X., Lan, J., Chen, S., et al. (2020). Diverse roles of the salicylic acid receptors NPR1 and NPR3/NPR4 in plant immunity. *Plant Cell*.

- Liu, Z., Wu, Y., Yang, F., Zhang, Y., Chen, S., Xie, Q., Tian, X., and Zhou, J.-M. (2013b). BIK1 interacts with PEPRs to mediate ethylene-induced immunity. *Proc. Natl. Acad. Sci. USA* *110*, 6205–6210.
- Livak, K.J., and Schmittgen, T.D. (2001). Analysis of relative gene expression data using real-time quantitative PCR and the 2(-Delta Delta C(T)) Method. *Methods* *25*, 402–408.
- Lopez, V.A., Park, B.C., Nowak, D., Sreelatha, A., Zembek, P., Fernandez, J., Servage, K.A., Gradowski, M., Hennig, J., Tomchick, D.R., et al. (2019). A bacterial effector mimics a host HSP90 client to undermine immunity. *Cell* *179*, 205–218.e21.
- Lorrain, S., Vaillau, F., Balagué, C., and Roby, D. (2003). Lesion mimic mutants: keys for deciphering cell death and defense pathways in plants? *Trends Plant Sci.* *8*, 263–271.
- Lu, D., Wu, S., Gao, X., Zhang, Y., Shan, L., and He, P. (2010). A receptor-like cytoplasmic kinase, BIK1, associates with a flagellin receptor complex to initiate plant innate immunity. *Proc. Natl. Acad. Sci. USA* *107*, 496–501.
- Lu, D., Lin, W., Gao, X., Wu, S., Cheng, C., Avila, J., Heese, A., Devarenne, T.P., He, P., and Shan, L. (2011). Direct ubiquitination of pattern recognition receptor FLS2 attenuates plant innate immunity. *Science* *332*, 1439–1442.
- Luderer, R., Takken, F.L.W., de Wit, P.J.G.M., and Joosten, M.H.A.J. (2002). *Cladosporium fulvum* overcomes Cf-2-mediated resistance by producing truncated AVR2 elicitor proteins. *Mol. Microbiol.* *45*, 875–884.
- Lukan, T., Pompe-Novak, M., Baebler, Š., Tušek-Žnidarič, M., Kladnik, A., Križnik, M., Blejec, A., Zagorščak, M., Stare, K., Dušak, B., et al. (2020). Precision transcriptomics of viral foci reveals the spatial regulation of immune-signaling genes and identifies RBOHD as an important player in the incompatible interaction between potato virus Y and potato. *Plant J.*
- Luna, E., Pastor, V., Robert, J., Flors, V., Mauch-Mani, B., and Ton, J. (2011). Callose deposition: a multifaceted plant defense response. *Mol. Plant Microbe Interact.* *24*, 183–193.
- Luu, D.D., Joe, A., Chen, Y., Parys, K., Bahar, O., Pruitt, R., Chan, L.J.G., Petzold, C.J., Long, K., Adamchak, C., et al. (2019). Biosynthesis and secretion of the microbial sulfated peptide RaxX and binding to the rice XA21 immune receptor. *Proc. Natl. Acad. Sci. USA* *116*, 8525–8534.
- Ma, C., Liu, Y., Bai, B., Han, Z., Tang, J., Zhang, H., Yaghmaiean, H., Zhang, Y., and Chai, J. (2017). Structural basis for BIR1-mediated negative regulation of plant immunity. *Cell Res.* *27*, 1521–1524.
- Ma, Q., Zhai, Y., Schneider, J.C., Ramseier, T.M., and Saier, M.H. (2003). Protein secretion systems of *Pseudomonas aeruginosa* and *P. fluorescens*. *Biochim. Biophys. Acta* *1611*, 223–233.
- Ma, X., Xu, G., He, P., and Shan, L. (2016). SERKING coreceptors for receptors. *Trends Plant Sci.* *21*, 1017–1033.
- Ma, X., Claus, L.A.N., Leslie, M.E., Tao, K., Wu, Z., Liu, J., Yu, X., Li, B., Zhou, J., Savatin, D.V., et al. (2020a). Ligand-induced monoubiquitination of BIK1 regulates plant immunity. *Nature* *581*, 199–203.

- Ma, X., Zhang, C., Kim, D.Y., Huang, Y., He, P., Vierstra, R.D., and Shan, L. (2020b). Ubiquitylome Analysis Reveals a Central Role for the Ubiquitin-Proteasome System in Plant Innate Immunity. *BioRxiv*.
- Ma, Y., Guo, H., Hu, L., Martinez, P.P., Moschou, P.N., Cevik, V., Ding, P., Duxbury, Z., Sarris, P.F., and Jones, J.D.G. (2018). Distinct modes of derepression of an Arabidopsis immune receptor complex by two different bacterial effectors. *Proc. Natl. Acad. Sci. USA* *115*, 10218–10227.
- Macho, A.P., and Zipfel, C. (2014). Plant PRRs and the activation of innate immune signaling. *Mol. Cell* *54*, 263–272.
- Macho, A.P., Boutrot, F., Rathjen, J.P., and Zipfel, C. (2012). Aspartate oxidase plays an important role in Arabidopsis stomatal immunity. *Plant Physiol.* *159*, 1845–1856.
- Macho, A.P., Schwessinger, B., Ntoukakis, V., Brutus, A., Segonzac, C., Roy, S., Kadota, Y., Oh, M.-H., Sklenar, J., Derbyshire, P., et al. (2014). A bacterial tyrosine phosphatase inhibits plant pattern recognition receptor activation. *Science* *343*, 1509–1512.
- Mackey, D., Holt, B.F., Wiig, A., and Dangl, J.L. (2002). RIN4 interacts with *Pseudomonas syringae* type III effector molecules and is required for RPM1-mediated resistance in Arabidopsis. *Cell* *108*, 743–754.
- Mackey, D., Belkhadir, Y., Alonso, J.M., Ecker, J.R., and Dangl, J.L. (2003). Arabidopsis RIN4 is a target of the type III virulence effector AvrRpt2 and modulates RPS2-mediated resistance. *Cell* *112*, 379–389.
- Maekawa, T., Kufer, T.A., and Schulze-Lefert, P. (2011). NLR functions in plant and animal immune systems: so far and yet so close. *Nat. Immunol.* *12*, 817–826.
- Maekawa, T., Kracher, B., Vernaldi, S., Ver Loren van Themaat, E., and Schulze-Lefert, P. (2012). Conservation of NLR-triggered immunity across plant lineages. *Proc. Natl. Acad. Sci. USA* *109*, 20119–20123.
- Mahdi, L.K., Huang, M., Zhang, X., Nakano, R.T., Kopp, L.B., Saur, I.M.L., Jacob, F., Kovacova, V., Lapin, D., Parker, J.E., et al. (2020). Discovery of a Family of Mixed Lineage Kinase Domain-like Proteins in Plants and Their Role in Innate Immune Signaling. *Cell Host Microbe*.
- Malinovsky, F.G., Batoux, M., Schwessinger, B., Youn, J.H., Stransfeld, L., Win, J., Kim, S.-K., and Zipfel, C. (2014). Antagonistic regulation of growth and immunity by the Arabidopsis basic helix-loop-helix transcription factor homolog of brassinosteroid enhanced expression2 interacting with increased leaf inclination1 binding bHLH1. *Plant Physiol.* *164*, 1443–1455.
- Mao, G., Meng, X., Liu, Y., Zheng, Z., Chen, Z., and Zhang, S. (2011). Phosphorylation of a WRKY transcription factor by two pathogen-responsive MAPKs drives phytoalexin biosynthesis in Arabidopsis. *Plant Cell* *23*, 1639–1653.
- MAPK Group (2002). Mitogen-activated protein kinase cascades in plants: a new nomenclature. *Trends Plant Sci.* *7*, 301–308.
- Martin, R., Qi, T., Zhang, H., Liu, F., King, M., Toth, C., Nogales, E., and Staskawicz, B.J. (2020). Structure of the activated Roq1 resistosome directly recognizing the pathogen effector XopQ. *BioRxiv*.

- Martins, S., Dohmann, E.M.N., Cayrel, A., Johnson, A., Fischer, W., Pojer, F., Satiat-Jeunemaître, B., Jaillais, Y., Chory, J., Geldner, N., et al. (2015). Internalization and vacuolar targeting of the brassinosteroid hormone receptor BRI1 are regulated by ubiquitination. *Nat. Commun.* *6*, 6151.
- McNellis, T.W., Mudgett, M.B., Li, K., Aoyama, T., Horvath, D., Chua, N.H., and Staskawicz, B.J. (1998). Glucocorticoid-inducible expression of a bacterial avirulence gene in transgenic *Arabidopsis* induces hypersensitive cell death. *Plant J.* *14*, 247–257.
- Meena, M.K., Prajapati, R., Krishna, D., Divakaran, K., Pandey, Y., Reichelt, M., Mathew, M.K., Boland, W., Mithöfer, A., and Vadassery, J. (2019). The  $Ca^{2+}$  channel CNGC19 regulates *Arabidopsis* defense against *Spodoptera* herbivory. *Plant Cell* *31*, 1539–1562.
- Meng, X., and Zhang, S. (2013). MAPK cascades in plant disease resistance signaling. *Annu. Rev. Phytopathol.* *51*, 245–266.
- Meng, X., Xu, J., He, Y., Yang, K.-Y., Mordorski, B., Liu, Y., and Zhang, S. (2013). Phosphorylation of an ERF transcription factor by *Arabidopsis* MPK3/MPK6 regulates plant defense gene induction and fungal resistance. *Plant Cell* *25*, 1126–1142.
- Menke, F.L.H., van Pelt, J.A., Pieterse, C.M.J., and Klessig, D.F. (2004). Silencing of the mitogen-activated protein kinase MPK6 compromises disease resistance in *Arabidopsis*. *Plant Cell* *16*, 897–907.
- Meteignier, L.-V., El Oirdi, M., Cohen, M., Barff, T., Matteau, D., Lucier, J.-F., Rodrigue, S., Jacques, P.-E., Yoshioka, K., and Moffett, P. (2017). Transcriptome analysis of an NB-LRR immune response identifies important contributors to plant immunity in *Arabidopsis*. *J. Exp. Bot.* *68*, 2333–2344.
- Miller, G., Schlauch, K., Tam, R., Cortes, D., Torres, M.A., Shulaev, V., Dangl, J.L., and Mittler, R. (2009). The plant NADPH oxidase RBOHD mediates rapid systemic signaling in response to diverse stimuli. *Sci. Signal.* *2*, ra45.
- Miya, A., Albert, P., Shinya, T., Desaki, Y., Ichimura, K., Shirasu, K., Narusaka, Y., Kawakami, N., Kaku, H., and Shibuya, N. (2007). CERK1, a LysM receptor kinase, is essential for chitin elicitor signaling in *Arabidopsis*. *Proc. Natl. Acad. Sci. USA* *104*, 19613–19618.
- Moeder, W., and Yoshioka, K. (2008). Lesion mimic mutants: A classical, yet still fundamental approach to study programmed cell death. *Plant Signal. Behav.* *3*, 764–767.
- Monaghan, J., Matschi, S., Shorinola, O., Rovenich, H., Matei, A., Segonzac, C., Malinovsky, F.G., Rathjen, J.P., MacLean, D., Romeis, T., et al. (2014). The calcium-dependent protein kinase CPK28 buffers plant immunity and regulates BIK1 turnover. *Cell Host Microbe* *16*, 605–615.
- Mur, L.A.J., Kenton, P., Lloyd, A.J., Ougham, H., and Prats, E. (2008). The hypersensitive response; the centenary is upon us but how much do we know? *J. Exp. Bot.* *59*, 501–520.
- Narusaka, M., Shirasu, K., Noutoshi, Y., Kubo, Y., Shiraishi, T., Iwabuchi, M., and Narusaka, Y. (2009). RRS1 and RPS4 provide a dual Resistance-gene system against fungal and bacterial pathogens. *Plant J.* *60*, 218–226.

- Návarová, H., Bernsdorff, F., Döring, A.-C., and Zeier, J. (2012). Pipecolic acid, an endogenous mediator of defense amplification and priming, is a critical regulator of inducible plant immunity. *Plant Cell* 24, 5123–5141.
- Navarro, L., Zipfel, C., Rowland, O., Keller, I., Robatzek, S., Boller, T., and Jones, J.D.G. (2004). The transcriptional innate immune response to flg22. Interplay and overlap with Avr gene-dependent defense responses and bacterial pathogenesis. *Plant Physiol.* 135, 1113–1128.
- Navarro, L., Dunoyer, P., Jay, F., Arnold, B., Dharmasiri, N., Estelle, M., Voinnet, O., and Jones, J.D.G. (2006). A plant miRNA contributes to antibacterial resistance by repressing auxin signaling. *Science* 312, 436–439.
- Navarro, L., Bari, R., Achard, P., Lisón, P., Nemri, A., Harberd, N.P., and Jones, J.D.G. (2008). DELLAs control plant immune responses by modulating the balance of jasmonic acid and salicylic acid signaling. *Curr. Biol.* 18, 650–655.
- Nawrath, C., Heck, S., Parinthewong, N., and Métraux, J.-P. (2002). EDS5, an essential component of salicylic acid-dependent signaling for disease resistance in Arabidopsis, is a member of the MATE transporter family. *Plant Cell* 14, 275–286.
- Ndamukong, I., Abdallat, A.A., Thurow, C., Fode, B., Zander, M., Weigel, R., and Gatz, C. (2007). SA-inducible Arabidopsis glutaredoxin interacts with TGA factors and suppresses JA-responsive PDF1.2 transcription. *Plant J.* 50, 128–139.
- Ngou, B.P.M., Ahn, H.-K., Ding, P., Redkar, A., Brown, H., Ma, Y., Youles, M., Tomlinson, L., and Jones, J.D.G. (2020a). Estradiol-inducible AvrRps4 expression reveals distinct properties of TIR-NLR-mediated effector-triggered immunity. *J. Exp. Bot.* 71, 2186–2197.
- Ngou, B.P.M., Ahn, H.-K., Ding, P., and Jones, J.D. (2020b). Mutual Potentiation of Plant Immunity by Cell-surface and Intracellular Receptors. *BioRxiv*.
- Niehl, A., Wyrsh, I., Boller, T., and Heinlein, M. (2016). Double-stranded RNAs induce a pattern-triggered immune signaling pathway in plants. *New Phytol.* 211, 1008–1019.
- Nishimura, M.T., Stein, M., Hou, B.-H., Vogel, J.P., Edwards, H., and Somerville, S.C. (2003). Loss of a callose synthase results in salicylic acid-dependent disease resistance. *Science* 301, 969–972.
- Nobori, T., Velásquez, A.C., Wu, J., Kvitko, B.H., Kremer, J.M., Wang, Y., He, S.Y., and Tsuda, K. (2018). Transcriptome landscape of a bacterial pathogen under plant immunity. *Proc. Natl. Acad. Sci. USA* 115, E3055–E3064.
- Nomura, K., Mecey, C., Lee, Y.-N., Imboden, L.A., Chang, J.H., and He, S.Y. (2011). Effector-triggered immunity blocks pathogen degradation of an immunity-associated vesicle traffic regulator in Arabidopsis. *Proc. Natl. Acad. Sci. USA* 108, 10774–10779.
- Ntoukakis, V., Schwessinger, B., Segonzac, C., and Zipfel, C. (2011). Cautionary notes on the use of C-terminal BAK1 fusion proteins for functional studies. *Plant Cell* 23, 3871–3878.
- O'Malley, R.C., Huang, S.-S.C., Song, L., Lewsey, M.G., Bartlett, A., Nery, J.R., Galli, M., Gallavotti, A., and Ecker, J.R. (2016). Cistrome and epicistrome features shape the regulatory DNA landscape. *Cell* 165, 1280–1292.

- Ochoa-Fernandez, R., Abel, N.B., Wieland, F.-G., Schlegel, J., Koch, L.-A., Miller, J.B., Engesser, R., Giuriani, G., Brandl, S.M., Timmer, J., et al. (2020). Optogenetic control of gene expression in plants in the presence of ambient white light. *Nat. Methods* *17*, 717–725.
- Ogasawara, Y., Kaya, H., Hiraoka, G., Yumoto, F., Kimura, S., Kadota, Y., Hishinuma, H., Senzaki, E., Yamagoe, S., Nagata, K., et al. (2008). Synergistic activation of the Arabidopsis NADPH oxidase AtrbohD by Ca<sup>2+</sup> and phosphorylation. *J. Biol. Chem.* *283*, 8885–8892.
- Okuyama, Y., Kanzaki, H., Abe, A., Yoshida, K., Tamiru, M., Saitoh, H., Fujibe, T., Matsumura, H., Shenton, M., Galam, D.C., et al. (2011). A multifaceted genomics approach allows the isolation of the rice Pia-blast resistance gene consisting of two adjacent NBS-LRR protein genes. *Plant J.* *66*, 467–479.
- Orlandi, E.W., Hutcheson, S.W., and Baker, C.J. (1992). Early physiological responses associated with race-specific recognition in soybean leaf tissue and cell suspensions treated with *Pseudomonas syringae* pv. *glycinea*. *Physiol. Mol. Plant Pathol.* *40*, 173–180.
- Ostergaard, L., Petersen, M., Mattsson, O., and Mundy, J. (2002). An Arabidopsis callose synthase. *Plant Mol. Biol.* *49*, 559–566.
- Pandey, S.P., Roccaro, M., Schön, M., Logemann, E., and Somssich, I.E. (2010). Transcriptional reprogramming regulated by WRKY18 and WRKY40 facilitates powdery mildew infection of Arabidopsis. *Plant J.* *64*, 912–923.
- Park, C.-J., Peng, Y., Chen, X., Dardick, C., Ruan, D., Bart, R., Canlas, P.E., and Ronald, P.C. (2008). Rice XB15, a protein phosphatase 2C, negatively regulates cell death and XA21-mediated innate immunity. *PLoS Biol.* *6*, e231.
- Parker, J.E., Holub, E.B., Frost, L.N., Falk, A., Gunn, N.D., and Daniels, M.J. (1996). Characterization of eds1, a mutation in Arabidopsis suppressing resistance to *Peronospora parasitica* specified by several different RPP genes. *Plant Cell* *8*, 2033–2046.
- Pauwels, L., Barbero, G.F., Geerinck, J., Tilleman, S., Grunewald, W., Pérez, A.C., Chico, J.M., Bossche, R.V., Sewell, J., Gil, E., et al. (2010). NINJA connects the co-repressor TOPLESS to jasmonate signalling. *Nature* *464*, 788–791.
- Peart, J.R., Lu, R., Sadanandom, A., Malcuit, I., Moffett, P., Brice, D.C., Schauser, L., Jaggard, D.A.W., Xiao, S., Coleman, M.J., et al. (2002). Ubiquitin ligase-associated protein SGT1 is required for host and nonhost disease resistance in plants. *Proc. Natl. Acad. Sci. USA* *99*, 10865–10869.
- Peart, J.R., Mestre, P., Lu, R., Malcuit, I., and Baulcombe, D.C. (2005). NRG1, a CC-NB-LRR protein, together with N, a TIR-NB-LRR protein, mediates resistance against tobacco mosaic virus. *Curr. Biol.* *15*, 968–973.
- Perraki, A., DeFalco, T.A., Derbyshire, P., Avila, J., Séré, D., Sklenar, J., Qi, X., Stransfeld, L., Schwessinger, B., Kadota, Y., et al. (2018). Phosphocode-dependent functional dichotomy of a common co-receptor in plant signalling. *Nature* *561*, 248–252.
- Picotti, P., and Aebersold, R. (2012). Selected reaction monitoring-based proteomics: workflows, potential, pitfalls and future directions. *Nat. Methods* *9*, 555–566.

- Pieterse, C.M., van Wees, S.C., van Pelt, J.A., Knoester, M., Laan, R., Gerrits, H., Weisbeek, P.J., and van Loon, L.C. (1998). A novel signaling pathway controlling induced systemic resistance in *Arabidopsis*. *Plant Cell* *10*, 1571–1580.
- Pogány, M., von Rad, U., Grün, S., Dongó, A., Pintye, A., Simoneau, P., Bahnweg, G., Kiss, L., Barna, B., and Durner, J. (2009). Dual roles of reactive oxygen species and NADPH oxidase RBOHD in an *Arabidopsis*-*Alternaria* pathosystem. *Plant Physiol.* *151*, 1459–1475.
- Poncini, L., Wyrsh, I., Dénervaud Tendon, V., Vorley, T., Boller, T., Geldner, N., Métraux, J.-P., and Lehmann, S. (2017). In roots of *Arabidopsis thaliana*, the damage-associated molecular pattern AtPep1 is a stronger elicitor of immune signalling than flg22 or the chitin heptamer. *PLoS One* *12*, e0185808.
- Pruitt, R.N., Joe, A., Zhang, W., Feng, W., Stewart, V., Schwessinger, B., Dinneny, J.R., and Ronald, P.C. (2017). A microbially derived tyrosine-sulfated peptide mimics a plant peptide hormone. *New Phytol.* *215*, 725–736.
- Qi, D., Dubiella, U., Kim, S.H., Sloss, D.I., Downen, R.H., Dixon, J.E., and Innes, R.W. (2014). Recognition of the protein kinase AVRPPHB SUSCEPTIBLE1 by the disease resistance protein RESISTANCE TO PSEUDOMONAS SYRINGAE5 is dependent on s-acylation and an exposed loop in AVRPPHB SUSCEPTIBLE1. *Plant Physiol.* *164*, 340–351.
- Qi, T., Seong, K., Thomazella, D.P.T., Kim, J.R., Pham, J., Seo, E., Cho, M.-J., Schultink, A., and Staskawicz, B.J. (2018). NRG1 functions downstream of EDS1 to regulate TIR-NLR-mediated plant immunity in *Nicotiana benthamiana*. *Proc. Natl. Acad. Sci. USA* *115*, E10979–E10987.
- Qi, Y., Tsuda, K., Glazebrook, J., and Katagiri, F. (2011). Physical association of pattern-triggered immunity (PTI) and effector-triggered immunity (ETI) immune receptors in *Arabidopsis*. *Mol. Plant Pathol.* *12*, 702–708.
- Qiao, Y., Liu, L., Xiong, Q., Flores, C., Wong, J., Shi, J., Wang, X., Liu, X., Xiang, Q., Jiang, S., et al. (2013). Oomycete pathogens encode RNA silencing suppressors. *Nat. Genet.* *45*, 330–333.
- Qiao, Y., Shi, J., Zhai, Y., Hou, Y., and Ma, W. (2015). *Phytophthora* effector targets a novel component of small RNA pathway in plants to promote infection. *Proc. Natl. Acad. Sci. USA* *112*, 5850–5855.
- Radojčić, A., Li, X., and Zhang, Y. (2018). Salicylic Acid: A Double-Edged Sword for Programed Cell Death in Plants. *Front. Plant Sci.* *9*, 1133.
- Ranf, S., Eschen-Lippold, L., Fröhlich, K., Westphal, L., Scheel, D., and Lee, J. (2014). Microbe-associated molecular pattern-induced calcium signaling requires the receptor-like cytoplasmic kinases, PBL1 and BIK1. *BMC Plant Biol.* *14*, 374.
- Ranf, S., Gisch, N., Schäffer, M., Illig, T., Westphal, L., Knirel, Y.A., Sánchez-Carballo, P.M., Zähringer, U., Hüchelhoven, R., Lee, J., et al. (2015). A lectin S-domain receptor kinase mediates lipopolysaccharide sensing in *Arabidopsis thaliana*. *Nat. Immunol.* *16*, 426–433.

- Rao, S., Zhou, Z., Miao, P., Bi, G., Hu, M., Wu, Y., Feng, F., Zhang, X., and Zhou, J.-M. (2018). Roles of Receptor-Like Cytoplasmic Kinase VII Members in Pattern-Triggered Immune Signaling. *Plant Physiol.* *177*, 1679–1690.
- Rasmussen, M.W., Roux, M., Petersen, M., and Mundy, J. (2012). MAP kinase cascades in arabidopsis innate immunity. *Front. Plant Sci.* *3*, 169.
- Ratcliff, F., Harrison, B.D., and Baulcombe, D.C. (1997). A similarity between viral defense and gene silencing in plants. *Science* *276*, 1558–1560.
- Rehmany, A.P., Gordon, A., Rose, L.E., Allen, R.L., Armstrong, M.R., Whisson, S.C., Kamoun, S., Tyler, B.M., Birch, P.R.J., and Beynon, J.L. (2005). Differential recognition of highly divergent downy mildew avirulence gene alleles by RPP1 resistance genes from two Arabidopsis lines. *Plant Cell* *17*, 1839–1850.
- Rekhter, D., Lüdke, D., Ding, Y., Feussner, K., Zienkiewicz, K., Lipka, V., Wiermer, M., Zhang, Y., and Feussner, I. (2019). Isochorismate-derived biosynthesis of the plant stress hormone salicylic acid. *Science* *365*, 498–502.
- Robatzek, S., Chinchilla, D., and Boller, T. (2006). Ligand-induced endocytosis of the pattern recognition receptor FLS2 in Arabidopsis. *Genes Dev.* *20*, 537–542.
- Roux, M., Schwessinger, B., Albrecht, C., Chinchilla, D., Jones, A., Holton, N., Malinovsky, F.G., Tör, M., de Vries, S., and Zipfel, C. (2011). The *Arabidopsis* leucine-rich repeat receptor-like kinases BAK1/SERK3 and BKK1/SERK4 are required for innate immunity to hemibiotrophic and biotrophic pathogens. *Plant Cell* *23*, 2440–2455.
- Rowland, O., Ludwig, A.A., Merrick, C.J., Baillieul, F., Tracy, F.E., Durrant, W.E., Fritz-Laylin, L., Nekrasov, V., Sjölander, K., Yoshioka, H., et al. (2005). Functional analysis of Avr9/Cf-9 rapidly elicited genes identifies a protein kinase, ACIK1, that is essential for full Cf-9-dependent disease resistance in tomato. *Plant Cell* *17*, 295–310.
- Ryals, J.A., Neuenschwander, U.H., Willits, M.G., Molina, A., Steiner, H.Y., and Hunt, M.D. (1996). Systemic Acquired Resistance. *Plant Cell* *8*, 1809–1819.
- Rybak, K., and Robatzek, S. (2019). Functions of extracellular vesicles in immunity and virulence. *Plant Physiol.* *179*, 1236–1247.
- Saile, S.C., Jacob, P., Castel, B., Jubic, L.M., Salas-Gonzalez, I., Bäcker, M., Jones, J.D.G., Dangl, J.L., and El Kasmi, F. (2020). Two unequally redundant “helper” immune receptor families mediate Arabidopsis thaliana intracellular “sensor” immune receptor functions. *PLoS Biol.* *18*, e3000783.
- Sainsbury, F., and Lomonosoff, G.P. (2014). Transient expressions of synthetic biology in plants. *Curr. Opin. Plant Biol.* *19*, 1–7.
- Santiago, J., Brandt, B., Wildhagen, M., Hohmann, U., Hothorn, L.A., Butenko, M.A., and Hothorn, M. (2016). Mechanistic insight into a peptide hormone signaling complex mediating floral organ abscission. *Elife* *5*.
- Sarris, P.F., Duxbury, Z., Huh, S.U., Ma, Y., Segonzac, C., Sklenar, J., Derbyshire, P., Cevik, V., Rallapalli, G., Saucet, S.B., et al. (2015). A Plant Immune Receptor Detects Pathogen Effectors that Target WRKY Transcription Factors. *Cell* *161*, 1089–1100.

- Saucet, S.B., Ma, Y., Sarris, P.F., Furzer, O.J., Sohn, K.H., and Jones, J.D.G. (2015). Two linked pairs of Arabidopsis TNL resistance genes independently confer recognition of bacterial effector AvrRps4. *Nat. Commun.* *6*, 6338.
- Schindelin, J., Arganda-Carreras, I., Frise, E., Kaynig, V., Longair, M., Pietzsch, T., Preibisch, S., Rueden, C., Saalfeld, S., Schmid, B., et al. (2012). Fiji: an open-source platform for biological-image analysis. *Nat. Methods* *9*, 676–682.
- Schwessinger, B., Roux, M., Kadota, Y., Ntoukakis, V., Sklenar, J., Jones, A., and Zipfel, C. (2011). Phosphorylation-dependent differential regulation of plant growth, cell death, and innate immunity by the regulatory receptor-like kinase BAK1. *PLoS Genet.* *7*, e1002046.
- Segonzac, C., Macho, A.P., Sanmartín, M., Ntoukakis, V., Sánchez-Serrano, J.J., and Zipfel, C. (2014). Negative control of BAK1 by protein phosphatase 2A during plant innate immunity. *EMBO J.* *33*, 2069–2079.
- Serrano, I., Audran, C., and Rivas, S. (2016). Chloroplasts at work during plant innate immunity. *J. Exp. Bot.* *67*, 3845–3854.
- Seybold, H., Trempel, F., Ranf, S., Scheel, D., Romeis, T., and Lee, J. (2014). Ca<sup>2+</sup> signalling in plant immune response: from pattern recognition receptors to Ca<sup>2+</sup> decoding mechanisms. *New Phytol.* *204*, 782–790.
- Shan, L., He, P., Li, J., Heese, A., Peck, S.C., Nürnberger, T., Martin, G.B., and Sheen, J. (2008). Bacterial effectors target the common signaling partner BAK1 to disrupt multiple MAMP receptor-signaling complexes and impede plant immunity. *Cell Host Microbe* *4*, 17–27.
- Shaner, N.C., Lambert, G.G., Chammas, A., Ni, Y., Cranfill, P.J., Baird, M.A., Sell, B.R., Allen, J.R., Day, R.N., Israelsson, M., et al. (2013). A bright monomeric green fluorescent protein derived from Branchiostoma lanceolatum. *Nat. Methods* *10*, 407–409.
- Shao, F., Golstein, C., Ade, J., Stoutemyer, M., Dixon, J.E., and Innes, R.W. (2003). Cleavage of Arabidopsis PBS1 by a bacterial type III effector. *Science* *301*, 1230–1233.
- She, J., Han, Z., Kim, T.-W., Wang, J., Cheng, W., Chang, J., Shi, S., Wang, J., Yang, M., Wang, Z.-Y., et al. (2011). Structural insight into brassinosteroid perception by BRI1. *Nature* *474*, 472–476.
- Sheard, L.B., Tan, X., Mao, H., Withers, J., Ben-Nissan, G., Hinds, T.R., Kobayashi, Y., Hsu, F.-F., Sharon, M., Browse, J., et al. (2010). Jasmonate perception by inositol-phosphate-potentiated COI1-JAZ co-receptor. *Nature* *468*, 400–405.
- Shimada, T.L., Shimada, T., and Hara-Nishimura, I. (2010). A rapid and non-destructive screenable marker, FAST, for identifying transformed seeds of *Arabidopsis thaliana*. *Plant J.* *61*, 519–528.
- Shirasu, K. (2009). The HSP90-SGT1 chaperone complex for NLR immune sensors. *Annu. Rev. Plant Biol.* *60*, 139–164.
- Shivaprasad, P.V., Chen, H.-M., Patel, K., Bond, D.M., Santos, B.A.C.M., and Baulcombe, D.C. (2012). A microRNA superfamily regulates nucleotide binding site-leucine-rich repeats and other mRNAs. *Plant Cell* *24*, 859–874.

- Sinapidou, E., Williams, K., Nott, L., Bahkt, S., Tör, M., Crute, I., Bittner-Eddy, P., and Beynon, J. (2004). Two TIR:NB:LRR genes are required to specify resistance to *Peronospora parasitica* isolate Cala2 in *Arabidopsis*. *Plant J.* 38, 898–909.
- Smakowska-Luzan, E., Mott, G.A., Parys, K., Stegmann, M., Howton, T.C., Layeghifard, M., Neuhold, J., Lehner, A., Kong, J., Grünwald, K., et al. (2018). An extracellular network of *Arabidopsis* leucine-rich repeat receptor kinases. *Nature* 553, 342–346.
- Sohn, K.H., Zhang, Y., and Jones, J.D.G. (2009). The *Pseudomonas syringae* effector protein, AvrRPS4, requires in planta processing and the KRVY domain to function. *Plant J.* 57, 1079–1091.
- Sohn, K.H., Segonzac, C., Rallapalli, G., Sarris, P.F., Woo, J.Y., Williams, S.J., Newman, T.E., Paek, K.H., Kobe, B., and Jones, J.D.G. (2014). The nuclear immune receptor RPS4 is required for RRS1SLH1-dependent constitutive defense activation in *Arabidopsis thaliana*. *PLoS Genet.* 10, e1004655.
- Soleimani, V.D., Palidwor, G.A., Ramachandran, P., Perkins, T.J., and Rudnicki, M.A. (2013). Chromatin tandem affinity purification sequencing. *Nat. Protoc.* 8, 1525–1534.
- Sreekanta, S., Bethke, G., Hatsugai, N., Tsuda, K., Thao, A., Wang, L., Katagiri, F., and Glazebrook, J. (2015). The receptor-like cytoplasmic kinase PCRK1 contributes to pattern-triggered immunity against *Pseudomonas syringae* in *Arabidopsis thaliana*. *New Phytol.* 207, 78–90.
- Stegmann, M., Monaghan, J., Smakowska-Luzan, E., Rovenich, H., Lehner, A., Holton, N., Belkhadir, Y., and Zipfel, C. (2017). The receptor kinase FER is a RALF-regulated scaffold controlling plant immune signaling. *Science* 355, 287–289.
- Steinbrenner, A.D., Munoz-Amatriain, M., Venegas, J.M.A., Lo, S., Shi, D., Holton, N., Zipfel, C., Abagyan, R., Huffaker, A., Close, T.J., et al. (2019). A receptor for herbivore-associated molecular patterns mediates plant immunity. *BioRxiv*.
- Su, J., Zhang, M., Zhang, L., Sun, T., Liu, Y., Lukowitz, W., Xu, J., and Zhang, S. (2017). Regulation of Stomatal Immunity by Interdependent Functions of a Pathogen-Responsive MPK3/MPK6 Cascade and Abscisic Acid. *Plant Cell* 29, 526–542.
- Su, J., Yang, L., Zhu, Q., Wu, H., He, Y., Liu, Y., Xu, J., Jiang, D., and Zhang, S. (2018). Active photosynthetic inhibition mediated by MPK3/MPK6 is critical to effector-triggered immunity. *PLoS Biol.* 16, e2004122.
- Sun, T., Zhang, Y., Li, Y., Zhang, Q., Ding, Y., and Zhang, Y. (2015). ChIP-seq reveals broad roles of SARD1 and CBP60g in regulating plant immunity. *Nat. Commun.* 6, 10159.
- Sun, T., Busta, L., Zhang, Q., Ding, P., Jetter, R., and Zhang, Y. (2018). TGACG-BINDING FACTOR 1 (TGA1) and TGA4 regulate salicylic acid and piperolic acid biosynthesis by modulating the expression of SYSTEMIC ACQUIRED RESISTANCE DEFICIENT 1 (SARD1) and CALMODULIN-BINDING PROTEIN 60g (CBP60g). *New Phytol.* 217, 344–354.
- Sun, T., Huang, J., Xu, Y., Verma, V., Jing, B., Sun, Y., Ruiz Orduna, A., Tian, H., Huang, X., Xia, S., et al. (2020). Redundant CAMTA Transcription Factors Negatively

- Regulate the Biosynthesis of Salicylic Acid and N-Hydroxy-pipecolic Acid by Modulating the Expression of SARD1 and CBP60g. *Mol. Plant* *13*, 144–156.
- Sun, Y., Li, L., Macho, A.P., Han, Z., Hu, Z., Zipfel, C., Zhou, J.-M., and Chai, J. (2013). Structural basis for flg22-induced activation of the *Arabidopsis* FLS2-BAK1 immune complex. *Science* *342*, 624–628.
- Takahashi, A., Casais, C., Ichimura, K., and Shirasu, K. (2003). HSP90 interacts with RAR1 and SGT1 and is essential for RPS2-mediated disease resistance in *Arabidopsis*. *Proc. Natl. Acad. Sci. USA* *100*, 11777–11782.
- Takken, F.L.W., and Tameling, W.I.L. (2009). To nibble at plant resistance proteins. *Science* *324*, 744–746.
- Takken, F.L., Albrecht, M., and Tameling, W.I. (2006). Resistance proteins: molecular switches of plant defence. *Curr. Opin. Plant Biol.* *9*, 383–390.
- Tao, Y., Xie, Z., Chen, W., Glazebrook, J., Chang, H.-S., Han, B., Zhu, T., Zou, G., and Katagiri, F. (2003). Quantitative nature of *Arabidopsis* responses during compatible and incompatible interactions with the bacterial pathogen *Pseudomonas syringae*. *Plant Cell* *15*, 317–330.
- Thilmony, R., Underwood, W., and He, S.Y. (2006). Genome-wide transcriptional analysis of the *Arabidopsis thaliana* interaction with the plant pathogen *Pseudomonas syringae* pv. tomato DC3000 and the human pathogen *Escherichia coli* O157:H7. *Plant J.* *46*, 34–53.
- Thines, B., Katsir, L., Melotto, M., Niu, Y., Mandaokar, A., Liu, G., Nomura, K., He, S.Y., Howe, G.A., and Browse, J. (2007). JAZ repressor proteins are targets of the SCF<sup>COI1</sup> complex during jasmonate signalling. *Nature* *448*, 661–665.
- Thomas, C.M., Jones, D.A., Parniske, M., Harrison, K., Balint-Kurti, P.J., Hatzixanthis, K., and Jones, J.D. (1997). Characterization of the tomato Cf-4 gene for resistance to *Cladosporium fulvum* identifies sequences that determine recognitional specificity in Cf-4 and Cf-9. *Plant Cell* *9*, 2209–2224.
- Thomas, W.J., Thireault, C.A., Kimbrel, J.A., and Chang, J.H. (2009). Recombineering and stable integration of the *Pseudomonas syringae* pv. *syringae* 61 hrp/hrc cluster into the genome of the soil bacterium *Pseudomonas fluorescens* Pf0-1. *Plant J.* *60*, 919–928.
- Thor, K., Jiang, S., Michard, E., George, J., Scherzer, S., Huang, S., Dindas, J., Derbyshire, P., Leitão, N., DeFalco, T.A., et al. (2020). The calcium-permeable channel OSCA1.3 regulates plant stomatal immunity. *Nature* *585*, 569–573.
- Thordal-Christensen, H., Zhang, Z., Wei, Y., and Collinge, D.B. (1997). Subcellular localization of H<sub>2</sub>O<sub>2</sub> in plants. H<sub>2</sub>O<sub>2</sub> accumulation in papillae and hypersensitive response during the barley-powdery mildew interaction. *Plant J.* *11*, 1187–1194.
- Tian, W., Hou, C., Ren, Z., Wang, C., Zhao, F., Dahlbeck, D., Hu, S., Zhang, L., Niu, Q., Li, L., et al. (2019). A calmodulin-gated calcium channel links pathogen patterns to plant immunity. *Nature* *572*, 131–135.
- Tornero, P., Chao, R.A., Luthin, W.N., Goff, S.A., and Dangl, J.L. (2002). Large-scale structure-function analysis of the *Arabidopsis* RPM1 disease resistance protein. *Plant Cell* *14*, 435–450.

- Torrens-Spence, M.P., Bobokalonova, A., Carballo, V., Glinkerman, C.M., Pluskal, T., Shen, A., and Weng, J.-K. (2019). PBS3 and EPS1 complete salicylic acid biosynthesis from isochorismate in Arabidopsis. *BioRxiv*.
- Torres, M.A., Dangl, J.L., and Jones, J.D.G. (2002). Arabidopsis gp91phox homologues AtrbohD and AtrbohF are required for accumulation of reactive oxygen intermediates in the plant defense response. *Proc. Natl. Acad. Sci. USA* *99*, 517–522.
- Toyota, M., Spencer, D., Sawai-Toyota, S., Jiaqi, W., Zhang, T., Koo, A.J., Howe, G.A., and Gilroy, S. (2018). Glutamate triggers long-distance, calcium-based plant defense signaling. *Science* *361*, 1112–1115.
- Trujillo, M., Ichimura, K., Casais, C., and Shirasu, K. (2008). Negative regulation of PAMP-triggered immunity by an E3 ubiquitin ligase triplet in Arabidopsis. *Curr. Biol.* *18*, 1396–1401.
- Tsuda, K., Mine, A., Bethke, G., Igarashi, D., Botanga, C.J., Tsuda, Y., Glazebrook, J., Sato, M., and Katagiri, F. (2013). Dual regulation of gene expression mediated by extended MAPK activation and salicylic acid contributes to robust innate immunity in Arabidopsis thaliana. *PLoS Genet.* *9*, e1004015.
- van der Biezen, E.A., Freddie, C.T., Kahn, K., Parker, J.E., and Jones, J.D.G. (2002). Arabidopsis RPP4 is a member of the RPP5 multigene family of TIR-NB-LRR genes and confers downy mildew resistance through multiple signalling components. *Plant J.* *29*, 439–451.
- van der Burgh, A.M., and Joosten, M.H.A.J. (2019). Plant immunity: thinking outside and inside the box. *Trends Plant Sci.* *24*, 587–601.
- van Wees, S.C.M., and Glazebrook, J. (2003). Loss of non-host resistance of Arabidopsis NahG to Pseudomonas syringae pv. phaseolicola is due to degradation products of salicylic acid. *Plant J.* *33*, 733–742.
- Verma, D.P., and Hong, Z. (2001). Plant callose synthase complexes. *Plant Mol. Biol.* *47*, 693–701.
- Voigt, C.A. (2014). Callose-mediated resistance to pathogenic intruders in plant defense-related papillae. *Front. Plant Sci.* *5*, 168.
- Voigt, C.A., and Somerville, S.C. (2009). Callose in biotic stress (pathogenesis). In *Chemistry, Biochemistry, and Biology of 1-3 Beta Glucans and Related Polysaccharides*, (Elsevier), pp. 525–562.
- Wagner, S., Stuttmann, J., Rietz, S., Guerois, R., Brunstein, E., Bautor, J., Niefind, K., and Parker, J.E. (2013). Structural basis for signaling by exclusive EDS1 heteromeric complexes with SAG101 or PAD4 in plant innate immunity. *Cell Host Microbe* *14*, 619–630.
- Wan, J., Zhang, X.-C., Neece, D., Ramonell, K.M., Clough, S., Kim, S.-Y., Stacey, M.G., and Stacey, G. (2008). A LysM receptor-like kinase plays a critical role in chitin signaling and fungal resistance in Arabidopsis. *Plant Cell* *20*, 471–481.
- Wan, J., Tanaka, K., Zhang, X.-C., Son, G.H., Brechenmacher, L., Nguyen, T.H.N., and Stacey, G. (2012). LYK4, a lysin motif receptor-like kinase, is important for chitin signaling and plant innate immunity in Arabidopsis. *Plant Physiol.* *160*, 396–406.

- Wan, L., Essuman, K., Anderson, R.G., Sasaki, Y., Monteiro, F., Chung, E.-H., Osborne Nishimura, E., DiAntonio, A., Milbrandt, J., Dangl, J.L., et al. (2019). TIR domains of plant immune receptors are NAD<sup>+</sup>-cleaving enzymes that promote cell death. *Science* 365, 799–803.
- Wang, D., Pajerowska-Mukhtar, K., Culler, A.H., and Dong, X. (2007). Salicylic acid inhibits pathogen growth in plants through repression of the auxin signaling pathway. *Curr. Biol.* 17, 1784–1790.
- Wang, G., Roux, B., Feng, F., Guy, E., Li, L., Li, N., Zhang, X., Lautier, M., Jardinaud, M.-F., Chabannes, M., et al. (2015). The Decoy Substrate of a Pathogen Effector and a Pseudokinase Specify Pathogen-Induced Modified-Self Recognition and Immunity in Plants. *Cell Host Microbe* 18, 285–295.
- Wang, J., Grubb, L.E., Wang, J., Liang, X., Li, L., Gao, C., Ma, M., Feng, F., Li, M., Li, L., et al. (2018). A regulatory module controlling homeostasis of a plant immune kinase. *Mol. Cell* 69, 493–504.e6.
- Wang, J., Hu, M., Wang, J., Qi, J., Han, Z., Wang, G., Qi, Y., Wang, H.-W., Zhou, J.-M., and Chai, J. (2019a). Reconstitution and structure of a plant NLR resistosome conferring immunity. *Science* 364.
- Wang, J., Wang, J., Hu, M., Wu, S., Qi, J., Wang, G., Han, Z., Qi, Y., Gao, N., Wang, H.-W., et al. (2019b). Ligand-triggered allosteric ADP release primes a plant NLR complex. *Science* 364.
- Wang, K., Senthil-Kumar, M., Ryu, C.-M., Kang, L., and Mysore, K.S. (2012). Phytosterols play a key role in plant innate immunity against bacterial pathogens by regulating nutrient efflux into the apoplast. *Plant Physiol.* 158, 1789–1802.
- Wang, L., Tsuda, K., Sato, M., Cohen, J.D., Katagiri, F., and Glazebrook, J. (2009). Arabidopsis CaM binding protein CBP60g contributes to MAMP-induced SA accumulation and is involved in disease resistance against *Pseudomonas syringae*. *PLoS Pathog.* 5, e1000301.
- Wang, W., Yang, J., Zhang, J., Liu, Y.-X., Tian, C., Qu, B., Gao, C., Xin, P., Cheng, S., Zhang, W., et al. (2020a). An arabidopsis secondary metabolite directly targets expression of the bacterial type III secretion system to inhibit bacterial virulence. *Cell Host Microbe* 27, 601–613.e7.
- Wang, W., Withers, J., Li, H., Zwack, P.J., Rusnac, D.-V., Shi, H., Liu, L., Yan, S., Hinds, T.R., Guttman, M., et al. (2020b). Structural basis of salicylic acid perception by Arabidopsis NPR proteins. *Nature* 586, 311–316.
- Wang, Y., Li, J., Hou, S., Wang, X., Li, Y., Ren, D., Chen, S., Tang, X., and Zhou, J.-M. (2010). A *Pseudomonas syringae* ADP-ribosyltransferase inhibits Arabidopsis mitogen-activated protein kinase kinases. *Plant Cell* 22, 2033–2044.
- Weiss, D., and Ori, N. (2007). Mechanisms of cross talk between gibberellin and other hormones. *Plant Physiol.* 144, 1240–1246.
- Whitham, S., McCormick, S., and Baker, B. (1996). The N gene of tobacco confers resistance to tobacco mosaic virus in transgenic tomato. *Proc. Natl. Acad. Sci. USA* 93, 8776–8781.

- Wildermuth, M.C., Dewdney, J., Wu, G., and Ausubel, F.M. (2001). Isochorismate synthase is required to synthesize salicylic acid for plant defence. *Nature* *414*, 562–565.
- Williams, S.J., Sohn, K.H., Wan, L., Bernoux, M., Sarris, P.F., Segonzac, C., Ve, T., Ma, Y., Saucet, S.B., Ericsson, D.J., et al. (2014). Structural basis for assembly and function of a heterodimeric plant immune receptor. *Science* *344*, 299–303.
- Willmann, R., Lajunen, H.M., Erbs, G., Newman, M.-A., Kolb, D., Tsuda, K., Katagiri, F., Fliegmann, J., Bono, J.-J., Cullimore, J.V., et al. (2011). Arabidopsis lysin-motif proteins LYM1 LYM3 CERK1 mediate bacterial peptidoglycan sensing and immunity to bacterial infection. *Proc. Natl. Acad. Sci. USA* *108*, 19824–19829.
- Wu, C.-H., Abd-El-Halim, A., Bozkurt, T.O., Belhaj, K., Terauchi, R., Vossen, J.H., and Kamoun, S. (2017). NLR network mediates immunity to diverse plant pathogens. *Proc. Natl. Acad. Sci. USA* *114*, 8113–8118.
- Wu, C.-H., Derevnina, L., and Kamoun, S. (2018). Receptor networks underpin plant immunity. *Science* *360*, 1300–1301.
- Wu, F., Chi, Y., Jiang, Z., Xu, Y., Xie, L., Huang, F., Wan, D., Ni, J., Yuan, F., Wu, X., et al. (2020a). Hydrogen peroxide sensor HPCA1 is an LRR receptor kinase in Arabidopsis. *Nature* *578*, 577–581.
- Wu, Y., Xun, Q., Guo, Y., Zhang, J., Cheng, K., Shi, T., He, K., Hou, S., Gou, X., and Li, J. (2016). Genome-Wide Expression Pattern Analyses of the Arabidopsis Leucine-Rich Repeat Receptor-Like Kinases. *Mol. Plant* *9*, 289–300.
- Wu, Z., Li, M., Dong, O.X., Xia, S., Liang, W., Bao, Y., Wasteneys, G., and Li, X. (2019). Differential regulation of TNL-mediated immune signaling by redundant helper CNLs. *New Phytol.* *222*, 938–953.
- Wu, Z., Tong, M., Tian, L., Zhu, C., Liu, X., Zhang, Y., and Li, X. (2020b). Plant E3 ligases SNIPER1 and SNIPER2 broadly regulate the homeostasis of sensor NLR immune receptors. *EMBO J.* *39*, e104915.
- Xiang, T., Zong, N., Zou, Y., Wu, Y., Zhang, J., Xing, W., Li, Y., Tang, X., Zhu, L., Chai, J., et al. (2008). Pseudomonas syringae effector AvrPto blocks innate immunity by targeting receptor kinases. *Curr. Biol.* *18*, 74–80.
- Xiao, Y., Stegmann, M., Han, Z., DeFalco, T.A., Parys, K., Xu, L., Belkhadir, Y., Zipfel, C., and Chai, J. (2019). Mechanisms of RALF peptide perception by a heterotypic receptor complex. *Nature* *572*, 270–274.
- Xin, X.-F., Nomura, K., Aung, K., Velásquez, A.C., Yao, J., Boutrot, F., Chang, J.H., Zipfel, C., and He, S.Y. (2016). Bacteria establish an aqueous living space in plants crucial for virulence. *Nature* *539*, 524–529.
- Xing, W., Zou, Y., Liu, Q., Liu, J., Luo, X., Huang, Q., Chen, S., Zhu, L., Bi, R., Hao, Q., et al. (2007). The structural basis for activation of plant immunity by bacterial effector protein AvrPto. *Nature* *449*, 243–247.
- Xiong, Q., Ye, W., Choi, D., Wong, J., Qiao, Y., Tao, K., Wang, Y., and Ma, W. (2014). Phytophthora suppressor of RNA silencing 2 is a conserved RxLR effector that promotes infection in soybean and Arabidopsis thaliana. *Mol. Plant Microbe Interact.* *27*, 1379–1389.

- Xu, G., Greene, G.H., Yoo, H., Liu, L., Marqués, J., Motley, J., and Dong, X. (2017). Global translational reprogramming is a fundamental layer of immune regulation in plants. *Nature* 545, 487–490.
- Xu, J., Xie, J., Yan, C., Zou, X., Ren, D., and Zhang, S. (2014). A chemical genetic approach demonstrates that MPK3/MPK6 activation and NADPH oxidase-mediated oxidative burst are two independent signaling events in plant immunity. *Plant J.* 77, 222–234.
- Yamada, K., Yamaguchi, K., Shirakawa, T., Nakagami, H., Mine, A., Ishikawa, K., Fujiwara, M., Narusaka, M., Narusaka, Y., Ichimura, K., et al. (2016a). The Arabidopsis CERK1-associated kinase PBL27 connects chitin perception to MAPK activation. *EMBO J.* 35, 2468–2483.
- Yamada, K., Saijo, Y., Nakagami, H., and Takano, Y. (2016b). Regulation of sugar transporter activity for antibacterial defense in Arabidopsis. *Science* 354, 1427–1430.
- Yamaguchi, Y., Pearce, G., and Ryan, C.A. (2006). The cell surface leucine-rich repeat receptor for *AtPep1*, an endogenous peptide elicitor in *Arabidopsis*, is functional in transgenic tobacco cells. *Proc. Natl. Acad. Sci. USA* 103, 10104–10109.
- Yamaguchi, Y., Huffaker, A., Bryan, A.C., Tax, F.E., and Ryan, C.A. (2010). PEPR2 is a second receptor for the *Pep1* and *Pep2* peptides and contributes to defense responses in *Arabidopsis*. *Plant Cell* 22, 508–522.
- Yan, S., and Dong, X. (2014). Perception of the plant immune signal salicylic acid. *Curr. Opin. Plant Biol.* 20, 64–68.
- Yan, H., Zhao, Y., Shi, H., Li, J., Wang, Y., and Tang, D. (2018). BRASSINOSTEROID-SIGNALING KINASE1 Phosphorylates MAPKKK5 to Regulate Immunity in Arabidopsis. *Plant Physiol.* 176, 2991–3002.
- Yoo, H., Greene, G.H., Yuan, M., Xu, G., Burton, D., Liu, L., Marqués, J., and Dong, X. (2020). Translational Regulation of Metabolic Dynamics during Effector-Triggered Immunity. *Mol. Plant* 13, 88–98.
- Yu, G., Xian, L., Xue, H., Yu, W., Rufian, J.S., Sang, Y., Morcillo, R.J.L., Wang, Y., and Macho, A.P. (2020). A bacterial effector protein prevents MAPK-mediated phosphorylation of SGT1 to suppress plant immunity. *PLoS Pathog.* 16, e1008933.
- Yu, I.C., Parker, J., and Bent, A.F. (1998). Gene-for-gene disease resistance without the hypersensitive response in Arabidopsis *dnd1* mutant. *Proc. Natl. Acad. Sci. USA* 95, 7819–7824.
- Yu, X., Xu, G., Li, B., de Souza Vespoli, L., Liu, H., Moeder, W., Chen, S., de Oliveira, M.V.V., Ariádina de Souza, S., Shao, W., et al. (2019). The Receptor Kinases BAK1/SERK4 Regulate Ca<sup>2+</sup> Channel-Mediated Cellular Homeostasis for Cell Death Containment. *Curr. Biol.* 29, 3778–3790.e8.
- Yuan, M., Jiang, Z., Bi, G., Nomura, K., Liu, M., He, S.Y., Zhou, J.-M., and Xin, X.-F. (2020). Pattern-recognition receptors are required for NLR-mediated plant immunity. *BioRxiv*.

- Yun, B.-W., Feechan, A., Yin, M., Saidi, N.B.B., Le Bihan, T., Yu, M., Moore, J.W., Kang, J.-G., Kwon, E., Spoel, S.H., et al. (2011). S-nitrosylation of NADPH oxidase regulates cell death in plant immunity. *Nature* *478*, 264–268.
- Zavaliev, R., Mohan, R., Chen, T., and Dong, X. (2020). Formation of NPR1 Condensates Promotes Cell Survival during the Plant Immune Response. *Cell* *182*, 1093–1108.e18.
- Zhai, C., Lin, F., Dong, Z., He, X., Yuan, B., Zeng, X., Wang, L., and Pan, Q. (2011). The isolation and characterization of Pik, a rice blast resistance gene which emerged after rice domestication. *New Phytol.* *189*, 321–334.
- Zhang, N., and Fan, Z. (2020). Transcriptional reprogramming during effector/flg22-triggered immune is independent of defense phytohormone signaling networks. *BioRxiv*.
- Zhang, S., and Klessig, D.F. (1998). Resistance gene N-mediated de novo synthesis and activation of a tobacco mitogen-activated protein kinase by tobacco mosaic virus infection. *Proc. Natl. Acad. Sci. USA* *95*, 7433–7438.
- Zhang, X.-C., and Gassmann, W. (2007). Alternative splicing and mRNA levels of the disease resistance gene RPS4 are induced during defense responses. *Plant Physiol.* *145*, 1577–1587.
- Zhang, J., Shao, F., Li, Y., Cui, H., Chen, L., Li, H., Zou, Y., Long, C., Lan, L., Chai, J., et al. (2007). A *Pseudomonas syringae* effector inactivates MAPKs to suppress PAMP-induced immunity in plants. *Cell Host Microbe* *1*, 175–185.
- Zhang, J., Li, W., Xiang, T., Liu, Z., Laluk, K., Ding, X., Zou, Y., Gao, M., Zhang, X., Chen, S., et al. (2010a). Receptor-like cytoplasmic kinases integrate signaling from multiple plant immune receptors and are targeted by a *Pseudomonas syringae* effector. *Cell Host Microbe* *7*, 290–301.
- Zhang, W., Fraiture, M., Kolb, D., Löffelhardt, B., Desaki, Y., Boutrot, F.F.G., Tör, M., Zipfel, C., Gust, A.A., and Brunner, F. (2013). Arabidopsis receptor-like protein30 and receptor-like kinase suppressor of BIR1-1/EVERSHED mediate innate immunity to necrotrophic fungi. *Plant Cell* *25*, 4227–4241.
- Zhang, X., Bernoux, M., Bentham, A.R., Newman, T.E., Ve, T., Casey, L.W., Raaymakers, T.M., Hu, J., Croll, T.I., Schreiber, K.J., et al. (2017). Multiple functional self-association interfaces in plant TIR domains. *Proc. Natl. Acad. Sci. USA* *114*, E2046–E2052.
- Zhang, Y., Fan, W., Kinkema, M., Li, X., and Dong, X. (1999). Interaction of NPR1 with basic leucine zipper protein transcription factors that bind sequences required for salicylic acid induction of the PR-1 gene. *Proc. Natl. Acad. Sci. USA* *96*, 6523–6528.
- Zhang, Y., Tessaro, M.J., Lassner, M., and Li, X. (2003). Knockout analysis of Arabidopsis transcription factors TGA2, TGA5, and TGA6 reveals their redundant and essential roles in systemic acquired resistance. *Plant Cell* *15*, 2647–2653.
- Zhang, Y., Cheng, Y.T., Qu, N., Zhao, Q., Bi, D., and Li, X. (2006). Negative regulation of defense responses in Arabidopsis by two NPR1 paralogs. *Plant J.* *48*, 647–656.
- Zhang, Y., Xu, S., Ding, P., Wang, D., Cheng, Y.T., He, J., Gao, M., Xu, F., Li, Y., Zhu, Z., et al. (2010b). Control of salicylic acid synthesis and systemic acquired resistance by

- two members of a plant-specific family of transcription factors. *Proc. Natl. Acad. Sci. USA* *107*, 18220–18225.
- Zhao, Y., Thilmony, R., Bender, C.L., Schaller, A., He, S.Y., and Howe, G.A. (2003). Virulence systems of *Pseudomonas syringae* pv. tomato promote bacterial speck disease in tomato by targeting the jasmonate signaling pathway. *Plant J.* *36*, 485–499.
- Zhou, C., Zhang, L., Duan, J., Miki, B., and Wu, K. (2005). HISTONE DEACETYLASE19 is involved in jasmonic acid and ethylene signaling of pathogen response in *Arabidopsis*. *Plant Cell* *17*, 1196–1204.
- Zhou, J., Wu, S., Chen, X., Liu, C., Sheen, J., Shan, L., and He, P. (2014). The *Pseudomonas syringae* effector HopF2 suppresses *Arabidopsis* immunity by targeting BAK1. *Plant J.* *77*, 235–245.
- Zhu, H., Li, G.-J., Ding, L., Cui, X., Berg, H., Assmann, S.M., and Xia, Y. (2009). *Arabidopsis* extra large G-protein 2 (XLG2) interacts with the G $\beta$  subunit of heterotrimeric G protein and functions in disease resistance. *Mol. Plant* *2*, 513–525.
- Zhu, Z., Xu, F., Zhang, Y., Cheng, Y.T., Wiermer, M., Li, X., and Zhang, Y. (2010). *Arabidopsis* resistance protein SNC1 activates immune responses through association with a transcriptional corepressor. *Proc. Natl. Acad. Sci. USA* *107*, 13960–13965.
- Zhu, Z., An, F., Feng, Y., Li, P., Xue, L., A, M., Jiang, Z., Kim, J.M., To, T.K., Li, W., et al. (2011). Derepression of ethylene-stabilized transcription factors (EIN3/EIL1) mediates jasmonate and ethylene signaling synergy in *Arabidopsis*. *Proc. Natl. Acad. Sci. USA* *108*, 12539–12544.
- Zipfel, C. (2014). Plant pattern-recognition receptors. *Trends Immunol.* *35*, 345–351.
- Zipfel, C., Kunze, G., Chinchilla, D., Caniard, A., Jones, J.D.G., Boller, T., and Felix, G. (2006). Perception of the bacterial PAMP EF-Tu by the receptor EFR restricts *Agrobacterium*-mediated transformation. *Cell* *125*, 749–760.
- Zuo, J., Niu, Q.-W., and Chua, N.-H. (2000). An estrogen receptor-based transactivator XVE mediates highly inducible gene expression in transgenic plants. *Plant J.* *24*, 265–273.
- Shaner, N.C., Lambert, G.G., Chammas, A., Ni, Y., Cranfill, P.J., Baird, M.A., Sell, B.R., Allen, J.R., Day, R.N., Israelsson, M., et al. (2013). A bright monomeric green fluorescent protein derived from *Branchiostoma lanceolatum*. *Nat. Methods* *10*, 407–409.
- Shao, F., Golstein, C., Ade, J., Stoutemyer, M., Dixon, J.E., and Innes, R.W. (2003). Cleavage of *Arabidopsis* PBS1 by a bacterial type III effector. *Science* *301*, 1230–1233.
- She, J., Han, Z., Kim, T.-W., Wang, J., Cheng, W., Chang, J., Shi, S., Wang, J., Yang, M., Wang, Z.-Y., et al. (2011). Structural insight into brassinosteroid perception by BRI1. *Nature* *474*, 472–476.
- Sheard, L.B., Tan, X., Mao, H., Withers, J., Ben-Nissan, G., Hinds, T.R., Kobayashi, Y., Hsu, F.-F., Sharon, M., Browse, J., et al. (2010). Jasmonate perception by inositol-phosphate-potentiated COI1-JAZ co-receptor. *Nature* *468*, 400–405.

- Shimada, T.L., Shimada, T., and Hara-Nishimura, I. (2010). A rapid and non-destructive screenable marker, FAST, for identifying transformed seeds of *Arabidopsis thaliana*. *Plant J.* *61*, 519–528.
- Shirasu, K. (2009). The HSP90-SGT1 chaperone complex for NLR immune sensors. *Annu. Rev. Plant Biol.* *60*, 139–164.
- Sinapidou, E., Williams, K., Nott, L., Bahkt, S., Tör, M., Crute, I., Bittner-Eddy, P., and Beynon, J. (2004). Two TIR:NB:LRR genes are required to specify resistance to *Peronospora parasitica* isolate Cala2 in *Arabidopsis*. *Plant J.* *38*, 898–909.
- Smakowska-Luzan, E., Mott, G.A., Parys, K., Stegmann, M., Howton, T.C., Layeghifard, M., Neuhold, J., Lehner, A., Kong, J., Grünwald, K., et al. (2018). An extracellular network of *Arabidopsis* leucine-rich repeat receptor kinases. *Nature* *553*, 342–346.
- Sohn, K.H., Zhang, Y., and Jones, J.D.G. (2009). The *Pseudomonas syringae* effector protein, AvrRPS4, requires in planta processing and the KRVY domain to function. *Plant J.* *57*, 1079–1091.
- Sohn, K.H., Segonzac, C., Rallapalli, G., Sarris, P.F., Woo, J.Y., Williams, S.J., Newman, T.E., Paek, K.H., Kobe, B., and Jones, J.D.G. (2014). The nuclear immune receptor RPS4 is required for RRS1SLH1-dependent constitutive defense activation in *Arabidopsis thaliana*. *PLoS Genet.* *10*, e1004655.
- Soleimani, V.D., Palidwor, G.A., Ramachandran, P., Perkins, T.J., and Rudnicki, M.A. (2013). Chromatin tandem affinity purification sequencing. *Nat. Protoc.* *8*, 1525–1534.
- Sreekanta, S., Bethke, G., Hatsugai, N., Tsuda, K., Thao, A., Wang, L., Katagiri, F., and Glazebrook, J. (2015). The receptor-like cytoplasmic kinase PCRK1 contributes to pattern-triggered immunity against *Pseudomonas syringae* in *Arabidopsis thaliana*. *New Phytol.* *207*, 78–90.
- Stegmann, M., Monaghan, J., Smakowska-Luzan, E., Rovenich, H., Lehner, A., Holton, N., Belkhadir, Y., and Zipfel, C. (2017). The receptor kinase FER is a RALF-regulated scaffold controlling plant immune signaling. *Science* *355*, 287–289.
- Steinbrenner, A.D., Munoz-Amatriain, M., Venegas, J.M.A., Lo, S., Shi, D., Holton, N., Zipfel, C., Abagyan, R., Huffaker, A., Close, T.J., et al. (2019). A receptor for herbivore-associated molecular patterns mediates plant immunity. *BioRxiv*.
- Su, J., Zhang, M., Zhang, L., Sun, T., Liu, Y., Lukowitz, W., Xu, J., and Zhang, S. (2017). Regulation of Stomatal Immunity by Interdependent Functions of a Pathogen-Responsive MPK3/MPK6 Cascade and Abscisic Acid. *Plant Cell* *29*, 526–542.
- Su, J., Yang, L., Zhu, Q., Wu, H., He, Y., Liu, Y., Xu, J., Jiang, D., and Zhang, S. (2018). Active photosynthetic inhibition mediated by MPK3/MPK6 is critical to effector-triggered immunity. *PLoS Biol.* *16*, e2004122.
- Sun, T., Zhang, Y., Li, Y., Zhang, Q., Ding, Y., and Zhang, Y. (2015). ChIP-seq reveals broad roles of SARD1 and CBP60g in regulating plant immunity. *Nat. Commun.* *6*, 10159.
- Sun, T., Busta, L., Zhang, Q., Ding, P., Jetter, R., and Zhang, Y. (2018). TGACG-BINDING FACTOR 1 (TGA1) and TGA4 regulate salicylic acid and pipecolic acid biosynthesis by modulating the expression of SYSTEMIC ACQUIRED RESISTANCE

- DEFICIENT 1 (SARD1) and CALMODULIN-BINDING PROTEIN 60g (CBP60g). *New Phytol.* 217, 344–354.
- Sun, T., Huang, J., Xu, Y., Verma, V., Jing, B., Sun, Y., Ruiz Orduna, A., Tian, H., Huang, X., Xia, S., et al. (2020). Redundant CAMTA Transcription Factors Negatively Regulate the Biosynthesis of Salicylic Acid and N-Hydroxyphenylacetic Acid by Modulating the Expression of SARD1 and CBP60g. *Mol. Plant* 13, 144–156.
- Sun, Y., Li, L., Macho, A.P., Han, Z., Hu, Z., Zipfel, C., Zhou, J.-M., and Chai, J. (2013). Structural basis for flg22-induced activation of the *Arabidopsis* FLS2-BAK1 immune complex. *Science* 342, 624–628.
- Takahashi, A., Casais, C., Ichimura, K., and Shirasu, K. (2003). HSP90 interacts with RAR1 and SGT1 and is essential for RPS2-mediated disease resistance in *Arabidopsis*. *Proc. Natl. Acad. Sci. USA* 100, 11777–11782.
- Takken, F.L.W., and Tameling, W.I.L. (2009). To nibble at plant resistance proteins. *Science* 324, 744–746.
- Takken, F.L., Albrecht, M., and Tameling, W.I. (2006). Resistance proteins: molecular switches of plant defence. *Curr. Opin. Plant Biol.* 9, 383–390.
- Tao, Y., Xie, Z., Chen, W., Glazebrook, J., Chang, H.-S., Han, B., Zhu, T., Zou, G., and Katagiri, F. (2003). Quantitative nature of *Arabidopsis* responses during compatible and incompatible interactions with the bacterial pathogen *Pseudomonas syringae*. *Plant Cell* 15, 317–330.
- Thilmony, R., Underwood, W., and He, S.Y. (2006). Genome-wide transcriptional analysis of the *Arabidopsis thaliana* interaction with the plant pathogen *Pseudomonas syringae* pv. tomato DC3000 and the human pathogen *Escherichia coli* O157:H7. *Plant J.* 46, 34–53.
- Thines, B., Katsir, L., Melotto, M., Niu, Y., Mandaokar, A., Liu, G., Nomura, K., He, S.Y., Howe, G.A., and Browse, J. (2007). JAZ repressor proteins are targets of the SCF<sup>COI1</sup> complex during jasmonate signalling. *Nature* 448, 661–665.
- Thomas, C.M., Jones, D.A., Parniske, M., Harrison, K., Balint-Kurti, P.J., Hatzixanthis, K., and Jones, J.D. (1997). Characterization of the tomato Cf-4 gene for resistance to *Cladosporium fulvum* identifies sequences that determine recognitional specificity in Cf-4 and Cf-9. *Plant Cell* 9, 2209–2224.
- Thomas, W.J., Thireault, C.A., Kimbrel, J.A., and Chang, J.H. (2009). Recombineering and stable integration of the *Pseudomonas syringae* pv. *syringae* 61 hrp/hrc cluster into the genome of the soil bacterium *Pseudomonas fluorescens* Pf0-1. *Plant J.* 60, 919–928.
- Thor, K., Jiang, S., Michard, E., George, J., Scherzer, S., Huang, S., Dindas, J., Derbyshire, P., Leitão, N., DeFalco, T.A., et al. (2020). The calcium-permeable channel OSCA1.3 regulates plant stomatal immunity. *Nature* 585, 569–573.
- Thordal-Christensen, H., Zhang, Z., Wei, Y., and Collinge, D.B. (1997). Subcellular localization of H<sub>2</sub>O<sub>2</sub> in plants. H<sub>2</sub>O<sub>2</sub> accumulation in papillae and hypersensitive response during the barley-powdery mildew interaction. *Plant J.* 11, 1187–1194.

- Tian, W., Hou, C., Ren, Z., Wang, C., Zhao, F., Dahlbeck, D., Hu, S., Zhang, L., Niu, Q., Li, L., et al. (2019). A calmodulin-gated calcium channel links pathogen patterns to plant immunity. *Nature* 572, 131–135.
- Tornero, P., Chao, R.A., Luthin, W.N., Goff, S.A., and Dangl, J.L. (2002). Large-scale structure-function analysis of the Arabidopsis RPM1 disease resistance protein. *Plant Cell* 14, 435–450.
- Torrens-Spence, M.P., Bobokalonova, A., Carballo, V., Glinkerman, C.M., Pluskal, T., Shen, A., and Weng, J.-K. (2019). PBS3 and EPS1 complete salicylic acid biosynthesis from isochorismate in Arabidopsis. *BioRxiv*.
- Torres, M.A., Dangl, J.L., and Jones, J.D.G. (2002). Arabidopsis gp91phox homologues AtrbohD and AtrbohF are required for accumulation of reactive oxygen intermediates in the plant defense response. *Proc. Natl. Acad. Sci. USA* 99, 517–522.
- Toyota, M., Spencer, D., Sawai-Toyota, S., Jiaqi, W., Zhang, T., Koo, A.J., Howe, G.A., and Gilroy, S. (2018). Glutamate triggers long-distance, calcium-based plant defense signaling. *Science* 361, 1112–1115.
- Trujillo, M., Ichimura, K., Casais, C., and Shirasu, K. (2008). Negative regulation of PAMP-triggered immunity by an E3 ubiquitin ligase triplet in Arabidopsis. *Curr. Biol.* 18, 1396–1401.
- Tsuda, K., Mine, A., Bethke, G., Igarashi, D., Botanga, C.J., Tsuda, Y., Glazebrook, J., Sato, M., and Katagiri, F. (2013). Dual regulation of gene expression mediated by extended MAPK activation and salicylic acid contributes to robust innate immunity in Arabidopsis thaliana. *PLoS Genet.* 9, e1004015.
- van der Biezen, E.A., Freddie, C.T., Kahn, K., Parker, J.E., and Jones, J.D.G. (2002). Arabidopsis RPP4 is a member of the RPP5 multigene family of TIR-NB-LRR genes and confers downy mildew resistance through multiple signalling components. *Plant J.* 29, 439–451.
- van der Burgh, A.M., and Joosten, M.H.A.J. (2019). Plant immunity: thinking outside and inside the box. *Trends Plant Sci.* 24, 587–601.
- van Wees, S.C.M., and Glazebrook, J. (2003). Loss of non-host resistance of Arabidopsis NahG to Pseudomonas syringae pv. phaseolicola is due to degradation products of salicylic acid. *Plant J.* 33, 733–742.
- Verma, D.P., and Hong, Z. (2001). Plant callose synthase complexes. *Plant Mol. Biol.* 47, 693–701.
- Voigt, C.A. (2014). Callose-mediated resistance to pathogenic intruders in plant defense-related papillae. *Front. Plant Sci.* 5, 168.
- Voigt, C.A., and Somerville, S.C. (2009). Callose in biotic stress (pathogenesis). In *Chemistry, Biochemistry, and Biology of 1-3 Beta Glucans and Related Polysaccharides*, (Elsevier), pp. 525–562.
- Wagner, S., Stuttmann, J., Rietz, S., Guerois, R., Brunstein, E., Bautor, J., Niefind, K., and Parker, J.E. (2013). Structural basis for signaling by exclusive EDS1 heteromeric complexes with SAG101 or PAD4 in plant innate immunity. *Cell Host Microbe* 14, 619–630.

- Wan, J., Zhang, X.-C., Neece, D., Ramonell, K.M., Clough, S., Kim, S.-Y., Stacey, M.G., and Stacey, G. (2008). A LysM receptor-like kinase plays a critical role in chitin signaling and fungal resistance in Arabidopsis. *Plant Cell* 20, 471–481.
- Wan, J., Tanaka, K., Zhang, X.-C., Son, G.H., Brechenmacher, L., Nguyen, T.H.N., and Stacey, G. (2012). LYK4, a lysin motif receptor-like kinase, is important for chitin signaling and plant innate immunity in Arabidopsis. *Plant Physiol.* 160, 396–406.
- Wan, L., Essuman, K., Anderson, R.G., Sasaki, Y., Monteiro, F., Chung, E.-H., Osborne Nishimura, E., DiAntonio, A., Milbrandt, J., Dangl, J.L., et al. (2019). TIR domains of plant immune receptors are NAD<sup>+</sup>-cleaving enzymes that promote cell death. *Science* 365, 799–803.
- Wang, D., Pajeroska-Mukhtar, K., Culler, A.H., and Dong, X. (2007). Salicylic acid inhibits pathogen growth in plants through repression of the auxin signaling pathway. *Curr. Biol.* 17, 1784–1790.
- Wang, G., Roux, B., Feng, F., Guy, E., Li, L., Li, N., Zhang, X., Lautier, M., Jardinaud, M.-F., Chabannes, M., et al. (2015). The Decoy Substrate of a Pathogen Effector and a Pseudokinase Specify Pathogen-Induced Modified-Self Recognition and Immunity in Plants. *Cell Host Microbe* 18, 285–295.
- Wang, J., Grubb, L.E., Wang, J., Liang, X., Li, L., Gao, C., Ma, M., Feng, F., Li, M., Li, L., et al. (2018). A regulatory module controlling homeostasis of a plant immune kinase. *Mol. Cell* 69, 493–504.e6.
- Wang, J., Hu, M., Wang, J., Qi, J., Han, Z., Wang, G., Qi, Y., Wang, H.-W., Zhou, J.-M., and Chai, J. (2019a). Reconstitution and structure of a plant NLR resistosome conferring immunity. *Science* 364.
- Wang, J., Wang, J., Hu, M., Wu, S., Qi, J., Wang, G., Han, Z., Qi, Y., Gao, N., Wang, H.-W., et al. (2019b). Ligand-triggered allosteric ADP release primes a plant NLR complex. *Science* 364.
- Wang, K., Senthil-Kumar, M., Ryu, C.-M., Kang, L., and Mysore, K.S. (2012). Phytosterols play a key role in plant innate immunity against bacterial pathogens by regulating nutrient efflux into the apoplast. *Plant Physiol.* 158, 1789–1802.
- Wang, L., Tsuda, K., Sato, M., Cohen, J.D., Katagiri, F., and Glazebrook, J. (2009). Arabidopsis CaM binding protein CBP60g contributes to MAMP-induced SA accumulation and is involved in disease resistance against *Pseudomonas syringae*. *PLoS Pathog.* 5, e1000301.
- Wang, W., Yang, J., Zhang, J., Liu, Y.-X., Tian, C., Qu, B., Gao, C., Xin, P., Cheng, S., Zhang, W., et al. (2020a). An arabidopsis secondary metabolite directly targets expression of the bacterial type III secretion system to inhibit bacterial virulence. *Cell Host Microbe* 27, 601–613.e7.
- Wang, W., Withers, J., Li, H., Zwack, P.J., Rusnac, D.-V., Shi, H., Liu, L., Yan, S., Hinds, T.R., Guttman, M., et al. (2020b). Structural basis of salicylic acid perception by Arabidopsis NPR proteins. *Nature* 586, 311–316.

- Wang, Y., Li, J., Hou, S., Wang, X., Li, Y., Ren, D., Chen, S., Tang, X., and Zhou, J.-M. (2010). A *Pseudomonas syringae* ADP-ribosyltransferase inhibits Arabidopsis mitogen-activated protein kinase kinases. *Plant Cell* 22, 2033–2044.
- Weiss, D., and Ori, N. (2007). Mechanisms of cross talk between gibberellin and other hormones. *Plant Physiol.* 144, 1240–1246.
- Whitham, S., McCormick, S., and Baker, B. (1996). The N gene of tobacco confers resistance to tobacco mosaic virus in transgenic tomato. *Proc. Natl. Acad. Sci. USA* 93, 8776–8781.
- Wildermuth, M.C., Dewdney, J., Wu, G., and Ausubel, F.M. (2001). Isochorismate synthase is required to synthesize salicylic acid for plant defence. *Nature* 414, 562–565.
- Williams, S.J., Sohn, K.H., Wan, L., Bernoux, M., Sarris, P.F., Segonzac, C., Ve, T., Ma, Y., Saucet, S.B., Ericsson, D.J., et al. (2014). Structural basis for assembly and function of a heterodimeric plant immune receptor. *Science* 344, 299–303.
- Willmann, R., Lajunen, H.M., Erbs, G., Newman, M.-A., Kolb, D., Tsuda, K., Katagiri, F., Fliegmann, J., Bono, J.-J., Cullimore, J.V., et al. (2011). Arabidopsis lysin-motif proteins LYM1 LYM3 CERK1 mediate bacterial peptidoglycan sensing and immunity to bacterial infection. *Proc. Natl. Acad. Sci. USA* 108, 19824–19829.
- Wu, C.-H., Abd-El-Haliem, A., Bozkurt, T.O., Belhaj, K., Terauchi, R., Vossen, J.H., and Kamoun, S. (2017). NLR network mediates immunity to diverse plant pathogens. *Proc. Natl. Acad. Sci. USA* 114, 8113–8118.
- Wu, C.-H., Derevnina, L., and Kamoun, S. (2018). Receptor networks underpin plant immunity. *Science* 360, 1300–1301.
- Wu, F., Chi, Y., Jiang, Z., Xu, Y., Xie, L., Huang, F., Wan, D., Ni, J., Yuan, F., Wu, X., et al. (2020a). Hydrogen peroxide sensor HPCA1 is an LRR receptor kinase in Arabidopsis. *Nature* 578, 577–581.
- Wu, Y., Xun, Q., Guo, Y., Zhang, J., Cheng, K., Shi, T., He, K., Hou, S., Gou, X., and Li, J. (2016). Genome-Wide Expression Pattern Analyses of the Arabidopsis Leucine-Rich Repeat Receptor-Like Kinases. *Mol. Plant* 9, 289–300.
- Wu, Z., Li, M., Dong, O.X., Xia, S., Liang, W., Bao, Y., Wasteneys, G., and Li, X. (2019). Differential regulation of TNL-mediated immune signaling by redundant helper CNLs. *New Phytol.* 222, 938–953.
- Wu, Z., Tong, M., Tian, L., Zhu, C., Liu, X., Zhang, Y., and Li, X. (2020b). Plant E3 ligases SNIPER1 and SNIPER2 broadly regulate the homeostasis of sensor NLR immune receptors. *EMBO J.* 39, e104915.
- Xiang, T., Zong, N., Zou, Y., Wu, Y., Zhang, J., Xing, W., Li, Y., Tang, X., Zhu, L., Chai, J., et al. (2008). *Pseudomonas syringae* effector AvrPto blocks innate immunity by targeting receptor kinases. *Curr. Biol.* 18, 74–80.
- Xiao, Y., Stegmann, M., Han, Z., DeFalco, T.A., Parys, K., Xu, L., Belkhadir, Y., Zipfel, C., and Chai, J. (2019). Mechanisms of RALF peptide perception by a heterotypic receptor complex. *Nature* 572, 270–274.

- Xin, X.-F., Nomura, K., Aung, K., Velásquez, A.C., Yao, J., Boutrot, F., Chang, J.H., Zipfel, C., and He, S.Y. (2016). Bacteria establish an aqueous living space in plants crucial for virulence. *Nature* 539, 524–529.
- Xing, W., Zou, Y., Liu, Q., Liu, J., Luo, X., Huang, Q., Chen, S., Zhu, L., Bi, R., Hao, Q., et al. (2007). The structural basis for activation of plant immunity by bacterial effector protein AvrPto. *Nature* 449, 243–247.
- Xiong, Q., Ye, W., Choi, D., Wong, J., Qiao, Y., Tao, K., Wang, Y., and Ma, W. (2014). Phytophthora suppressor of RNA silencing 2 is a conserved RxLR effector that promotes infection in soybean and *Arabidopsis thaliana*. *Mol. Plant Microbe Interact.* 27, 1379–1389.
- Xu, G., Greene, G.H., Yoo, H., Liu, L., Marqués, J., Motley, J., and Dong, X. (2017). Global translational reprogramming is a fundamental layer of immune regulation in plants. *Nature* 545, 487–490.
- Xu, J., Xie, J., Yan, C., Zou, X., Ren, D., and Zhang, S. (2014). A chemical genetic approach demonstrates that MPK3/MPK6 activation and NADPH oxidase-mediated oxidative burst are two independent signaling events in plant immunity. *Plant J.* 77, 222–234.
- Yamada, K., Yamaguchi, K., Shirakawa, T., Nakagami, H., Mine, A., Ishikawa, K., Fujiwara, M., Narusaka, M., Narusaka, Y., Ichimura, K., et al. (2016a). The *Arabidopsis* CERK1-associated kinase PBL27 connects chitin perception to MAPK activation. *EMBO J.* 35, 2468–2483.
- Yamada, K., Saijo, Y., Nakagami, H., and Takano, Y. (2016b). Regulation of sugar transporter activity for antibacterial defense in *Arabidopsis*. *Science* 354, 1427–1430.
- Yamaguchi, Y., Pearce, G., and Ryan, C.A. (2006). The cell surface leucine-rich repeat receptor for *AtPep1*, an endogenous peptide elicitor in *Arabidopsis*, is functional in transgenic tobacco cells. *Proc. Natl. Acad. Sci. USA* 103, 10104–10109.
- Yamaguchi, Y., Huffaker, A., Bryan, A.C., Tax, F.E., and Ryan, C.A. (2010). PEPR2 is a second receptor for the *Pep1* and *Pep2* peptides and contributes to defense responses in *Arabidopsis*. *Plant Cell* 22, 508–522.
- Yan, H., Zhao, Y., Shi, H., Li, J., Wang, Y., and Tang, D. (2018). BRASSINOSTEROID-SIGNALING KINASE1 Phosphorylates MAPKKK5 to Regulate Immunity in *Arabidopsis*. *Plant Physiol.* 176, 2991–3002.
- Yoo, H., Greene, G.H., Yuan, M., Xu, G., Burton, D., Liu, L., Marqués, J., and Dong, X. (2020). Translational Regulation of Metabolic Dynamics during Effector-Triggered Immunity. *Mol. Plant* 13, 88–98.
- Yu, G., Xian, L., Xue, H., Yu, W., Rufian, J.S., Sang, Y., Morcillo, R.J.L., Wang, Y., and Macho, A.P. (2020). A bacterial effector protein prevents MAPK-mediated phosphorylation of SGT1 to suppress plant immunity. *PLoS Pathog.* 16, e1008933.
- Yu, I.C., Parker, J., and Bent, A.F. (1998). Gene-for-gene disease resistance without the hypersensitive response in *Arabidopsis dnd1* mutant. *Proc. Natl. Acad. Sci. USA* 95, 7819–7824.

- Yu, X., Xu, G., Li, B., de Souza Vespoli, L., Liu, H., Moeder, W., Chen, S., de Oliveira, M.V.V., Ariádina de Souza, S., Shao, W., et al. (2019). The Receptor Kinases BAK1/SERK4 Regulate Ca<sup>2+</sup> Channel-Mediated Cellular Homeostasis for Cell Death Containment. *Curr. Biol.* 29, 3778–3790.e8.
- Yuan, M., Jiang, Z., Bi, G., Nomura, K., Liu, M., He, S.Y., Zhou, J.-M., and Xin, X.-F. (2020). Pattern-recognition receptors are required for NLR-mediated plant immunity. *BioRxiv*.
- Yun, B.-W., Feechan, A., Yin, M., Saidi, N.B.B., Le Bihan, T., Yu, M., Moore, J.W., Kang, J.-G., Kwon, E., Spoel, S.H., et al. (2011). S-nitrosylation of NADPH oxidase regulates cell death in plant immunity. *Nature* 478, 264–268.
- Zavaliev, R., Mohan, R., Chen, T., and Dong, X. (2020). Formation of NPR1 Condensates Promotes Cell Survival during the Plant Immune Response. *Cell* 182, 1093–1108.e18.
- Zhai, C., Lin, F., Dong, Z., He, X., Yuan, B., Zeng, X., Wang, L., and Pan, Q. (2011). The isolation and characterization of Pik, a rice blast resistance gene which emerged after rice domestication. *New Phytol.* 189, 321–334.
- Zhang, N., and Fan, Z. (2020). Transcriptional reprogramming during effector/flg22-triggered immune is independent of defense phytohormone signaling networks. *BioRxiv*.
- Zhang, S., and Klessig, D.F. (1998). Resistance gene N-mediated de novo synthesis and activation of a tobacco mitogen-activated protein kinase by tobacco mosaic virus infection. *Proc. Natl. Acad. Sci. USA* 95, 7433–7438.
- Zhang, X.-C., and Gassmann, W. (2007). Alternative splicing and mRNA levels of the disease resistance gene RPS4 are induced during defense responses. *Plant Physiol.* 145, 1577–1587.
- Zhang, J., Shao, F., Li, Y., Cui, H., Chen, L., Li, H., Zou, Y., Long, C., Lan, L., Chai, J., et al. (2007). A *Pseudomonas syringae* effector inactivates MAPKs to suppress PAMP-induced immunity in plants. *Cell Host Microbe* 1, 175–185.
- Zhang, J., Li, W., Xiang, T., Liu, Z., Laluk, K., Ding, X., Zou, Y., Gao, M., Zhang, X., Chen, S., et al. (2010a). Receptor-like cytoplasmic kinases integrate signaling from multiple plant immune receptors and are targeted by a *Pseudomonas syringae* effector. *Cell Host Microbe* 7, 290–301.
- Zhang, W., Fraiture, M., Kolb, D., Löffelhardt, B., Desaki, Y., Boutrot, F.F.G., Tör, M., Zipfel, C., Gust, A.A., and Brunner, F. (2013). Arabidopsis receptor-like protein30 and receptor-like kinase suppressor of BIR1-1/EVERSHED mediate innate immunity to necrotrophic fungi. *Plant Cell* 25, 4227–4241.
- Zhang, X., Bernoux, M., Bentham, A.R., Newman, T.E., Ve, T., Casey, L.W., Raaymakers, T.M., Hu, J., Croll, T.I., Schreiber, K.J., et al. (2017). Multiple functional self-association interfaces in plant TIR domains. *Proc. Natl. Acad. Sci. USA* 114, E2046–E2052.
- Zhang, Y., Fan, W., Kinkema, M., Li, X., and Dong, X. (1999). Interaction of NPR1 with basic leucine zipper protein transcription factors that bind sequences required for salicylic acid induction of the PR-1 gene. *Proc. Natl. Acad. Sci. USA* 96, 6523–6528.

- Zhang, Y., Tessaro, M.J., Lassner, M., and Li, X. (2003). Knockout analysis of Arabidopsis transcription factors TGA2, TGA5, and TGA6 reveals their redundant and essential roles in systemic acquired resistance. *Plant Cell* *15*, 2647–2653.
- Zhang, Y., Cheng, Y.T., Qu, N., Zhao, Q., Bi, D., and Li, X. (2006). Negative regulation of defense responses in Arabidopsis by two NPR1 paralogs. *Plant J.* *48*, 647–656.
- Zhang, Y., Xu, S., Ding, P., Wang, D., Cheng, Y.T., He, J., Gao, M., Xu, F., Li, Y., Zhu, Z., et al. (2010b). Control of salicylic acid synthesis and systemic acquired resistance by two members of a plant-specific family of transcription factors. *Proc. Natl. Acad. Sci. USA* *107*, 18220–18225.
- Zhao, Y., Thilmony, R., Bender, C.L., Schaller, A., He, S.Y., and Howe, G.A. (2003). Virulence systems of *Pseudomonas syringae* pv. tomato promote bacterial speck disease in tomato by targeting the jasmonate signaling pathway. *Plant J.* *36*, 485–499.
- Zhou, C., Zhang, L., Duan, J., Miki, B., and Wu, K. (2005). HISTONE DEACETYLASE19 is involved in jasmonic acid and ethylene signaling of pathogen response in Arabidopsis. *Plant Cell* *17*, 1196–1204.
- Zhou, J., Wu, S., Chen, X., Liu, C., Sheen, J., Shan, L., and He, P. (2014). The *Pseudomonas syringae* effector HopF2 suppresses Arabidopsis immunity by targeting BAK1. *Plant J.* *77*, 235–245.
- Zhu, H., Li, G.-J., Ding, L., Cui, X., Berg, H., Assmann, S.M., and Xia, Y. (2009). Arabidopsis extra large G-protein 2 (XLG2) interacts with the Gbeta subunit of heterotrimeric G protein and functions in disease resistance. *Mol. Plant* *2*, 513–525.
- Zhu, Z., Xu, F., Zhang, Y., Cheng, Y.T., Wiermer, M., Li, X., and Zhang, Y. (2010). Arabidopsis resistance protein SNC1 activates immune responses through association with a transcriptional corepressor. *Proc. Natl. Acad. Sci. USA* *107*, 13960–13965.
- Zhu, Z., An, F., Feng, Y., Li, P., Xue, L., A, M., Jiang, Z., Kim, J.M., To, T.K., Li, W., et al. (2011). Derepression of ethylene-stabilized transcription factors (EIN3/EIL1) mediates jasmonate and ethylene signaling synergy in *Arabidopsis*. *Proc. Natl. Acad. Sci. USA* *108*, 12539–12544.
- Zipfel, C. (2014). Plant pattern-recognition receptors. *Trends Immunol.* *35*, 345–351.
- Zipfel, C., Kunze, G., Chinchilla, D., Caniard, A., Jones, J.D.G., Boller, T., and Felix, G. (2006). Perception of the bacterial PAMP EF-Tu by the receptor EFR restricts *Agrobacterium*-mediated transformation. *Cell* *125*, 749–760.
- Zuo, J., Niu, Q.-W., and Chua, N.-H. (2000). An estrogen receptor-based transactivator XVE mediates highly inducible gene expression in transgenic plants. *Plant J.* *24*, 265–273.